Molecular Diversity from *N*-phenylquinoneimine

Newcastle University

ADEBIMPE DORCAS ADESINA

Submitted in partial fulfilment of the requirements for the degree of Doctor of Philosophy

April 2020

Acknowledgements

All thanks to the Almighty God for the successful completion of this study.

I would like to extend my thanks and gratitude to my supervisor Dr Michael A. Carroll for his continuous support, guidance and encouragement throughout this project.

I would like to thank Dr Corrine Wills for support with the NMR spectroscopy, Dr Paul G. Waddell with the X-ray crystallography, the SAgE mass spectrometry facility (Newcastle University), London Metropolitan University for elemental analyses, Newcastle University and TetFund for the sponsorship.

Finally, I would like to thank my family for their encouragement and support to be able to succeed in my endeavours throughout the course at Newcastle University.

Abstract

Diversity-oriented synthesis (DOS) continues to grow as an area of importance in the disciplines of organic synthesis and chemical biology.[1-3] It involves the preparation of diverse scaffolds of varying complexity and enables the exploration of a greater range of 'chemical space' than hitherto possible through multicomponent-coupling and tandem reactions.

Tandem reactions, also known as cascade or domino reactions, link several transformations together in a single process step. Simple starting materials can be used to rapidly build complex structures with high selectivity. The use and production of toxic and/or hazardous intermediates can be avoided/minimised and novel avenues of research and new reactions can be developed.[4]

In this work, azaquinone **1** has been studied as a new key intermediate in multicomponent coupling and tandem reactions (Scheme 1). As all six carbon atoms in the quinoid ring are different, it has the potential to serve as a novel building block to access a range of useful structural motifs as part of scaffold diversity synthesis and drug discovery.

Conjugate addition to azaquinone **1** with nitrogen nucleophiles (aromatic amines) has been investigated, giving di-substituted arylamino compounds **2** in good yields (56–68%). Although the basic process has been reported,[5] the regiochemistry of these compounds has now been confirmed by 2D NMR (COSY and NOESY) and also by determination of the crystal structure of the products. The reaction of aromatic amines with azaquinone occurred by both 1,4-conjugate addition to the α,β-unsaturated imine and the α,β-unsaturated ketone, resulting only in di-addition products. These diarylamino products **2** are coloured compounds which may be of importance in the dye industry, and those interested in development of diagnostic tools. Further reactions of compounds **2** could result in the production of azine, oxazine, and thiazine dyes.

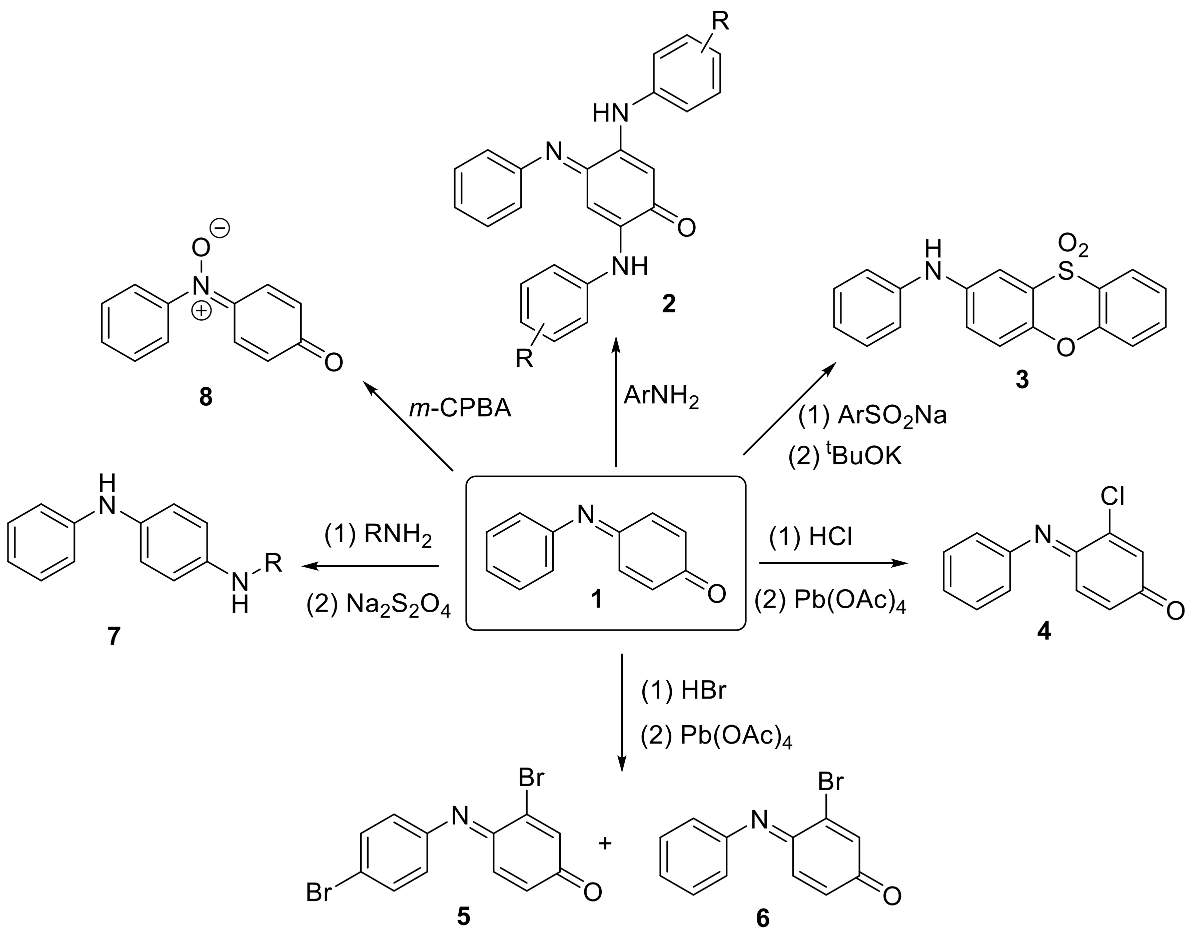

Scheme 1: Reactions of azaquinone, **1**

The reaction of aliphatic amines was found to occur by direct addition to the carbonyl group of azaquinone, giving 1,4-diaminoarenes **7** following reductive work-up. These *N*-substituted phenylenediamines **7** are useful for the production of drugs, agricultural products, as antioxidants, gel inhibitors and polymerization inhibitors.[6]

Azaquinone also reacts with sulfur nucleophiles (e.g. sodium arenesulfinates) and a further oxidative cyclisation has served as a new route to synthesizing phenoxathiins **3** which can serve as sulfone containing scaffolds in pharmaceutical molecules.[7]

Halogenation of azaquinone is selective depending on the reaction conditions used, allowing targeted functionalisation which enables the application of metal catalysed cross-coupling reactions, extending the sequence of potential reactions further.[8,9] The bromination of the phenyl ring also occurs as a competing process, but this can be suppressed by the addition of radical scavengers (e.g. resorcinol) to the reaction mixture. The chlorination of azaquinone is more selective and gives only the mono-substituted product **4** with the chloro group on the quinoid ring. Halogenation of the *N*-oxide **8** was also investigated and this results in direct bromination of the phenyl ring, changing the selectivity of the reaction. The concurrent loss of the *N*-oxide functionality in the products from the bromination reactions suggests that the mechanism of bromination of the phenyl group in the *N*-oxide is from nucleophilic addition rather than the radical reaction, which is observed with azaquinone as the substrate.

The order of addition of the aromatic amines to azaquinone was also investigated using computational methods. Although the proposed mono-addition products **9** and **10** (Scheme 2) have not been observed or isolated in the reaction, computational studies has shown that the reaction intermediate results from single addition to the α,β-ketone (before oxidation) which the second nucleophile then adds to.

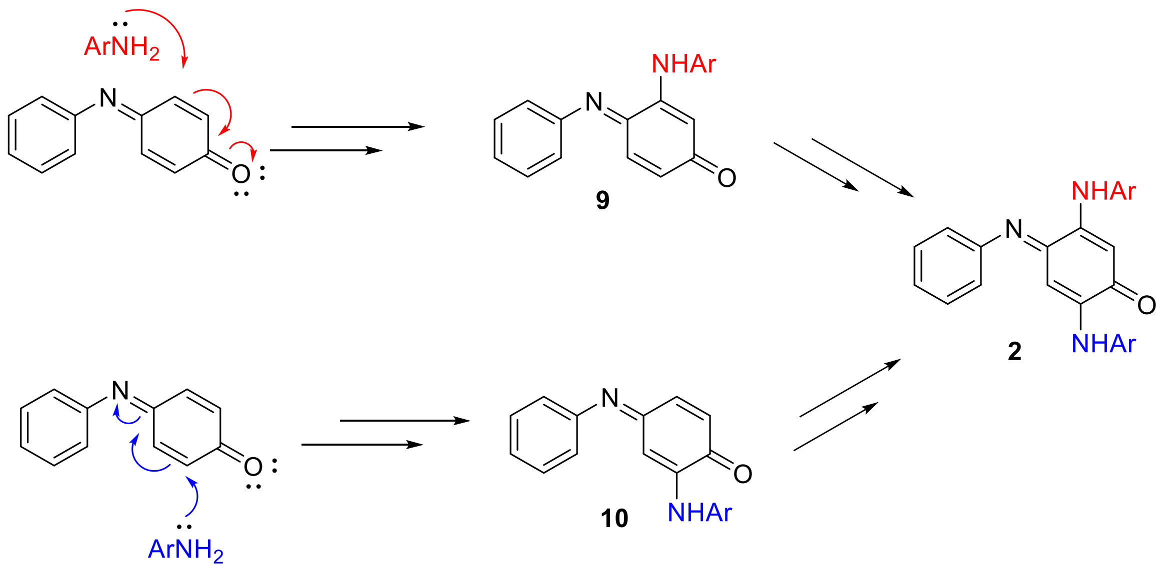

Scheme 2: Mechanism of the reaction of azaquinone with aromatic amines

As mentioned before, the introduction of halogens offers the possibility of further elaboration of the structure. 3-Bromoazaquinone **6** gave the expected products resulting from cross-coupling reactions while 3-chloroazaquinone **4** was found to be unreactive towards these coupling reactions. In general, Suzuki and Stille reactions (13–66% **11**) were more successful than Sonogashira and Kumada reactions (10% **12**, **13**) with Buchwald-Hartwig conditions also giving good yields of the amino product (29–79% **9**). The mono-addition product, **9** derived from the

Buchwald-Hartwig reaction has also been used to investigate the order of addition in the formation of product **2** which is derived from the direct reaction of aromatic amines with azaquinone.

These coupling reactions has served as a means of incorporating both new R and Ar groups into the quinoid ring of the azaquinone, and so elaborating the structure.

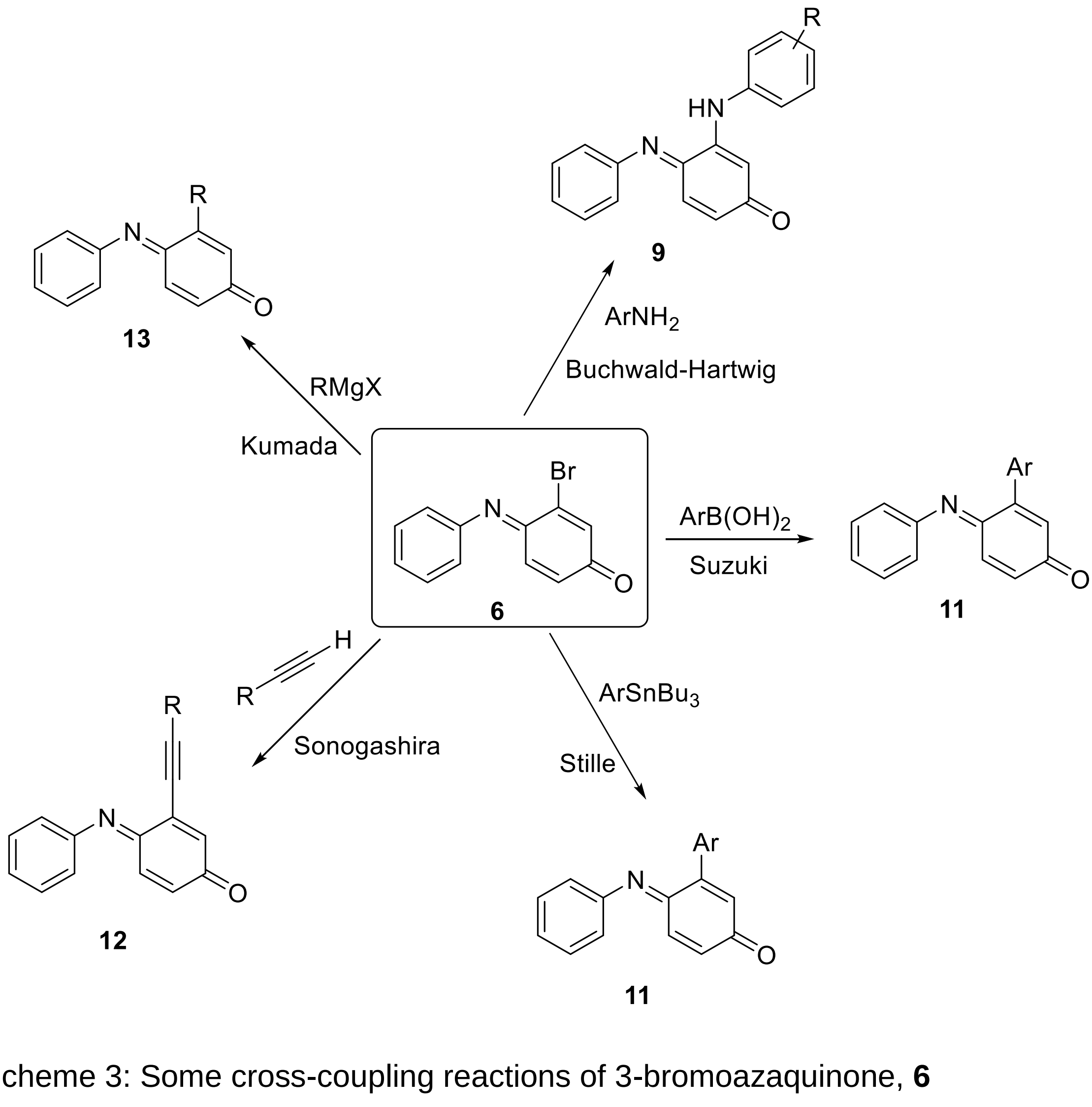

Scheme 3: Some cross-coupling reactions of 3-bromoazaquinone, **6**

Abbreviations

AcOH	acetic acid
AIBN	2,2'-azobis(2-methylpropionitrile)
Anal. Calcd	analytical calculated
Aq	aqueous
Ar	aryl
BINAP	2,2'-bis(diphenylphosphino)-1,1'-binaphthyl
Bn	benzyl
Bu	butyl
°C	degree Celsius
$CDCl_3$	deuterated chloroform
COSY	correlation spectroscopy
d	doublet
DABCO	1,4-diazabicyclo[2.2.2]octane
dba	dibenzylideneacetone
DCM	dichloromethane
DMF	*N,N*-dimethylformamide
DMP	Dess-Martin Periodinane
DMSO	dimethyl sulfoxide
DNA	deoxyribonucleic acid
DPPE	1,2-bis(diphenylphosphino)ethane

DPPF	1,1'-bis(diphenylphosphino)ferrocene
EDG	electron-donating group
Equiv.	equivalent
Et	ethyl
Et_3N	triethylamine
EtOAc	ethyl acetate
EtOH	ethanol
EWG	electron-withdrawing group
g	gram
h	hour(s)
HFIP	1,1,1,3,3,3-hexafluoro-2-propanol
HMBC	heteronuclear multiple bond correlation
HMDS	hexamethyldisilazane
HOMO	highest occupied molecular orbital
HPLC	High Performance/Pressure Liquid Chromatography
hv	light
Hz	hertz
IBX	2-iodoxybenzoic acid
IR	infrared
J	coupling constant
L	ligand/litres

LAB	lithium *N,N*-dialkylaminoborohydride
LUMO	lowest unoccupied molecular orbital
M	molar
m	multiplet
***m*-CPBA**	meta-chloroperoxybenzoic acid
Me	methyl
MeCN	acetonitrile
MeO	methoxy
mg	milligram
min	minute(s)
mL	millilitre
mmol	millimole
MOM	methoxymethyl
Mp	melting point
mRNA	messenger ribonucleic acid
m/z	mass/charge ratio
NaHMDS	sodium bis(trimethylsilyl)amide
NMR	nuclear magnetic resonance
NOESY	nuclear Overhauser effect spectroscopy
Nu	nucleophile
OAc	acetate

OTf	trifluoromethanesulfonate (triflate)
OTs	*p*-toluenesulfonate (tosylate)
Ph	phenyl
Piv	pivalate
ppm	parts per million
R_f	Retention factor
RP	reverse phase
rt	room temperature
s	singlet
$SnBu_3$	tributyltin
S_NAr	nucleophilic aromatic substitution
t	triplet
THF	tetrahydrofuran
TIPS	triisopropylsilyl
TMS	trimethylsilyl / tetramethysilane
TMSOTf	trimethylsilyl trifluoromethanesulfonate
V	volts
xantphos	4,5-bis(diphenyl-phosphino)-9,9-dimethylxanthene

Contents

Chapter 1. Introduction

1.1 Diversity-Oriented Synthesis

The art of organic synthesis provides chemists with a great toolbox for the creation of novel structures with new properties and thereby prodigiously impacts on human life.[10,11] The use of small molecules in chemical biology, nanomedicine and chemical genetics, for example, has undoubtedly broadened the horizons of chemical synthesis.[12,13] The search for biologically active small molecules, often identified through high-throughput screenings (HTS) of compound libraries marked the beginning of divergent chemical synthesis approaches.[14,15]

The scaffold is the core molecular framework that provides the basic shape, rigidity, or flexibility of a molecule,[16] and exposes various substituents over its periphery in three-dimensional space, which can interact with diverse biological targets. Scaffold diversity is therefore the most important feature of a compound library that determines its success in screening endeavours, in particular when identifying bioactive molecules in unbiased phenotypic screenings or novel biological targets. In such scenarios, a compound collection rich in scaffold diversity stands better chances to identify hit and lead molecules.[17]

Whereas, the synthesis of small molecules focused around a lead structure (the target molecule) is relatively easy, the efficient synthesis of structurally diverse small molecules has been distinguished from target-oriented synthesis (e.g. natural product synthesis and focused 'library' synthesis) and termed diversity-oriented synthesis (DOS) (Fig. 1.1).[3,18]

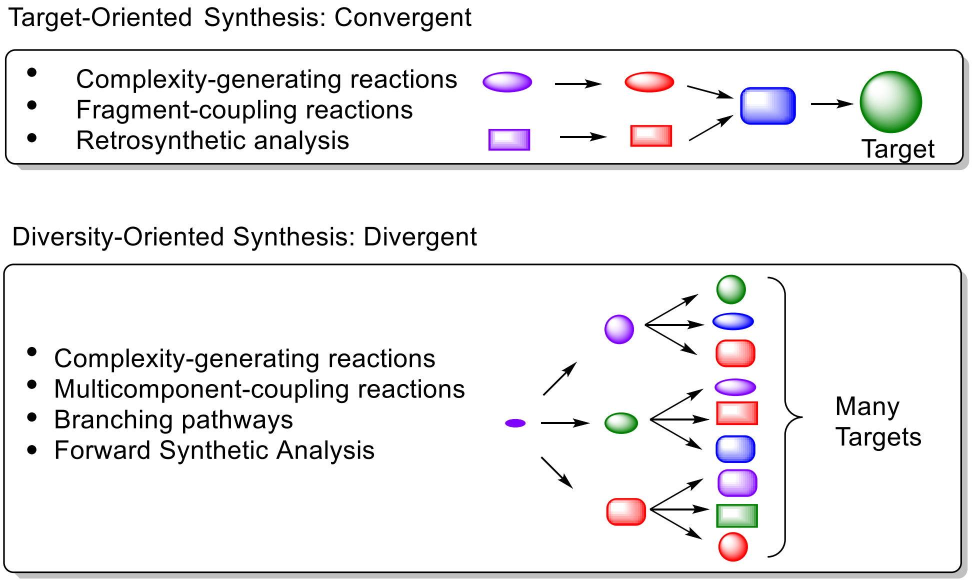

Figure 1.1: Comparison of target-oriented synthesis (TOS) versus diversity-oriented synthesis (DOS). No specific meaning is implied by the colours or shapes except that each unit represents a different compound.

In target-oriented synthesis, retrosynthetic analysis is employed to find an efficient and convergent route using complexity-generating reactions such as the Diels-Alder reaction, where two C–C bonds are made regioselectively.[19] DOS requires a planning algorithm to deliver an efficient but divergent route. Although DOS aims to achieve a diverse and non-focused coverage of biologically active chemical space, the results of DOS may find use in other fields in future years. Complexity-generating reactions are again important for efficiency (multicomponent-coupling, cascade and tandem complexity-generating reactions are the most valuable); however, pathways need to be identified that give structurally diverse targets. In order to achieve the highest levels of structural diversity: (i) the building blocks, (ii) the stereochemistry, (iii) the functional groups and, most importantly, (iv) the molecular framework must be varied. The key to the structural complexity is the complexity-generating reactions while the key to the structural diversity is the branch points and building blocks.[3] The identification in the forward direction of pairwise relationships, where the product of one complexity-generating reaction is the substrate for another, can lead to high levels of molecular complexity in a very efficient manner.[2,20]

Diversity-oriented synthesis (DOS) continues to grow as an area of importance in the disciplines of organic synthesis and chemical biology.[1-3] One important area that should benefit significantly from DOS is drug discovery. The existing chemical space can be expanded with new synthetic molecules, hoping to identify novel and better drug and probe molecules.[17]

Lead generation can be approached broadly in two ways. The first approach looks for small molecules (drugs are most often organic, small molecules) that give you a desired physiological outcome, such as toxicity to bacteria. This approach has been incredibly successful historically, identifying the clinical antibiotics vancomycin, penicillins, streptomycin, tetracyclines, erythromycin, sulphonamides etc. The second approach starts with a target such as a protein and looks for small molecules that modulate or attenuate its function. Both approaches require the availability of collections of small molecules. DOS has the potential to deliver this ideal collection of small molecules efficiently. Moreover, structure-activity relationships of identified 'hit' structures can be rapidly obtained with different building blocks, facilitating the 'hits to leads' process.[3]

1.2 Multicomponent Reactions

Arguably, one of the most promising synthetic strategies for generating collections of small molecules by DOS involves the sequencing of multicomponent reactions (MCRs) with subsequent transformations, including cyclizations and refunctionalizations, that form new compounds possessing increased molecular complexity and diversity.[21] This process of sequencing MCRs with subsequent cyclizations is commonly referred to as the build/couple/pair (B/C/P) strategy of DOS.[1,22]

In the build phase, building blocks are synthesized. Asymmetric syntheses of chiral building blocks containing orthogonal sets of functionalities suitable for subsequent coupling and pairing steps are performed. These chiral building blocks can be prepared by using either enantio- and diastereoselective reactions or compounds from the "chiral pool". To minimize the overall number of synthetic steps, functional groups needed for subsequent coupling and pairing reactions should be embedded within these building blocks. In the simplest form of the B/C/P strategy, all stereogenic elements of the final products reside within the chiral building blocks and are obtained by a simple mix-and-match process.[23]

In the couple phase, intermolecular coupling reactions that join the building blocks are performed resulting in compounds with a dense array of functional groups that can undergo intramolecular reactions in distinct pairwise combinations – either without stereochemical consequences or with complete control of all possible stereochemical outcomes.

In the pair phase, intramolecular coupling reactions that join pairwise combinations of functional groups incorporated in the "build" phase (termed functional-group-pairing reactions[24]) are performed. This process provides the basis for structural diversity.

The diversification of enantioenriched Michael adducts through functional group pairing to access highly functionalised modular scaffolds has been reported.[24] A range of five- to ten-membered complex fused and bridged ring systems and investigation of their synthetic utility to produce novel structural types was described. In the generalized structure **1.1**, the nitro group may be paired in chemical reactions with the ester functional group or with the alkyne. Likewise, incorporation of an *o*-allyl moiety into nitrostyrene **1.1** (Scheme 1.1, R^2 = allyl) enables pairing between R^2 and the alkyne/alkene. Further diversification was achieved by performing a Diels-Alder reaction with the 1,3-diene substrate **1.4** to yield another molecular skeleton. Where the folding reactions left the nitro and ester groups of the densely functionalized starting material untouched (e.g. **1.1**→**1.4**), their pairing in a later reaction sequence led to the construction of further molecular skeletons.[25]

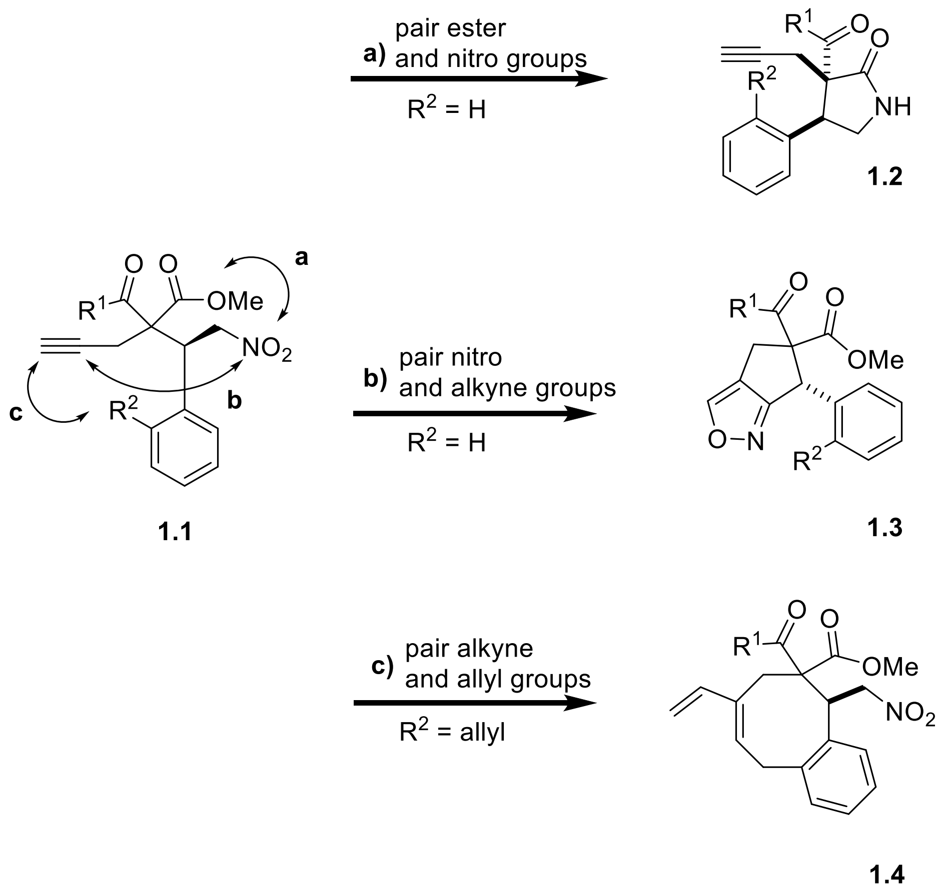

Scheme 1.1: Skeletal diversity through functional group pairing

Most reactions involve two stoichiometric reactants and give one product. Reactions in which more than two reactants come together to produce a product are called multi-component reactions. Multicomponent reactions generally involve two reactants forming a reactive intermediate that then reacts with another reagent to form products.

In contrast to two-component reactions, MCRs are especially favourable. Very many products can be synthesized from only a few starting substances. Many common MCRs fall back on easily accessible, archetypical functional groups, which are available in a great variety, that is an MCR is economical with resources. As MCRs, being one-pot reactions, are practically single-step conversions, they are easier to carry out than multistep syntheses.[26]

The classic multicomponent reaction, the Ugi four-component reaction (U-4CR), has certainly been well recognised and utilized for its ability to unite building blocks from four diverse and yet readily available functional group families: carboxylic acids, carbonyls, amines, and the much rarer isonitriles.[21,26] The U-4CR is extraordinarily functional group tolerant, and each of the four components can contain functionality that can be used in subsequent transformations, thus allowing for access to a number of cyclisation manifolds. It thus does not occasion surprise that a substantial body of work has been devoted to post condensation modifications of U-4CR adducts.[27,28] The products of an Ugi reaction are *N*-acyl α-amino amides, and thus are closely related to peptides. This is a virtue both because of the important biological properties of peptides and because the differences between Ugi products and native peptides may make the former more valuable as drug candidates.

The Ugi reaction has an interesting mechanism (Scheme 1.2).[29] The formation of an imine between the carbonyl and an amine is a classical reaction in organic chemistry. The initial formation of an imine from the reaction of **1.5** and **1.6** means that preformed imines or imine-like functional groups may also be used in Ugi-type coupling processes. The imine is protonated by the carboxylic acid, making it electrophilic as the iminium ion **1.7**. The dipolar isonitrile group **1.8** carries significant negative charge character on its carbon and can therefore act as a nucleophile toward the iminium ion. The product of this process is an iminacylium ion **1.9** that can react with the carboxylate ion **1.10** to form what is effectively a mixed anhydride **1.11** between a carboxylic acid and an imide. This is a reactive acylating agent, and the nitrogen that was made nucleophilic by the addition of the isonitrile to the iminium ion can perform an intramolecular acyl substitution reaction to give the condensation product **1.12**.

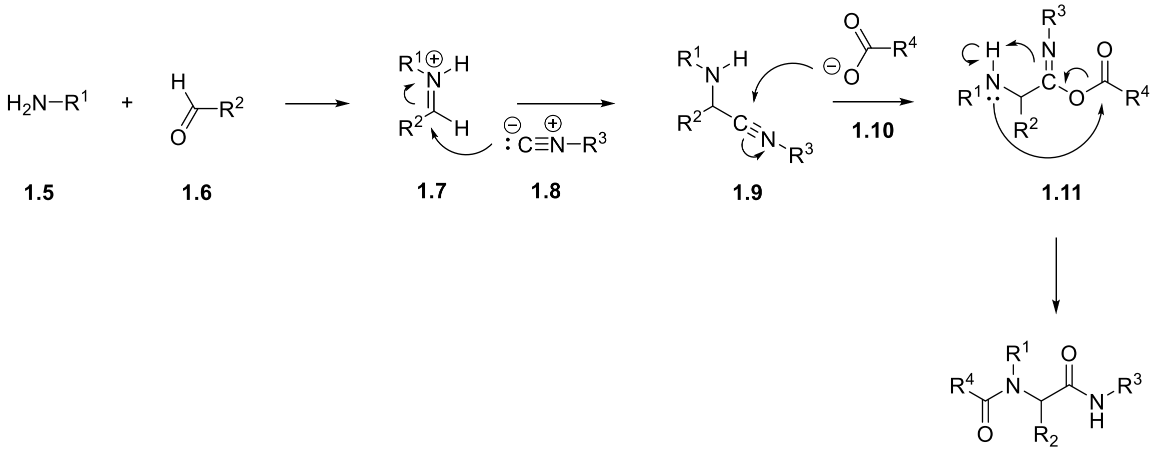

1.5 1.6 1.7 1.8 1.9 1.10 1.11 1.12

Scheme 1.2: Mechanism of the Ugi condensation

A diversity-oriented synthesis of fused dihydropyrazin-2(1H)-ones through a Ugi 4CR/deprotection/Heck sequence has been reported by Amador-Sanchez et al.[30] A collection of highly substituted fused-dihydropyrazinones **1.19** was prepared by a practical approach from dimethylacetamide Ugi adducts **1.17**. The dimethylacetamide Ugi adducts were formed from the reaction of *o*-haloarene/heteroarene **1.13**, aminoacetaldehyde dimethyl acetal **1.14**, the corresponding aldehydes **1.15** and isocyanides **1.16**. The protocol included a C–N bond formation between the primary amide and the transitory oxocarbenium ion formed under acidic conditions, and then the construction of the polycyclic system after an intramolecular C(sp^2)-C(sp^2) Heck reaction, under one pot conditions (Scheme 1.3). Structurally diverse poly aza-heterocycles were generated, screened for cytotoxicity, and found to show important activity against prostate, breast and lung cancer cell lines.

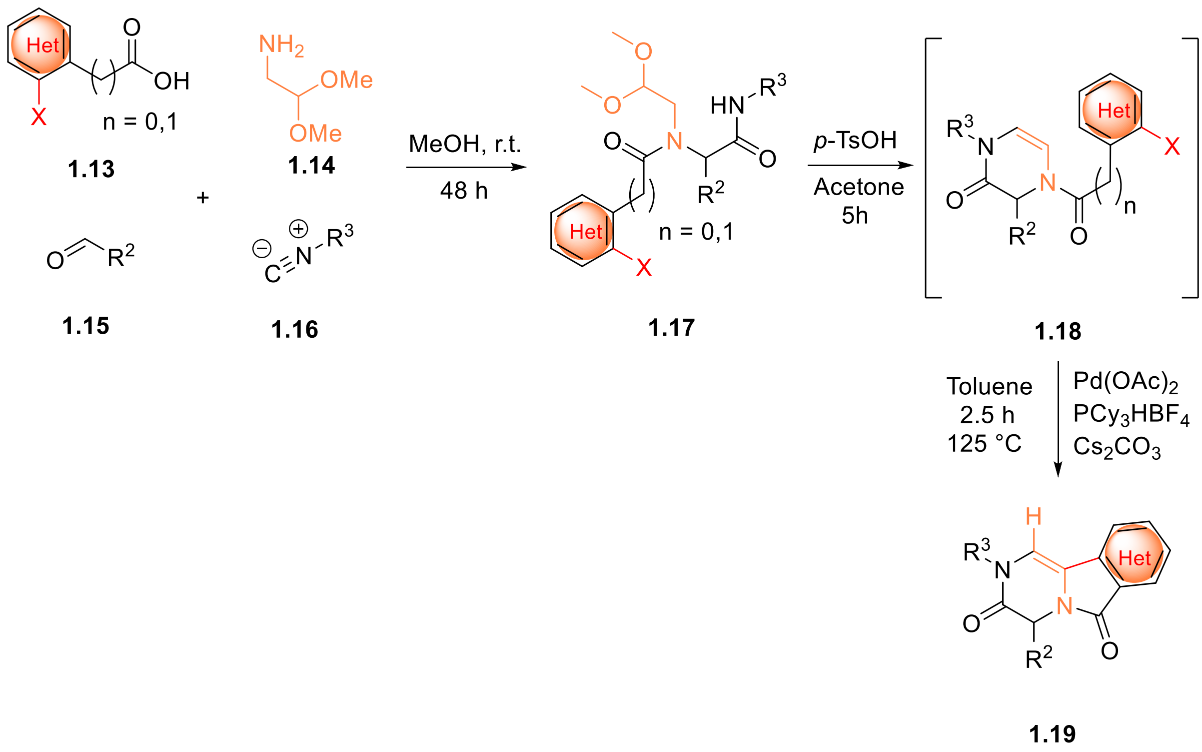

Scheme 1.3: Ugi 4CR/Deprotection/Heck sequence for the DOS of fused dihydropyrazinones

A highly efficient and chemoselective one-pot diversity-oriented synthesis of coumarin derivatives has been described by Yang et al.[31] Furo[3,2-c]coumarins **1.23** and 3-benzofuranyl chromenones **1.24** were prepared through an initial chemoselective acylation of functionalized phosphorus zwitterions **1.22** and a subsequent chemoselective intramolecular Wittig reaction. The functional zwitterions were prepared through a tandem three-component reaction of 4-hydroxycoumarin **1.20** and various 2-hydroxybenzaldehydes **1.21** (Scheme 1.4). Benzofuranyl coumarins are a class of heterocyclic scaffolds that are known to possess remarkable therapeutic activities, such as antibacterial, analgesic, and even anticancer properties.[32,33]

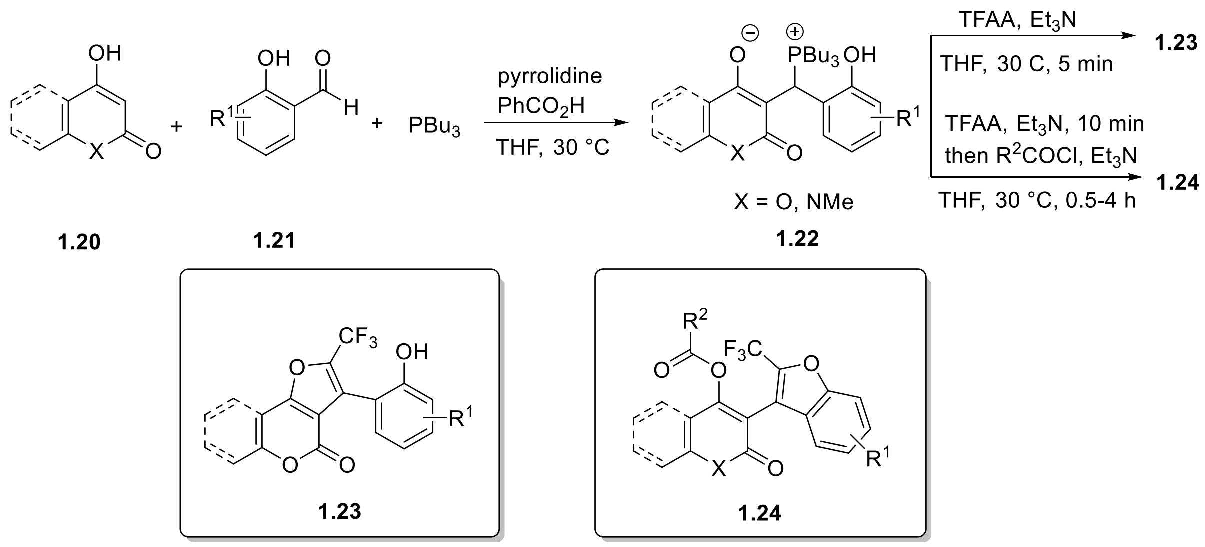

Scheme 1.4: Diversity-oriented synthesis of coumarin derivatives

A Mannich-type 4CR that involved combining aldehydes, amines, acid chlorides, and nucleophiles to provide access to highly functionalized amide products that could be further transformed by cyclizations involving ring-closing metathesis (RCM), Dieckmann and Heck reactions, and Diels-Alder and dipolar cycloadditions to give a diverse collection of heterocyclic scaffolds has been reported.[1,34] Methyl 2-formylbenzoate **1.25** was condensed with either allyl or propargyl amine to give intermediate imines that were treated sequentially with acetyl chloride and allylzinc bromide to furnish adduct **1.26** in a one-pot operation (Scheme 1.5). Compound **1.26a** was then converted into the benzazepine **1.27** via an RCM using Grubbs catalyst followed by a Dieckmann cyclization. In a related process, **1.26b** was transformed via an enyne RCM/cross metathesis cascade that was catalysed by the Hoveyda-Grubbs catalyst and in which styrene served as a fifth component to give an intermediate that was cyclized by a Dieckmann condensation to give **1.28**. These two examples illustrate how simply changing one of the inputs for the 4CR allows for differential processing of the initial adduct into targets of varying complexity. Importantly, the keto amide and alkene groups in **1.27** and **1.28** serve as potential initiation sites for further diversification.

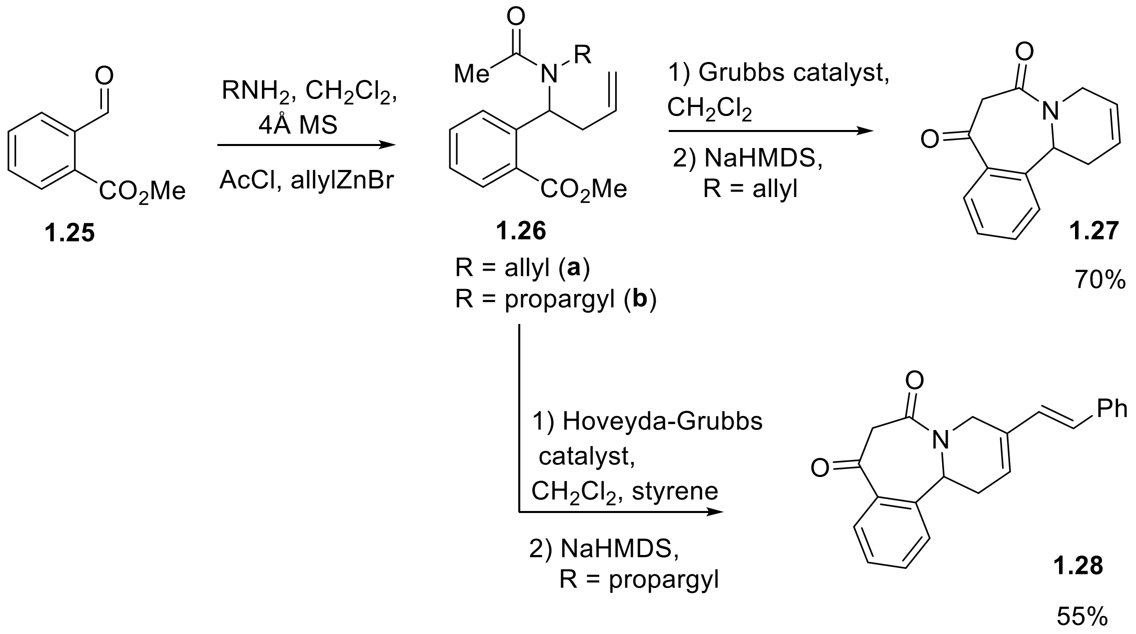

Scheme 1.5: Sequential Mannich-type 4CR/RCM/Dieckmann cyclization

Another multicomponent reaction that has been applied to combinatorial chemistry is the Biginelli condensation, which uses aldehydes **1.29**, β-ketoesters **1.30**, and ureas **1.31** to form pyrimidines **1.32**. This reaction has been performed with a fluorous tag attached to the urea, as in **1.33**, to facilitate purification of the condensation product (Scheme 1.6). The fluorous silyl group is removed with fluoride ion to give the benzoate.[29]

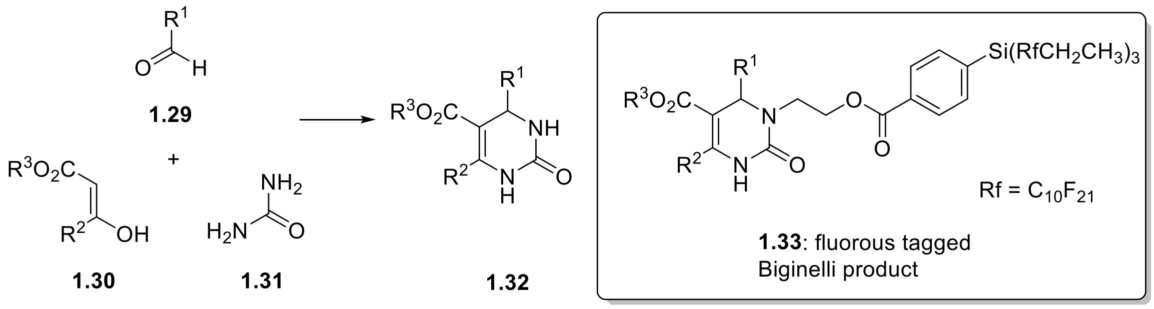

Scheme 1.6: Biginelli condensation

1.3 Tandem Reactions in Organic Synthesis

A tandem reaction comprises at least two consecutive reactions such that each subsequent reaction occurs only by virtue of the chemical functionality formed in the previous step. Although often composed solely of intramolecular transformations, tandem reactions can also occur intermolecularly, in which case they also fall under the category of multicomponent reactions.

Tandem reactions, also known as cascade reactions, domino reactions, or telescoped reactions[35-37] link several transformations together in a single process. Typically, an initial reaction produces an intermediate that undergoes further transformations with strategically positioned reactive centres in the same molecule, with other compounds in the reaction mixture, or with additional reagents introduced after the initial transformation takes place.[38] The advantages are that

- simple starting materials can be used to rapidly build complex structures with high selectivity in one process
- there are reduced operating costs and labour
- novel avenues of research and new reactions are developed
- the production is more sustainable whilst also avoiding the use and isolation of toxic and/or hazardous substances
- potential additional environmental benefits through reduced waste and processing (Figure 1.2)

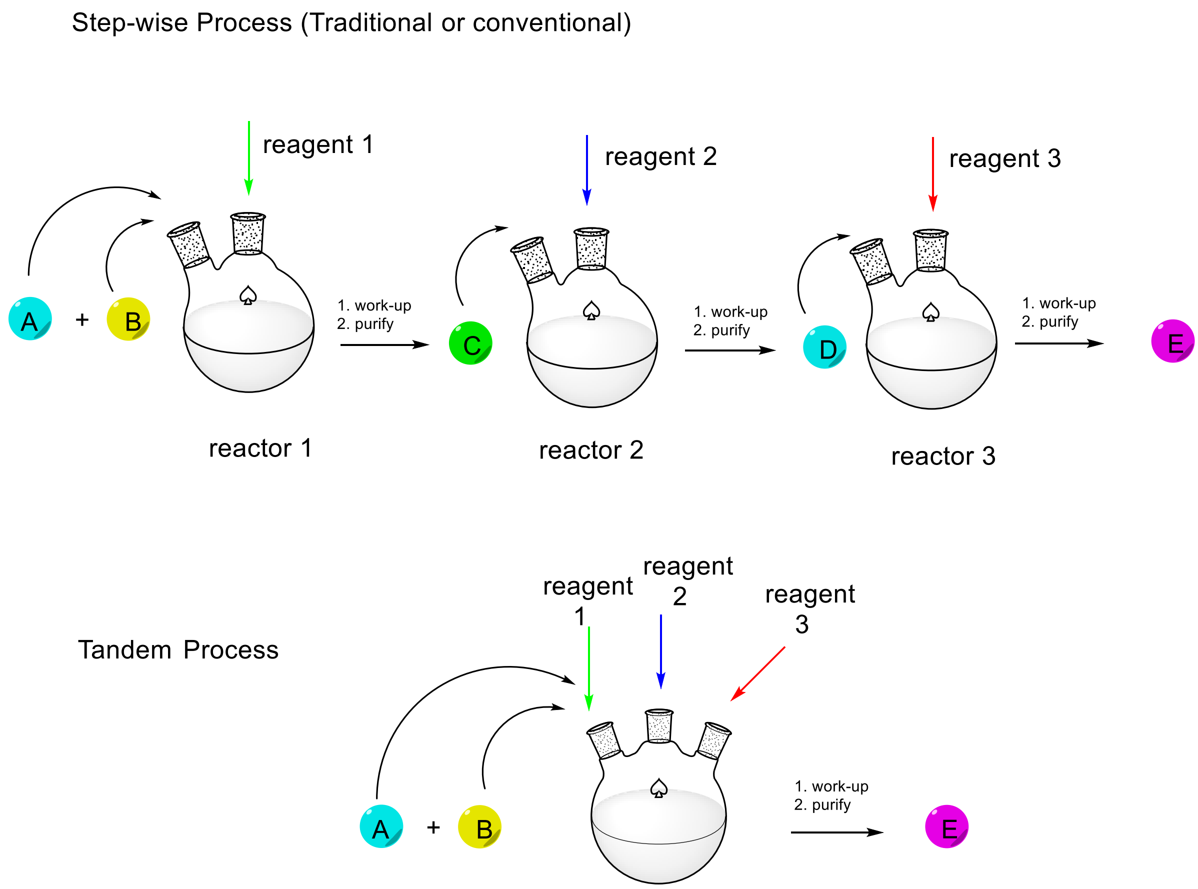

Figure 1.2: Stepwise and tandem processes

The usefulness of a tandem reaction is correlated firstly to the number of bonds which are formed in one sequence – the bond-forming efficiency, secondly, the increase in structural complexity, and, thirdly, to its suitability for a general application.[20]

The earliest example of a tandem reaction is arguably the synthesis of tropinone reported in 1917 by Robinson.[39] Schöpf and Robinson[39,40] put together a mixture of succindialdehyde **1.34**, methylamine **1.35**, and acetonedicarboxylic acid **1.36** to give eventually the bicyclic tropinone **1.37** which is a structural component of several alkaloids such as cocaine **1.38** and atropine **1.39** (Scheme 1.7).[41] The key step in this synthesis is a double Mannich reaction.

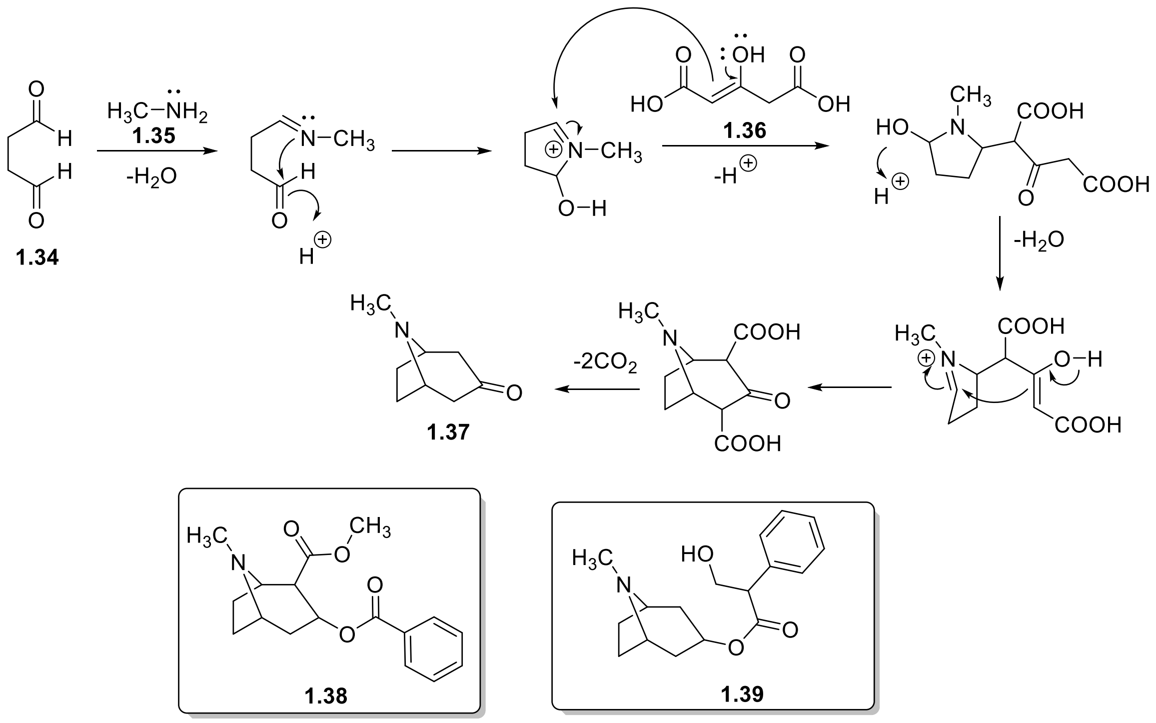

Scheme 1.7: Biomimetic tandem synthesis of tropinone **1.37**

Since then, the use of tandem reactions has proliferated in the area of total synthesis and is reflected by the relevant review articles published over the past couple of decades.[20,39,41-47]

1.3.1 Tandem Nucleophilic Reactions

Tandem nucleophilic reactions are defined as a reaction sequence in which the key step constitutes a nucleophilic attack. An example of such a reaction is seen in the synthesis of the broad-spectrum antibiotic (–)-chloramphenicol, reported by Rao et al (Scheme 1.8). The chiral epoxy-alcohol **1.40** was first treated with dichloroacetonitrile in the presence of NaH. The resulting intermediate **1.41** then underwent a $BF_3 \cdot Et_2O$-mediated tandem reaction – intramolecular opening of the epoxide ring – yielding intermediate **1.42**, which, after an *in situ* hydrolysis facilitated by excess $BF_3 \cdot Et_2O$, afforded (–)-chloramphenicol **1.43** in 71% yield.[43,48]

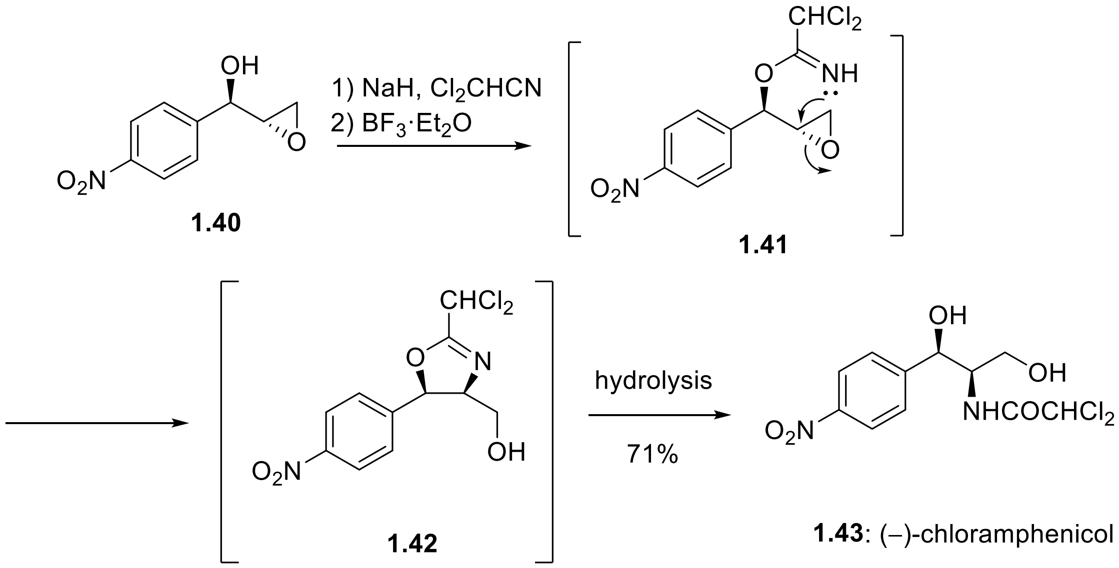

Scheme 1.8: Synthesis of (–)-chloramphenicol via a nucleophilic sequence

A subcategory of tandem nucleophilic reactions is organocatalytic sequences, in which the key nucleophilic attack is driven by organocatalysis.

Sorensen and co-workers[49] reported an organocatalytic sequence in the total synthesis of the natural product (+)-harziphilone, **1.50**, a naturally occurring inhibitor of the binding interaction between HIV-1 Rev protein and the Rev-responsive element (RRE) of viral mRNA (Scheme 1.9).[44] The starting material enone **1.44**, when treated with 1,4-diazabicyclo[2.2.2]octane (DABCO) **1.45**, yielded intermediate **1.46** via conjugate addition. Subsequent cyclization by the intramolecular Michael addition of the enolate into the triple bond of the system gave species **1.47**, which afforded intermediate **1.48** after proton transfer and tautomerization. The reaction was completed by elimination of the organocatalyst, DABCO, and a spontaneous 6π-electrocyclic ring closure of the resultant *cis*-dienone **1.49** to give (+)-harziphilone **1.50** in 70% overall yield.[44,49]

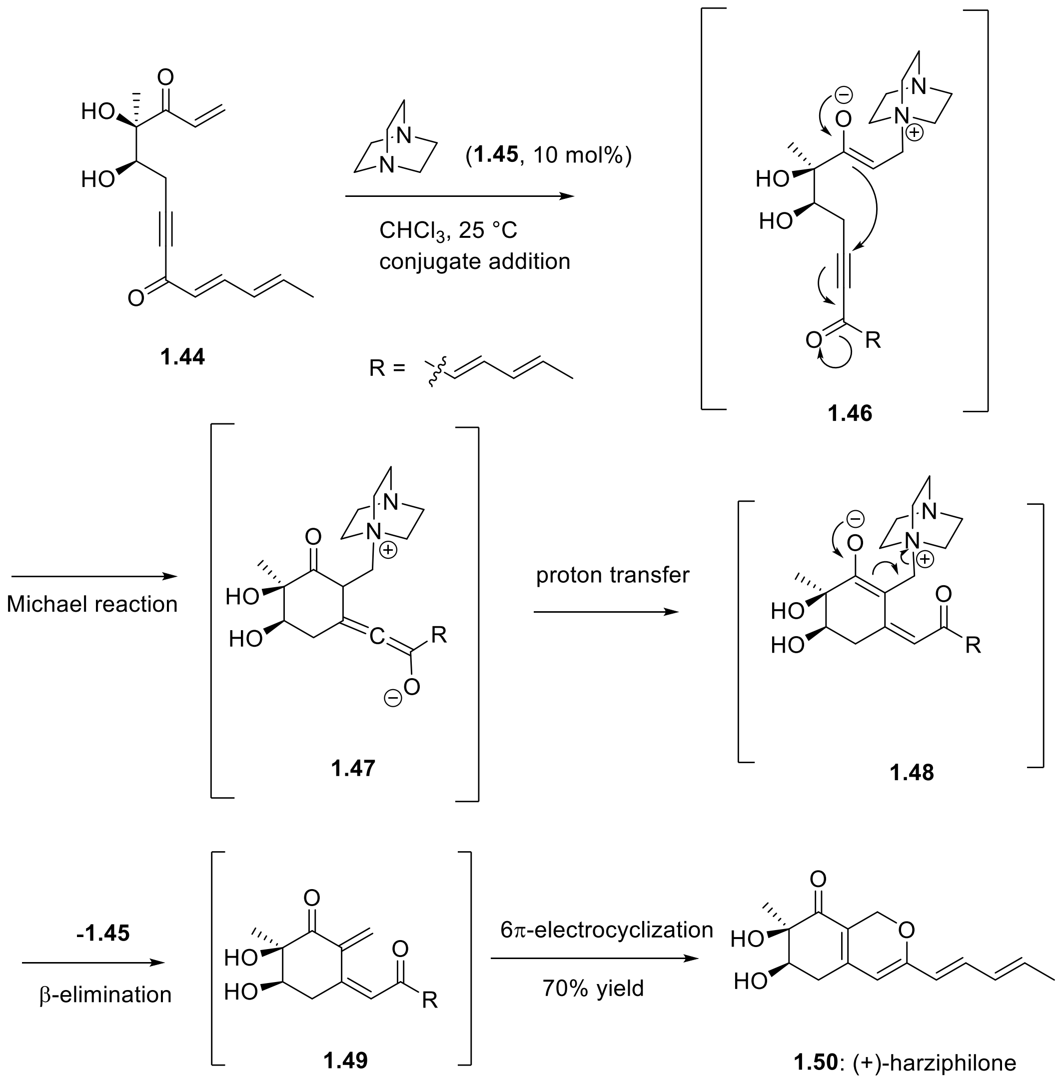

Scheme 1.9: Organocatalytic cascade in the total synthesis of (+)-harziphilone **1.50**

1.3.2 Tandem Electrophilic Reactions

A biomimetic electrophilic cascade[50-52] was employed by Holton and co-workers in their total synthesis of hemibrevetoxin B, a marine polycyclic ether with potent biological activities such as neurotoxicity, cytotoxicity, and antiviral and antifungal activities (**1.55,** Scheme 1.10).[53] The substrate epoxy alkene **1.51** was treated with *N*-phenylselenophthalimide **1.52** and led to sequential ring closure to give the advanced intermediate **1.53** as a single stereoisomer due to the S_N2-type reactions involved. The highly polar but non-nucleophilic solvent 1,1,1,3,3,3-hexafluoro-2-propanol (HFIP) was chosen for its ability to stabilize such charged species without interfering in the progress of the reaction. Fusion of the oxepane ring onto intermediate **1.53** followed by the appropriate side-chain manipulations then completed the total synthesis.[54,55]

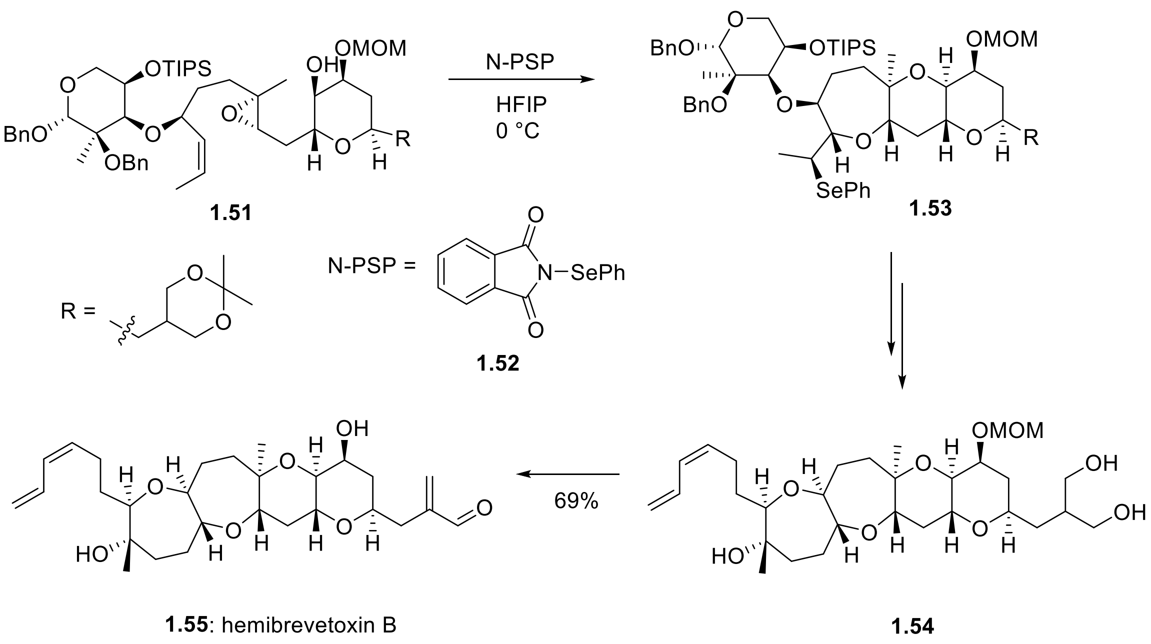

Scheme 1.10: Total Synthesis of hemibrevetoxin B using an epoxy-olefin cyclization

1.3.3 Tandem Radical-mediated Reactions

Radical cascades are those in which the key step constitutes a radical reaction. The high reactivity of free radical species renders radical-based synthetic approaches desirable for cascade reactions.[44] A wide variety of radical cascades have been designed and executed.[56,57] The potential of these reactions is very high due to the mild conditions under which radicals may be generated. These gentle reaction conditions tolerate a wide range of functionality in the substrates; thus, complex synthetic targets can be prepared with minimal use of protecting groups. An additional advantage to the use of radicals is that they add to unactivated double and triple bonds as well as to those bearing polarizing groups.

One of the most widely recognized examples of the synthetic utility of radical cascades is the cyclization sequence employed in the total synthesis of (±)-hirsutene **1.60**, which is known to possess remarkable biological properties (Scheme 1.11).[44,58] Herein, alkyl iodide **1.56** was converted to the primary radical intermediate **1.57**, which underwent a 5-exo-dig radical cyclization to afford reactive species **1.58**. A subsequent 5-exo-dig radical cyclization led to intermediate **1.59**, which upon quenching gave the target (±)-hirsutene **1.60** in 80% overall yield.[44,58]

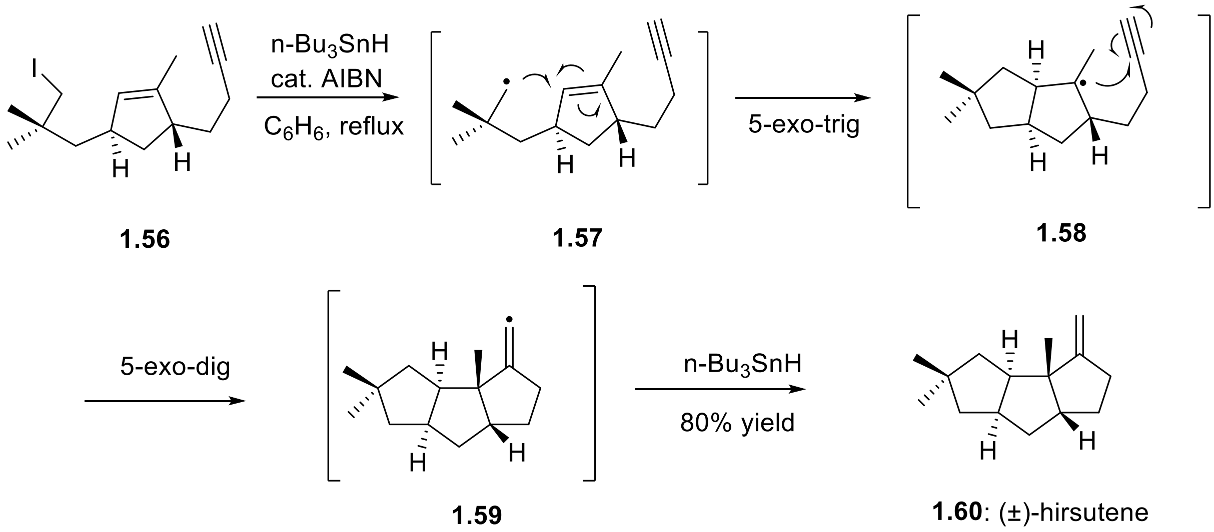

Scheme 1.11: Cascade radical cyclization in the total synthesis of (±)-hirsutene **1.60**

In their synthesis of (–)-morphine **1.66** (Scheme 1.12), Parker and Fokas used a cascade radical process to form two rings and install the all-carbon quaternary stereocentre in a single step. Treatment of bromide **1.61** with tri-n-butyltin hydride and 2,2'-azobis(2-methylpropionitrile), AIBN in dry benzene heated in a degassed sealed tube at 120-130 °C gave tetracyclic product **1.65** in moderate yield.[59,60] The reaction proceeds by the initial generation of aryl radical **1.62**, which cyclizes onto the tethered cyclohexene to form the dihydrobenzofuran system and the quaternary center in **1.63**. The approach of the aryl radical to the lower face of the alkene (as drawn in **1.62**) is governed by the stereochemistry of the ether linkage. Secondary radical **1.63** then cyclizes in a 6-*endo*-trig fashion to generate benzylic radical **1.64**. The geometric constraints imposed by the tricyclic framework of **1.63** discourage the alternative, and otherwise generally kinetically favoured, 5-exo-trig mode of cyclization. Finally, elimination of phenylsulfinyl radical forms the olefin required for the completion of this formal total synthesis of morphine, one of the most widely used drugs for the treatment of severe pain.[61,62]

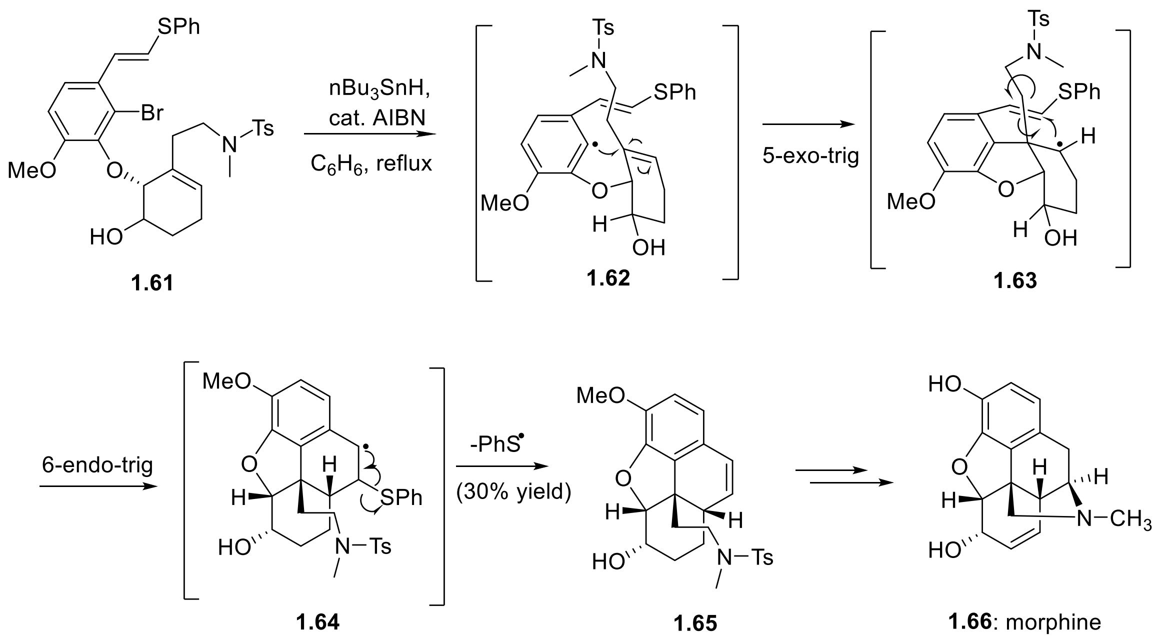

Scheme 1.12: Tandem radical cyclization in the synthesis of (–)-morphine **1.66**

1.3.4 Tandem Pericyclic Reactions

Pericyclic reactions are perhaps the most widely encountered kind of process in cascade transformations. They include cycloadditions, sigmatropic rearrangements and electrocyclic reactions, all of which have been employed in cascades en route to natural product targets.[44] However, by combining two or more pericyclic reactions the effect can be multiplied. There are considerable advances in the use of pericyclic processes to start inter and intramolecular sequences. In particular, tandem sequences involving asymmetric cycloaddition reactions are highly effective processes for the rapid elaboration of complex polycyclic systems, since each cycloaddition event generates a new ring and two new covalent bonds.[63] In this set of reactions, there are sequences often including a Diels-Alder reaction in the first step.[43]

A representative example of a pericyclic cascade is the endiandric acid cascade reported by Nicolaou et al. (Scheme 1.13).[44,64] Herein the highly unsaturated system **1.67** first underwent selective hydrogenation of the alkynes to give the conjugated tetraene species **1.68**, which upon heating underwent an 8π-conrotatory electrocyclic ring closure, yielding cyclic intermediate **1.69**. A second spontaneous electrocyclization, a 6π-disrotatory ring closure, converted **1.69** to the bicyclic species **1.70**, the geometry of which favoured a subsequent intramolecular Diels-Alder reaction. The methyl ester of endiandric acid B **1.71,** having antibacterial activity, was thus obtained in 23% overall yield.

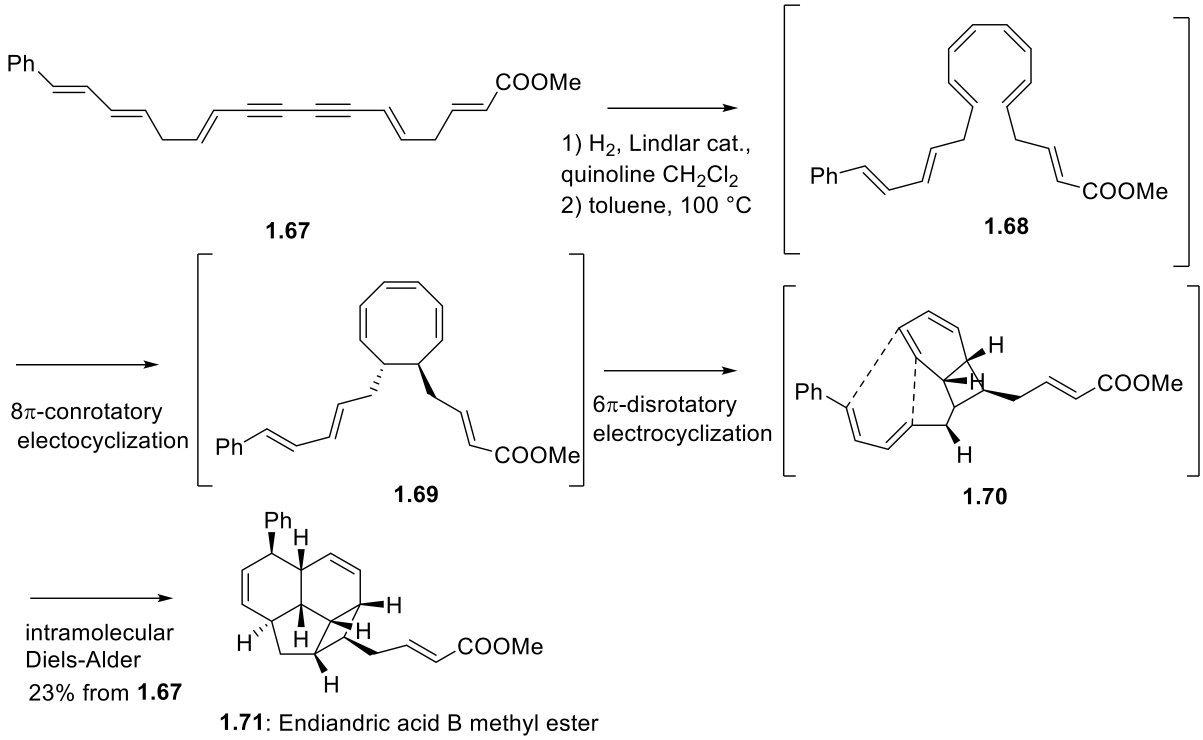

Scheme 1.13: Pericyclic cascade in the synthesis of endiandric acid derivatives

1.3.5 Transition Metal-catalysed Reactions

Transition metal-catalysed cascades combine the novelty and power of organometallic chemistry with the synthetic utility and economy of cascade reactions, providing a more ecologically friendly and economical approach to organic synthesis.[44]

The Heck reaction is an important way to couple aryl and vinyl systems in the presence of palladium, and it forms the keystone to many tandem processes.[65-69] Pursuant to a strategy for the synthesis of illudin M **1.76**, a compound with antitumor antibiotic properties, a Heck vinylation /Diels-Alder reaction has been investigated as a route to fused-ring bicyclic systems. Heck cyclization of 2-bromo-1,6-diene **1.72** afforded the bis(exomethylene)cyclopentane **1.73** which, in the presence of methyl-2-chloro-2-cyclopropylideneacetate **1.74**, afforded an 83% yield of bicyclic spirane **1.75**. The reaction proceeded best when the entire transformation was carried out without isolation of the intermediate diene **1.73** (Scheme 1.14).[38]

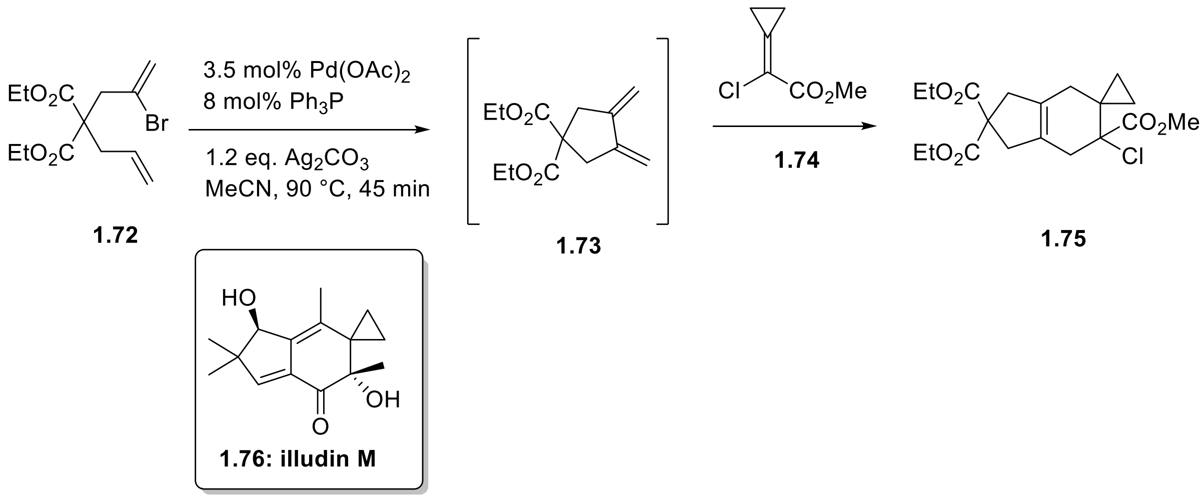

Scheme 1.14: Heck vinylation cascade route to the synthesis of bicyclic spirane **1.75**

1.3.6 Tandem Photochemical Reactions

The advantage of using light to drive reactions lies in the fact that it is an environmentally safe "reagent" that tolerates many functional groups. Since photochemical reactions usually proceed from an excited electronic state, reactions often produce unique products that are not available from ground state reactants. On the other hand, photochemical reactions do not always meet the selectivity requirements needed for organic synthesis, and the chromophores required for light absorption generally leave unwanted functionality in the product.[38]

A photochemical process to receive attention in tandem organic synthesis was a novel sequential cycloaddition / iminium ion formation / propargylsilane cyclization to generate quinolizidines and pyrido[1,2-a]azepines.[70] As an example, enamino aldehyde **1.77** was irradiated in the presence of 50 equivalents of *tert*-butyl acrylate **1.78** to afford 2-hydroxytetrahydropyridine **1.79**. Cyclization with TMSOTf then gave the quinolizidine **1.80** in 73% overall yield as a 35.5:1 mixture of α:β epimers at C(9a). In a formal sense, product **1.79** could arise from an initial [2+2] reaction to the imino enol form of **1.77** followed by a ring expansion (Scheme 1.15).

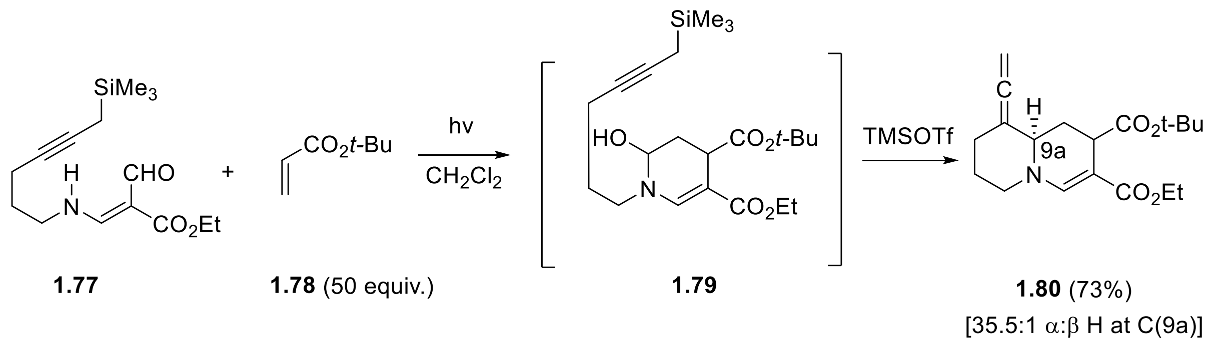

Scheme 1.15: Photochemically induced tandem reaction

1.3.7 Tandem Carbene Reactions

Electrophilic carbenes and carbenoids formed in the vicinity of heteroatom-containing functional groups (especially ethers, amines, and carbonyls) react to form ylides capable of undergoing further transformations. Processes initiated by heteroatom addition to a carbene centre include [2,3]-sigmatropic rearrangements,[71-73] Stevens [1,2]-alkyl shifts,[74-79] and 1,3-dipolar cycloaddition of carbonyl ylides.[80-84]

Two syntheses based on [2,3]-sigmatropic rearrangement of carbene-derived ylides have been reported. Pirrung and co-workers[71] have utilized a carbene-based tandem reaction in an enantioselective synthesis of (+)-griseofulvin **1.85**. Griseofulvin is a classical antifungal agent still used in the treatment of a number of types of dermatophytosis (ringworm).[85] The diazoketoester **1.82** was prepared from 3,5-dimethoxyphenol **1.81** in six steps with an overall yield of 32%. Decomposition of **1.82** in the presence of $Rh_2(OPiv)_4$ produced oxonium ylide **1.83**, which underwent a [2,3]-sigmatropic rearrangement to afford a 62% yield of **1.84** as a single stereoisomer. A six-step sequence converted **1.84** to the natural product in 26% overall yield (Scheme 1.16).

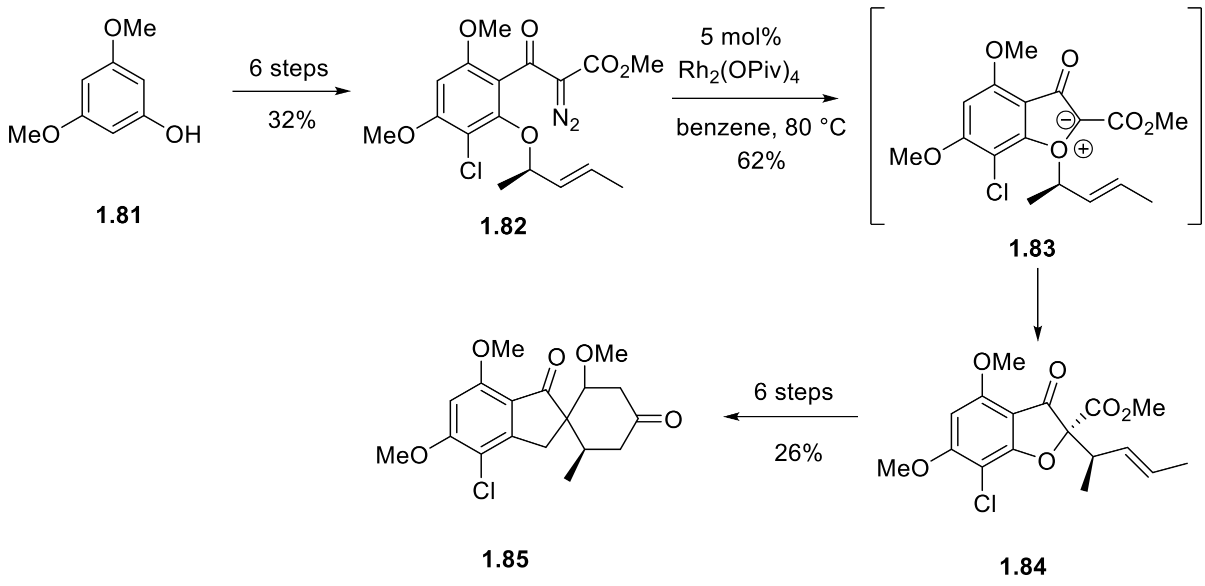

Scheme 1.16: Tandem carbene reactions

1.4 Quinones

To explain the chemistry of azaquinone which is what this project is about, it is worth considering the chemistry of 1,4-benzoquinone since it is similar in structure to azaquinone.

Quinones are a group of cyclic, conjugated diketone compounds that are widely distributed in nature, and are used in the dye industry because they are mostly coloured substances e.g. alizarin **1.86** and purpurin **1.87** (Fig. 1.3). Quinone molecules are well known as electron acceptors and emit virtually no light in the visible region. The introduction of donors and/or acceptors into the quinone nucleus produces visible absorption with intramolecular charge-transfer character.[86] Quinones have also been used as analytic reagents, polymer modifiers, photoresistors, and catalysts.[87]

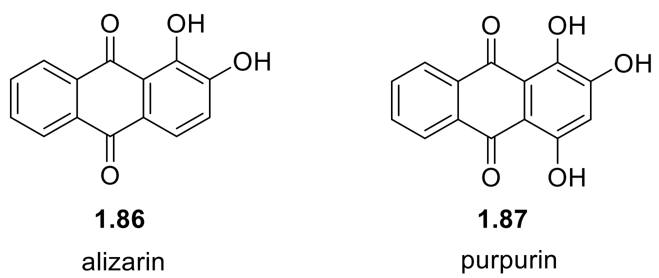

Figure 1.3: Some useful quinone compounds

The quinone of interest is 1,4-benzoquinone, because it is closest in structure to *N*-phenylquinonimine (azaquinone). The addition of nucleophiles to 1,4-benzoquinone is shown in Scheme 1.17.[87] A large proportion of the quinone chemistry involves 1,4-addition to the α,β-unsaturated system for which a large range of nucleophiles can be used.

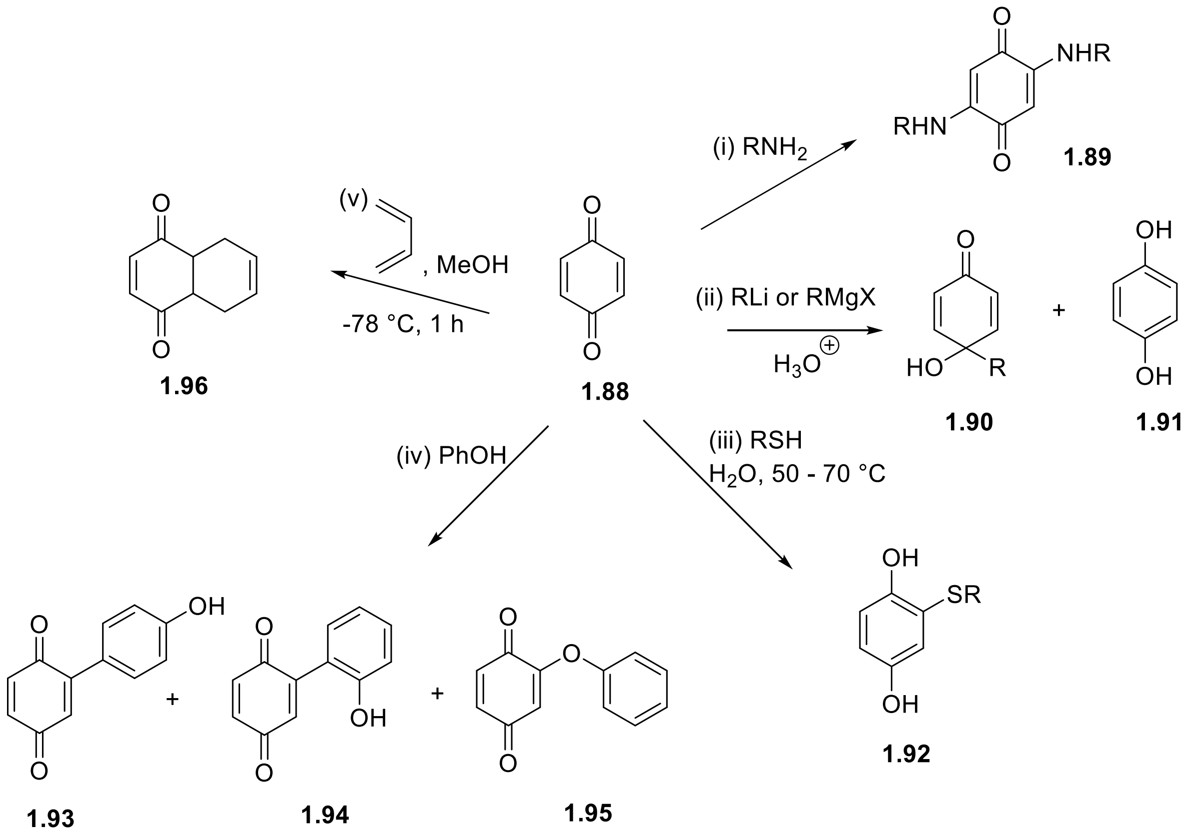

Scheme 1.17: Nucleophilic addition reactions of Quinone

(i) nitrogen nucleophiles (ii) 1,2-addition (iii) sulfur nucleophiles (iv) oxygen nucleophiles (v) cycloadditions

1.5 Azaquinones

Azaquinones are highly coloured compounds[88-92] and constitute a core structure in several important natural products (Fig. 1.4),[93,94] some of which are key abiotic and biological compounds, which intercalate with DNA.[95] New avenues for molecular sensors[96] and ligands,[97,98] for drug delivery,[99,100] and controlled material growth have been provided through many of these hybrid materials.[101] Azaquinones can also be used as building blocks to other useful synthetic compounds, and therefore represent a new frontier for the design and generation of molecular complexity.[101]

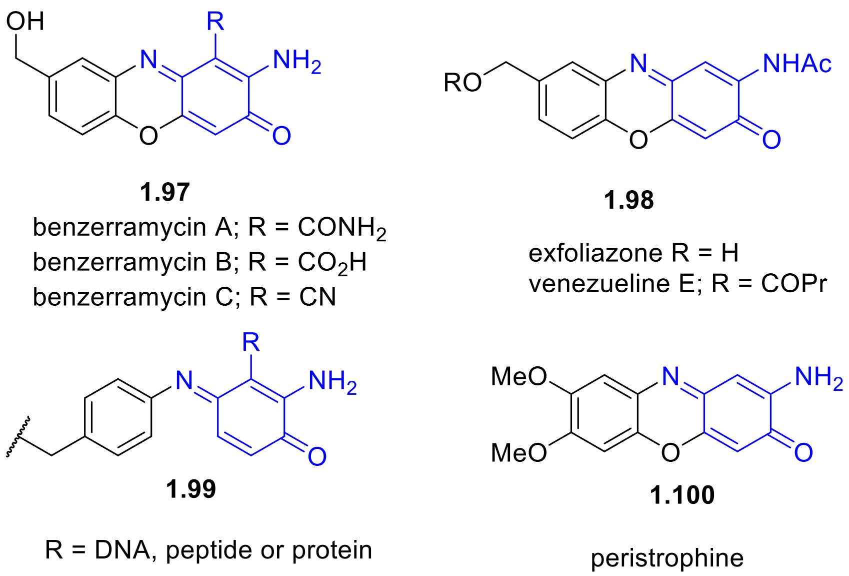

Figure 1.4: Some azaquinone containing natural products[101]

1.5.1 Chemistry of Azaquinone

Azaquinone can react with nucleophiles by 1,2-addition or 1,4-addition. Azaquinone has two unique sites susceptible to 1,2-addition – the ketone and the imine. If the nucleophile is an amine, for example RNH_2, attack at the carbonyl carbon followed by reduction gives 1,4-diaminoarenes **1.102**, whilst attack at the imino carbon converts the *N*-phenyl group to a new group **1.103** (Scheme 1.18).

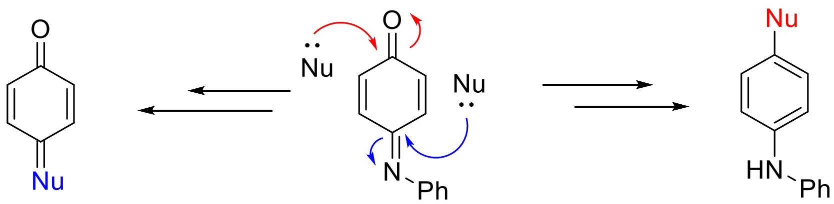

1.103 **1.101** **1.102**

Scheme 1.18: Nucleophilic attack by 1,2-addition to the ketone or the imine

As stated above, there are two possible α,β-unsaturated systems in azaquinone chemistry: α,β-keto and α,β-imino. All the four β-carbons are unique and have different reactivity. Scheme 1.19 shows the products of attack of a nucleophile at all four sites susceptible to 1,4-addition. By quenching the enolate with an electrophile other than $H^{\oplus}$, it may be possible to selectively add two substituents to the ring in a single reaction. The stereochemistry of the *N*-arylamine also introduces asymmetry. Nucleophilic addition to the α,β-ketone system generates products **1.104** and **1.105**, whilst addition to the α,β-imine generates products **1.106** and **1.107.**

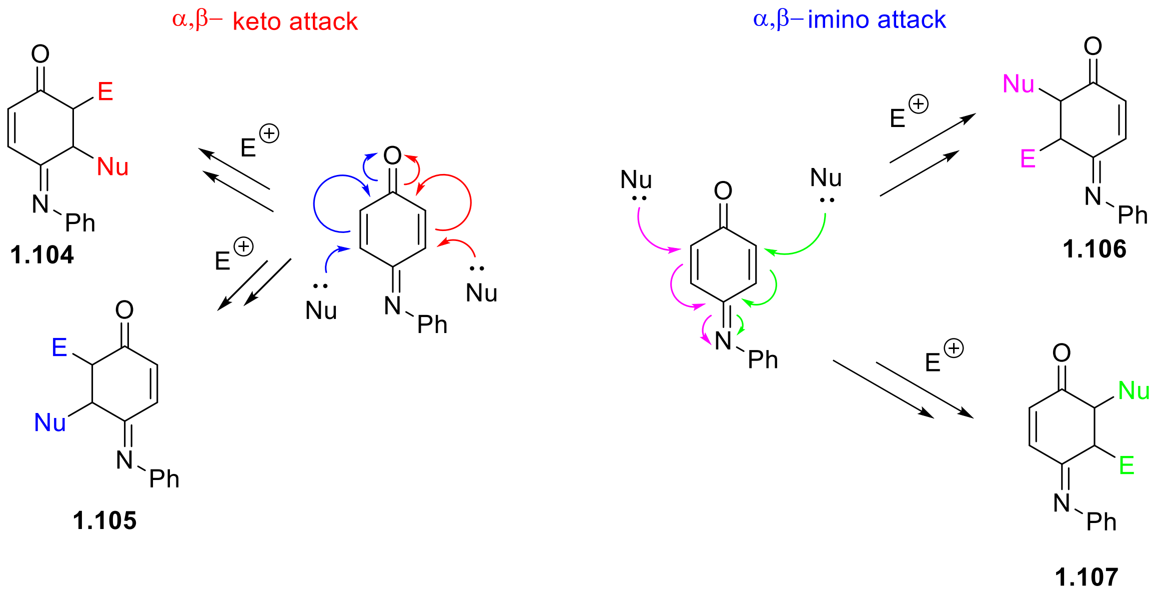

Scheme 1.19: Nucleophilic attack by 1,4-conjugate addition

1.5.2 Conjugate Addition

One of the largest and most diverse classes of reactions is composed of nucleophilic additions to a carbonyl group. Conjugation of a double bond to a carbonyl group transmits the electrophilic character of the carbonyl carbon to the β-carbon of the double bond. These conjugated carbonyl groups are called enones or α,β-unsaturated carbonyl groups. A resonance description of this transmission is shown in Scheme 1.20.[102] As a result, nucleophiles may attack either at the carbonyl carbon or at the β-carbon. These two modes of reaction are referred to as 1,2-addition and 1,4-addition respectively. A 1,4-addition is also called a Conjugate Addition or Michael Addition.

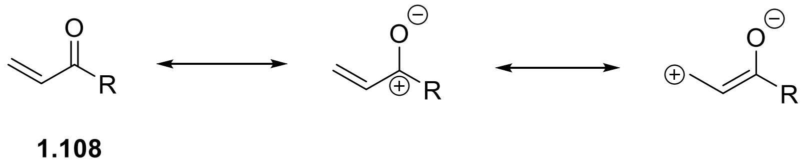

Scheme 1.20: Resonance structures of conjugated carbonyl groups

Nucleophilic conjugate addition is therefore a type of organic reaction in which a nucleophile reacts with an α,β-unsaturated carbonyl compound in the β-position. The negative charge carried by the nucleophile is delocalized in the alkoxide anion and the α-carbon carbanion by resonance. Protonation leads, through keto-enol tautomerism, to the saturated carbonyl compound (Scheme 1.21).

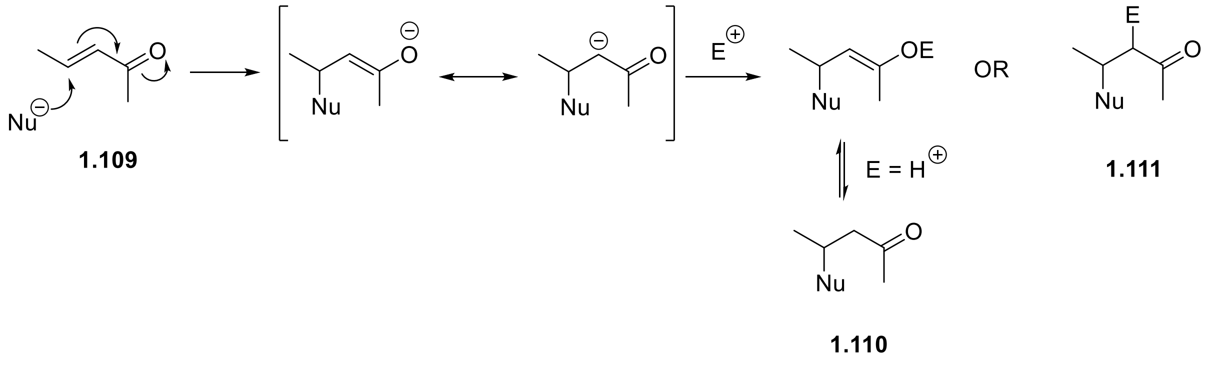

Scheme 1.21: Mechanism of conjugate addition

Nucleophiles that undergo conjugate addition with α,β-unsaturated carbonyl compounds include water, alcohols, thiols, primary and secondary amines, bromide, chloride and cyanide. The actual bond-forming step in the reaction must involve movement of electrons from the HOMO of the nucleophile to the LUMO of the unsaturated carbonyl compound (electrophile) (Scheme 1.22).[103]

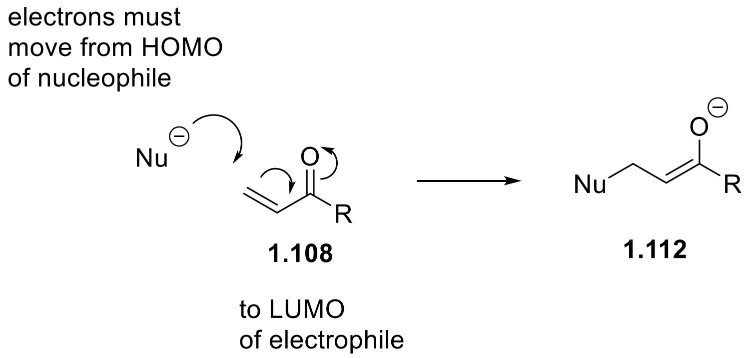

Scheme 1.22: Mechanism for 1,4-conjugate addition

Conjugate addition is effective in the formation of new carbon-carbon bonds with the aid of organometallic reagents such as the reaction of an organozinc iodide with methylvinylketone, **1.114** (Scheme 1.23).[104]

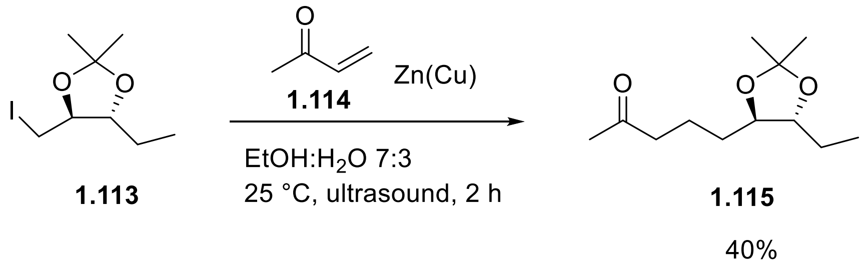

Scheme 1.23: Organozinc iodide reaction with methylvinylketone **1.114**

The way that nucleophiles react (either by conjugate addition or 1,2 addition) depends on

- The type of nucleophile
- The reaction conditions
- The nature of the α,β-unsaturated carbonyl compound

Hard nucleophiles are typically from the early rows of the periodic table and have higher charge density and tend to favour 1,2-addition, whereas soft nucleophiles tend to be from the later rows of the periodic table. They are either uncharged or have larger atoms with a more diffuse orbitals and tend to favour 1,4-addition.

Table 1.1: Hard and Soft Nucleophiles

Hard Nucleophiles	**Intermediate**	**Soft Nucleophiles**
F^-, HO^-, RO^-, Cl^-	N_3^-, ^-CN	I^-, RS^-, RSe^-
H_2O, ROH, R^1COR^2	RNH_2, R^1R^2NH	RSH, R_3P
NH_3, RMgBr, RLi	Br^-	Alkenes, aromatic rings

Treating an enone, **1.114** with cyanide and an acid catalyst at low temperature gives a cyanohydrin, **1.116** by direct attack at C=O, whilst heating the reaction mixture leads to conjugate addition product, **1.117** (Scheme 1.24).[103]

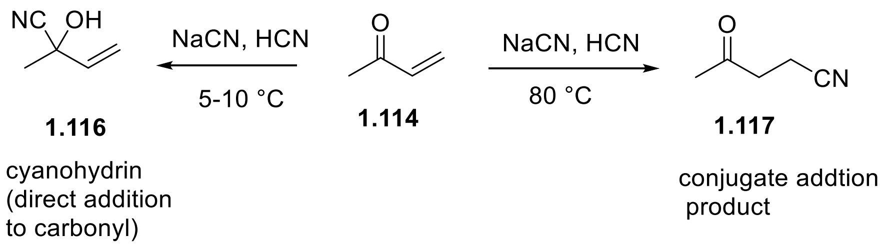

Scheme 1.24: Reactions of methylvinylketone with cyanide

The contrast between the two products is that the cyanohydrin is formed faster than the conjugate addition product, but the conjugate addition product is the more stable compound hence the thermodynamic conditions giving the conjugate addition product.

Typically, kinetic control involves lower temperatures and shorter reaction times, which ensures that only the fastest reaction has the chance to occur. And, typically, thermodynamic control involves higher temperatures and long reaction times to ensure that even the slower reactions have a chance to occur, and all the material is converted to the most stable compound (Scheme 1.25).[103]

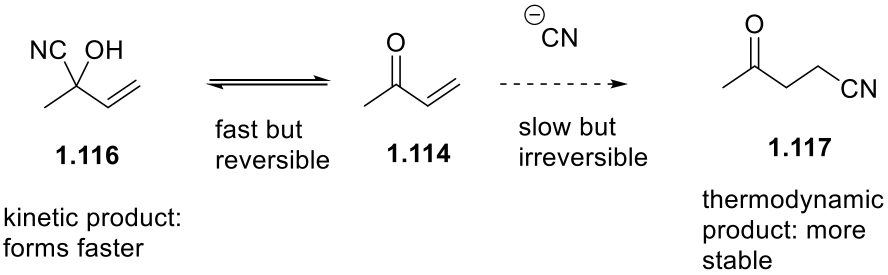

Scheme 1.25: Thermodynamic control versus Kinetic control

The site of nucleophilic attack is determined by reactivity: the more reactive the carbonyl group, the more direct addition to C=O will result. The most reactive carbonyl groups are those that are not conjugated with additional heteroatoms such as O or N (as they are in esters and amides), particularly reactive are acyl chlorides and aldehydes and ketones. For esters and other less reactive carbonyl compounds, conjugate addition is the only reaction that occurs.[103]

Steric hindrance also has a role to play: the more substituents there are at the β carbon, the less likely a nucleophile is to attack there, with preference therefore being 1,2-addition irrespective of the nucleophile.

1.5.3 Reactions of Azaquinone

The reactions of azaquinone, **1.101** reported in the literature are minimal with very limited examples; the scope and application remain to be established as does the regiochemistry of the transformations. Given the regiochemical possibilities of products resulting from nucleophilic addition, modern analytical techniques would be useful in confirming the structure of the products, which is critical if azaquinone is to be used as a versatile intermediate in tandem reactions. Scheme 1.26[5-7,105,106] shows some of these examples.

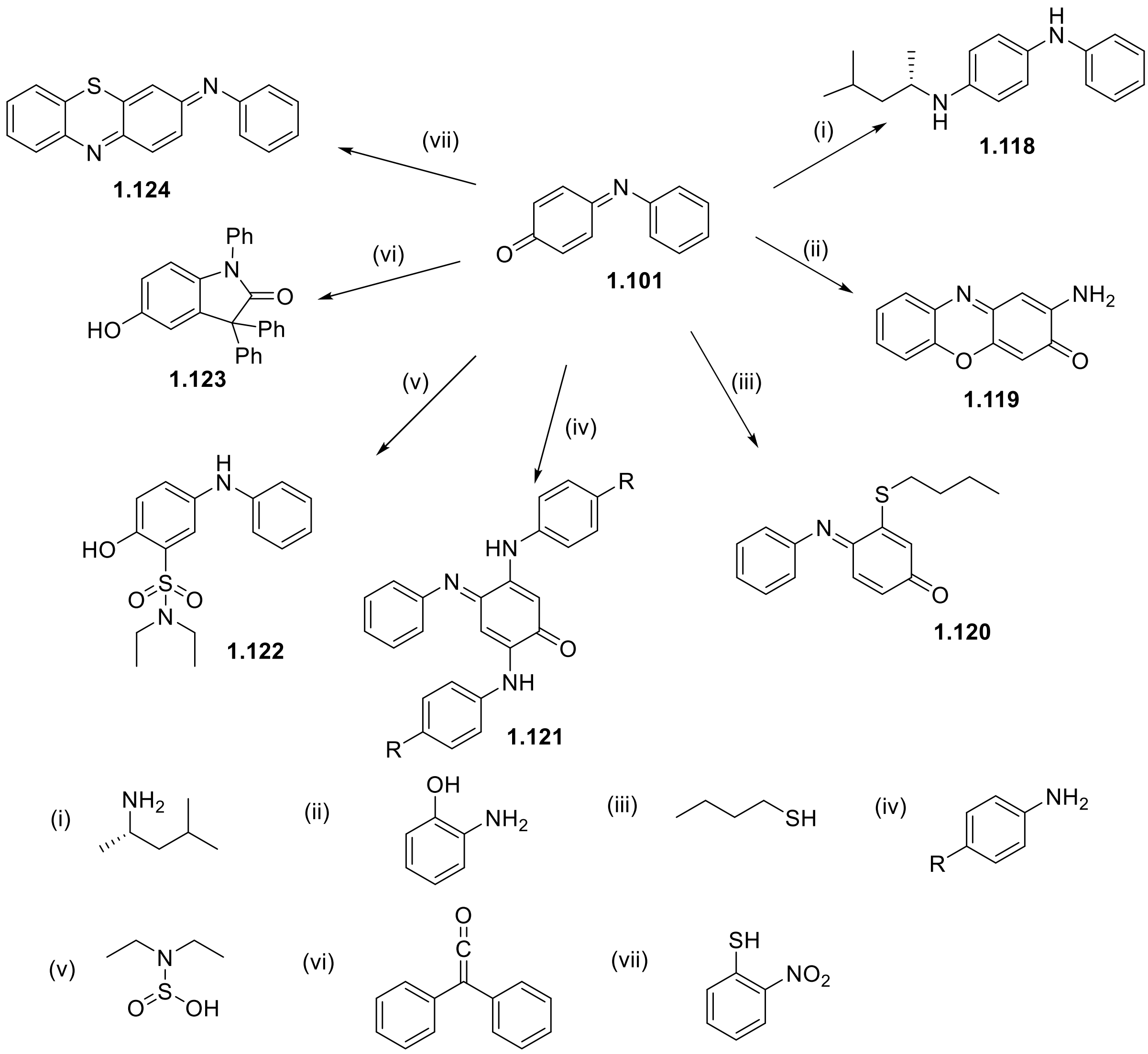

Scheme 1.26: Azaquinone reactions

1.6 The Chemistry of Hypervalent Iodine

In this project, azaquinone was initiated from arylation using diaryliodonium salts, making it important to understand the chemistry of hypervalent iodine. Iodine is commonly found in organoiodine compounds in the monovalent form with an oxidation state of -1. It generally forms weak bonds with carbon, with a bond dissociation energy of about 57 kcal/mol for a typical C–I bond[107] and plays an important role in organic reactions and synthesis. However, because it is a large, polarizable, electropositive and abundant group 17 element, it also forms stable polycoordinate, multivalent compounds.[108]

The first polyvalent organic iodine complex, $PhICl_2$, was prepared by German chemist C. Willgerodt in 1886. Although its oxidizing properties were known since 1893, a renaissance in the field of polyvalent iodine has occurred only in the past 20 years.[109,110]

The chemical properties and reactivity of hypervalent iodine is similar to the heavy metal reagents such as Hg(III), Tl(III), and Pb(IV) but without the toxicity and environmental issues. Reaction conditions are mild and there is commercial availability of key precursors such as $PhI(OAc)_2$.

Hypervalent compounds have a non-standard number of bonds. Therefore, they are given a λ-notation according to IUPAC nomenclature. Iodine compounds with three or five ligands are hence denoted as λ^3- and λ^5 -iodanes respectively. A λ^3-iodane forms a trigonal bipyramidal structure with its 10 valence electrons whereas a λ^5-compound has 12 valence electrons and adopts a distorted octahedral structure (Fig. 1.5).[111]

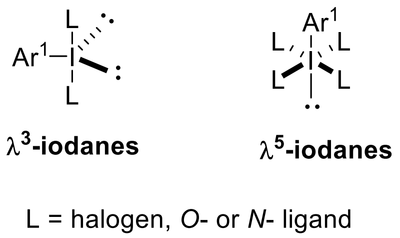

Figure 1.5: General structural types of hypervalent iodine compounds

1.6.1 Classes of Hypervalent Iodine

Hypervalent iodine chemistry is based on the strongly electrophilic nature of the iodine making it susceptible to nucleophilic attack, in combination with the leaving group ability of the phenyliodonio group – I(X)Ph (~10^6 times greater than triflate!!!).[108] The favourable reduction of the hypervalent iodide to normal valency by reductive elimination of iodobenzene is the key to its reactivity.

Iodine(V) reagents such as DMP, 2-iodoxybenzoic acid (Fig. 1.6) and their analogues[112,113] are frequently used as mild reagents for the oxidation of alcohols to the corresponding carbonyl compounds e.g. in the total synthesis of natural products.[114-116]

Iodine(III) compounds with two heteroatom ligands, such as $PhI(OAc)_2$, are also frequently employed in the oxidation of alcohols to carbonyl compounds, difunctionalization of alkenes, synthesis of quinones, in rearrangements and also in α-functionalization of carbonyl compounds.[117]

Iodine(III) compounds in which the iodine bears two carbon ligands can undergo reactions whereby they transfer one of the ligands to a range of nucleophiles. They can be used to oxidize metals to unusual oxidation states e.g. Pd(II→IV).[118] Moreover, they can also be used in sequential cyclizations for the synthesis of several important heterocyclic compounds.[119]

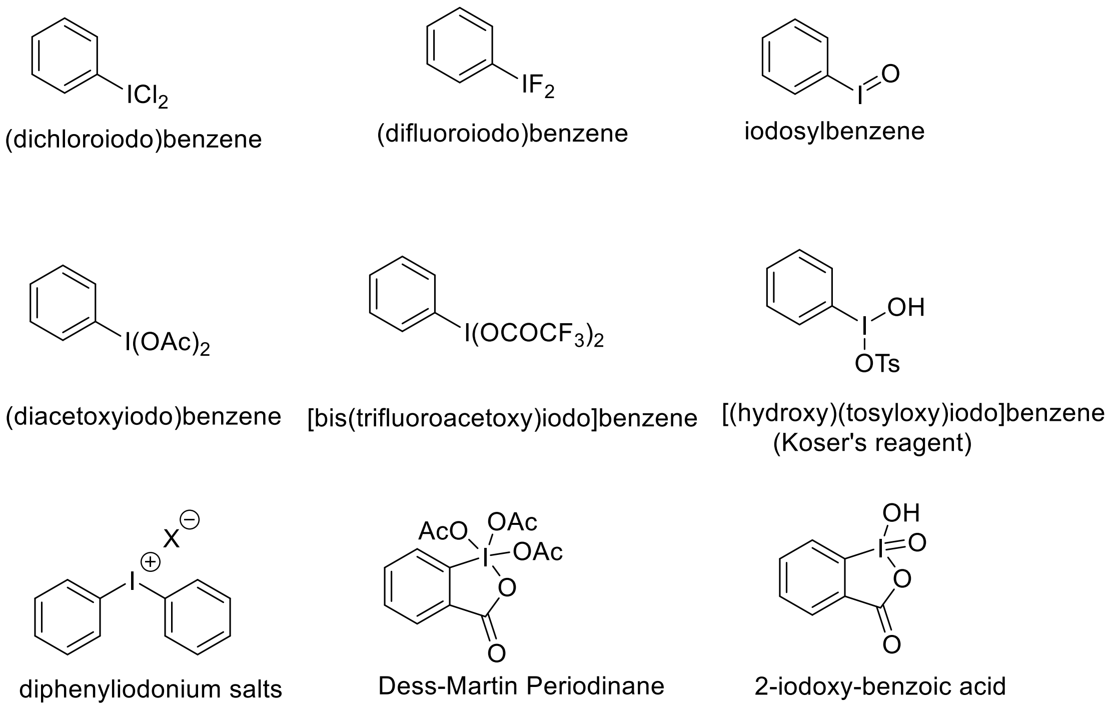

Figure 1.6: Most frequently used hypervalent iodide reagents[120]

Iodine(III) compounds are electrophilic at iodine, because of the node in the occupied non-bonding orbital of the hypervalent bond (Fig. 1.7). Thus, they react with various nucleophiles by initial Nu–I bond formation and release of one of the ligands.

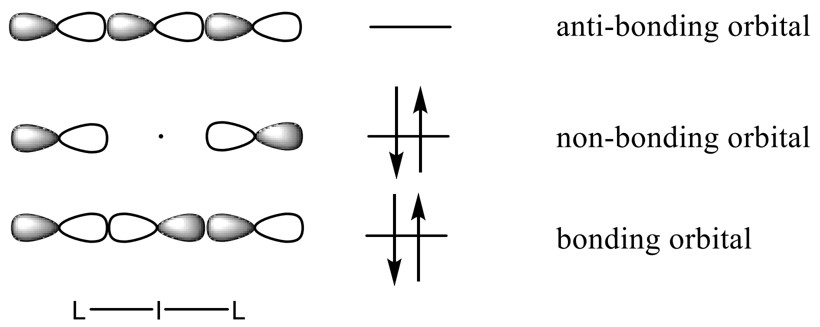

Figure 1.7: Orbital diagram of a hypervalent bond

Diaryliodonium salts are the best-known compounds in this class. Owing to their highly electron-deficient nature and the presence of an excellent leaving-group, they serve as versatile arylating agents with a variety of nucleophiles. This will be discussed in detail below.

1.7 Diaryliodonium Salts

1.7.1 Structure and Reactivity

Diaryliodonium salts are generally air and moisture stable compounds that were first reported by Hartmann and Meyer in 1894[121] and are the most investigated structural type amongst the iodonium salts. They adopt a trigonal bipyramidal structure with one aromatic moiety occupying the equatorial position and the other aryl group in the apical position together with a heteroatom ligand. The salt is referred to as a symmetric salt if $Ar^1 = Ar^2$, and as an asymmetric salt if $Ar^1 \neq Ar^2$ (Fig. 1.8).

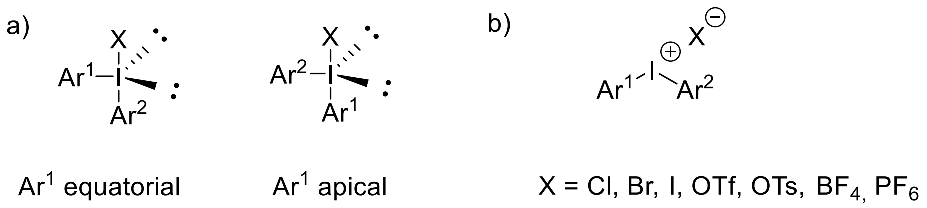

Figure 1.8: General structure of diaryliodonium salts a) T-shaped with a covalent bond to X b) Salt form

However, insufficient understanding of the hypervalent structure in solution makes depiction of asymmetric diaryliodonium salts as the T-shaped trigonal bipyramidal structure problematic. For example, which aryl group should reside in the equatorial position and which in the apical position. Instead, these salts are often illustrated as a positively charged iodine atom with two aryl ligands and an associated anion (Fig. 1.8b)[122] which does not always adequately reflect their reactivity.

Iodine(III) compounds with two heteroatom ligands are believed to retain this T-shape in solution, whereas the diaryliodonium salt structure in solution has been debated and could depend both on the anion $X^{\ominus}$ and the solvent.[123] The IUPAC nomenclature for this compound class is “diaryl-λ^3-iodanes”, although the old term diaryliodonium salt is the most common in use today.

Diaryliodonium salts can have a range of substituents on the aryl rings and a range of counter-ions can also be used. The anion $X^{\ominus}$ influences both the solubility and reactivity of the salts, diaryliodonium salts with halide anions are generally sparingly soluble in many organic solvents, whereas triflate salts have good solubility.[124] In general, non-nucleophilic and weakly nucleophilic anions such as triflate, tosylate, tetrafluoroborate or hexafluorophosphate are preferred over halides in synthetic applications so that the anion does not provide a competing nucleophile (Scheme 1.27).

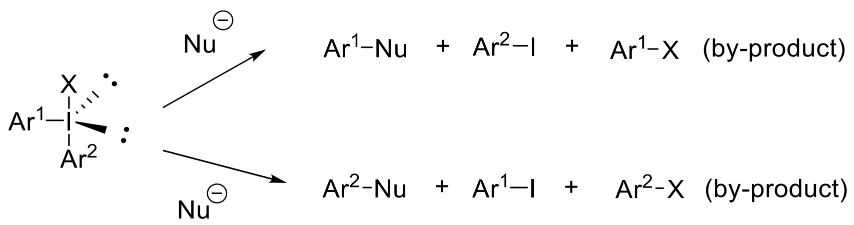

Scheme 1.27: General arylation of a nucleophile

1.7.2 Chemoselectivity of Asymmetric Diaryliodonium Salts

Asymmetric salts are often preferred over symmetric ones for a variety of reasons. Asymmetric diaryliodonium salts are desirable when the starting materials are of limited availability or expensive, as one aryl moiety can be selectively transferred, with the other aryl moiety behaving as a “dummy ligand” or non-participating group.

The most frequently used non-participating group, for metal-catalysed reactions is the mesityl group. In metal-mediated reactions with asymmetric salts, the least sterically hindered arene is selectively transferred. If steric bulk is not a factor, then the most electron-deficient arene is preferentially transferred as nucleophiles show a preference for the most electron-deficient ring, therefore the ring with the electron-withdrawing group ends up in the arylated product.[118] The aryl groups can often be differentiated from each other electronically or sterically as both properties are known to influence the outcome of the substitution reaction. The recycling of the non-participating aryl iodide may also be achieved by choosing an asymmetric salt, thereby making the process more efficient (Scheme 1.27).[122]

1.7.3 Synthesis of Diaryliodonium Salts

The first synthesis of a diaryliodonium salt was accomplished over 100 years ago by Victor Meyer[121] and refined by Beringer in the 1950s to a working one-pot reaction, albeit with a small substrate scope (Scheme 1.28).[125]

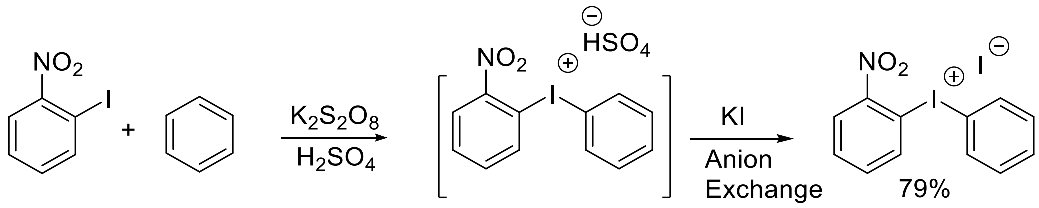

1.125 **1.126** **1.127**

Scheme 1.28: Beringer’s one-pot synthesis of a diaryliodonium salt

The first regiospecific synthesis of diaryliodonium tosylates **1.130** was discovered by Koser and co-workers in 1980. The reaction of hydroxy(tosyloxy)iodobenzene (PhI(OH)OTs, Koser’s reagent), **1.128** with arylsilanes, **1.129** under neutral conditions occurred by *ipso*-substitution regardless of the other functionality R^1 and R^2 (Scheme 1.29).[126,127]

Substituted versions of Koser’s reagent could also be employed, delivering both symmetric and asymmetric salts in moderate yields. Electron-rich arenes, such as thiophene, react with ArI(OH)OTs without the need for the trimethylsilyl (TMS) activating group and only give one regioisomer.[128]

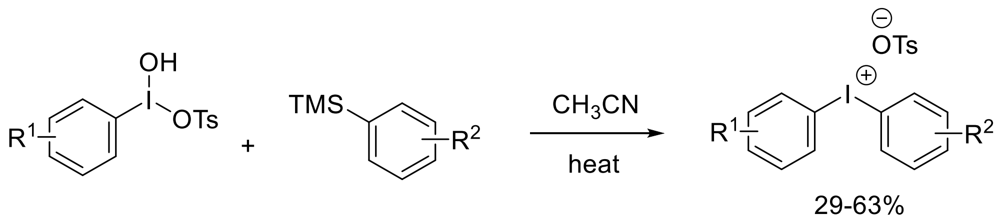

1.128 **1.129** **1.130**

Scheme 1.29: Koser and co-workers' synthesis of diaryliodonium salts

Oloffson and co-workers developed a new regiospecific sequential one-pot synthesis of symmetrical and asymmetrical diaryliodonium tetrafluoroborates based on the use of boronic acids (Scheme 1.30).[129] The reaction was fast, high yielding and gave a large substrate scope as the use of boron trifluoride etherate could give rise to diaryliodonium tetrafluoroborates without an extra anion-exchange step. In addition, the corresponding diaryliodonium triflates were conveniently obtained via an in-situ anion exchange.

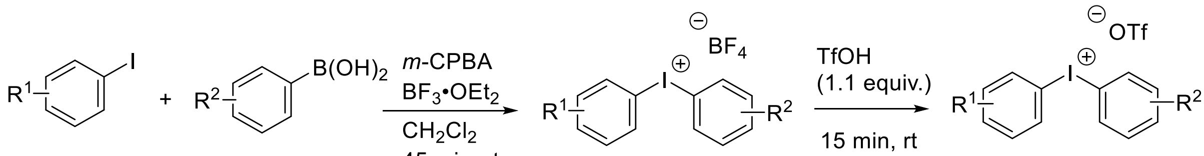

1.131 **1.132** **1.133** **1.134**

Scheme 1.30: One-pot synthesis of symmetrical and asymmetrical diaryliodonium tetrafluoroborates

The most common way of synthesizing diaryliodonium salts is a stepwise approach in which an aryl iodide, **1.135** is converted into an aryliodine(III) compound, **1.136** by treatment with an inorganic oxidant under acidic conditions (Scheme 1.31A). This aryliodine(III) species is isolated and subsequent ligand exchange with an arene, an arylstannane, an arylsilane, or an arylboronic acid delivers the diaryliodonium salt under acidic conditions.[118] The anion usually originates from the acid used, and an anion exchange is often performed to give a more easily isolated and/or applicable salt. Structurally diverse diaryliodonium salts can be obtained by employing different reagents depending on the electronic properties of the aryl moieties, although choosing the correct method can be difficult for non-specialists in the field. To shorten the synthetic route to symmetric diaryliodonium salts, preformed inorganic iodine (III) reagents, **1.137** e.g. iodosyl fluorosulfate can be employed. (Scheme 1.31C)[130]

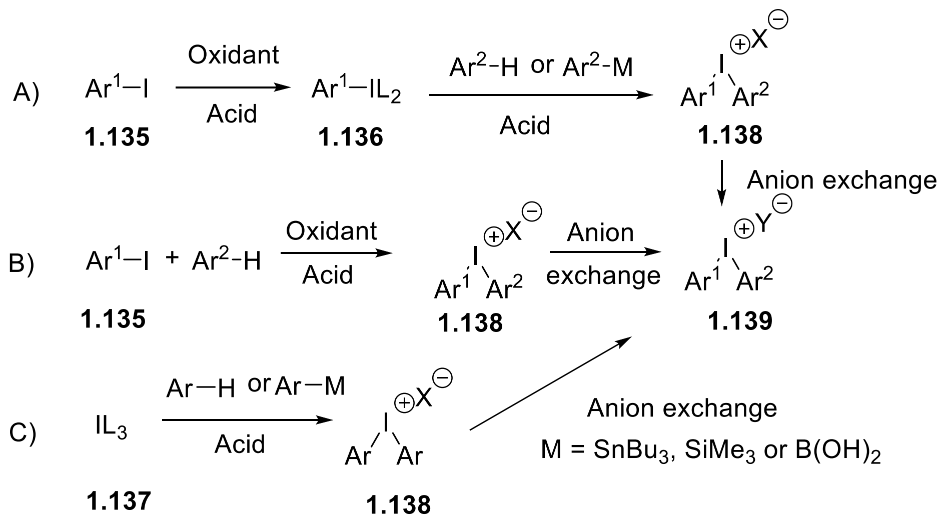

Scheme 1.31: General acidic routes to diaryliodonium salts

1.7.4 Applications of Diaryliodonium Salts in Organic Synthesis

Diaryliodonium salts are often applied in metal-catalyzed cross-coupling reactions,[108,131] in the α-arylation of carbonyl compounds,[132-135] as benzyne generators,[136] as precursors to ^{18}F-labeled radioligands[137] and as biologically active compounds in their own right.[138] In a specific example, a study of the *in vitro* activities of several diaryliodonium salts against oral and dental anaerobes has demonstrated that their activities are comparable to that of chlorhexidine and these compounds may be suitable for incorporation into an oral mouthwash.[138] It was noted that their activities were generally equivalent to that of chlorhexidine. However, the structure-activity relationships of the iodonium salts used were not determined and human trials were not considered.

Many applications of diaryliodonium salts in organic synthesis have emerged over the past decade and the field now encompasses such diverse elements as electrophilic arylation of a wide range of nucleophiles,[139,140] and dearomatization of phenols.[141] Encouragingly, advances are also being made in asymmetric synthesis[142,143] although this area remains in its infancy, providing a challenging target for future research. In addition, these versatile compounds are industrially applied as cationic photoinitiators in polymerization processes.[144,145]

In 1953, Beringer et al.,[146] demonstrated that diaryliodonium bromides were useful reagents for the phenylation of versatile organic and inorganic bases including alkoxides, phenoxides, benzoates, nitrites, sulfonamides, amines, sulfites, sulfonates, and cyanides under relatively mild conditions. These results have provided the basis for a new research field using diaryliodonium salts as reagents in organic transformations. Since these first discoveries, several methodologies have been developed for carbon and heteroatom arylations using diaryliodonium salts.[124]

1.8 Arylation Reactions

Arylation reactions are widely used in organic syntheses and various arylation reactions using diaryliodonium salts have been reported. Alcohols,[147] acids,[148] amines,[149] thiols,[150] and carbonyl compounds[132] have all been arylated successfully with diaryliodonium salts.

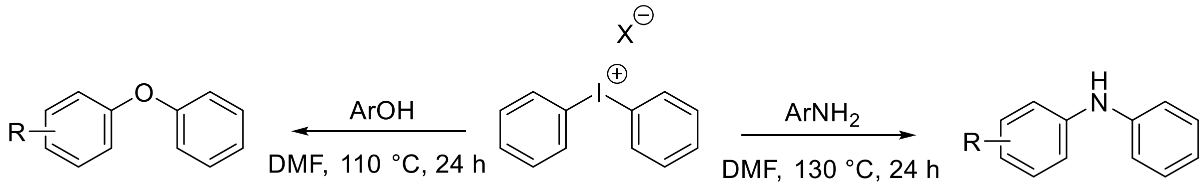

1.141 **1.140** **1.142**

Scheme 1.32: General arylation of anilines and phenols using diaryliodonium salts[151]

New 8-chloro-2-phenyl-2,7-naphthyridin-1(2*H*)-one building blocks bearing diverse substituents on the 2-phenyl group **1.145** have been synthesized via an efficient diaryliodonium salt-based *N*-arylation strategy. A small combinatorial library of 8-amino substituted 2-phenyl-2,7-naphthyridin-1(2*H*)-one **1.147** was further constructed using the mild acid-catalyzed nucleophilic substitution of chlorinated naphthyridinones **1.145** and substituted anilines **1.146** (Scheme 1.33).[152] Preliminary biochemical screening resulted in the discovery of the new 2,7-naphthyridone-based MET / AXL kinase inhibitors with comparable MET / AXL potency to that of commercial cabozantinib.

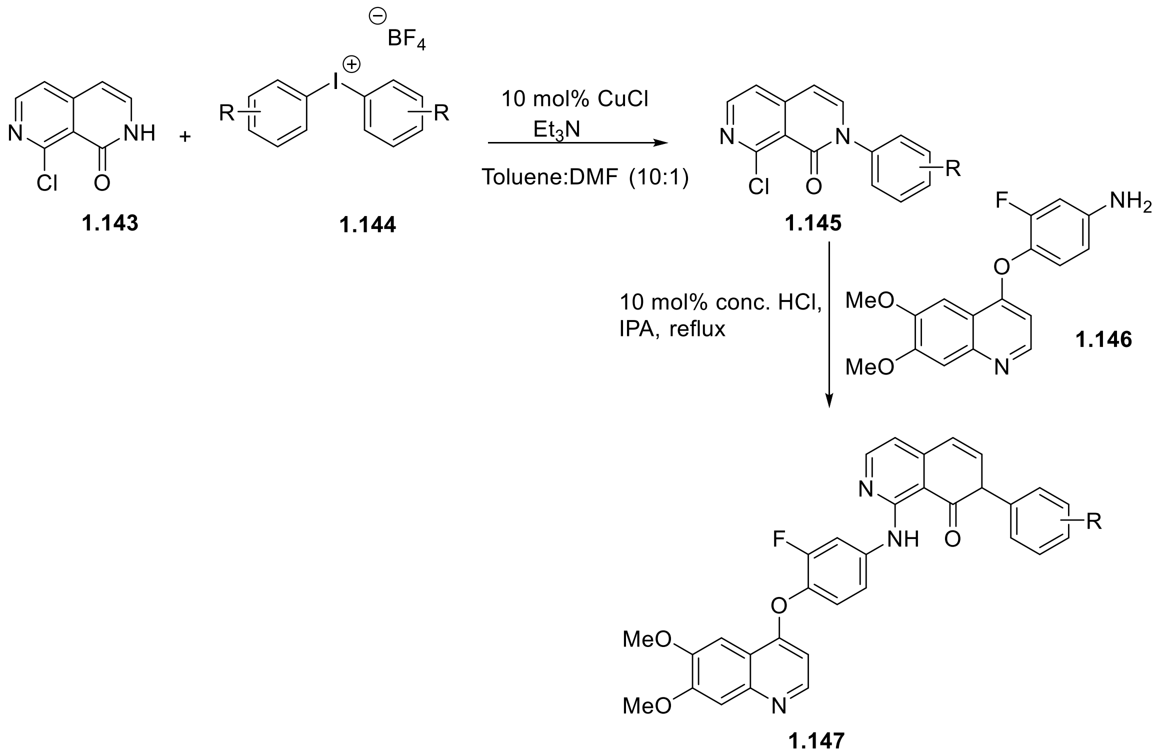

Scheme 1.33: Synthesis of N-Phenyl-2,7-naphthyridin-1(2*H*)-one-based MET / AXL inhibitors

1.9 Summary

This introduction chapter has served to be an overall guide through the important chemistry that will be discussed in this thesis. We have seen how diversity oriented syntheses can expand the chemical space and identify novel and better drug molecules. We have shown the great synthetic utility of complexity-generating reactions that allow structural complexity and building blocks leading to structural diversity. We have also seen how tandem reactions allow us to use simple starting materials to build complex structures with high selectivity in one process. Azaquinones, which can be initiated from arylation reactions using diaryliodonium salts, can serve as building blocks to other synthetic compounds, and therefore represent a new frontier for the design and generation of molecular complexity.

Chapter 2. Synthesis of azaquinone and investigation of the addition of nitrogen and sulfur nucleophiles to azaquinone

This project aims to study the possible tandem reactions of 4-(phenylimino)cyclohexa-2,5-dien-1-one (Azaquinone), via nucleophilic addition and oxidative cyclisation. Computational studies will also be used to investigate the mechanism where alternatives are possible. Azaquinone is an unexplored yet versatile building block. The chemistry of azaquinone with all six carbon atoms in the quinoid ring being different will form the basis for studies in this chapter as attack of nucleophiles is possible to both of the α,β-unsaturated systems, thus demonstrating the use of azaquinone as a potential key intermediate in tandem reactions and a new class of building block leading to structural complexity.

2.1 Arylation of binucleophiles

As arylation of amines and phenols has been reported to give mono-functionalised molecules, the group considered the relative arylation of these two functional groups, the amino and the hydroxyl groups viz: aminophenols to establish whether one could be arylated selectively in the presence of the other.

The arylation of 2-hydroxyaniline **2.2** with diaryliodonium trifluoroacetate **2.1** gave the *N*-arylation product in preference with only trace amounts of *N,O*-diarylation being detected[151] (Scheme 2.1).

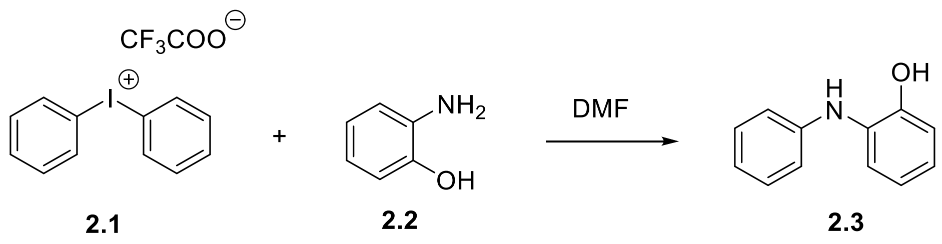

Scheme 2.1: *N*-Arylation of 2-hydroxyaniline, **2.2** with diaryliodonium trifluoroacetate

The arylation of 3-hydroxyaniline and 4-hydroxyaniline with diaryliodonium trifluoroacetate was also found to be *N*-selective.[151] However, in the case of 4-hydroxyaniline, the oxidised product – azaquinone – was also detected due to the oxidising property of hypervalent iodine species (Scheme 2.2).

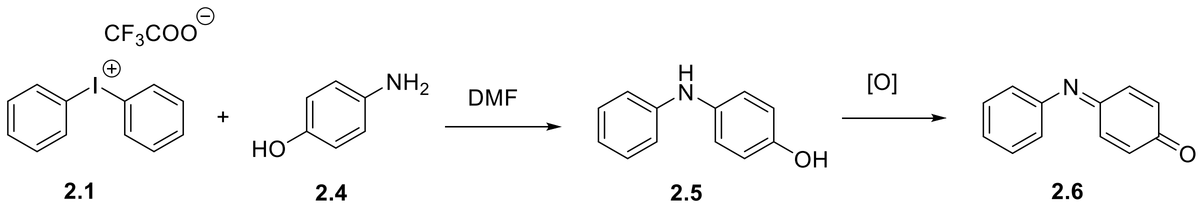

Scheme 2.2: *N*-Arylation of 4-hydroxyaniline, **2.4** with diaryliodonium trifluoroacetate

Arylation reactions of diaryliodonium salts with species containing multiple nucleophilic sites may show selectivity, as in the case of hydroxyanilines and the resulting products can undergo further transformations, extending the utility still further. For example, tandem reactions can be carried out on the product diarylamines of the *N*-arylation reactions of 2- and 4-hydroxyanilines as they generate azaquinones on oxidation. This will allow the preparation of diverse yet complex structures (e.g. post arylation ring formation) from simple, available starting materials without the need to isolate any of the intermediates.

In addition to batch conditions, the reaction was also conducted in a flow reactor using a copper coil which also acts as a catalyst for the reaction eliminating the need for the additional reagents (Fig. 2.1).[151]

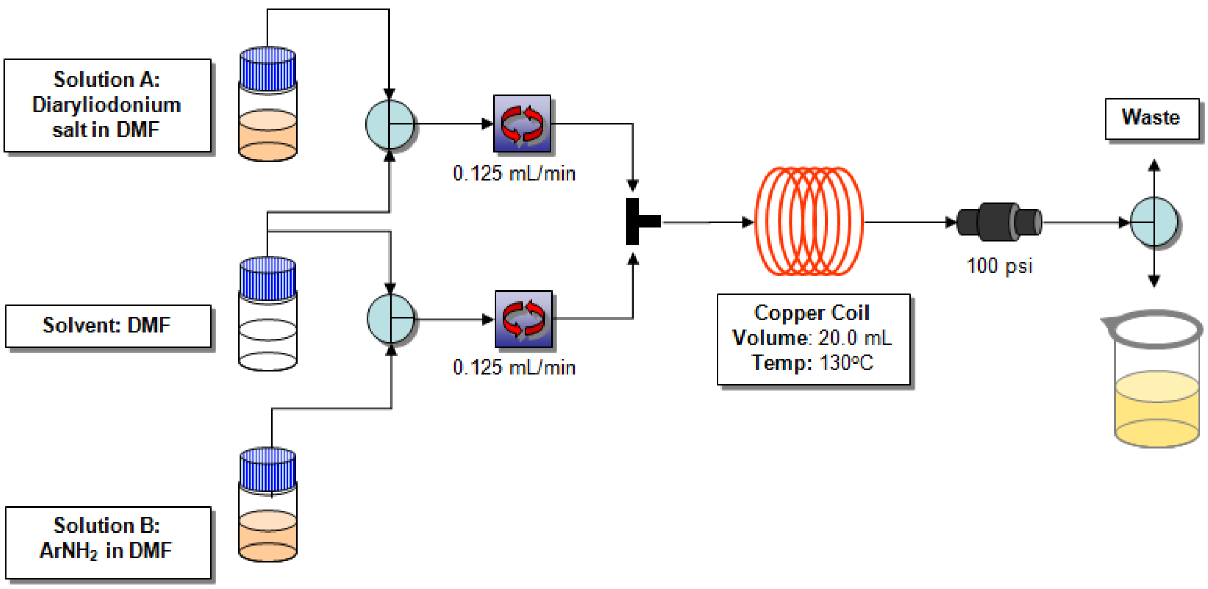

Figure 2.1: Transfer to Flow Chemistry

2.1.1 Synthesis of Diphenyliodonium salts

Diphenyliodonium salts were used in the arylation studies, iodobenzene **2.7** was used to synthesize (diacetoxyiodo)benzene **2.9** in excellent yield using sodium perborate as the oxidising agent (Scheme 2.3).[153]

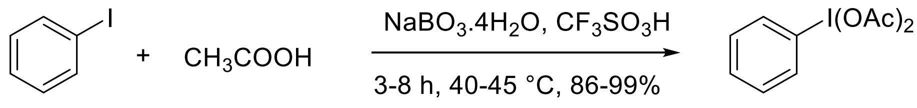

2.7 **2.8** **2.9**

Scheme 2.3: Formation of (diacetoxyiodo)benzene from iodobenzene

Diphenyliodonium trifluoroacetate **2.1** was then prepared from (diacetoxyiodo)benzene **2.9** and phenylboronic acid according to a reported procedure (Scheme 2.4).[149]

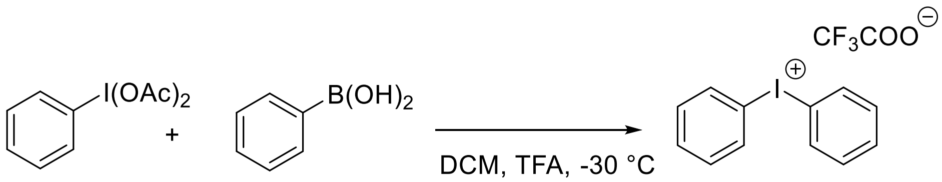

2.9 **2.10** **2.1**

64%

Scheme 2.4: Formation of diphenyliodonium trifluoroacetate from (diacetoxyiodo)benzene

2.1.2 Arylation with aniline

A preliminary arylation study (Scheme 2.5) was carried out to investigate the formation of diarylamines from diphenyliodonium trifluoroacetate **2.1** and aniline **2.11**, using reported conditions—DMF at 130 °C, for 24 h to serve as a control reaction for subsequent reactions using diaryliodonium salts and 4-hydroxyaniline.[154,155]

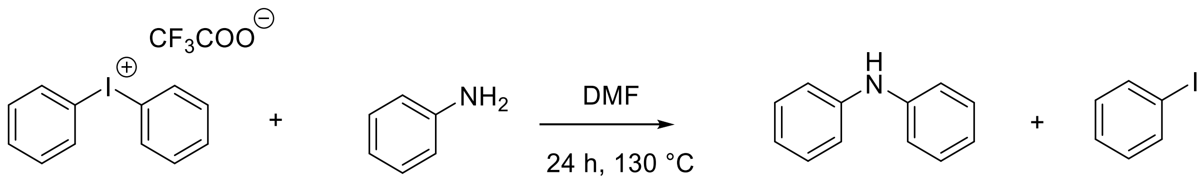

2.1 **2.11** **2.12** **2.7**

Scheme 2.5: Formation of diphenylamine **2.12** from diphenyliodonium trifluoroacetate

A HPLC method (see page 131) was also developed to allow rapid analysis of this reaction, once transferred to a flow chemistry protocol and this is shown below.

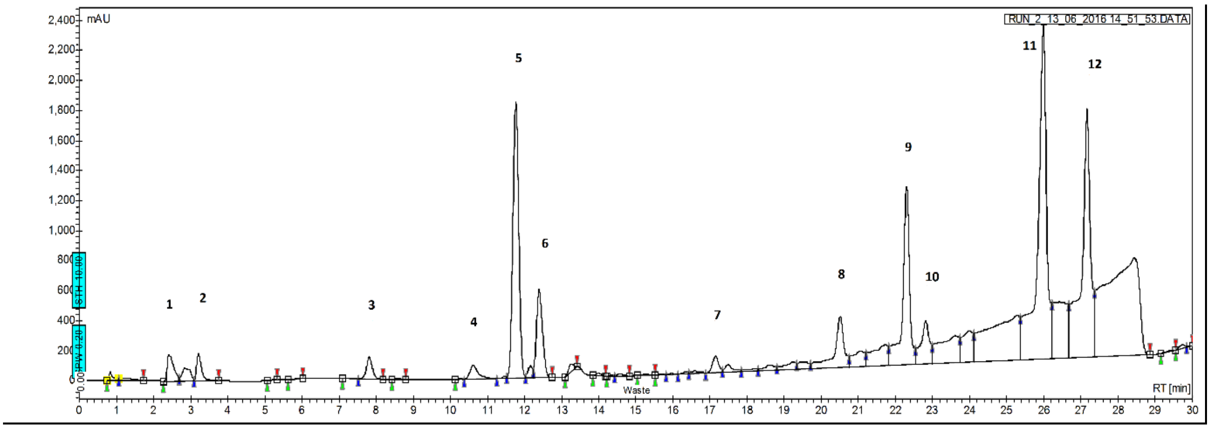

Figure 2.2: HPLC chromatogram of reaction of **2.1** with aniline

The presence of phenol **2.13** (Table 2.1; peak 5) as a by-product of the reaction can be attributed to possible hydrolysis of the diaryliodonium salt **2.1,** achieved by nucleophilic addition of water and then reductive elimination as shown in Scheme 2.6a or by addition of the counter-ion (trifluoroacetate) followed by hydrolysis of the resulting ester (Scheme 2.6b). The latter is more likely given the presence of phenyltrifluoroacetate **2.14** (Table 2.1; peak 6) in the crude reaction mixture.

Table 2.1. Peaks in Chromatogram (Fig. 1.6) from HPLC of standards

Peak	Retention Time (min)	Compound
4	10.60	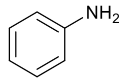 **2.11**
5	11.80	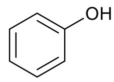 **2.13**
6	12.40	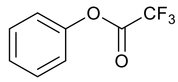 **2.14**
11	26.00	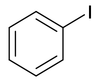 **2.7**
12	27.40	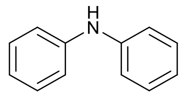 **2.12**

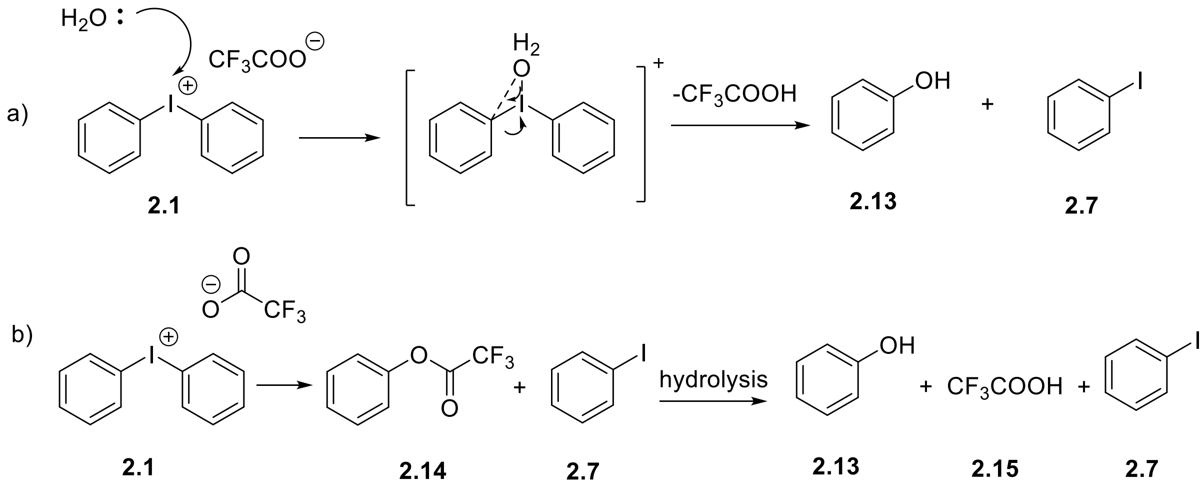

Scheme 2.6: Reaction mechanism for the formation of phenol **2.13** and phenyltrifluoroacetate **2.14**

2.1.3 Arylation with 4-hydroxyaniline

The result of this initial reaction (Scheme 2.5) provided the desired diarylamine **2.12** in good yield and prompted us to proceed to the reaction with 4-hydroxyaniline (Scheme 2.7) to determine the relative reactivity of anilines and phenols as both have been shown to undergo arylation using diphenyliodonium salts.[156]

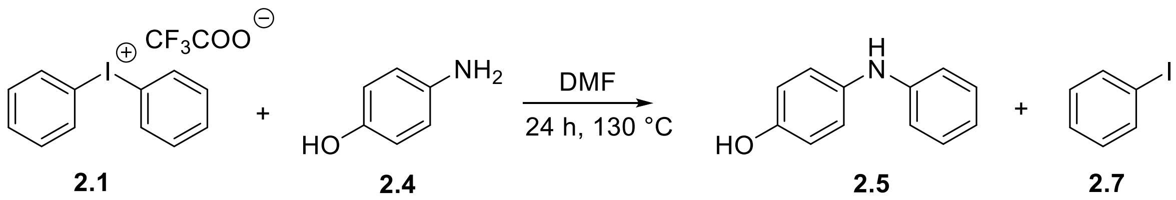

Scheme 2.7: Formation of 4-hydroxydiphenylamine **2.5** from **2.1**

The reaction was done under batch conditions using both one equivalent and two equivalents of the diaryliodonium salt **2.1** and the results are given in Table 2.2.

Table 2.2. Reaction of diphenyliodonium trifluoroacetate with 4-hydroxyaniline at 130 °C

Entry	**2.1**	**2.4**	**Time (h)**	**Solvent**	**2.5:2.7**[a]
1	1equiv. (5 mmol)	1equiv. (5 mmol)	24	DMF (50 mL)	1.6:1
2	2equiv. (10 mmol)	1equiv. (5 mmol)	24	DMF (50 mL)	1.2:1
3	2equiv. (2.5 mmol)	1equiv. (1.25 mmol)	24	DMF (25 mL)	1.1:1

[a] ratio by HPLC analysis of the crude reaction mixture of Scheme 2.7.

This was surprising as previous work in the group on the reaction of diphenyliodonium trifluoroacetate with 4-hydroxyaniline in a continuous flow process gave the *N*-arylation product as the major product. A product of oxidation, 4-(phenylimino)cyclohexa-2,5-dien-1-one (azaquinone) **2.6** was also detected when two equivalents of diphenyliodonium trifluoroacetate was used, as hypervalent iodine species have also been used as oxidising agents (Scheme 2.2).[155,157] This suggests different reaction preferences depending on the conditions used.

The formation of 4-hydroxydiphenylamine also suggests selectivity for *N*-arylation over *O*-arylation when both nucleophiles are present in the same substrate. The unidentified peaks in Table 2.3 could indicate the presence of *O*-arylation or *N,O*-diarylation products but standards were not available. However, identification of these peaks by accessing practical amounts of these compounds as analytical reference materials will constitute further work.

The chromatograms for the reactions given in Table 2.2 are as shown.

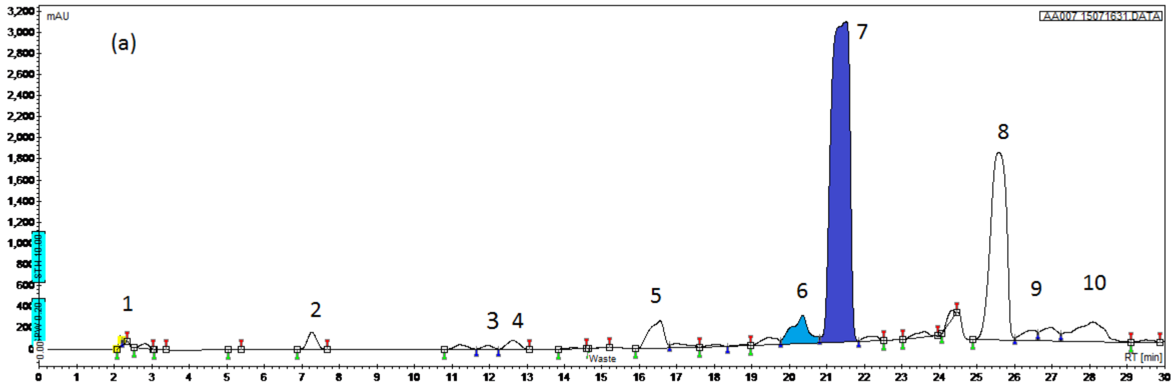

The reaction of diphenyliodonium trifluoroacetate **2.1** with 4-hydroxyaniline **2.4** (Table 2.2; Entry1)

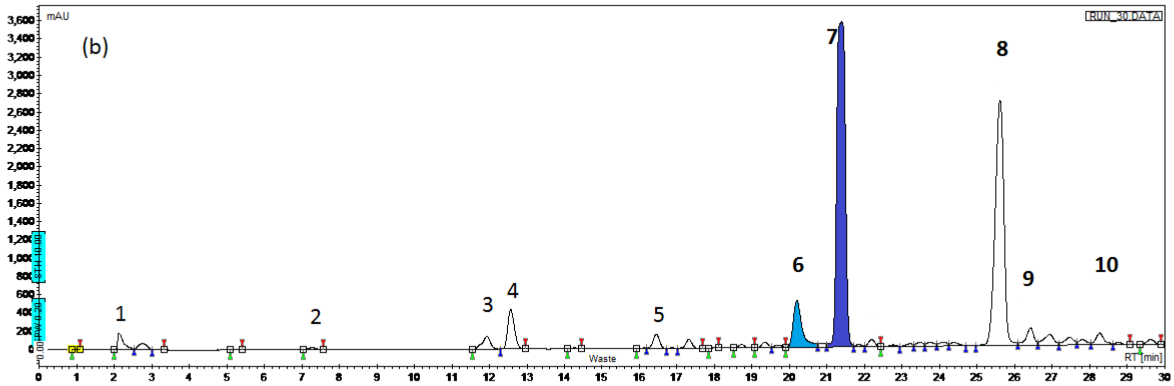

The reaction of diphenyliodonium trifluoroacetate **2.1** with 4-hydroxyaniline **2.4** (Table 2.2; Entry 2)

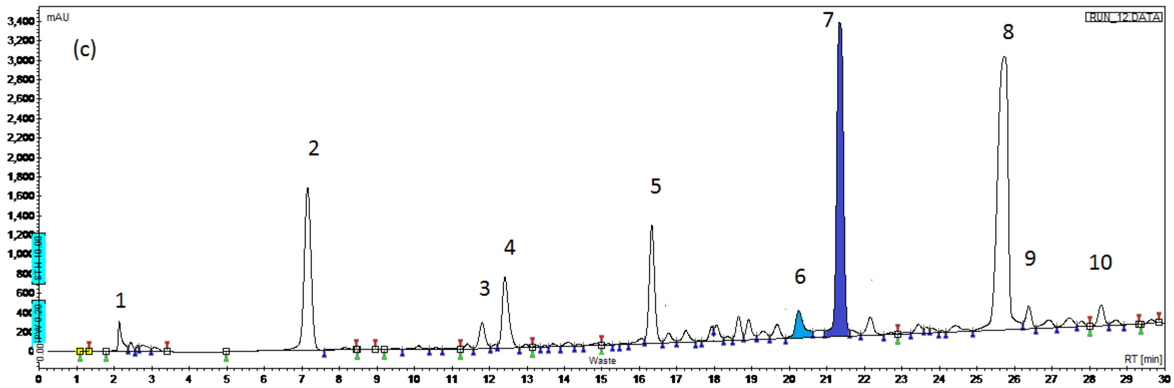

The reaction of diphenyliodonium trifluoroacetate **2.1** with 4-hydroxyaniline **2.4** (Table 2.2; Entry 3)

Figure 2.3: HPLC chromatograms for the reaction in Table 2.2

Table 2.3. Identification of HPLC peaks in the reaction of **2.1** and **2.4** (Fig. 1.7) by comparison to standards.

Peak	Retention Time (min)	Compound
1	2.2	Solvent (DMF)
2	7.2	n/i
3	11.8	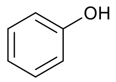 **2.13**
4	12.4	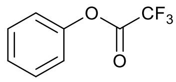 **2.14**
5	16.4	n/i
6	20.4	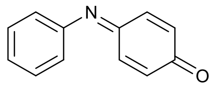 **2.6**
7	21.4	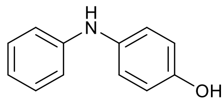 **2.5**
8	25.8	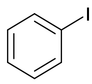 **2.7**
9	26.6	n/i
10	28.4	n/i

n/i = not identified

2.1.4 Counter-ion effect

The effect of the counter-ion of the diaryliodonium salt on the outcome of the reaction was also studied (Fig. 2.4). As mentioned previously, diaryliodonium salts with halide anions are generally sparingly soluble in many organic solvents, whereas triflate and tetrafluoroborate salts have good solubility. In general, non-nucleophilic anions such as triflate, tosylate, tetrafluoroborate or hexafluorophosphate are preferred over halides in synthetic applications because they limit competing nucleophilic substitution from the counter-ion for example leading to aryltrifluoroacetates in the case of **2.1** (see Table 2.3; peak 4).

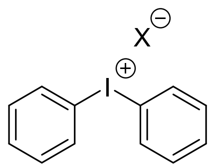

2.1, 2.16a-2.16d

X = CF_3COO **2.1**
X = Cl **2.16a**, OTf **2.16b**, OTs **2.16c**, PF_6 **2.16d**

Figure 2.4: Diphenyliodonium salts with counter-ion, **X**

It is evident from the results in Table 2.4 that where the counter-ion is less nucleophilic in nature, the reaction proceeds as expected providing **2.5** in good yield (Table 2.4; Entry 1). However, the other counter-ions give limited amounts of the desired product (**2.5**) with significant quantities of iodobenzene (**2.7**), the diaryliodonium salt with the hexafluorophosphate counter-ion did not give any **2.5** and only gave **2.7**. These excess amounts of iodobenzene could be as a result of the thermal decomposition or fluorination of **2.16d** (Table 2.4; Entry 5) being the preferred reaction path in these cases.

Table 2.4. Effect of counter-ion on the formation of 4-hydroxydiphenylamine **2.5**

Entry	**Compound**	**X**	**2.5:2.7**
1	**2.1**	CF_3COO	2.5:1
2	**2.16a**	Cl	1:10
3	**2.16b**	CF_3SO_3	1:34
4	**2.16c**	TsO	1:17
5	**2.16d**	PF_6	**2.7** only

The formation of benzene **2.17** and biphenyl **2.18** from the thermal decomposition suggests that these could also be some of the unidentified peaks in the HPLC chromatograms (Scheme 2.8).

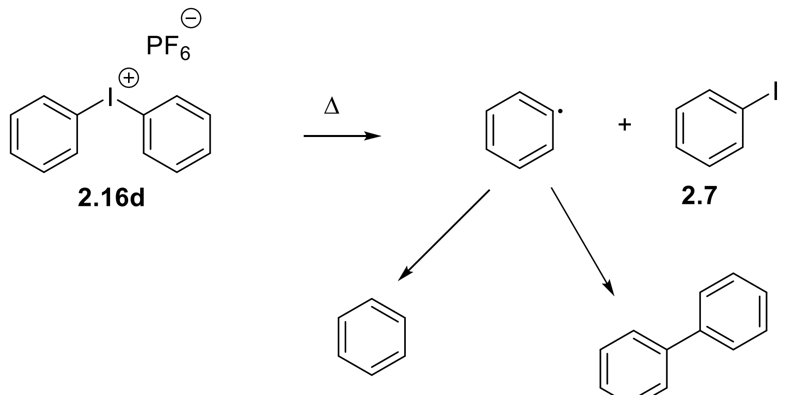

Scheme 2.8: Thermal decomposition of diaryliodonium salt

The chromatograms for the reactions given in Table 2.4 are as shown.

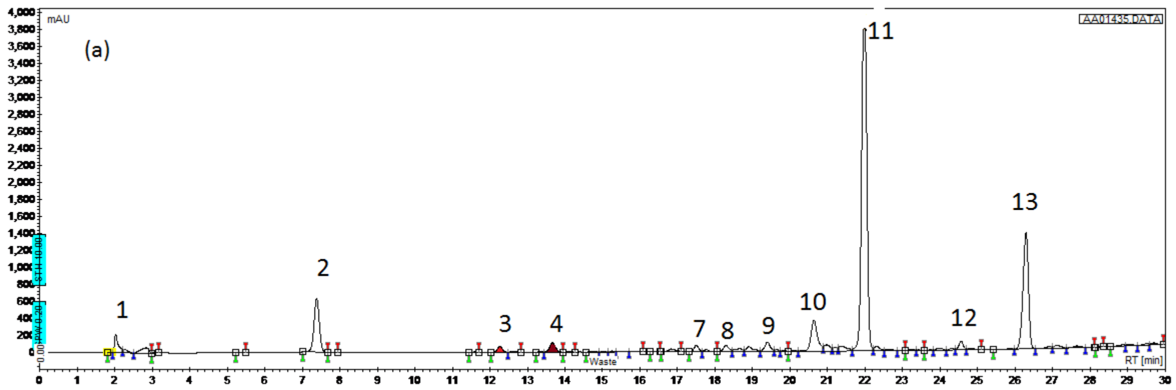

The reaction of **2.1** with **2.4** (Table 2.4; Entry 1)

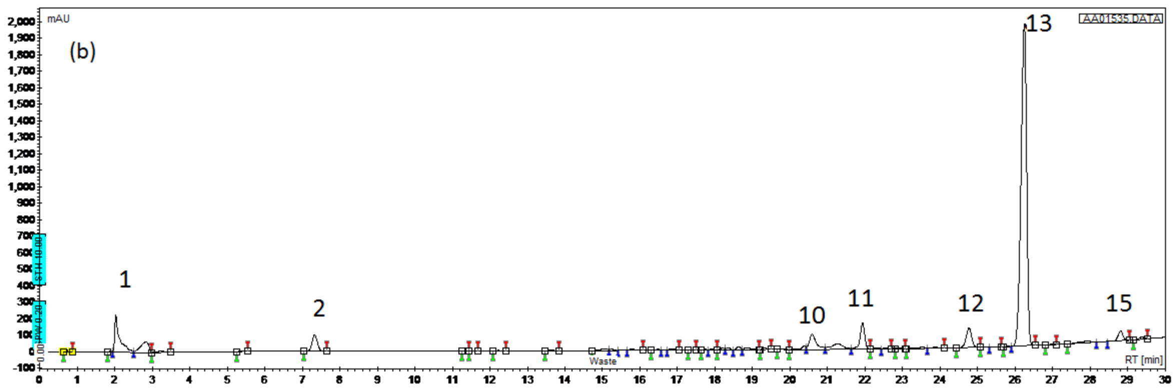

The reaction of **2.16a** with **2.4** (Table 2.4; Entry 2)

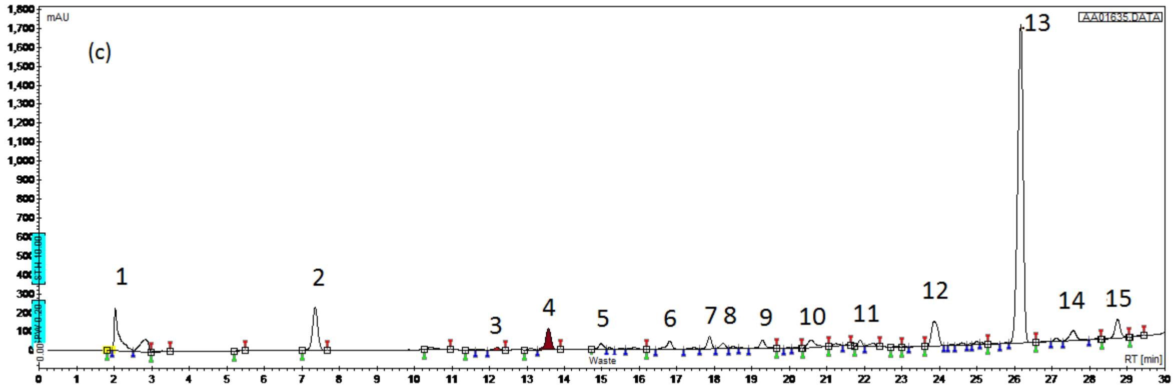

The reaction of **2.16b** with **2.4** (Table 2.4; Entry 3)

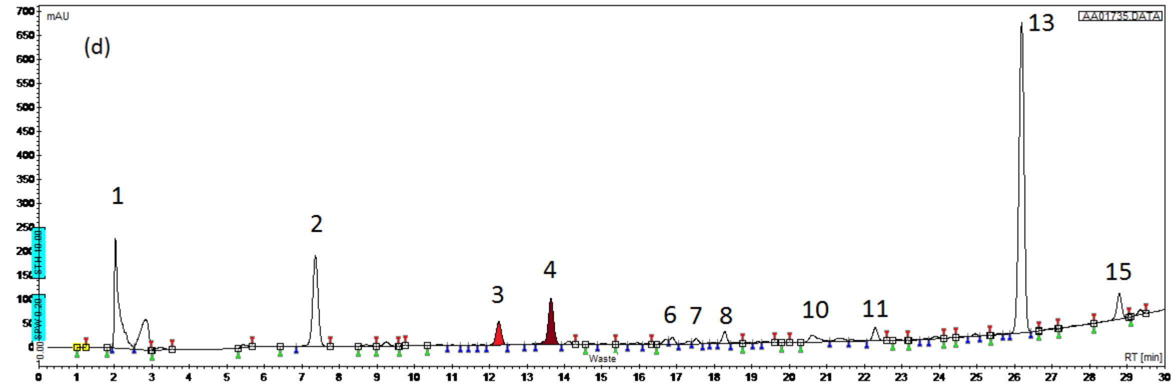

The reaction of **2.16c** with **2.4** (Table 2.4; Entry 4)

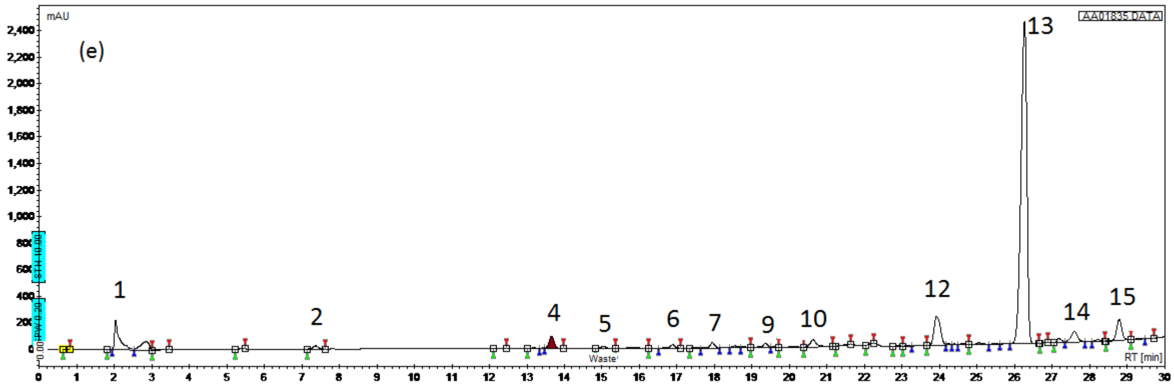

The reaction of **2.16d** with **2.4** (Table 2.4; Entry 5)

Figure 2.5: HPLC chromatograms for the reactions in Table 2.4 (see Table 2.5 for assignment of peaks)

The formation of multiple products by the addition of 4-hydroxyaniline to diphenyliodonium trifluoroacetate has been studied. Good yields of the desired products are obtained in DMF at 130 °C for 24 h. The effect of the counter-ion on the reactions of diphenyliodonium salts with 4-hydroxyaniline has also been studied and the reaction proceeds as expected using the trifluoroacetate ion, providing **2.5** in good yield (Table 2.4; entry 1). However, other counter-ions (Table 2.4) gave the by-product **2.7** as the major product. At this stage, it is not clear why the other counter-ions are not as successful in this role. The non-nucleophilic hexafluorophosphate gave **2.7** as the only product of the two desired suggesting that, in this case, the decomposition pathway is the preferred reaction.

Table 2.5. Identification of major HPLC peaks in the reaction of **2.1, 2.16a-2.16d** with 4-hydroxyaniline by comparison to standards (reaction in Table 2.4).

Peak	Retention Time(min)	Compound
1	2.2	Solvent (DMF)
2	7.2 – 19.4	n/i
3	20.6	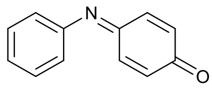 **2.6**
4	22.0	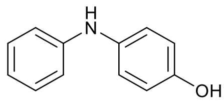 **2.5**
5	24.0	n/i
6	26.0	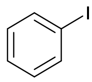 **2.7**
7	27.6	n/i
8	28.8	n/i

n/i = not identified

To investigate tandem reactions of the azaquinone **2.6** generated in this process, an alternative method would initially be used to access sufficient amounts of this species for evaluation.

2.2 *N*-Phenylquinoneimine: Azaquinone

Azaquinone is a bright orange crystalline powder related to benzoquinone by replacement of one atom of quinonoid oxygen by the imino group (Figure 2.6). Whilst quinone reactions have been extensively studied, the reactions of *N*-phenylquinoneimine have received surprising little attention over the years. Due to its α,β-keto and α,β-imino functionalities, azaquinone is highly reactive, with all six carbon atoms in the ring being different unlike 1,4-benzoquinone where there are only two types of carbon atoms due to the high degree of symmetry. Thus, this structure offers much potential for regioselective reactions. Different analogues of the azaquinone can be formed by varying the starting diaryliodonium salt or using a substituted 4-hydroxyaniline in the *N*-arylation reaction (Scheme 2.2). Azaquinone can be used as a building block to access useful synthetic compounds, and therefore as a potential key intermediate in tandem reactions.

2.6

Figure 2.6: Structure of Azaquinone

2.2.1 Synthesis of Azaquinone

The common method of preparing azaquinone is by the oxidation of 4-hydroxydiphenylamine, **2.5** by using various oxidising agents. This is shown in Table 2.6 below.

Table 2.6: Various oxidising agents used in the preparation of azaquinone

Oxidising agent	**Solvent**	**Temp (°C)**	**Time (min)**	**Yield (%)**	**Ref.**
HgO	benzene	80 °C	60	78	158
Ag_2CO_3 on Celite	toluene	rt	30	99	159
Hypochlorite	heptane	rt	60	99	160
Hydrogen peroxide	toluene	35	25	99	161
Activated carbon catalyst	methanol	50	60	90	162
$K_2Cr_2O_7$	acetone	40	45	97	6

In our work, the oxidising agent was prepared by the method of Fetizon,[163] a reaction of silver nitrate with sodium carbonate decahydrate to give a precipitate of silver carbonate adsorbed on celite (see Experimental section). The oxidation of **2.5** using silver carbonate adsorbed on Celite, a solid-supported oxidising agent (and so easily removed after the reaction) gives the azaquinone in excellent yield and is preferred to the other methods (Scheme 2.9).[159] The method uses two equivalents of Ag_2CO_3 and carried out at room temperature with 100% conversion to the product observed in 24 h.

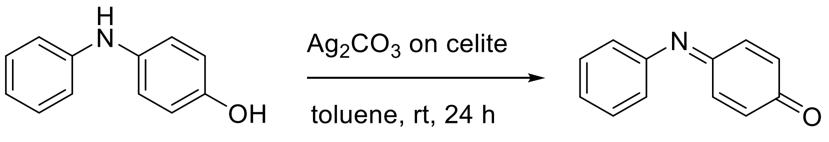

2.5 **2.6**

Scheme 2.9: Preparation of azaquinone

The ^1H NMR spectrum of azaquinone (Fig. 2.7) shows the four quinoid protons are different as predicted, having peaks as doublet of doublets, which demonstrates the potential different reactivity towards nucleophiles of the different positions.

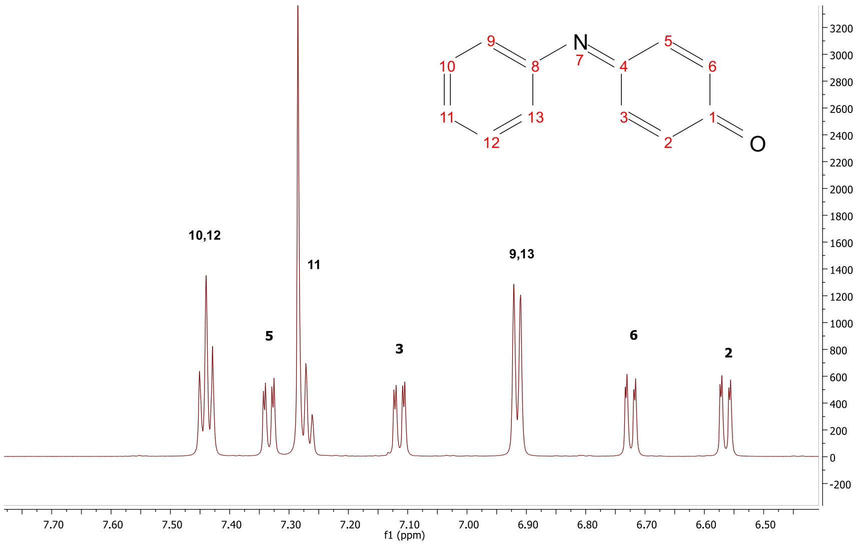

Figure 2.7: ^1H NMR spectrum of azaquinone

To date ^1H NMR prediction software does not demonstrate this important difference (Fig. 2.8). It predicts that both protons *ortho* to the carbonyl carbon are same and the protons ortho to the imino carbon are also the same. This highlights a significant limitation in the simulation software and is therefore of limited use in characterisation of this class of materials.

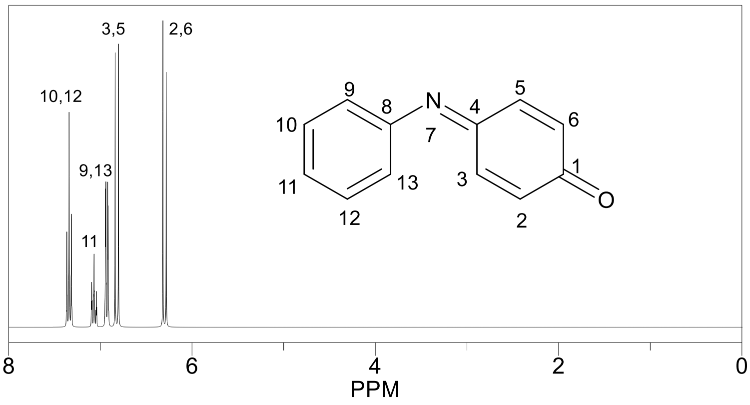

Figure 2.8: ChemBioDraw Ultra 14.0.0.117 ^{1}H NMR prediction for azaquinone **2.6**

The structure of azaquinone was also confirmed by the x-ray diffraction as shown in Figure 2.9. The dihedral angle C7 – N1 – C4 – C3 is -6.411° meaning that the phenyl ring is twisted relative to the quinoid ring which suggests that the phenyl ring is not in conjugation with the quinoid ring.

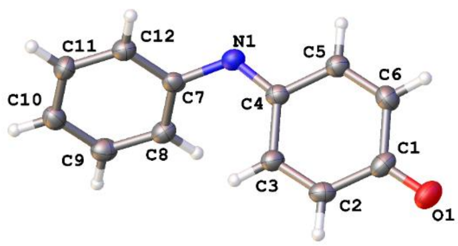

Figure 2.9: Crystal structure of azaquinone, **2.6**

2.2.2 Azaquinone as an oxidising agent

In a similar manner to 1,4-benzoquinone, azaquinone may act as an oxidising agent. This is seen from its reaction with 2-hydroxyaniline, **2.2**. 2-Hydroxyaniline was expected to react with azaquinone as a nucleophile, being an aniline derivative, but there was no evidence of the nucleophilic addition reaction, rather, the product was that of oxidative self-condensation of 2-hydroxyaniline giving a phenoxazinone, **1.26** (Scheme2.10).[5] Azaquinone appears to act as an oxidising agent in this reaction as it was also reduced to 4-hydroxydiphenylamine (40%).

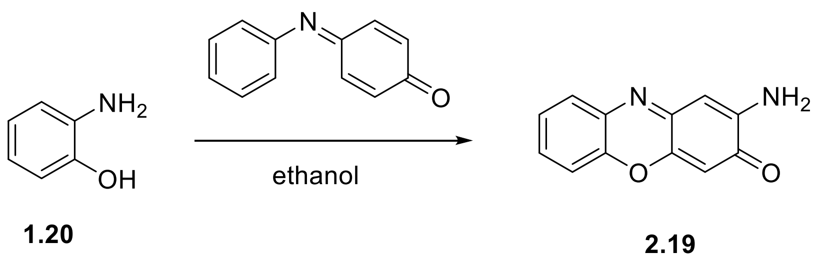

Scheme 2.10: Oxidation of 2-hydroxyaniline

2.3 Reaction with Nitrogen Nucleophiles

Nucleophilic addition of aromatic amines to azaquinone, **2.6** has been reported by Tsoi E. V. et al.[5] to give 2,5-diarylamino iminoquinones **2.21**, which are converted under oxidative conditions to products of intramolecular cyclisation, 2-arylamino-5-aryl-3-phenazinones **2.22** by heating in the presence of air or $K_3Fe(CN)_6$. The reported reactions (Scheme 2.11) were carried out in ethanol, at room temperature, and with two equivalents of the amine.

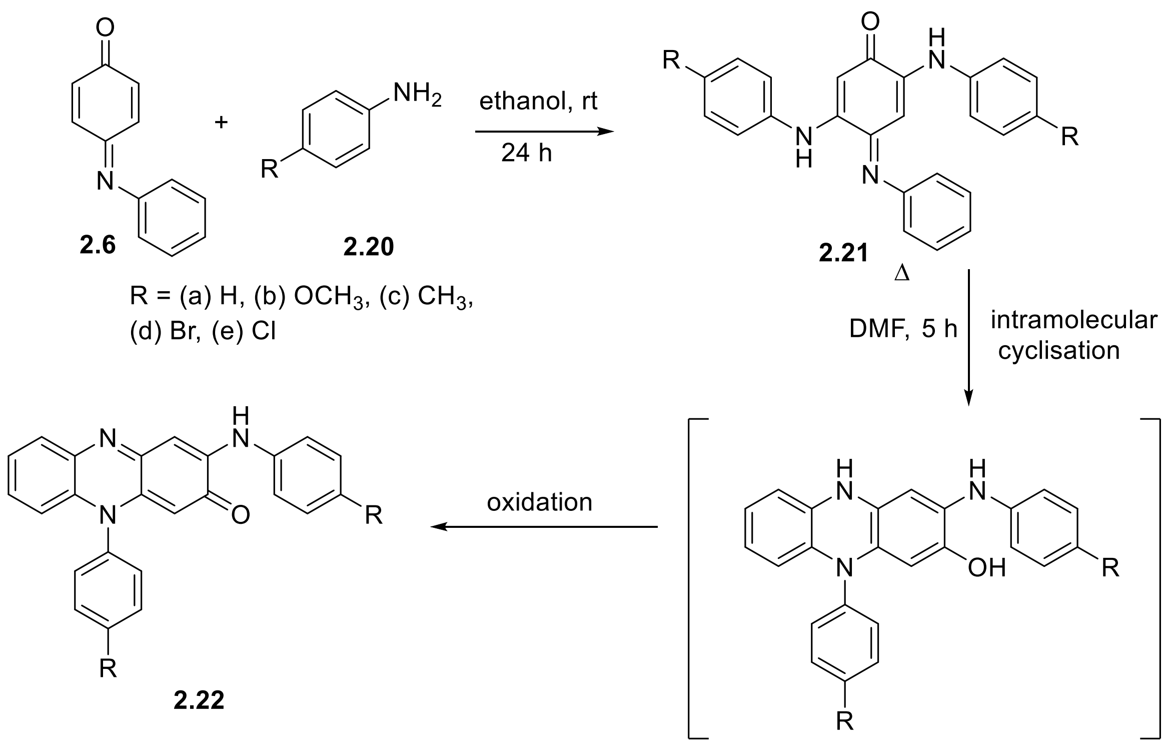

Scheme 2.11: Reaction of azaquinone, **2.6** with aromatic amines, **2.20**

Two singlets corresponding to the two quinoid protons were observed in the ^{1}H NMR spectra of 2,5-diarylamino derivatives, **2.21**, 6.12 ppm and 6.21 ppm for R=H,[5] which only indicates that the two arylamino substituents are attached to opposite sides of the quinoid ring but does not confirm they are para-oriented with respect to one another or their relative positions to the carbonyl group.

For example, if the two arylamino substituents were both para-oriented with respect to each other **2.21,** both ortho to the carbonyl carbon, **2.23**, both para to one another but with the substituent ortho to the imino carbon on the same side as the *N*-phenyl ring **2.24**, or both ortho to the imino carbon, **2.25**, the two singlets would still be observed (Fig. 2.10).

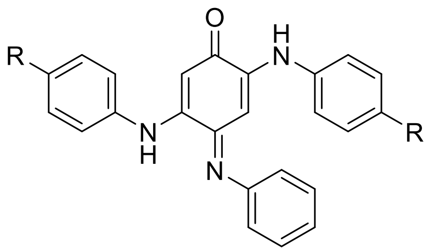

2.21

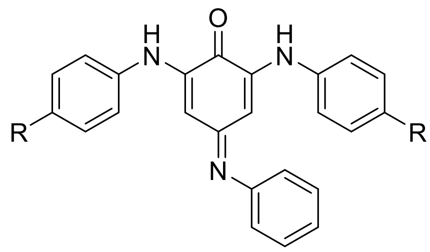

2.23

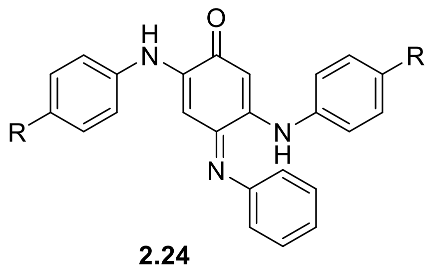

2.24

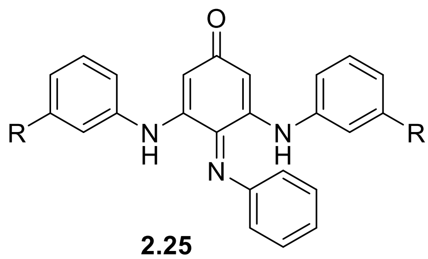

2.25

Fig 2.10: Possible structures of 2,5-diarylamino iminoquinones **2.21**

To date ^{1}H NMR prediction software (ChemBioDraw Ultra 14.0.0.117) however, does not take into account this important difference. Compounds **2.21** and **2.24** are predicted to have two singlets corresponding to the quinoid protons while the quinoid protons of **2.23** and **2.25** are predicted to have the same chemical shift i.e one singlet because the substituents are both ortho to the carbonyl carbon **2.23** or both ortho to the imino carbon **2.25**. However, this prediction does not take into consideration the *E/Z* isomerism arising from the position of the *N*-phenyl ring. This also highlights a significant limitation in the simulation software as was evident in the NMR data for azaquinone.

In the reported ^{1}H NMR data, the multiplicity and splitting patterns of the aromatic protons were not given, but rather reported as a range. Consequently, the data provided was insufficient to identify the correct regiochemistry of the product.

Also, as two equivalents of the arylamine were used and only the di-substituted products were reported, there was no mention of the result of using one equivalent of arylamine or whether any mono-addition products were isolated and therefore it was not possible to determine the position of the initial nucleophilic attack.

Since azaquinone has been identified as a key intermediate in tandem processes, it was therefore needful to consider these reactions in detail, to confirm the regiochemistry and structure of the products and also the order of addition if more than one group was added.

2.3.1 Aromatic amine addition

The reactions of aromatic amines with azaquinone are consistent with 1,4-conjugate addition to the α,β-unsaturated imine and/or the α,β-unsaturated ketone, resulting in di-addition products. The results of these studies are presented in Table 2.7.

Table 2.7: Aromatic Amine Addition

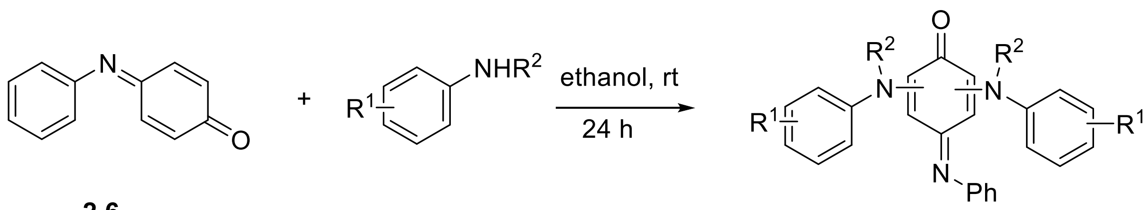

2.6 **2.26a-f** **2.27a-f**

Entry	Aniline 2.26	R^1	R^2	Yield (%) 2.27
1	**a**	H	H	56
2	**b**	4-OMe	H	60
3	**c**	4-Cl	H	62
4	**d**	4-CF_3	H	68
5	**e**	2-Me	H	67
6	**f**	H	Me	66

The reactions were conducted by adding two equivalents of the arylamine to azaquinone in ethanol and stirring the mixture at room temperature for 24 h. The crude products from the reaction mixture were purified by normal phase column chromatography. The two singlet signals characteristic of a di-substituted quinoid ring were observed for all the analogues in the ^{1}H NMR spectra. The NH protons were also different and two broad singlets were observed at 8.69 ppm and 7.67 ppm respectively for **2.27a**. The multiplicity of the protons was clearly seen, and the peaks were assigned using ^{1}H and COSY (Fig. 2.11), NOESY (Fig. 2.12) and HMBC N15 (Fig. 2.13) spectra.

The COSY spectrum of **2.27a** (Fig. 2.11) indicates all the spin-spin coupled protons and as such was used to assign the chemical shifts to the different protons of the aryl rings. The triplet at δ 7.45 is coupled to the doublet at δ 7.35 (cross peaks 1) and coupled to the triplet at δ 7.24 (cross peaks 2), corresponding to the chemical shifts for a phenyl ring. In the same way, the triplet at δ 7.41 is coupled to the doublet at δ 6.98 (cross peaks 5) and coupled to the triplet at δ 7.17 (cross peaks 3), corresponding to the chemical shifts for another phenyl ring. As before, the triplet at δ 7.29 is coupled to the doublet at δ 7.08 (cross peaks 4) and to the triplet at δ 7.06 (cross peaks 6).

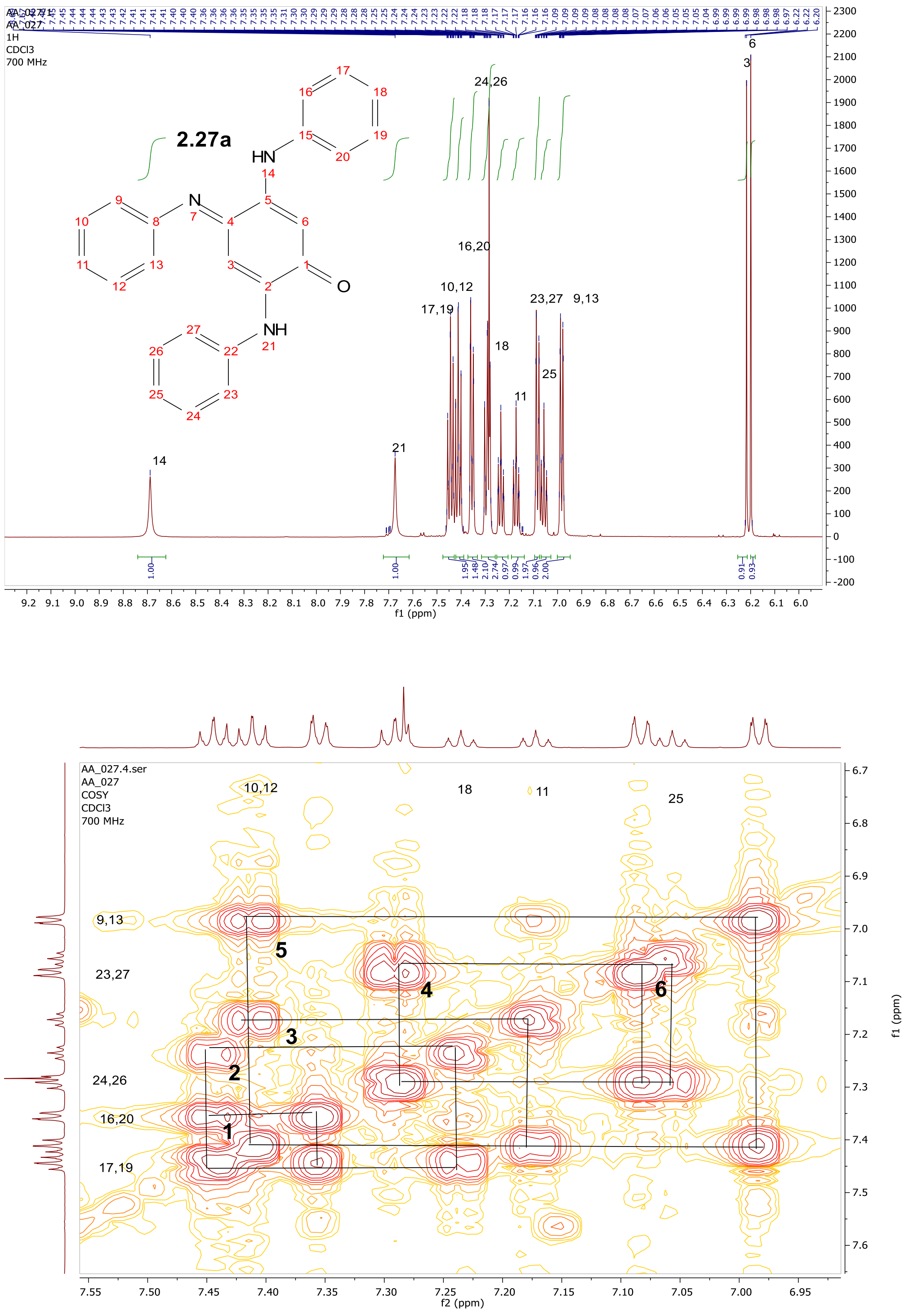

Figure 2.11: ^{1}H NMR and COSY spectra of **2.27a**

However, the data from the COSY spectrum was insufficient to determine the position of attachment of the two arylamines on the quinoid ring and the third phenyl ring (the imino *N*-phenyl group).

The 1D NOESY spectrum of **2.27a** (Fig. 2.12) was used to detect through-space interactions between the protons in the molecule. When one of the singlets at δ 6.22 corresponding to a quinoid proton was irradiated, a NOE correlation was observed with the peak at δ 6.98. This suggests that the phenyl ring with the peak at δ 6.98 is the *N*-phenyl group attached to the imine, suggesting the compound is the *E*-isomer. A NOE was also observed between the singlet at δ 6.22 and the peak at δ 7.08 which corresponds to a doublet. This suggests that the phenyl ring with the peak at δ 7.08 is the *N*-phenyl which is ortho to the carbonyl carbon and should be attached to carbon 2 of the quinoid ring rather than carbon 6. This is because there would be no proximity between the *N*-phenyl attached to the imine and the *N*-phenyl having the peak at δ 7.08 if it was attached to carbon 6 of the quinoid ring.

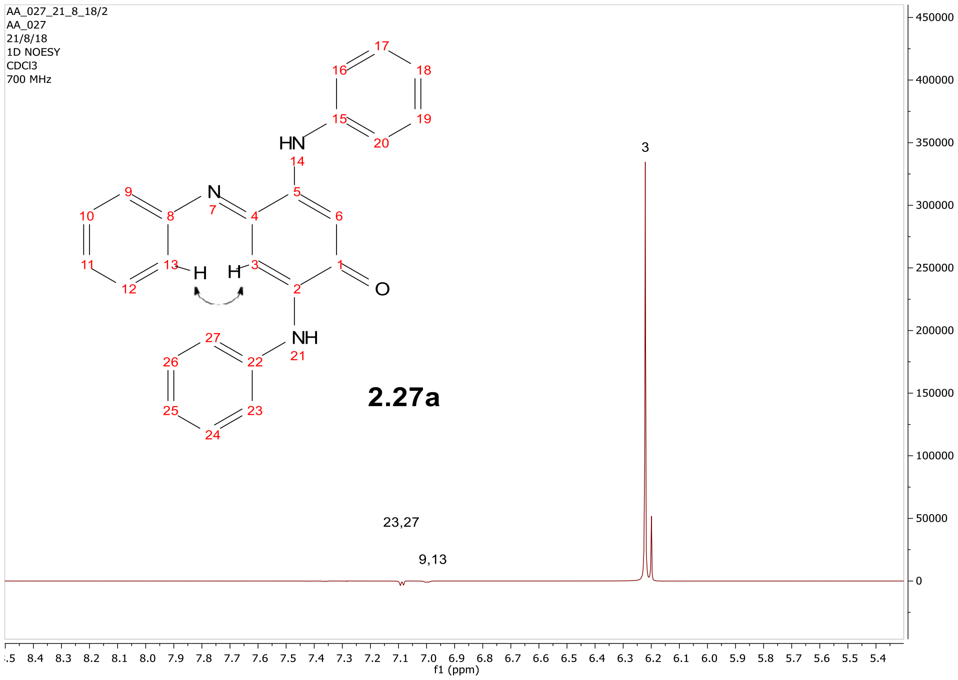

Figure 2.12: 1D NOESY spectrum of **2.27a**

The HMBC N15 spectrum (Fig. 2.13) was also used to determine the position of attachment of the NHs on the quinoid ring and the phenyl ring attached to them. A coupling between the NH at δ 8.69 and the doublet at δ 7.35 indicates that the phenyl ring with the doublet δ 7.35 is attached to the NH at δ 8.69. In the same way, a coupling between the NH at δ 7.67 and the doublet at δ 7.08 indicates that the phenyl ring with the doublet δ 7.08 is attached to the NH at δ 7.67. A coupling was also observed between the NH at δ 8.69 and the quinoid proton at δ 6.20, suggesting that the *N*-phenyl with NH δ 8.69 is ortho to the quinoid proton at δ 6.20. Similarly, a coupling between the NH at δ 7.67 and the quinoid proton at δ 6.22 suggests that the *N*-phenyl with NH δ 7.67 is ortho to the quinoid proton at δ 6.22.

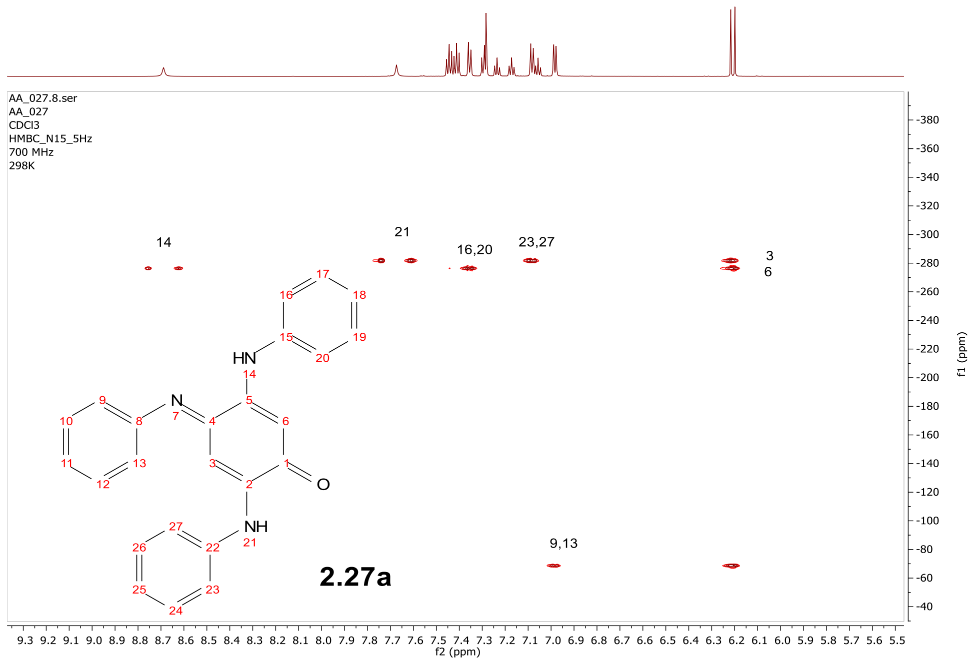

Figure 2.13: HMBC N15 spectrum of **2.27a**

A secondary amine, *N*-methylaniline **2.27f**, was also used in the reaction and it gave the expected result in good yield (66%), a similar percentage to the primary amine derivatives. The ^{1}H NMR spectrum (Fig. 2.14) shows the two singlets characteristic of the di-substituted quinoid ring at 5.80 ppm and 5.75 ppm and the two singlets of the methyl protons at 3.31 ppm and 3.04 ppm highlighting that the two methyl groups are different. It also confirms 1,4-addition and relative para-orientation of the two groups suggesting that the extra steric hindrance of a secondary aniline or change in pK_a did not affect the outcome of the reaction.

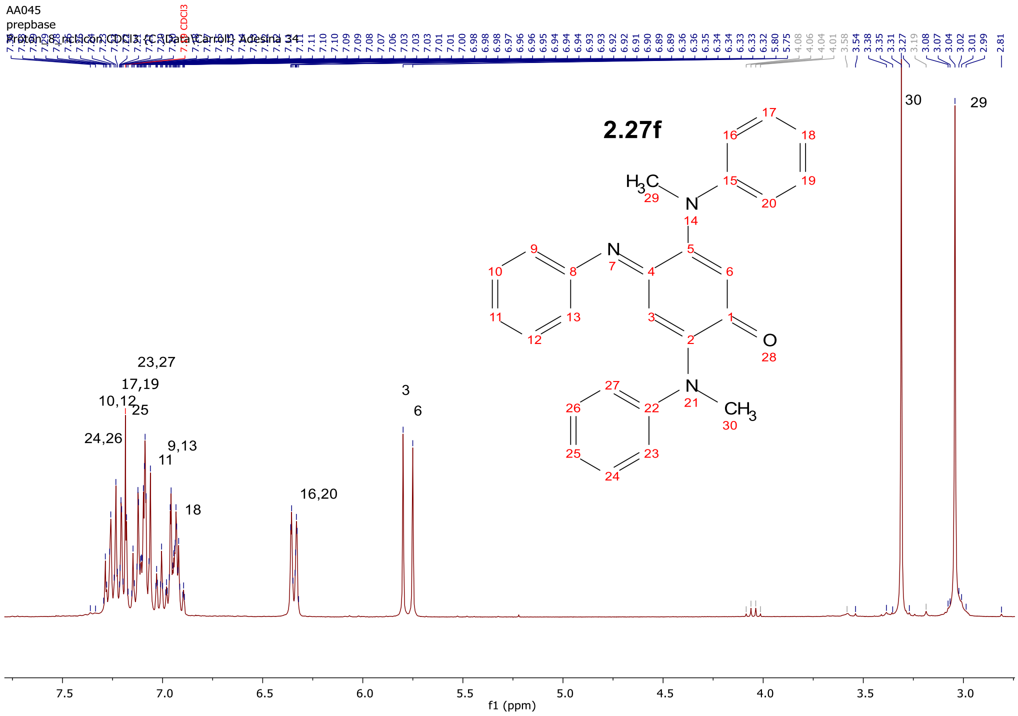

Figure 2.14: ^{1}H NMR spectrum of compound **2.27f**

The structural assignment was also confirmed by X-ray analysis of single crystals of **2.27c, 2.27d, 2.27e and 2.27f** (Fig. 2.15) and it shows the arylamino disubstituted product as one substituent ortho to the carbonyl carbon and the other ortho to the imino carbon as predicted by the 2D NMRs i.e **2.21** (Fig. 2.10). This data also confirms the *E*- conformation of the arylamino disubstituted product as shown by the NOESY spectrum. The crystal structures also show that the phenyl ring is twisted relative to the quinoid ring suggesting that the phenyl ring is not in conjugation with the quinoid ring. The dianilino compounds were coloured compounds, and their colour was found to be dependent on substitution. They may therefore be of importance in the dye industry.

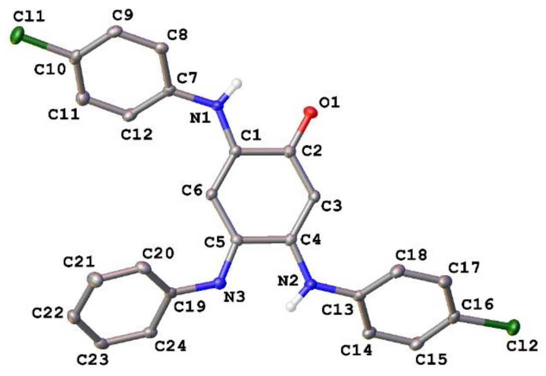

2.27c

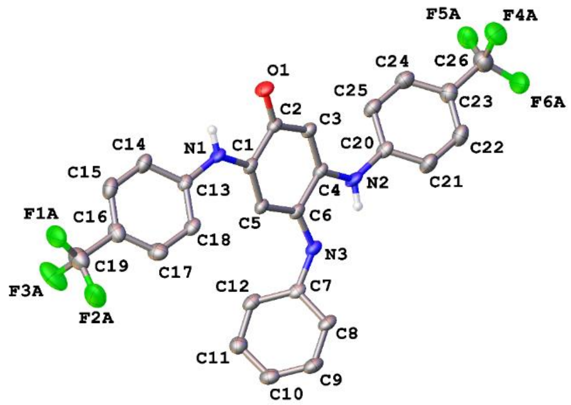

2.27d

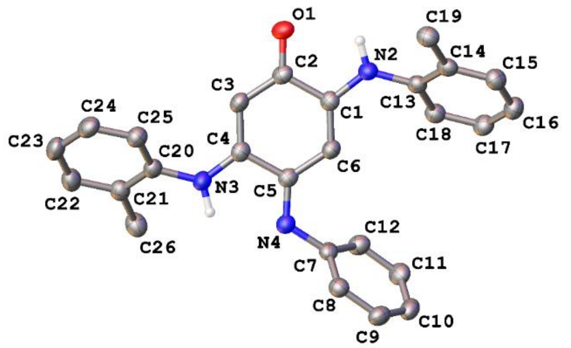

2.27e

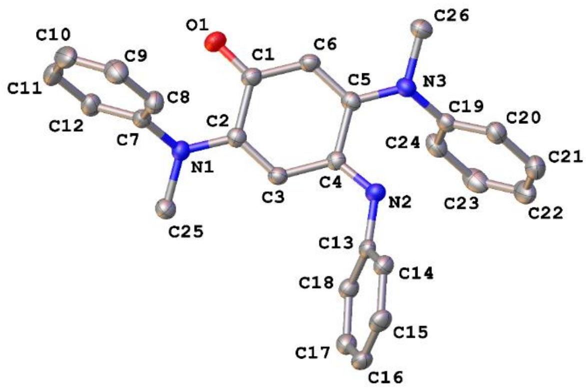

2.27f

Figure 2.15: Crystal Structures of **2.27c**, **2.27d, 2.27e** and **2.27f**

The structure of 2,5-diarylamino derivatives, **2.21**, confirmed by the crystal structures and 2D NMR data of some of the analogues, is therefore as shown in Scheme 2.12.

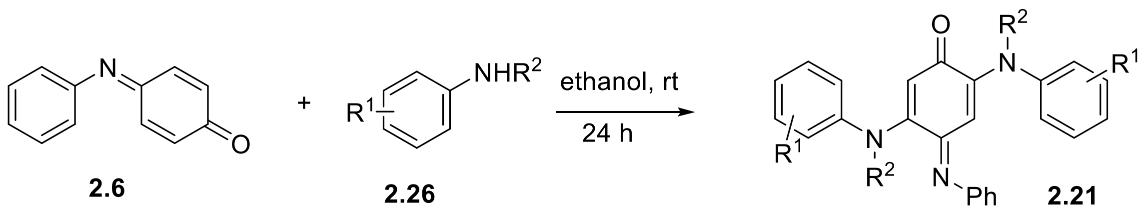

Scheme 2.12: Regiochemistry of 2,5-diarylamino-1,4-benzoquinone-4-phenylimines, **2.21**

The first addition of the aromatic amines could be either to the α,β-unsaturated ketone giving the mono-addition product **2.28** or to the α,β-unsaturated imine giving the mono-addition product **2.29** as shown in Scheme 2.13.

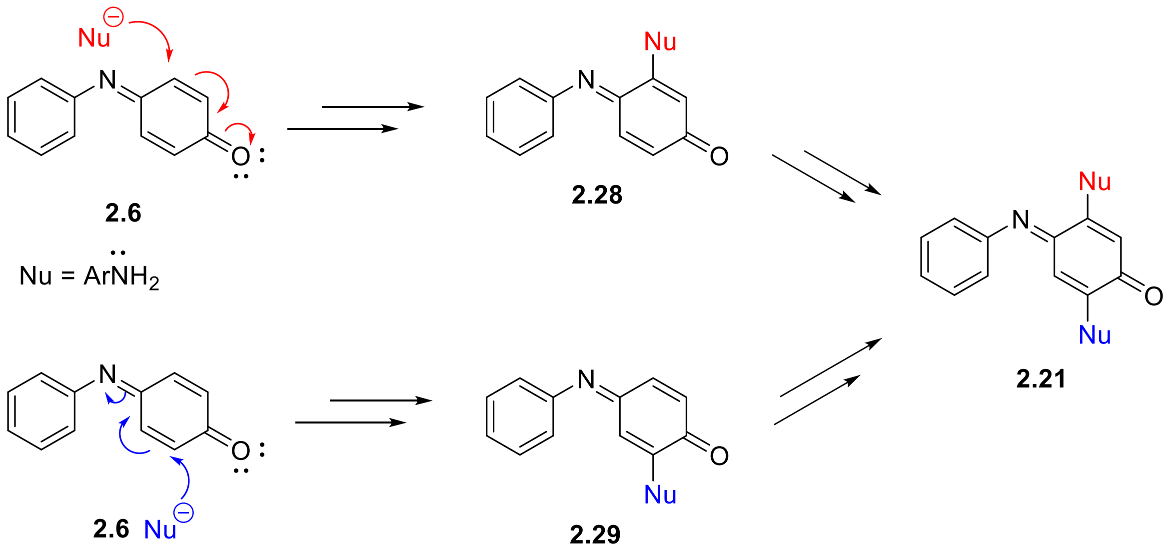

Scheme 2.13: Options of 1,4-Conjugate addition to give the di-aniline addition product **2.21**

The reactions of aniline with azaquinone were carried out using different equivalents of the amine in order to find out if the mono-addition products could be detected and isolated and thus determine the position of initial nucleophilic attack i.e. conjugate addition to the α,β-unsaturated imine or the α,β-unsaturated ketone. Surprisingly, it was observed that di-addition products were still formed with reduced equivalents of aniline, but in reduced yields, giving more unreacted starting material as the amine equivalents were reduced, the results are shown in Table 2.8.

Table 2.8: Reaction of aniline with azaquinone using different equivalents

Azaquinone 2.6	Aniline	2.21a:2.6
1 equiv.	2 equiv.	3:1
1 equiv.	1 equiv.	1:1
1 equiv.	0.5 equiv.	1:5

Polar aprotic solvents (acetonitrile, DMF, and DCM) and non-polar solvents (dioxane and toluene) under anaerobic conditions were also used to investigate the generation of the mono-addition products. All solvents gave the same di-addition product with no trace of the mono-addition product(s) by ^{1}H NMR. Timed experiments (1 h to 24 h) were done to monitor the progress of the reaction but the di-addition product and unreacted azaquinone were the only components observed. This suggests that the mono-addition products **2.28** and **2.29** may not be the intermediates in the reaction of azaquinone with aniline.

It was reported by E. V. Tsoi[5] et al that when 2,5-diarylamino iminoquinones **2.21** were heated in the presence of air or $K_3Fe(CN)_6$, they were converted to phenazinones **2.22** in good yields, resulting from the intramolecular nucleophilic substitution of the hydrogen atom ortho to the nitrogen in the *N*-phenyl ring by the spatially close arylamine residue (Scheme 2.14). The structures were confirmed by ^{1}H NMR spectra and the identical character of **2.22a** to 2-phenylamino-5-phenyl-3-phenazinone which was obtained by an alternative route.

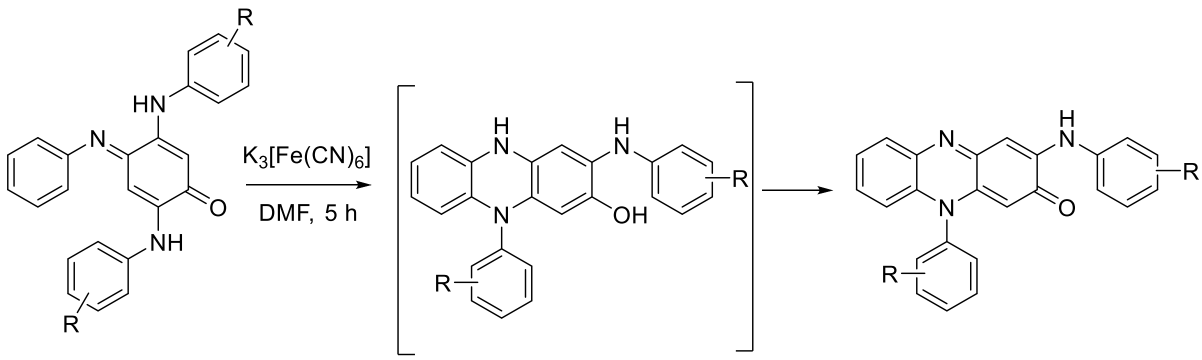

2.21 R = (a) H, (b) OCH_3, (c) CH_3, (d) Br, (e) Cl **2.22**

Scheme 2.14: Intramolecular oxidation of **2.21** to give phenazinones **2.22**

Now that the dianilino azaquinone derivatives were available, the oxidative cyclisation step to give phenazinones **2.22** had been attempted in DMF with two equivalents of $K_3[Fe(CN)_6]$, and the mixture heated at reflux for 5 h. However, no visible change was observed as the ^{1}H NMR spectrum was the same as the diarylamino substituted products. This could be due to the *E*-isomerism of the dianilino compounds, as it has been reported in a comparative study that the *Z*-isomer of 2-benzamido-3-phenylacrylohydrazide **2.31** underwent cyclization to give the imidazole derivative **2.33** and triazinone derivative **2.34**, whereas the *E*-isomer **2.32** did not undergo such cyclization (Scheme 2.15).[164]

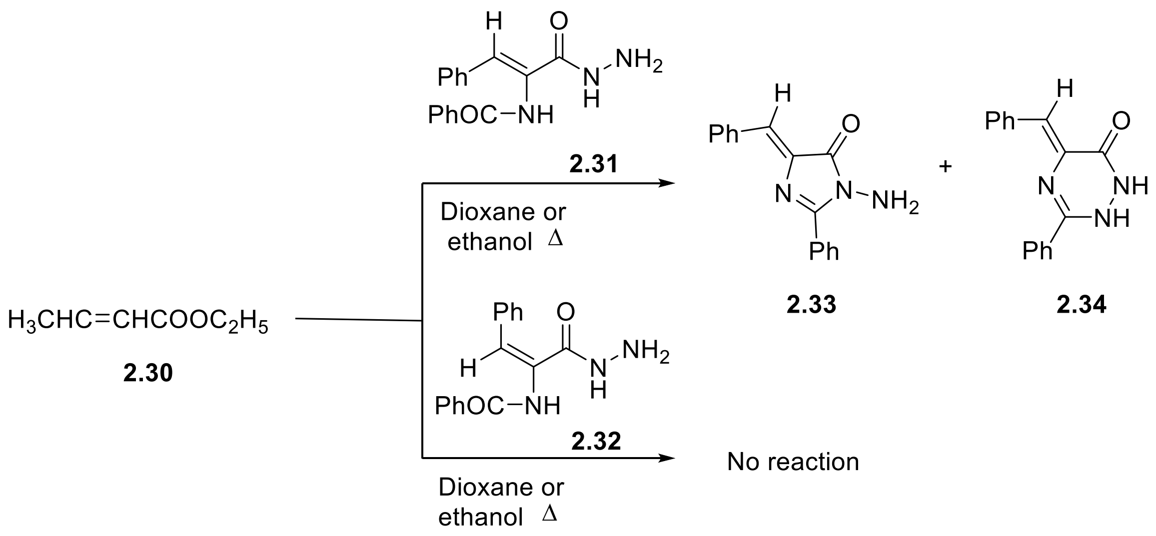

Scheme 2.15: Cyclization of 2-benzamido-3-phenylacrylohydrazide

2.3.2 Aliphatic amine Addition

Since the nucleophilic addition of aromatic amines to azaquinone was found to be 1,4-selective and results in double addition, it would be interesting to investigate the addition of aliphatic amines to azaquinone and compare results.

The addition of primary aliphatic amines to azaquinone has been reported by K.S. Cottman[6] as a process for preparing *N*-substituted phenylenediamines. The reaction proceeds via 1,2-addition to the carbonyl group which on reduction gives 1,4-diaminoarenes (Scheme 2.16). Solvents which may be used in the reaction include methanol, tetrahydrofuran, toluene, dichloromethane, and ethanol.[6] The reported solvent was toluene and the reaction was conducted at 110 °C. The reaction was also conducted in the presence of an acid catalyst, to facilitate addition to the carbonyl group. Reductive work-up, using aqueous sodium hydrosulfite, converted the product *N*-phenyl-*N*'-diimines, **2.36** to the desired *N*-substituted phenylenediamines, **2.37**. These *N*-substituted phenylenediamines have found utility in the production of drugs, agricultural products, and are also useful as dyes, antioxidants, antiozonants, gel inhibitors and anti-degradants in rubber.[6,165,166]

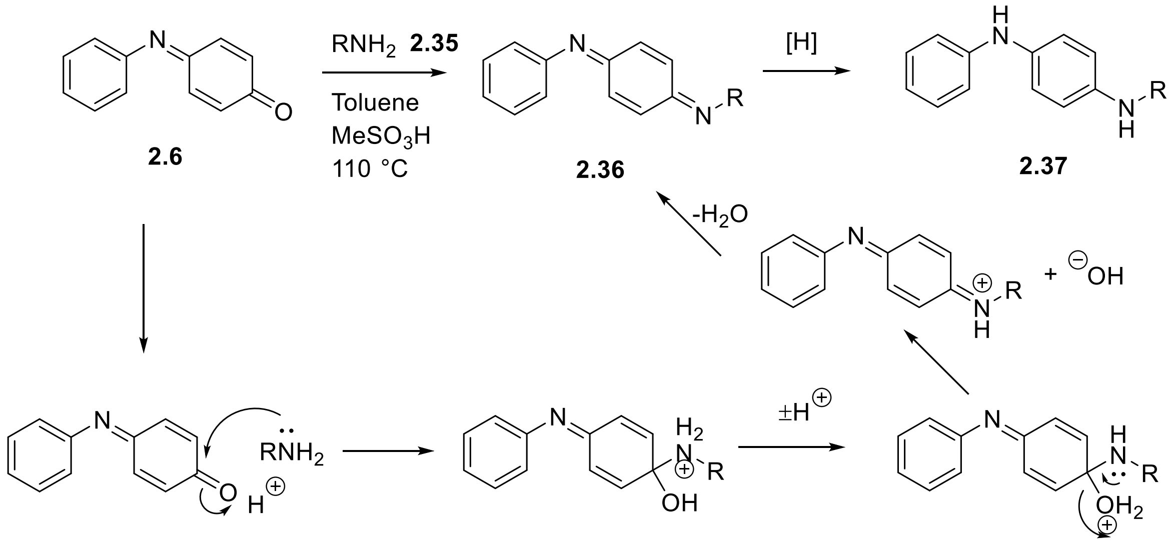

Scheme 2.16: Addition of aliphatic amines to azaquinone

The reactions were repeated by ourselves by adding two equivalents of the primary amine to azaquinone in toluene at 110 °C (Scheme 2.17). Methanesulfonic acid was used as the acid catalyst, and aqueous sodium hydrosulfite for the reduction step. Some of the targeted compounds were isolated in good yields first by tandem reverse phase chromatography and then acid-base extraction. The results are given in Table 2.9.

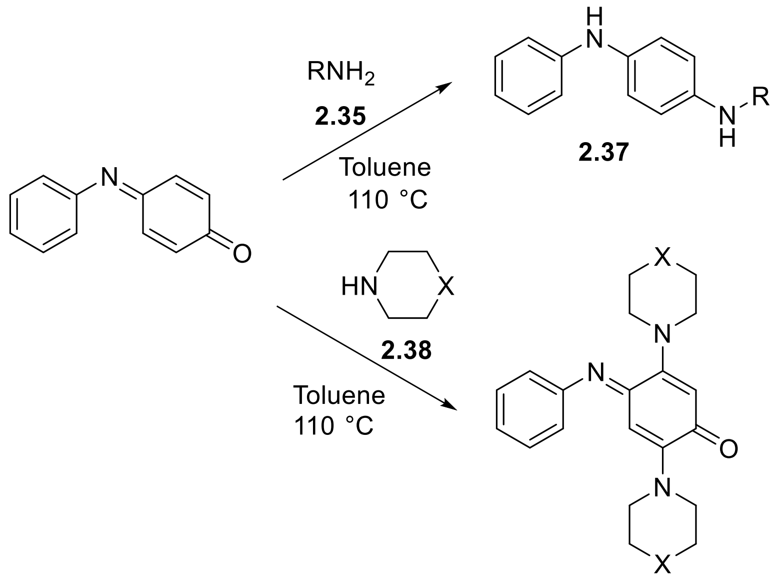

Scheme 2.17: Reaction of azaquinone with aliphatic amines

Table 2.9: Aliphatic Amine Addition

Entry		**Amine**	**Yield (%) 2.37**
1	**2.35a**	R = $PhCH_2$	60
2	**2.35b**	R = C_8H_{17}	62
3	**2.35c**	R = C_6H_{11}	84[a]
4	**2.35d**	R = $(CH_3)_2CH$	78[a]
5	**2.38a**	X = CH_2	**2.39a** 82[a]
6	**2.38b**	X = O	**2.39b** 80[a]

[a] yield determined from the ^{1}H NMR of the crude mixture

Two secondary amines were also considered in this reaction, piperidine **2.38a** and morpholine **2.38b** and they both seem to react like the aromatic amines, having the two singlets at 5.66 ppm and 5.57 ppm for the reaction with piperidine (spectrum 1) and at 5.66 ppm and 5.62 ppm for the reaction with morpholine (spectrum 2). These singlets are characteristic of the di-substituted quinoid ring, although the products were only present in low yields (Fig. 2.16). This change in reactivity observed with the secondary aliphatic amines could be due to the cyclic nature of the amines considered, pKa changes or increased steric hindrance around the *N* lone pair.

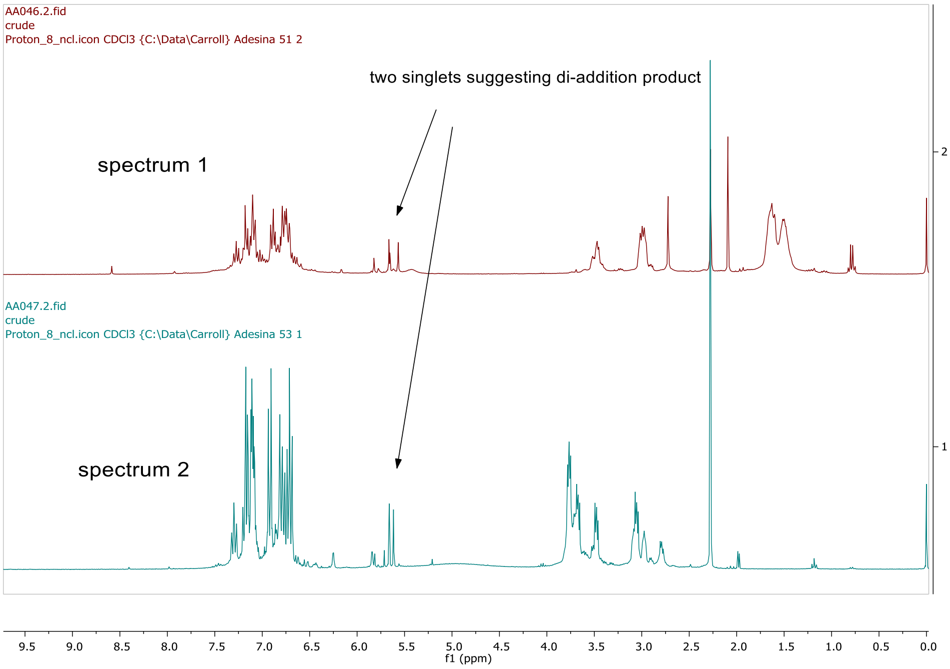

Figure 2.16: ^{1}H NMR of crude mixture of the reaction of azaquinone with piperidine **2.38a** (spectrum 1) and the reaction of azaquinone with morpholine **2.38b** (spectrum 2)

In summary, the reaction of aromatic amines proceeds via 1,4-conjugate addition process and always results in di-addition irrespective of the relative amounts of aniline whilst primary aliphatic amines result in direct 1,2-addition to the carbonyl group which on reductive work-up gives 1,4-diaminoarenes.

The outcome with secondary amines varied however, with anilines such as *N*-methylaniline performing as demonstrated for aniline whereas in the case of aliphatic amines the result is different with 1,4-conjugate addition rather than 1,2-addition now being the preferred reaction pathway.

2.3.3 Computational studies of azaquinone and its reactions with amines

Initial calculations were carried out using Gaussian software for the azaquinone structure to determine the charges on each carbon atom and hence establish a possible order of reactivity for the different positions.[167] The calculation type used for the studies is FOPT, calculation method is RHF (Restricted Hartree-Fock) and the basis set is 6-31G.

The relative charge distribution of the molecule is as expected for C1 and C4 given that they are both attached to electronegative elements (O and N respectively). The positive charge on C1 is higher than that on C4 because oxygen is more electronegative than nitrogen suggesting this would be the preferred site of reaction for 'hard' nucleophiles (Fig. 2.17). Carbons 2, 3, 5 and 6 are surprisingly seen to all have negative charges. The α,β-keto carbons, C3 and C5, have smaller negative values and therefore are likely to be the most reactive towards nucleophiles than the α,β-imino carbons, C2 and C6. This means that C3 and C5 are more electrophilic than C2 and C6 and will be the preferred position of the two unsaturated systems of attack for 'soft' nucleophiles. Indeed, experimental results of 1,4-addition of nucleophiles[5,168] suggest these sites are electrophilic in nature.

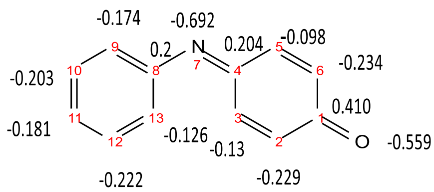

Figure 2.17: Azaquinone structure with charge distribution

Transition states can be localized in many cases through scanning one structural degree of freedom. This will be successful if the reaction pathway can be described by essentially one structural parameter. In order to cover the relevant part of a potential energy surface, a series of calculations must be performed in which one of the structural parameters is fixed to a certain value, while all other parameters are optimized to their most favourable values. This is the relaxed potential energy surface (PES) scan. The PES is calculated for the attack of the aromatic amines on the different carbon positions, giving HOMO and LUMO values. The HOMO-LUMO gap is then calculated from these values obtained (Table 2.10).

Table 2.10: Optimisation Result Summary of Azaquinone

E(RHF)	-588.69419476 au
RMS Gradient Norm	0.00001785 au
Dipole Moment	5.0583 Debye
HOMO value	-0.31369 au
LUMO value	0.01126 au
HOMO-LUMO gap	-0.32495 au

Reactions with Aromatic amines:

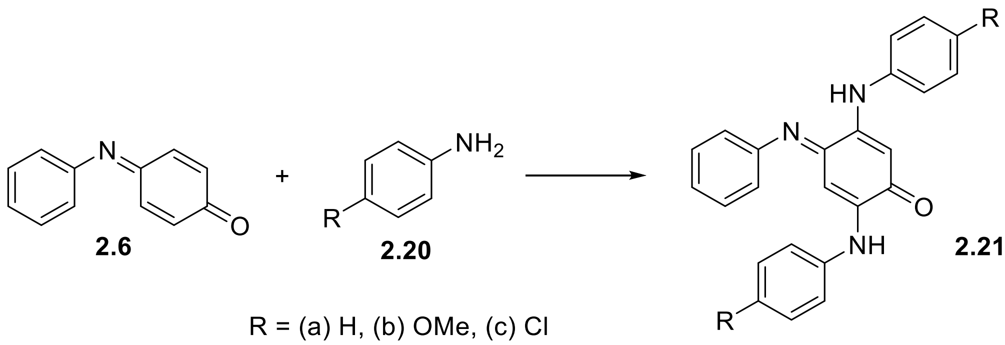

Scheme 2.18: Reaction of aromatic amines with azaquinone

a) Aniline

Since the conjugate addition of nucleophiles involves the movement of electrons from the HOMO of nucleophile (amines in this case) to the LUMO of electrophile (the six carbon atoms in the quinoid ring), it is expected that the smallest difference obtainable will be the preferred position of attack as it has the lowest value. The lowest HOMO-LUMO gap is for carbon position 2 and this matches the position of attack from experimental data.

Table 2.11: Potential Energy Surface Scan

Carbon Position	HOMO (au)	LUMO (au)	HOMO-LUMO gap (au)
1	-0.29576	0.08110	-0.37686
2	-0.20589	0.06059	-0.26648
3	-0.23369	0.07619	-0.30988
4	-0.22742	0.06458	-0.29200
5	-0.24623	0.07712	-0.32335
6	-0.20638	0.06518	-0.27156

b) 4-Methoxyaniline

As observed in the PES scan of azaquinone with aniline, the smallest difference obtainable in the movement of electrons from the HOMO of the nucleophile to the LUMO of the electrophile is seen to be the preferred position of attack by conjugate addition (carbon position 2).

Table 2.12: Potential Energy Surface Scan

Carbon Position	**HOMO (au)**	**LUMO (au)**	**HOMO-LUMO (au)**
1	-0.29408	0.08519	-0.37927
2	-0.20371	0.06283	-0.26654
3	-0.23421	0.07777	-0.31198
4	-0.22058	0.06376	-0.28434
5	-0.24536	0.07967	-0.32503
6	-0.21424	0.06590	-0.28014

c) 4-Chloroaniline

As before, the PES scan of azaquinone with 4-chloroaniline also shows position 2 as the preferred position of attack by the nucleophile, given by the shortest distance obtained for the movement of electrons from the HOMO of the nucleophile to the LUMO of the electrophile.

Table 2.13: Potential Energy Surface Scan

Carbon Position	**HOMO (au)**	**LUMO (au)**	**HOMO-LUMO (au)**
1	-0.30762	0.05932	-0.36694
2	-0.21000	0.05654	-0.26654
3	-0.24145	0.07084	-0.31229
4	-0.22519	0.06139	-0.28658
5	-0.24392	0.07068	-0.31460
6	-0.22304	0.06211	-0.28515

The HOMO-LUMO difference of the PES for the analogues are approximately the same for carbon position 2 (Table 2.14). This also suggests that position 2 is the first preferred position of attack for the aromatic amines.

Table 2.14: Comparison of the analogues for the aromatic amines

R	E(RHF)	Dipole Moment	HOMO-LUMO (au)	HOMO-LUMO of PES Carbon position 2 (au)
H	-874.34	5.67	-0.27687	-0.26648
OMe	-988.16	5.56	-0.30195	-0.26654
Cl	-1333.22	6.78	-0.28709	-0.26654

Reaction with Aliphatic Amines:

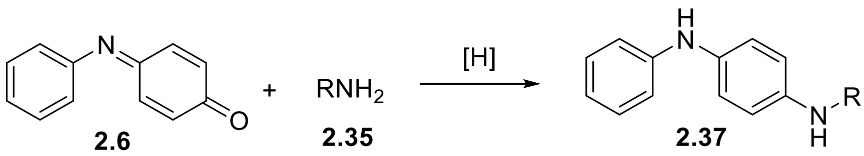

R = (a) C_8H_{17}, (b) C_6H_{11}, (c) CH_3

Scheme 2.19: Reaction of aliphatic amines with azaquinone

a) Octylamine

Table 2.15: Potential Energy Surface Scan

Carbon Position	HOMO (au)	LUMO (au)	HOMO-LUMO (au)
1	-0.28741	0.08755	-0.37496
2	-0.20682	0.06486	-0.27168
3	-0.23979	0.08024	-0.32003
4	-0.22012	0.06567	-0.28579
5	-0.23510	0.08034	-0.31544
6	-0.20967	0.07174	-0.28141

b) Cyclohexylamine

Table 2.16: Potential Energy Surface Scan

Carbon Position	HOMO (au)	LUMO (au)	HOMO-LUMO (au)
1	-0.29235	0.08664	-0.37899
2	-0.20451	0.06149	-0.26600
3	-0.23518	0.07991	-0.31509
4	-0.21931	0.06244	-0.28175
5	-0.24234	0.07698	-0.31932
6	-0.28618	0.02406	-0.31024

c) Methylamine

Table 2.17: Potential Energy Surface Scan

Carbon Position	HOMO (au)	LUMO (au)	HOMO-LUMO (au)
1	-0.30002	0.08114	-0.38116
2	-0.20722	0.06925	-0.27647
3	-0.22963	0.08239	-0.31202
4	-0.21624	0.06401	-0.28025
5	-0.23525	0.08292	-0.31817
6	-0.21089	0.07353	-0.28442

From the PES of the aliphatic amines, the shortest distance from the HOMO of the nucleophile to the LUMO of the electrophile is for position 2. This does not match the experimental data, which gives the position of attack as carbon position 1.

Table 2.18: Comparison of the analogues for the aliphatic amines

R	E(RHF)	Dipole Moment	HOMO-LUMO (au)	HOMO-LUMO of PES Carbon position 1 (au)
C_8H_{17}	-957.01	4.43	-0.33509	-0.37496
C_6H_{11}	-877.81	5.02	-0.33980	-0.37899
CH_3	-683.88	3.10	-0.33300	-0.38116

It is not clear why the lowest HOMO-LUMO difference matches the experimental position of attack for the aromatic amines (position 2) while the lowest HOMO-LUMO difference does not match the experimental position of attack for the aliphatic amines (position 1). This suggests that this molecular modelling method needs modification to accurately predict the reactivity of this type of compounds.

Another method used to investigate the reactivity, position of nucleophilic attack for azaquinone and the preferred reaction pathway for the reaction of azaquinone with amines was by using ArgusLab software.[169] The chemical structure of azaquinone was generated and geometry optimisation was performed on a computer. The AM1 method was used to generate the heat of formation, SCF energy, Mulliken atomic charges, ground state dipole (debye) and ZDO atomic charges of azaquinone (Tables 2.19 and 2.20). The AM1 as a semiempirical method, addresses two limitations of the Hartree-Fock calculations – low speed and low accuracy, by omitting or parameterizing certain integrals based on experimental data, such as ionization energies of atoms, or dipole moments of molecules.[170]

Table 2.19: Ground State Dipole (debye)

X	**Y**	**Z**	**Length**
-3.76662256	-0.40777185	0.00023632	3.78863081

Heat of formation of azaquinone was 59.7567 kcal/mol and the SCF energy was found to be -80.2961482703 au (-50386.6392 kcal/mol) as calculated by AM1 method using ArgusLab 3.0.

Table 2.20: Mulliken Atomic Charges and ZDO Atomic Charges of azaquinone

S.No	Atoms	ZDO atomic charges	Mulliken atomic charges
1	C	-0.0068	0.0015
2	C	-0.1345	-0.1914
3	C	-0.1335	-0.1941
4	C	-0.1104	-0.1736
5	C	-0.1389	-0.2024
6	C	-0.0814	-0.1367
7	C	-0.2131	-0.2808
8	C	0.2720	0.2999
9	C	-0.1844	-0.2510
10	C	-0.1274	-0.1887
11	C	-0.0677	-0.1262
12	C	0.0502	0.0703
13	N	-0.1435	-0.2016
14	O	-0.2738	-0.3005
15	H	0.1310	0.1902
16	H	0.1357	0.1987
17	H	0.1369	0.2003
18	H	0.1380	0.2015
19	H	0.1495	0.2166
20	H	0.1569	0.2252
21	H	0.1540	0.2220
22	H	0.1372	0.1986
23	H	0.1539	0.2223

A mapped surface was generated for azaquinone. This is a surface where one property is superimposed onto a surface created by another property. Fig. 2.18 shows HOMO-LUMO difference mapped onto the electron density surface for the ground state of azaquinone. The colour map shows the energy (in hartrees) for the various colours. The red colour on the surface shows region of high electron density. Nucleophilic attack is less likely to occur at these regions but more likely to occur at the α,β-keto carbons since they have low electron density. This matches experimental result which shows that the α,β-keto carbons are more electrophilic in nature.

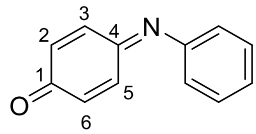

2.6

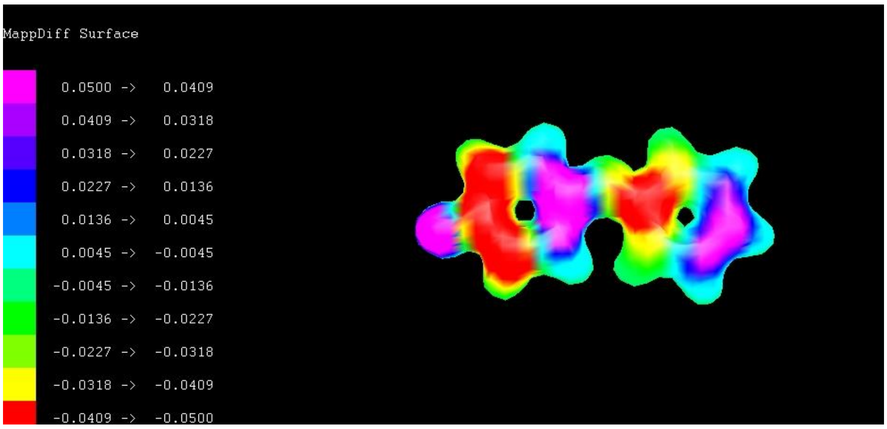

Figure 2.18: HOMO-LUMO mapped electron density surface of azaquinone

The HOMO-LUMO difference mapped onto the electron density surfaces for the two possible mono-addition products are as shown (Fig. 2.19 and 2.20). The red end of the spectrum shows regions of highest stability for a positive test charge, magenta/ blue shows the regions of least stability for a positive test charge.

Fig. 2.19 suggests that a second nucleophilic attack would be at carbon 5 (the more electrophilic carbon), giving a di-addition product with both nucleophiles ortho to the imino carbon. This implies that the mono-addition product **2.28** may not be the proposed intermediate for the reaction of azaquinone with anilines. Similarly, Fig. 2.20 suggests that a second nucleophile would attack carbon 2, giving a di-addition product with both nucleophiles ortho to the carbonyl carbon. The mono-addition product **2.29** may therefore not be the intermediate.

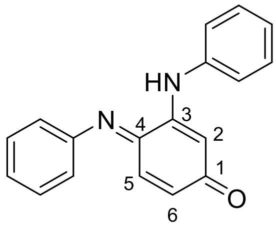

2.28

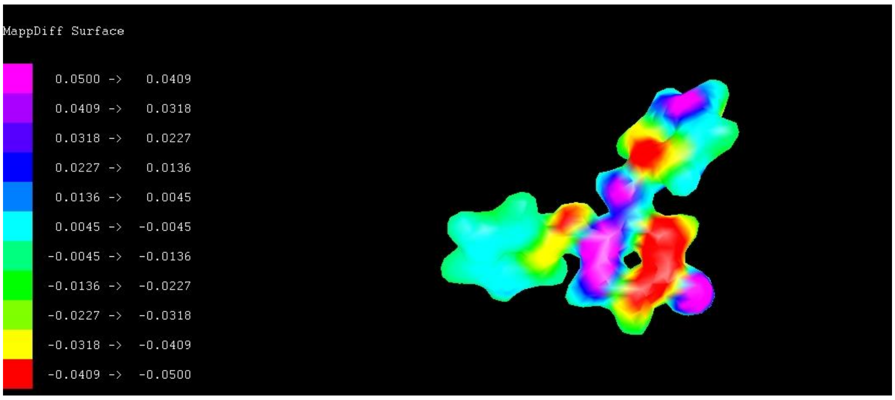

Figure 2.19: HOMO-LUMO mapped electron density surface of α,β-keto mono-addition product **2.28**

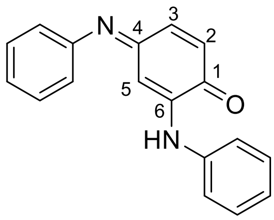

2.29

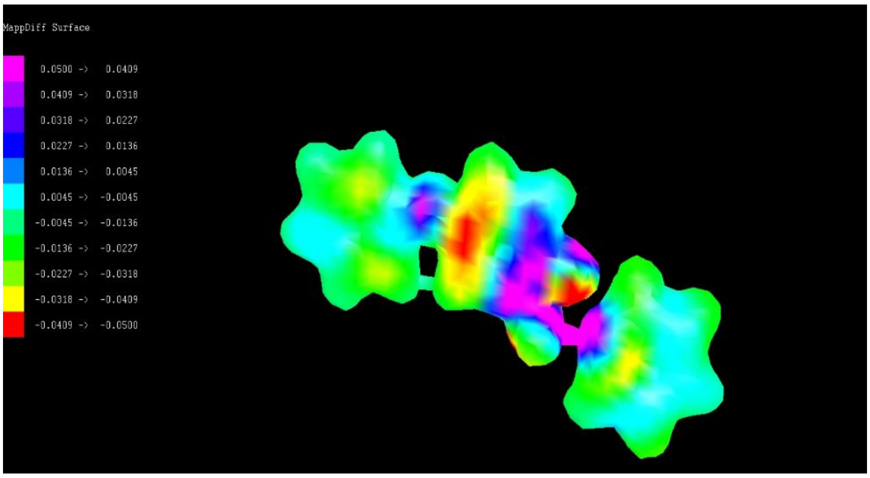

Figure 2.20: HOMO-LUMO mapped electron density surface of α,β-imino mono-addition product **2.29**

Another option considered was to generate the mapped electron density surfaces for the proposed intermediates **2.40** and **2.41** (Scheme 2.20).

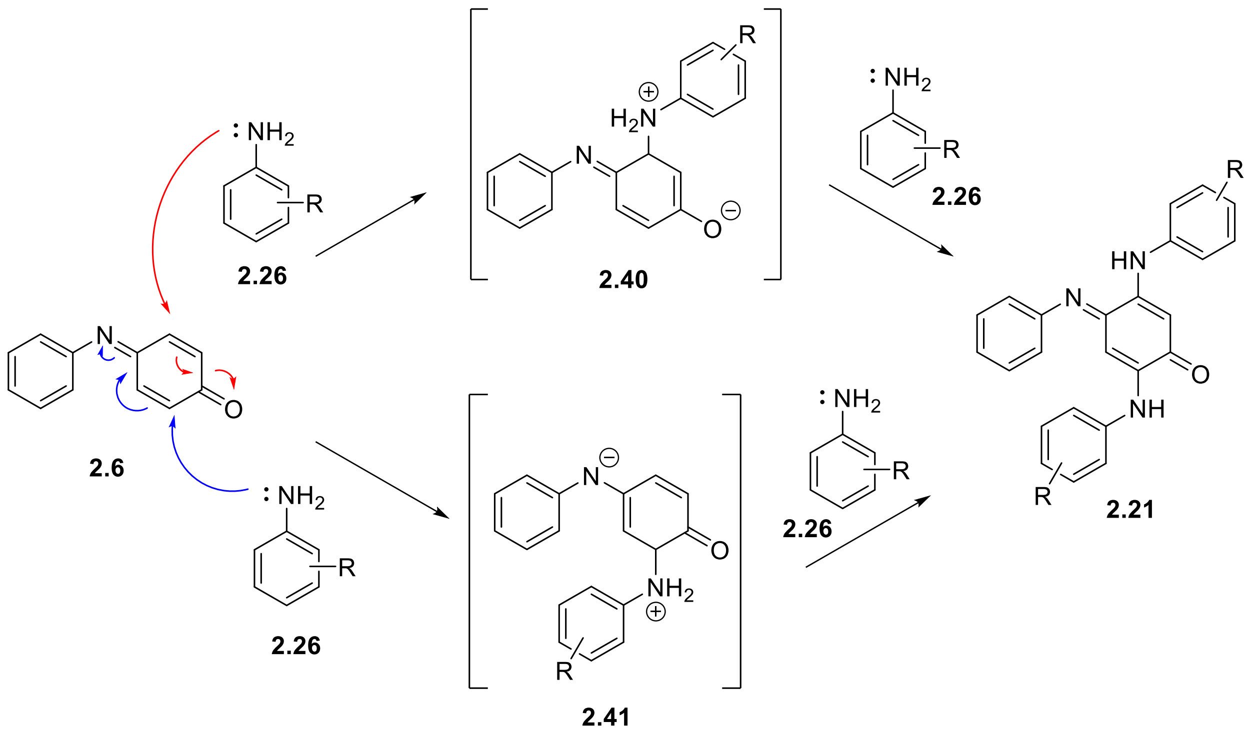

Scheme 2.20: Conjugate addition of aromatic amines to the α,β-unsaturated ketone and imine of azaquinone

Fig. 2.21 suggests that a second nucleophilic attack would preferably be at carbon position 6 which would give the di-addition product **2.21** with both nucleophiles para-oriented with respect to each other. On the other hand, Fig. 2.22 suggests that a second nucleophile would attack carbon 2, giving a di-addition product with both nucleophiles ortho to the carbonyl carbon. This implies that the intermediate for the reaction would be **2.40** and would give the preferred reaction pathway as shown in Scheme 2.20. This explains why no mono-addition product is detected in the reaction since the intermediate **2.40** is readily converted to the di-addition product **2.21** by a second nucleophilic attack.

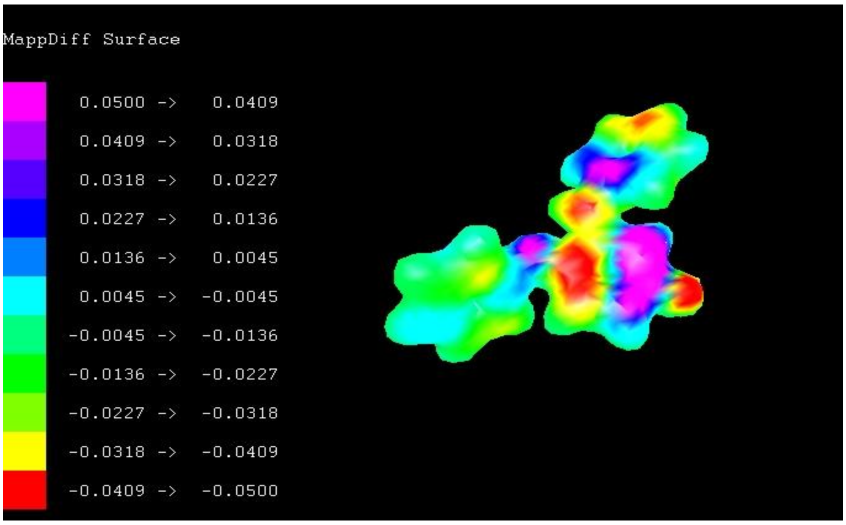

Figure 2.21: HOMO-LUMO mapped electron density surface of α,β-keto intermediate **2.40**

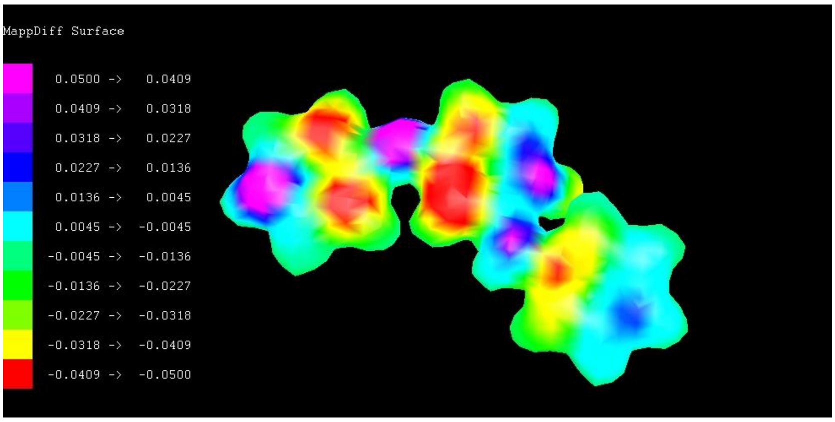

Figure 2.22: HOMO-LUMO mapped electron density surface of α,β-imino intermediate **2.41**

This approach to predict reactivity can be related to the Fukui function which describes the electron density after adding or removing some number of electrons. It can predict where the most electrophilic and nucleophilic sites on a molecule are. The Fukui equation for the electrophilic attack, f^-, for when 1 electron is removed is given by $f^- = \rho(N) - \rho(N-1)$. Equally, the Fukui function for the nucleophilic attack, f^+, for when 1 electron is added is given by $f^+ = \rho(N+1) - \rho(N)$.

The Dual Descriptor is a way to combine the two Fukui functions. It has a positive value where it is electrophilic and negative where it is nucleophilic. It is implemented as the difference between the Fukui plus and Fukui minus functions, given by $f(r) = f^{+} - f^{-}$.

The Fukui function has been widely applied to the interpretation of reactivity in organic molecules. The "dual descriptor", which has been more recently introduced, provides particularly powerful insight into chemical reactivity in a clear and simple way.[171,172]

2.4 Reaction with Sulfur Nucleophiles

2.4.1 Addition of sodium arenesulfinates

The reaction of azaquinone derivatives with sodium arenesulfinates **2.43** has been reported by Konovalova et al.[7] The reactions were carried out in acetic acid using two equivalents of the nucleophile, however the reactions afforded exclusively the product of single 1,4-addition to the α,β-unsaturated imino system **2.44**. This was then oxidised with lead (IV) acetate to the corresponding 1,4-benzoquinone imine derivatives **2.45** (Scheme 2.21).

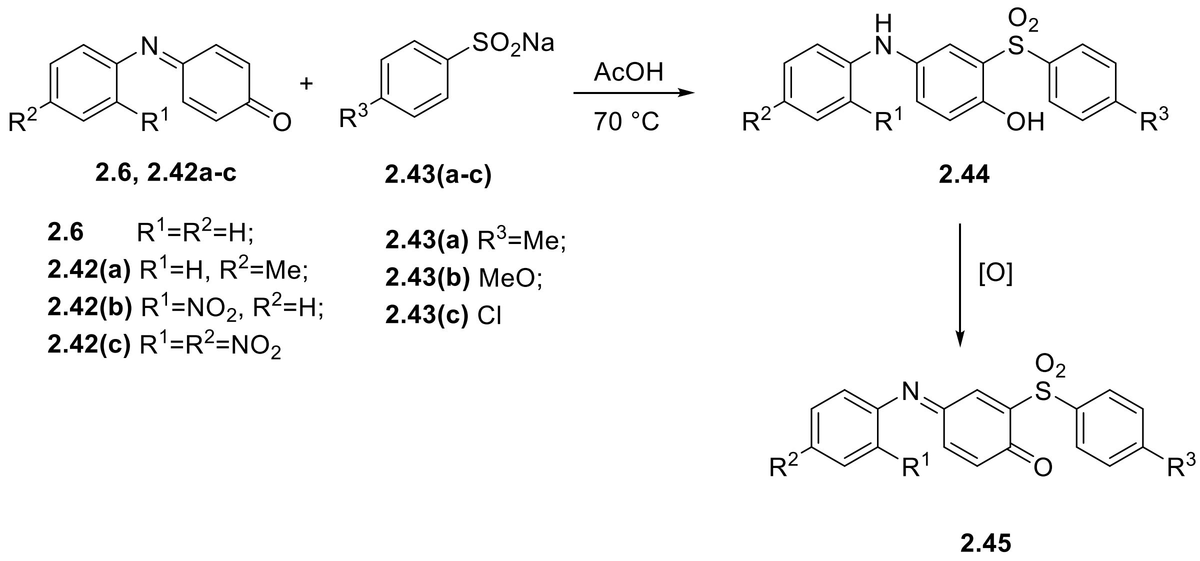

Scheme 2.21: Addition of sodium arenesulfinates to azaquinone derivatives

The reactions of azaquinone with sodium arenesulfinates **2.46** were repeated by ourselves by adding the sodium arenesulfinates to azaquinone **2.6** in acetic acid, and heating to 70 °C until the mixture turned colourless. After cooling, water was added until complete precipitation of the solid occurred which was then removed by filtration to give the product **2.47** as shown in Scheme 2.22. The reaction of sodium arenesulfinates with azaquinone occured by 1,4-addition to the α,β-unsaturated imine, giving mono-addition products only. This method is an alternative route to making this type of sulfones.

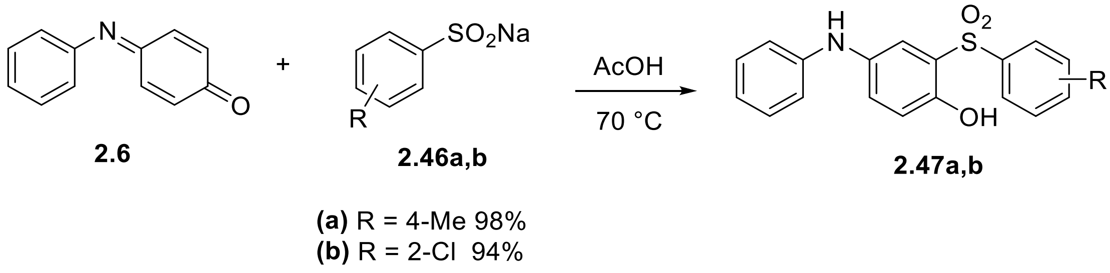

Scheme 2.22: Reaction of azaquinone with sodium arenesulfinates

Some polymers containing sulfone groups are useful engineering plastics as they exhibit high strength and resistance to oxidation, corrosion, high temperatures, and creep under stress, for example, some are valuable as replacements for copper in domestic hot water plumbing.[173] Precursors to such polymers are the sulfones bisphenol S **2.48** and 4,4'-dichlorodiphenyl sulfone **2.49** (Fig. 2.23). Examples of sulfones in pharmacology include dapsone **2.50**, a drug formerly used as an antibiotic to treat leprosy. Several of its derivatives, such as promin, have similarly been studied or applied in medicine.[174]

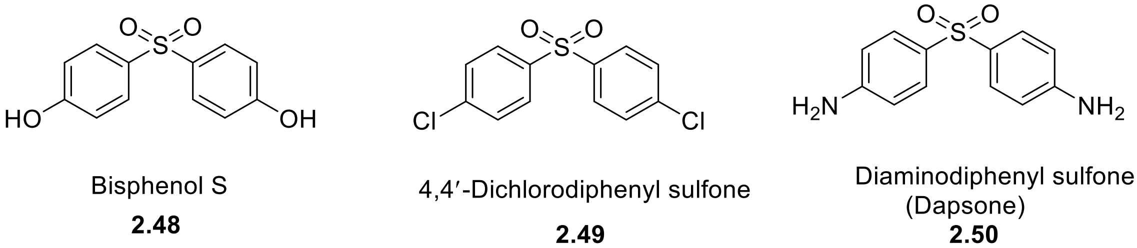

Figure 2.23: Some useful sulfone-containing compounds

2.4.2 Subsequent tandem reactions: A new route to phenoxathiin dioxide

Since many natural products and druglike compounds possess heterocyclic subunits, the ability to synthesize efficiently diverse heterocyclic compounds is critical. A method of preparing phenoxathiin-10,10-dioxide has been reported by

C. L. Deasy.[175] Phenoxathiin-10,10-dioxide, **2.53** is formed when phenoxathiin, **2.52** is oxidised by chromic acid, by potassium permanganate, or by prolonged treatment with hydrogen peroxide, it is obtained as colourless needles after recrystallization from dilute acetic acid.[176,177] Phenoxathiin was made by the Ferrario reaction,[178] the reaction between diphenyl ether, **2.51** and sulfur in the presence of anhydrous aluminium chloride (Scheme 2.23).

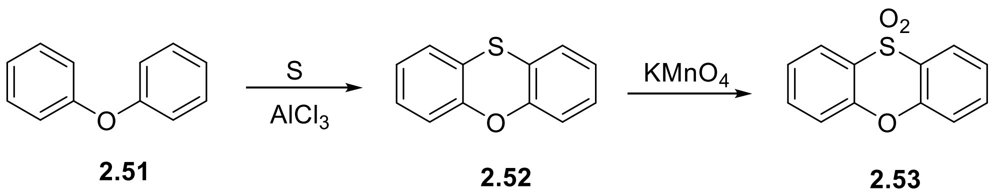

Scheme 2.23: Preparation of phenoxathiin-10,10-dioxide using the Ferrario reaction

Various alkyl or cycloalkylphenoxathiins, their oxides and dioxides and their halogen derivatives are recommended for use as insecticides in dusts or sprays, as modifiers in plastic materials, as intermediates, as antioxidants, and as rubber and gum inhibitors (Figure 2.24).[175,179]

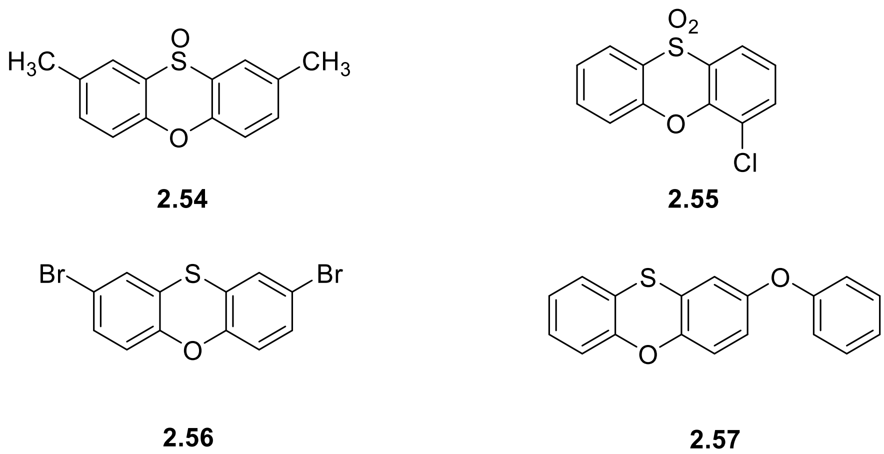

Figure 2.24: Some phenoxathiin derivatives

The cyclisation of compound **2.47b** was considered as a new route to making phenoxathiin-10,10-dioxide as part of tandem processes and an alternative route with mild reaction conditions versus the oxidation of sulfur with strong oxidising reagents. Addition of potassium tert-butoxide to a solution of **2.47b** in DMF at 90

°C for 24 h, followed by extraction with ethylacetate, and recrystallization of the resulting solid from THF afforded the cyclised product **2.58** as colourless crystals in excellent yield (Scheme 2.24). This occurs by an intramolecular cyclisation reaction resulting from an S_NAr reaction between the phenol and the chloroarene to form the new six-membered ring.

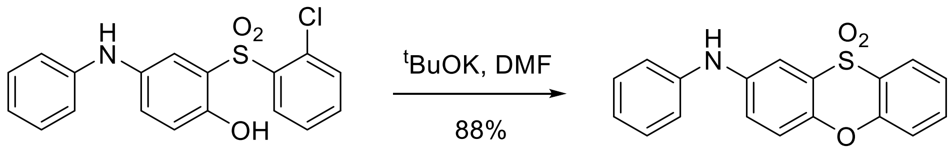

2.47b **2.58**

Scheme 2.24: Cyclisation of **2.47b** using potassium tert-butoxide

Compound **2.58** was confirmed by the ^{1}H NMR, ^{13}C NMR analysis and determination of the crystal structure (Figure 2.25).

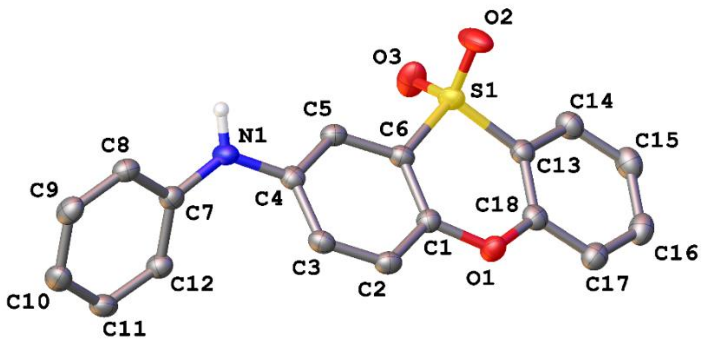

Figure 2.25: Crystal structure of compound **2.58**

Aromatic heterocyclic structures are largely used as scaffolds for generating combinatorial libraries in drug discovery research.[180] Sulfones are found in numerous medicines and drug candidate under development for the treatment of a host of diseases impacting human health worldwide (Fig. 2.26).[181] For example, Diazoxide is often used as a vasodilator in the treatment of acute hypertension or malignant hypertension.[182]

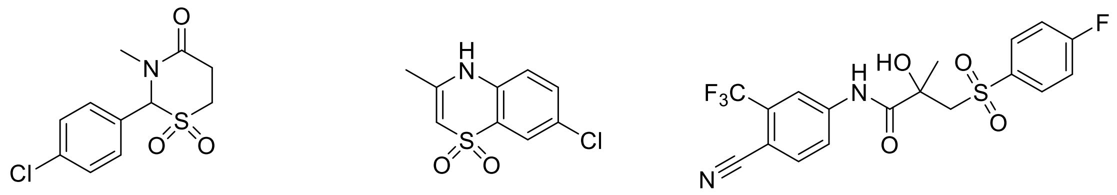

Trancopal **2.59** | Hypestat **2.60** | Casodex **2.61**

Chlormezone
Musculo-skeletal 1960

Diazoxide
Cardiovascular 1973

Bicalutamide
Endocrine system 1995

Figure 2.26: Some sulfone containing scaffolds in pharmaceutical molecules

2.5 Summary

The multiple products formed by the arylation of 4-hydroxyaniline with diphenyliodonium salts have been identified. Azaquinone has been observed as a product resulting from the in-situ oxidation of 4-hydroxydiphenylamine during these reactions and has been prepared by the oxidation of 4-hydroxydiphenylamine using Fetizon's reagent.

The nucleophilic addition of aliphatic amines to azaquinone is 1,2-selective and gives diaminoarenes. Conjugate addition to azaquinone, with aromatic amines resulted in diarylamino compounds, with the regiochemistry of the products being confirmed.

The reaction of azaquinone with arenesulfinates gives1,4-addition products and a further oxidative cyclisation has served as a new route to synthesizing phenoxathiins as part of tandem processes. This group of compounds can serve as sulfone containing scaffolds in pharmaceutical molecules.

Chapter 3. Halogenation of azaquinone and its derivatives

3.1 Halogenation reactions

Halogenation is the process in which one or more halogen atoms are introduced into an organic compound. This reaction is a basic and fundamental transformation in organic chemistry because it opens a gateway to further chemical reactions through the reactivity of the carbon-halogen bond e.g. via modern cross-coupling reactions such as the Suzuki-Miyaura and Mizoroki-Heck reactions.[183,184] This bond can be used as a precursor in forming a range of bonds such as carbon-carbon,[185] carbon-nitrogen,[186] and carbon-oxygen[187] bonds (Scheme 3.1). This is of great interest in the development of the reactions of azaquinone as it will allow subsequent elaboration of the structure extending the utility of this new building block still further.

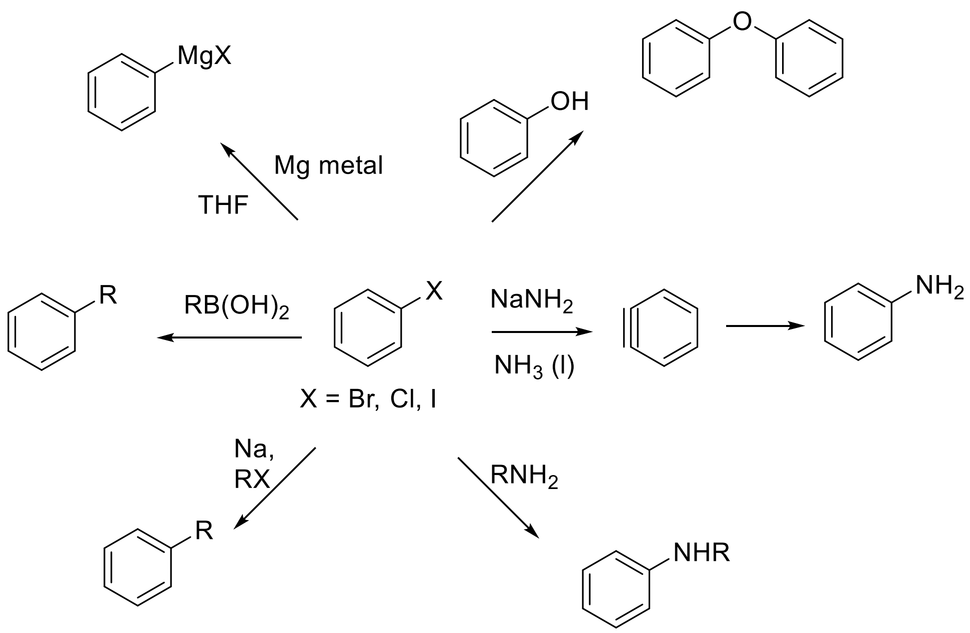

Scheme 3.1: Some reactions of arylhalides

3.2 Azaquinone reaction with hydrobromic acid

Initial studies on the reaction of hydrobromic acid with azaquinone, **3.1** have been reported by Burmistrov et al.[8] It was reported that the nucleophilic addition of bromide was to the α,β-unsaturated ketone, however the position relative to the *N*-Ar substituent was not discussed. Aqueous hydrobromic acid was added to azaquinone in acetic acid at room temperature, and organic extracts from the reaction mixture were treated with lead (IV) oxide (Scheme 3.2) to convert the phenol intermediate to the azaquinone system.

From the reaction, compounds **3.2**, **3.3**, and **3.4** were isolated in 36%, 32%, and 3% respectively although ^{1}H NMR data was provided only for **3.3**.[8] Compound **3.2** was characterised using melting point and elemental analysis only while melting point data was given for **3.4**. This level of characterisation is surprising given the amount of compound **3.2** that was isolated (94 mg). These are insufficient data to correctly assign the regiochemistry of any substitution and thus the identity of these compounds. It was therefore needful to consider this reaction process in detail.

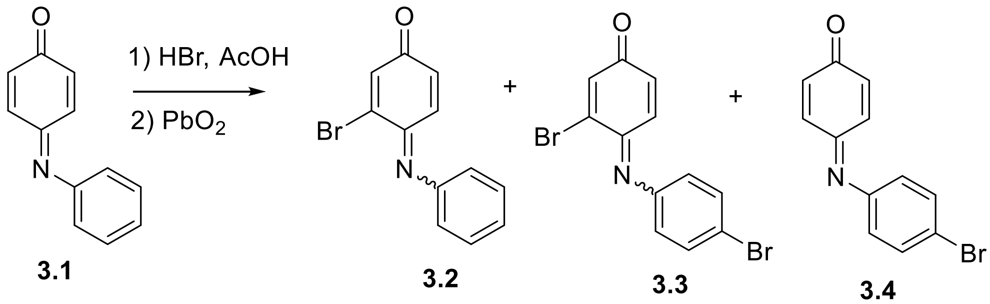

Scheme 3.2: Addition of hydrobromic acid to azaquinone

The reported reactions were repeated by ourselves by adding aqueous hydrobromic acid to azaquinone in acetic acid and stirring at room temperature for 30 min. Preliminary studies were done using lead (IV) oxide, however lead (IV) acetate was also considered as an alternative for the oxidation step as it is a more selective oxidising agent.[188] However, the results were similar, therefore, lead (IV) acetate was used for the remaining studies because it resulted in less by-products evident by TLC. The combined organic products were oxidised, and compounds **3.5** and **3.6** (Scheme 3.3) were isolated by two-stage column chromatography (SiO_2 1:4 ethylacetate-petrol followed by RP (C18) 1:1 MeCN-H_2O) from the crude reaction mixture (32% and 36% respectively).

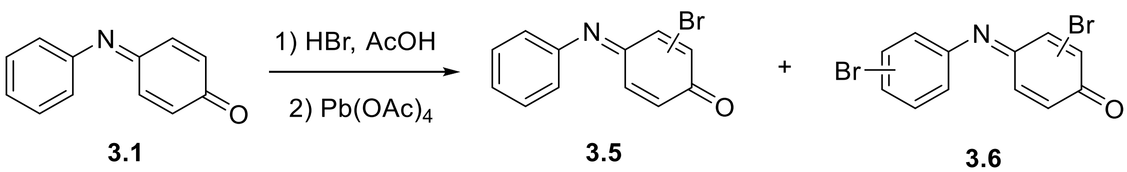

Scheme 3.3: Reaction of HBr with azaquinone

The [1]H NMR spectra for **3.5** and **3.6** are shown in Figure 3.1. The spectra show a bromine atom substituent on the quinoid ring, but this is not sufficient to assign which carbon it is attached to. The two doublet peaks at 7.45 and 6.69 ppm are characteristic of a para-substituted phenyl ring, indicating that the bromine on the phenyl ring is at the para position to the nitrogen.

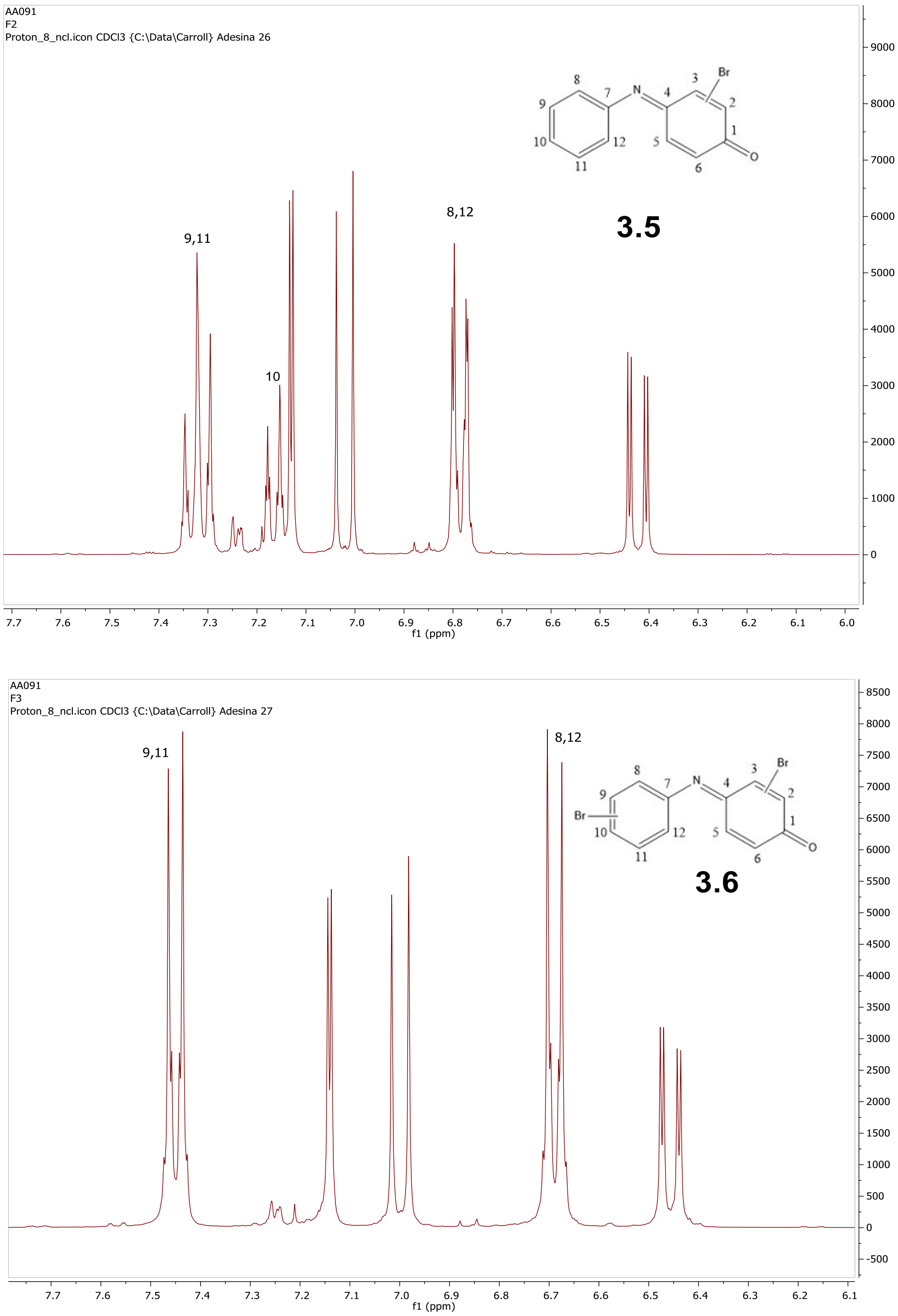

Figure 3.1: [1]H NMR spectra of compounds **3.5** and **3.6** respectively

The possible positions of a bromine atom substituent on the quinoid ring for compound **3.6** are shown in Figure 3.2. Surprisingly, the NMR prediction software (ChemBioDraw Ultra version 14.0.0.117) does not distinguish between these isomers.

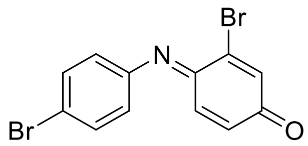

3.3

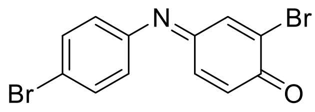

3.7

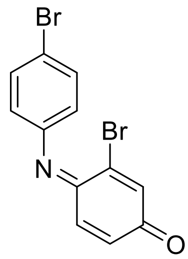

3.8

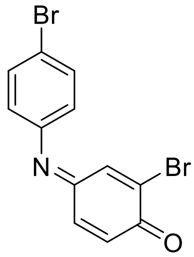

3.9

Figure 3.2: Possible structures of a bromine substituent on the quinoid ring of a disubstituted azaquinone

COSY and NOESY spectra (Fig. 3.3) were used respectively to determine coupled protons and protons that are close in space. The COSY spectrum shows coupling between protons 5 and 6 which suggests they are next to each other. The COSY spectrum also shows some coupling between protons 2 and 6, which is observed in the NOESY spectrum also (arrow 3). This suggests that the bromine substituent on the quinoid ring is ortho to the imine, eliminating the options of compounds **3.7** and **3.9**. The NOESY spectrum also shows that protons 5 and 12 were close in space (arrows 1 and 2). This confirms that the bromine substituent on the quinoid ring was oriented away from the phenyl ring. This eliminates the options of compounds **3.8** and **3.9**, leaving compound **3.3** as the structure of the product.

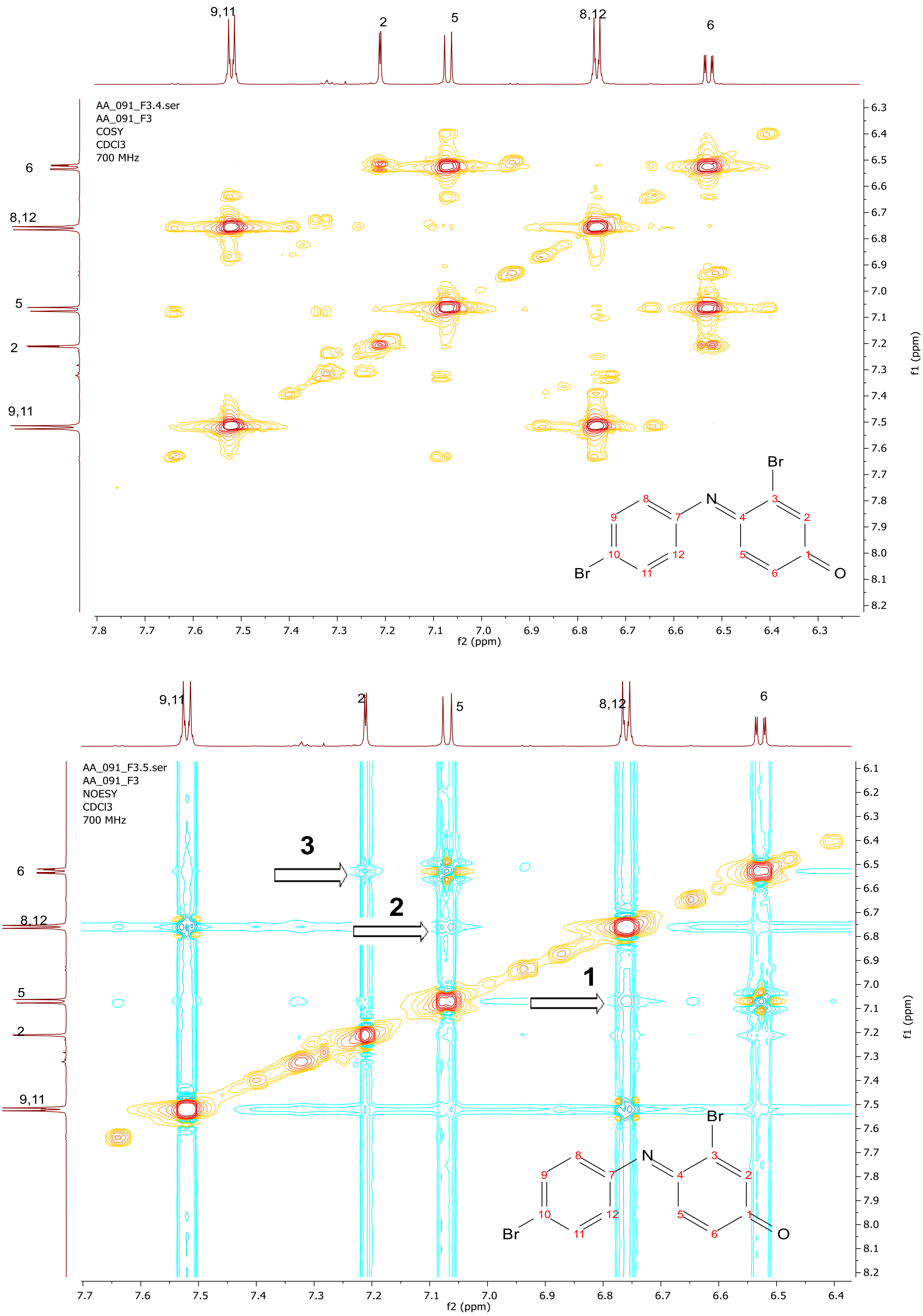

Figure 3.3: COSY (top) and NOESY (bottom) spectra of compound **3.6**

As a result, the position to which the bromine substituent was attached on the quinoid ring was also confirmed by determination of the crystal structure (Fig. 3.4), confirming the substitution at C3, which is compound **3.3**. The dihedral angle C4 – N1 – C7 – C8 is 129.763° which suggests that the overall structure is not flat, and that the phenyl ring is not in conjugation with the quinoid ring as is observed with the azaquinone.

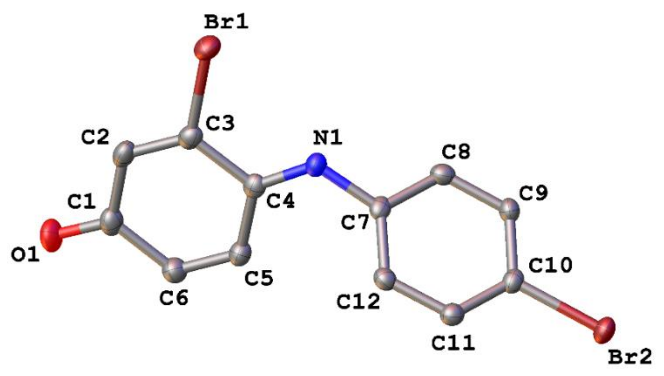

Figure 3.4: Crystal structure of **3.3**

This first confirmation of the actual structure of the product suggests that the reactions of hydrobromic acid with azaquinone occurs by nucleophilic addition to the α,β-unsaturated ketone to give the 4-hydroxydiphenylamine **3.10** after imine/enamine tautomerism which is then oxidised to give the bromoazaquinone **3.2** (Scheme 3.4).

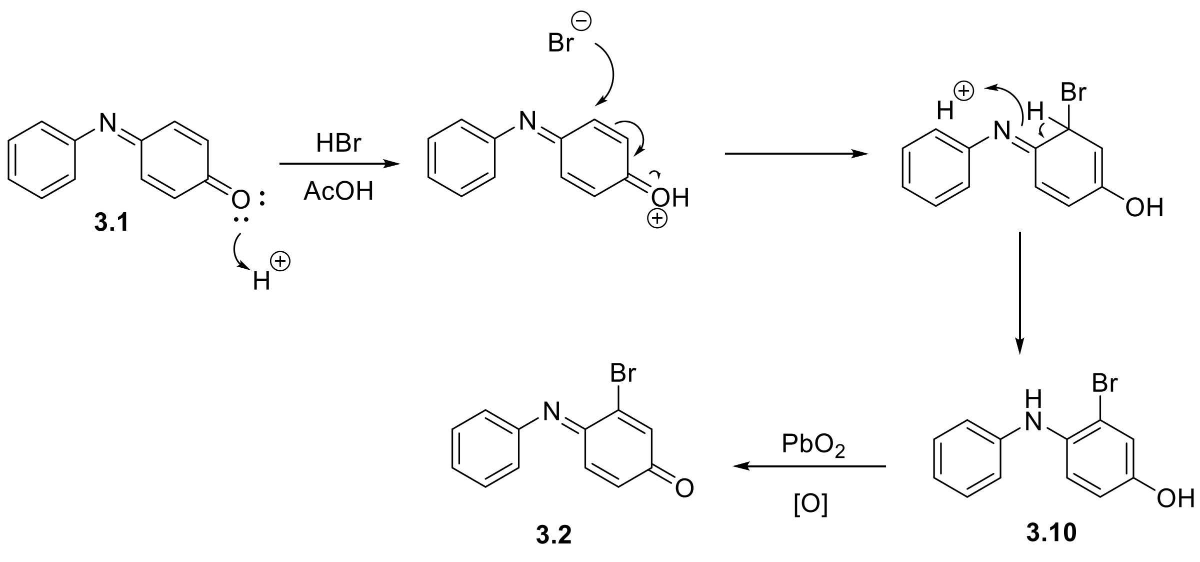

Scheme 3.4: Bromination of azaquinone

Bromination of the phenyl ring at the para position was also found to occur as a competing process, giving the di-substituted compound **3.3** (Scheme 3.5) and will be discussed in the next section.

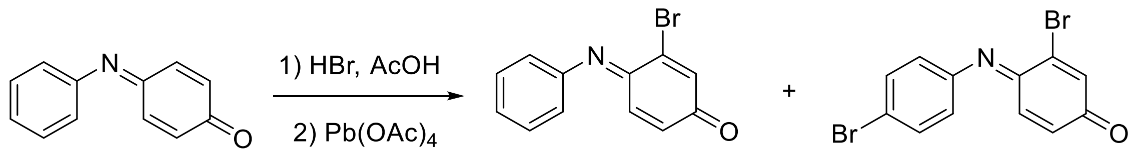

3.1 3.2 3.3

Scheme 3.5: Reaction of HBr with azaquinone

3.2.1. Addition of resorcinol to the bromination of azaquinone, 3.1

As observed in the reaction of azaquinone, **3.1** with hydrobromic acid, the bromination of the phenyl ring is a competing process, but this can be suppressed by the addition of resorcinol or other radical scavengers to the reaction mixture. Due to the relatively high value of the oxidation potential of azaquinone, –0.67 V (as measured by our colleagues in electrochemistry) on the hydrogen scale, (lit., value –0.71 V),[189,190] the bromide ion from HBr is capable of being oxidised. The resulting bromine radicals (or free bromine) attack the aromatic nucleus (phenyl ring). With such a mechanism for the process, the introduction of radical scavengers into the reaction mixture should inhibit the substitution process on the phenyl ring.[8] Resorcinol was also used as a radical scavenger by Toropin et al. in the reaction of hydrogen bromide with *N*-(4-tolyl)-1,4-benzoquinone monoimines and *N*-(4-tolylsulfonyl)-1,4-benzoquinone monoimines,[191] the excellent scavenging property of polyphenols (e.g. resorcinol) is attributed to the phenolic OH's present and their activity is characterised by its hydrogen atom donating ability to scavenge the radicals and the easy formation of a quinone.[192] The addition of resorcinol to the reaction of azaquinone, **3.1** with hydrobromic acid clearly changed the composition of the reaction mixture, eliminating the bromination of the phenyl group and giving the mono-substituted product **3.2** in 60% yield with unreacted azaquinone making up the remainder (Scheme 3.6).

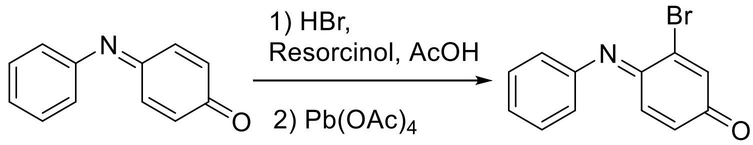

3.1 **3.2**

Scheme 3.6: Addition of resorcinol to the bromination of azaquinone

3.3 Azaquinone reaction with hydrochloric acid

The addition of hydrochloric acid to azaquinone was also reported by Burmistrov et al.[9] The regioselectivity of nucleophilic addition to *N*-phenylquinoneimine is determined by electrophilicity of the substrate, nucleophilicity of the reagent, and hardness of the latter.[7] Hard nucleophiles ($Cl^{\ominus}$, $Br^{\ominus}$) add to *N*-phenylquinoneimine in protic media at the ortho position to the nitrogen atom i.e. to the α,β unsaturated ketone (Scheme 3.7).[193]

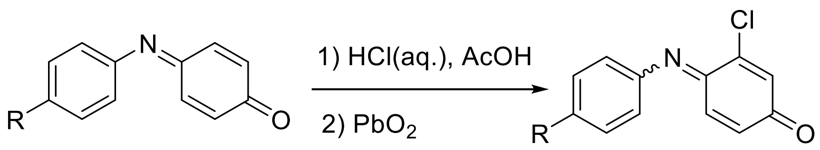

3.1, 3.11a,b **3.12, 3.13a,b**

R = H **(3.1)**, R = OMe **(3.11a),** R = I **(3.11b)**

Scheme 3.7: Reaction of hydrochloric acid with azaquinones

However, when strong electron-withdrawing substituents are introduced into the *N*-aryl fragment, the electrophilicity of the quinoneimine is increased and products from addition to the α,β unsaturated imine are formed (Scheme 3.8).[9,194]

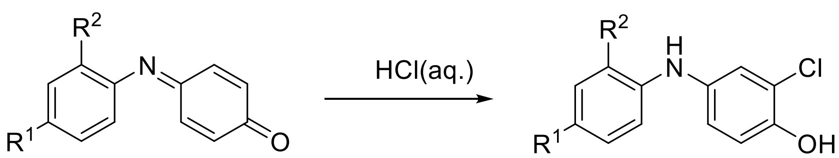

3.14a,b **3.15a,b**

R^1 = H, R^2 = NO_2 **(a)**, R^1 = NO_2, R^2 = H **(b)**

Scheme 3.8: Influence of electron-withdrawing groups on the chlorination of azaquinones

In the literature,[9] the synthesized compounds from this reaction were analysed by their melting points, infrared spectroscopy and elemental analyses. However, in a similar fashion to the bromination reaction, these data could not have unambiguously assigned the position of the chlorine atom, hence the regiochemistry of compound **3.12** remains to be confirmed.

The reaction was conducted by adding concentrated hydrochloric acid (37%) to azaquinone in acetic acid, and the mixture heated under reflux for 24 h. As before, the organic products were oxidised from the initial phenol product **3.17** using lead (IV) acetate. Purification by chromatography (SiO_2 1:9 ethylacetate-petrol) gave compound **3.16** as the major product (60%) with the remainder being unreacted azaquinone (Scheme 3.9). It should be noted that the chlorination of the phenyl group was not observed in the treatment of azaquinone with HCl.

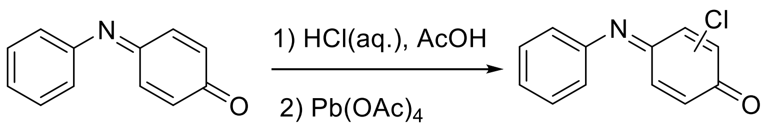

Scheme 3.9: Treatment of azaquinone with HCl(aq.)

The mechanism for the chlorination of azaquinone is shown in Scheme 3.10.

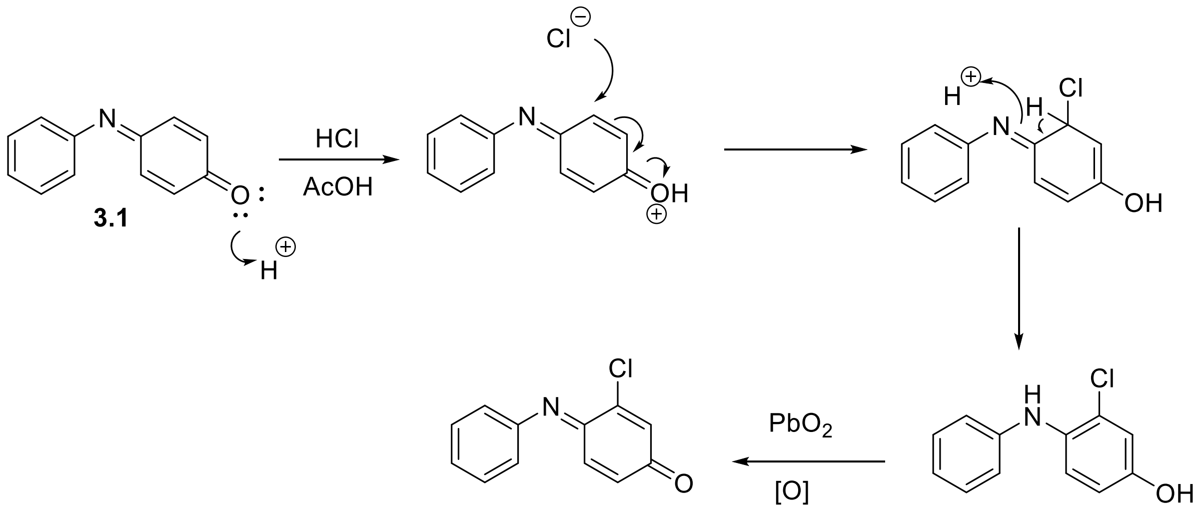

Scheme 3.10: Chlorination of azaquinone[9,195]

The ^1H NMR spectrum of **3.16** (Figure 3.5) indicates the presence of a chlorine atom substituent on the quinoid ring but as in the bromination reaction, does not confirm the position of attachment, with COSY and NOESY spectra being used to determine the regiochemistry of the compound as **3.12**.

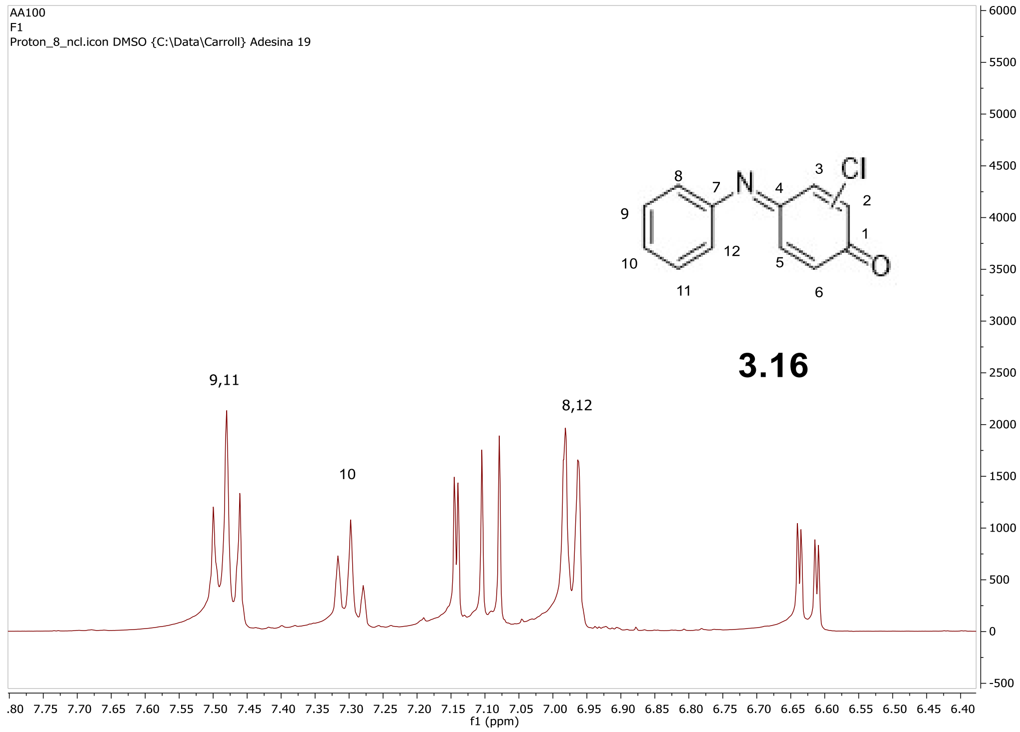

Figure 3.5: [1]H NMR spectrum of compound **3.16**

3.3.1 Addition of Resorcinol to the chlorination of azaquinone, 3.1

As in the bromination reaction, the reaction of azaquinone with hydrochloric acid was also carried out with the addition of resorcinol although the chlorination of the phenyl group was not observed, giving the mono-substituted product **3.12** in 60% yield and unreacted azaquinone as the only other component in the reaction mixture (Scheme 3.11). The product(s) of this reaction is the same as when resorcinol was not added to the mixture.

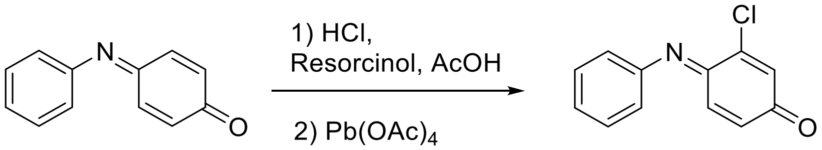

3.1 **3.12**

Scheme 3.11: Addition of resorcinol to the chlorination of azaquinone

3.4 Oxidation of azaquinone: synthesis of iminium oxide

As the halogenation reactions of azaquinone were successful, it would be interesting to also do the halogenation reactions with azaquinone *N*-oxide so as to compare the reactivity of both as Burmistrov[9] suggested that electron-withdrawing groups may impact the outcome. It was also of interest to see if the *N*-oxide can serve as a directing and/or protecting group as with pyridine, **3.18** and pyridine *N*-oxide, **3.19** (for an example see Scheme 3.12).

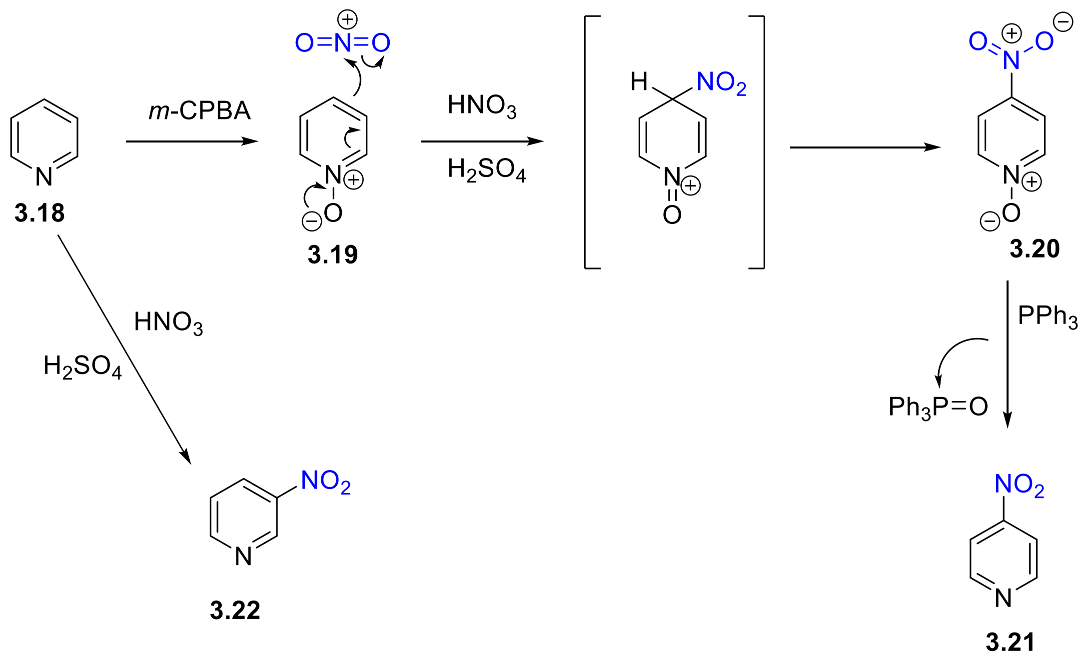

Scheme 3.12: Reaction of pyridine *N*-oxide, **3.19** as both a protecting and directing group

In a similar fashion, azaquinone *N*-oxide was prepared from the oxidation of azaquinone using meta-chloroperoxybenzoic acid (*m*-CPBA) in DCM at room temperature for 24 h (Scheme 3.13).[196]

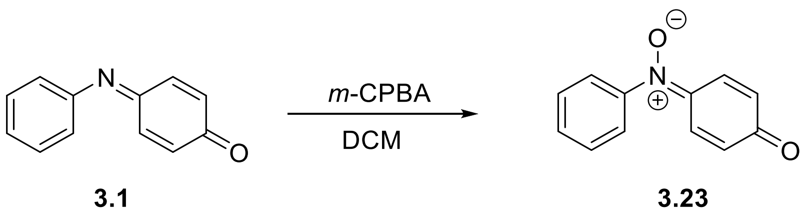

Scheme 3.13: Oxidation of azaquinone, **3.1** to azaquinone *N*-oxide, **3.23**

The changes in the chemical shifts in the ^{1}H NMR spectrum of azaquinone *N*-oxide when compared to azaquinone are consistent with the presence of an electron-withdrawing group. The largest differences are for protons 8 (from 6.91 ppm to 7.50 ppm) and 3 (from 7.33 ppm to 8.06 ppm) as expected when considering their proximity to the *N*-oxide. A relatively smaller downshift of peaks for the other protons, which are further away from the oxygen, should therefore be expected and is observed in the spectrum (Fig. 3.6).

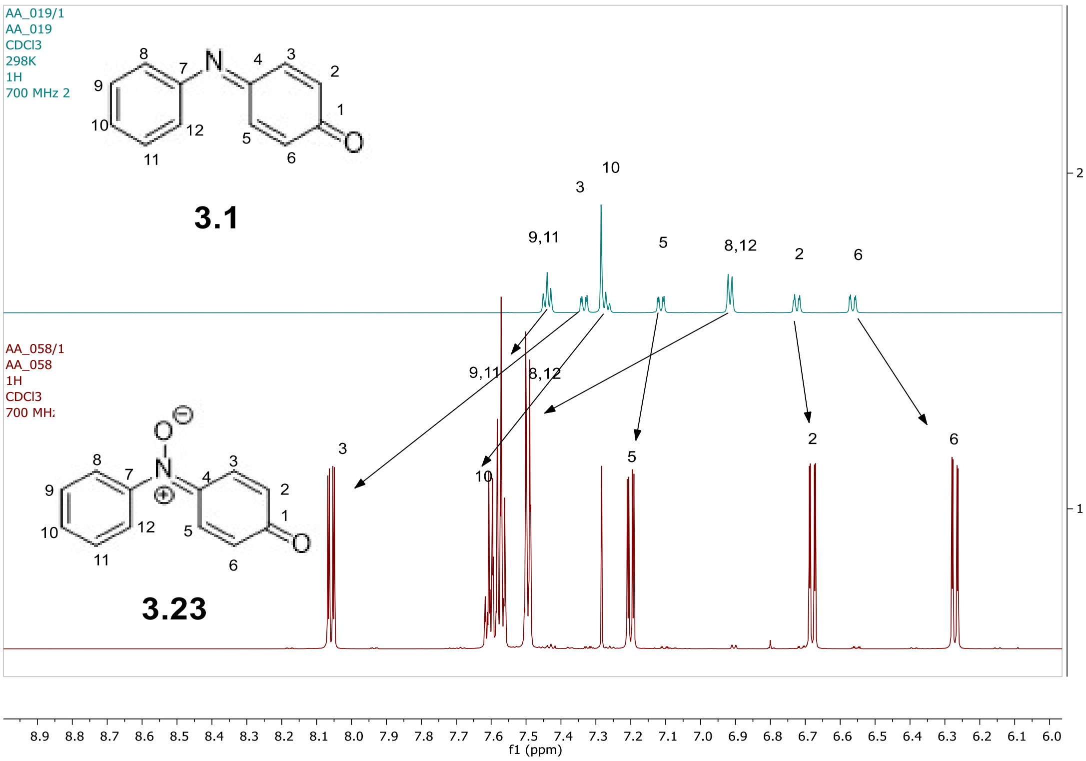

Figure 3.6: ^{1}H NMR spectrum of azaquinone *N*-oxide, **3.23** compared to azaquinone, **3.1**

The structure of this compound was also confirmed by determination of the crystal structure (Figure 3.7). The dihedral angle C3 – C4 – N1 – C7 is 9.125° which suggests that, like the dibromoazaquinone **3.3**, the structure is not flat, and the phenyl ring is not in conjugation with the quinoid ring. This was also observed in the azaquinone structure.

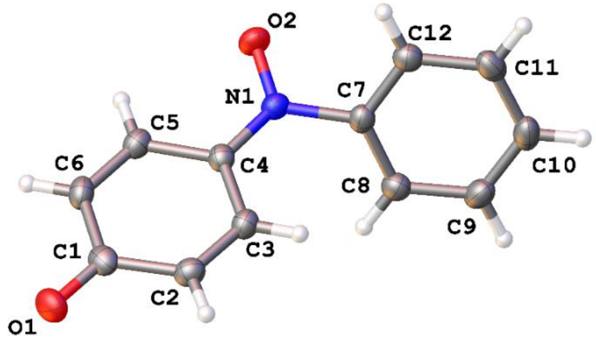

Figure 3.7: Crystal structure of **3.23**

3.5 Reaction of azaquinone *N*-oxide with hydrobromic acid

As the reaction of azaquinone *N*-oxide, **3.23** with hydrobromic acid is a new and unexplored reaction, the same method that was used for the bromination of azaquinone was employed. Purification by chromatography (SiO_2 1:9 ethylacetate-petrol, RP (C18) 7:3 MeCN-H_2O) gave the tri-substituted product **3.24** (30%), the di-substituted product **3.3** (37%), and the mono-substituted product (phenyl ring) **3.25** (7%) as shown in Scheme 3.14. It should be noted that no *N*-oxides, including **3.23** were recovered.

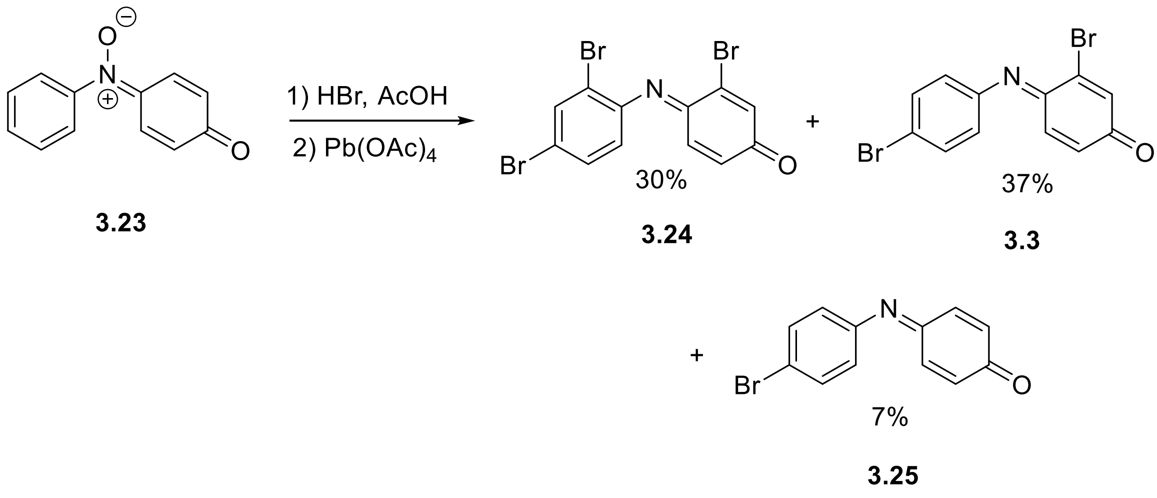

Scheme 3.14: Reaction of hydrobromic acid with azaquinone *N*-oxide **3.23**

Compound **3.3** is a common product from the bromination reactions of both the azaquinone, **3.1** and the *N*-oxide, **3.23**. The tri-substituted product **3.24** and the mono-substituted (phenyl ring) product **3.25**, however, was observed for the first time in the bromination of azaquinone *N*-oxide but not in the bromination of azaquinone. This suggests that the phenyl ring in the *N*-oxide is less electron-rich than in the azaquinone, and so more electrophilic than the azaquinone. The loss of the *N*-oxide in the products from the bromination reactions suggests that the mechanism of bromination of the phenyl group is nucleophilic addition rather than the radical reaction which is observed in the azaquinone bromination reactions (Scheme 3.15).

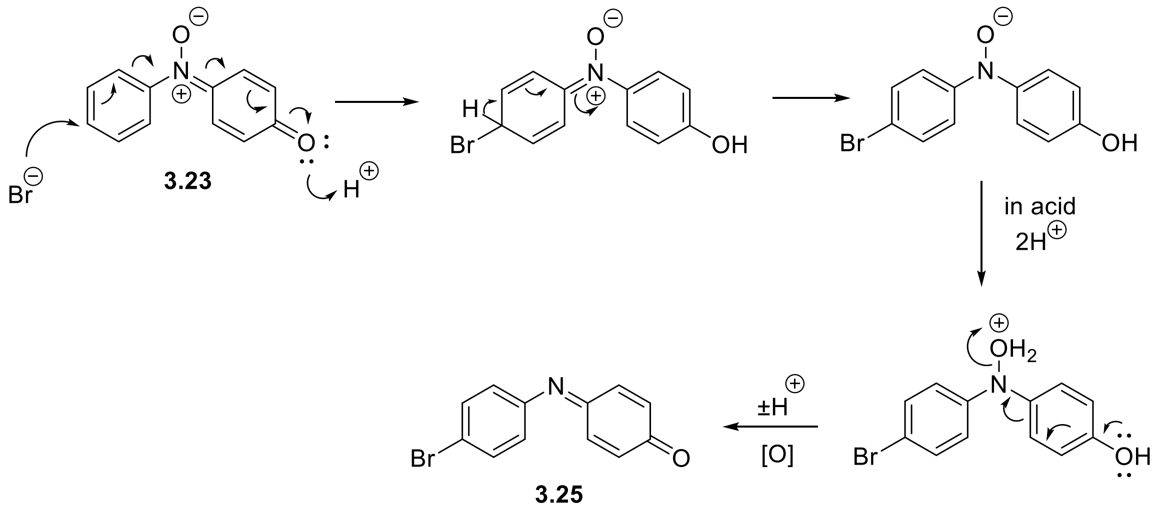

Scheme 3.15: Mechanism of bromination of azaquinone *N*-oxide to give **3.25**

Fig. 3.8 shows the ^{1}H NMR spectrum of compound **3.24**, confirming its identity.

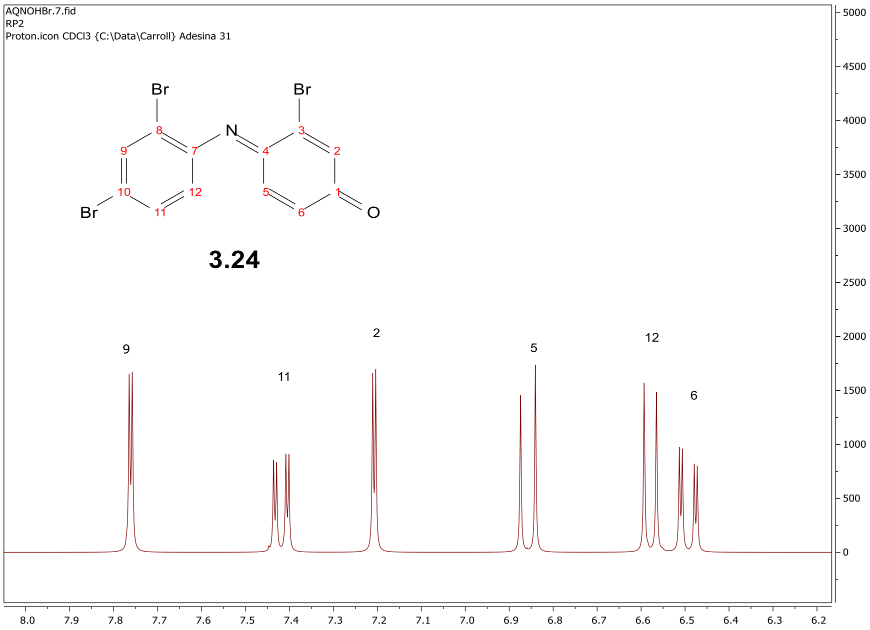

Figure 3.8: ^{1}H NMR spectrum of compound **3.24**

The mono-substituted product (phenyl ring), compound **3.25**, is also one of the products formed in the bromination of the *N*-oxide, suggesting that the *N*-oxide results in direct halogenation to the phenyl ring suggesting the order of reaction as no mono-substituted (phenyl ring) product was observed with the azaquinone i.e. bromination of the phenyl ring first and then bromination of the azaquinone group as described when the azaquinone itself was the substrate. The ^{1}H NMR spectrum of compound **3.25** is shown in Figure 3.9.

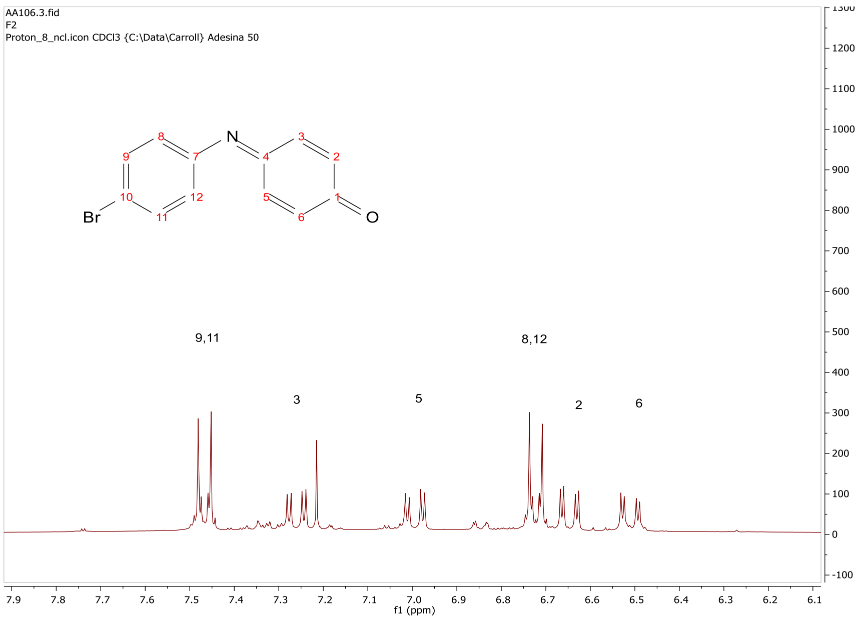

Figure 3.9: ^{1}H NMR spectrum of compound **3.25**

It was reported by Burmistrov et al.[8] that compound **3.24** can be formed by further brominating compound **3.3** in the absence of resorcinol (Scheme 3.16) but we have observed it as one of the products in the direct bromination of the *N*-oxide.

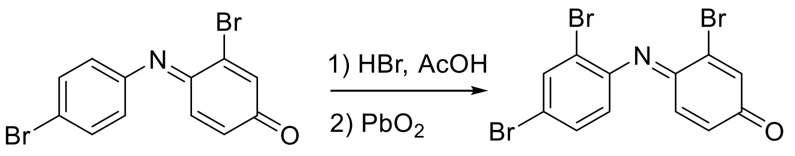

Scheme 3.16: Addition of hydrobromic acid to di-substituted azaquinone[8]

The observation that compound **3.24** can only be made from azaquinone under more forcing conditions suggests that the *N*-oxide is brominated before its loss of oxygen and conversion to azaquinone (Scheme 3.15). The order of reaction for the addition of hydrobromic acid to azaquinone-*N*-oxide should therefore be as shown in Scheme 3.17.

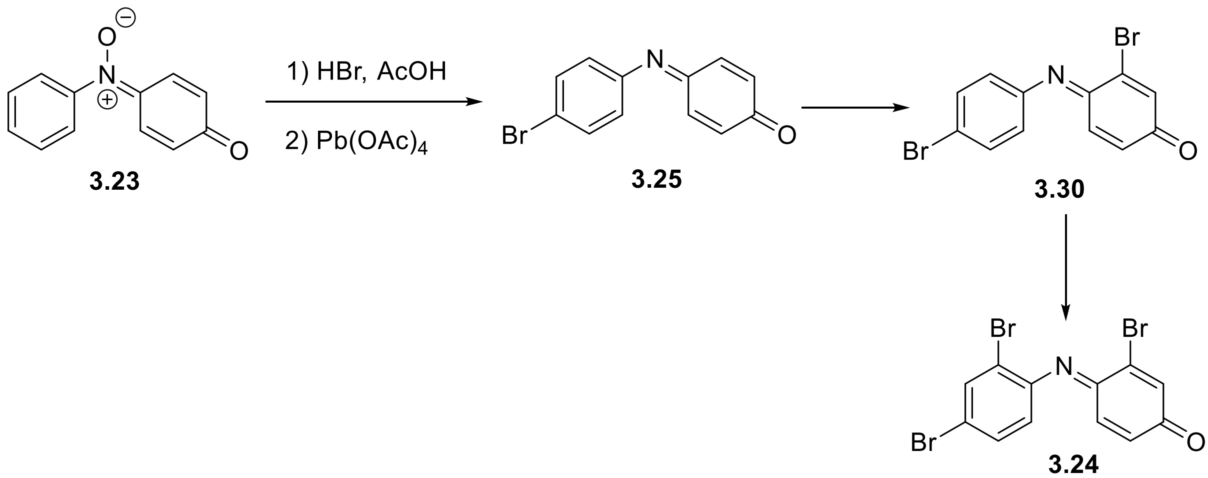

Scheme 3.17: Order of addition of hydrobromic acid to azaquinone *N*-oxide, **3.23**

3.5.1. Addition of resorcinol to the bromination of azaquinone N-oxide, 3.23

The reaction of azaquinone *N*-oxide, **3.23** with hydrobromic acid was also carried out with the addition of resorcinol. The di-substituted product **3.3** (47%) is still observed with the mono-substituted (quinoid ring) product **3.2** (26%) being formed together with unreacted azaquinone (Scheme 3.18). The observance of compound **3.3** suggests that the bromination of the phenyl ring is not eliminated in the bromination of the *N*-oxide using resorcinol and therefore is probably not a radical bromination process but a nucleophilic substitution.

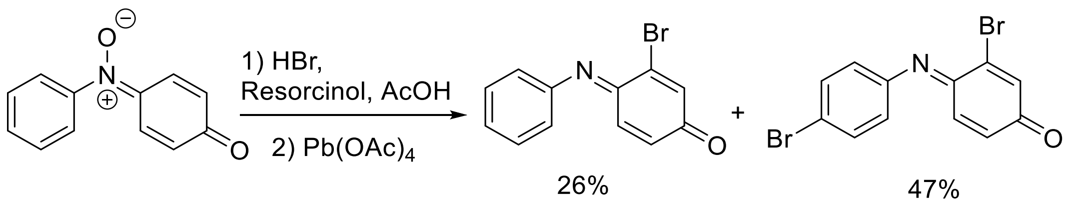

3.23 **3.2** **3.3**

Scheme 3.18: Addition of resorcinol to the bromination of azaquinone *N*-oxide

3.6 Reaction of azaquinone *N*-oxide with hydrochloric acid

The reaction of azaquinone *N*-oxide, **3.23** with hydrochloric acid was carried out using the same method for the chlorination of azaquinone (see section 3.3). Purification by chromatography (SiO_2 1:9 ethylacetate-petrol) gave **3.26** (70%) and **3.27** (12%) (Scheme 3.19).

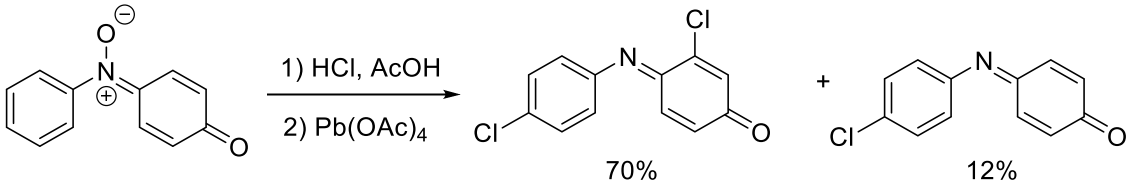

3.23 **3.26** **3.27**

Scheme 3.19: Reaction of hydrochloric acid with azaquinone *N*-oxide

As observed in the bromination of the *N*-oxide, there appears to be a different selectivity in this reaction from the chlorination of azaquinone. Whilst the chlorination of azaquinone gives the mono-substituted (quinoid ring) product **3.12**, the chlorination of its *N*-oxide gives the di-substituted product **3.26** and the mono-substituted (phenyl ring) product **3.27,** which indicates the preference of the *N*-oxide for the reaction of the phenyl ring and that this occurs first. This can be explained from the fact that the *N*-oxide is a more electrophilic substrate than the azaquinone similar to the bromination result, therefore making the *N*-oxide more reactive to nucleophiles. This selectivity and the non-observance of *N*-oxide products, which was also the case in the bromination of the *N*-oxide, suggests that the loss of oxygen occurs during or after the halogenation (Scheme 3.20).

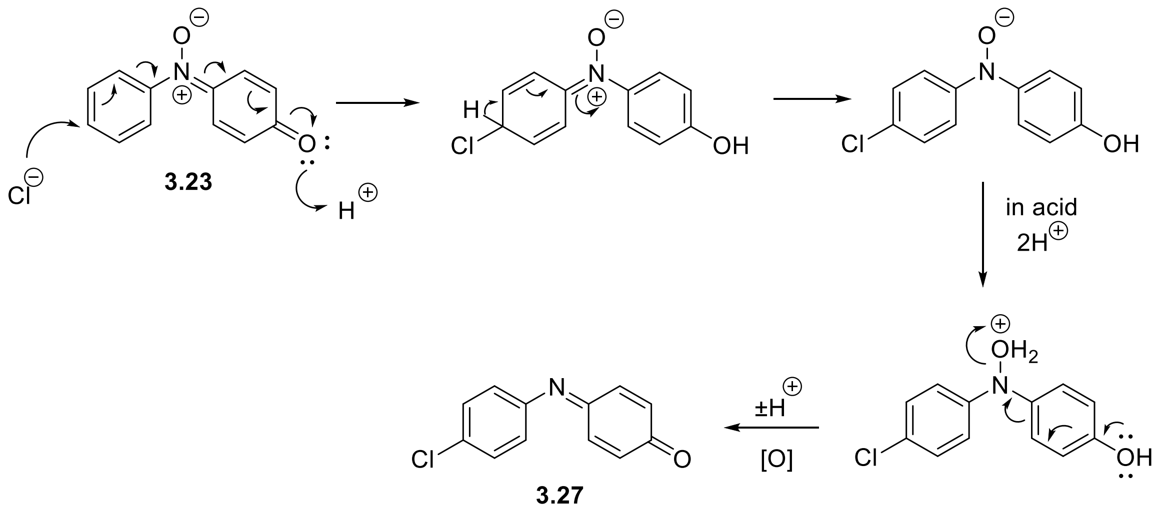

Scheme 3.20: Mechanism of chlorination of azaquinone to give **3.27**

As with the previous reactions, COSY and NOESY spectra were used to determine the regiochemistry of the compound but the position of chlorine attachment on the quinoid ring in compound **3.26** was also confirmed by determination of the crystal structure (Fig. 3.10).

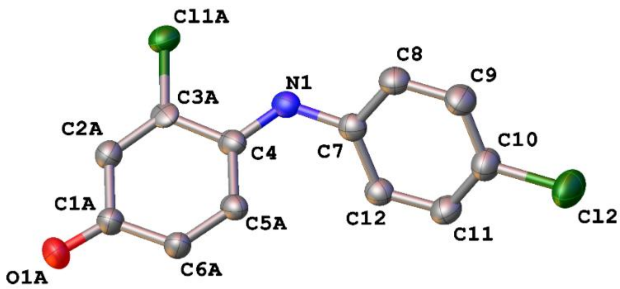

Figure 3.10: Crystal structure of **3.26**

3.6.1 Addition of resorcinol to the chlorination of azaquinone N-oxide, 3.23

The reaction of azaquinone *N*-oxide with hydrochloric acid was also carried out with the addition of resorcinol. The di-substituted product **3.26** is observed together with the mono-substituted product (quinoid ring) **3.12** and unreacted azaquinone (Scheme 3.21).

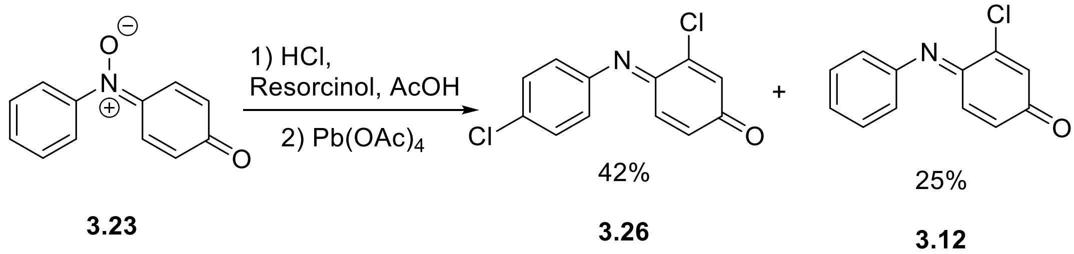

Scheme 3.21: Addition of resorcinol to the chlorination of azaquinone *N*-oxide

This observation is similar to that seen as a result of the addition of resorcinol to the bromination of the *N*-oxide (Scheme 3.18). Two possible substitution products – di-substituted product and mono-substituted product (quinoid ring) are formed when resorcinol is added to the halogenation of azaquinone *N*-oxide.

The results of the halogenation reactions of azaquinone and azaquinone *N*-oxide are summarised in Table 3.1.

Table 3.1: Results of the halogenation reactions of azaquinone **3.1** and azaquinone *N*-oxide **3.23** with/without resorcinol

Entry		**HBr/ HCl**	**Trihalo Yield**	**Dihalo Yield**	**Monohalo (quinoid ring) Yield**	**Monohalo (phenyl ring) Yield**
1	**3.1**	HBr	nd	36% **(3.3)**	32% **(3.2)**	nd
2	**3.1**	HBr[a]	nd	nd	60% **(3.2)**	nd
3	**3.1**	HCl	nd	nd	60% **(3.12)**	nd
4	**3.1**	HCl[a]	nd	nd	60% **(3.12)**	nd
5	**3.23**	HBr	30% **(3.24)**	37% **(3.3)**	nd	7% **(3.25)**
6	**3.23**	HBr[a]	nd	47% **(3.3)**	26% **(3.2)**	nd
7	**3.23**	HCl	nd	70% **(3.26)**	nd	12% **(3.27)**
8	**3.23**	HCl[a]	nd	42% **(3.26)**	25% **(3.12)**	nd

[a] with resorcinol 100 mol%, 'nd' not detected

The bromination of azaquinone gives both mono-substituted (quinoid ring) and di-substituted (phenyl and quinoid rings) products. The use of a radical scavenger (resorcinol) eliminates the bromination of the phenyl ring. The chlorination of azaquinone, however, is more selective and gives only the mono-substituted (quinoid ring) product under these conditions. Halogenation of the *N*-oxide results in direct bromination/chlorination of the phenyl ring, changing the selectivity of the reaction suggesting both the order of addition and a change in mechanism (Scheme 3.22). The C–Cl/Br bond can facilitate metal-catalysed cross-coupling reactions such as the Suzuki reaction allowing further elaboration of the structure.

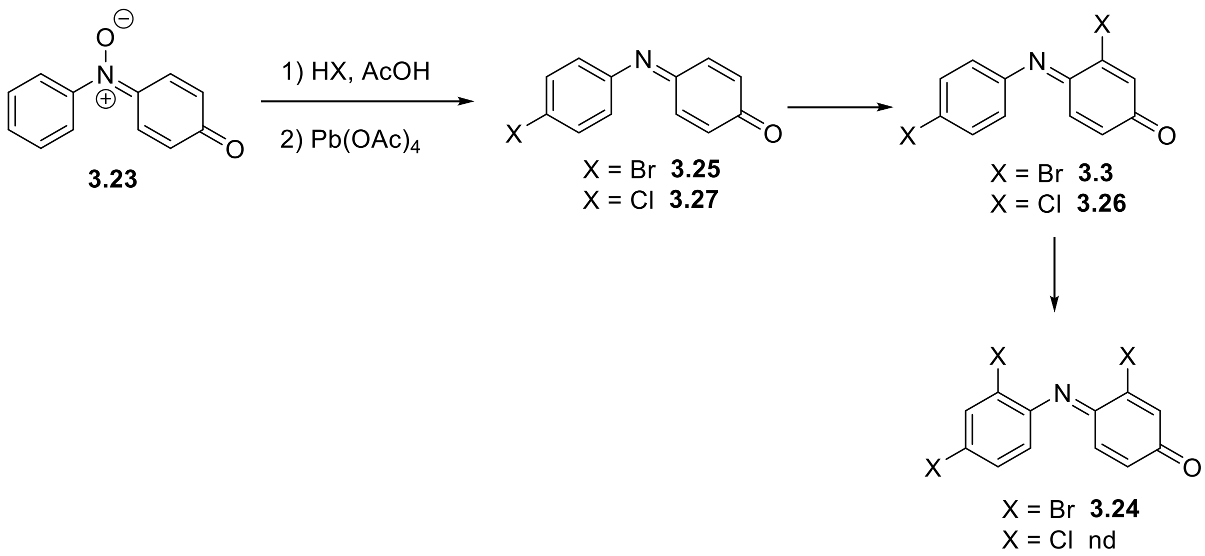

Scheme 3.22: General mechanism for the halogenation of azaquinone *N*-oxide, **3.23**

3.7 Summary

The halogenation of azaquinone has been found to be selective depending on the reaction conditions used, and allows targeted functionalisation. The halogenation of azaquinone *N*-oxide was also investigated and this gives direct halogenation to the phenyl ring, changing the selectivity of the reaction. The concurrent loss of the *N*-oxide functionality in the products from the halogenation reactions suggests that the mechanism of halogenation of the phenyl group in the *N*-oxide is from the nucleophilic addition rather than the radical reaction which is observed with azaquinone as the substrate.

Chapter 4. Cross-Coupling Reactions of Haloazaquinone

4.1 Introduction to cross-coupling reactions

Cross-coupling reactions are transformations that form (usually) carbon-carbon bonds, enabling the preparation of an enormous structural diversity of complex molecules, essential in the pharmaceutical industry and for preparing organic materials.[197] They typically use transition metal catalysts (such as palladium, nickel, copper and iron), an organic halide, and a nucleophilic coupling partner.

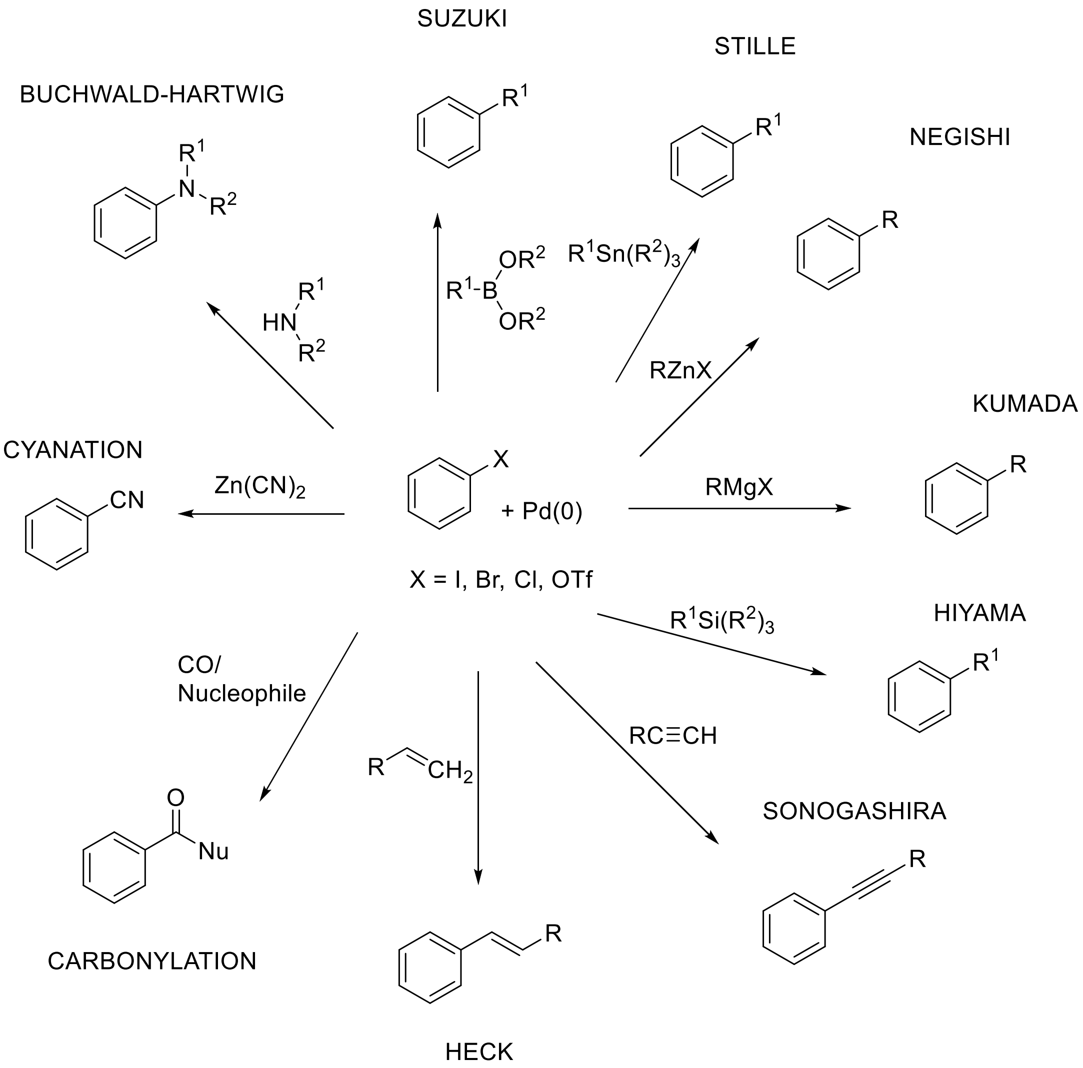

Scheme 4.1: Cross-coupling Reactions

Several coupling reactions have been developed and these are specific to different substrates: Suzuki,[198] Stille,[199] Negishi,[200] Kumada,[201] Hiyama,[202] Sonogashira,[203] Heck,[204] Buchwald-Hartwig,[205] cyanation,[206] carbonylation[207] (Scheme 4.1). The Suzuki, Stille, Sonogashira, Kumada and Buchwald-Hartwig reactions were investigated as part of our research as they are among the most commonly utilised reactions in present time within the drug discovery community and are discussed in detail later.

Most palladium catalysed reactions are believed to follow a similar catalytic cycle (Scheme 4.2). The catalytic species can be formed *in situ* using a palladium source, such as $Pd_2(dba)_3$ or $Pd(OAc)_2$ and the necessary ligand or introduced as a preformed catalyst such as $Pd(PPh_3)_4$, $PdCl_2(PPh_3)_2$ or $PdP(^tBu_3)_2$. Careful choice of ligand can facilitate two steps of the catalytic cycle. The use of strong σ-donating ligands, such as trialkylphosphines, increases the electron density around the metal, accelerating the oxidative addition of the catalyst to the substrate, this is most commonly believed to be the rate determining step. Choice of ligand also determines the mechanism by which oxidative addition occurs. The elimination step is accelerated by the use of bulky ligands, in particular phosphine ligands exhibiting a large cone angle (also known as Tolman angle).[208]

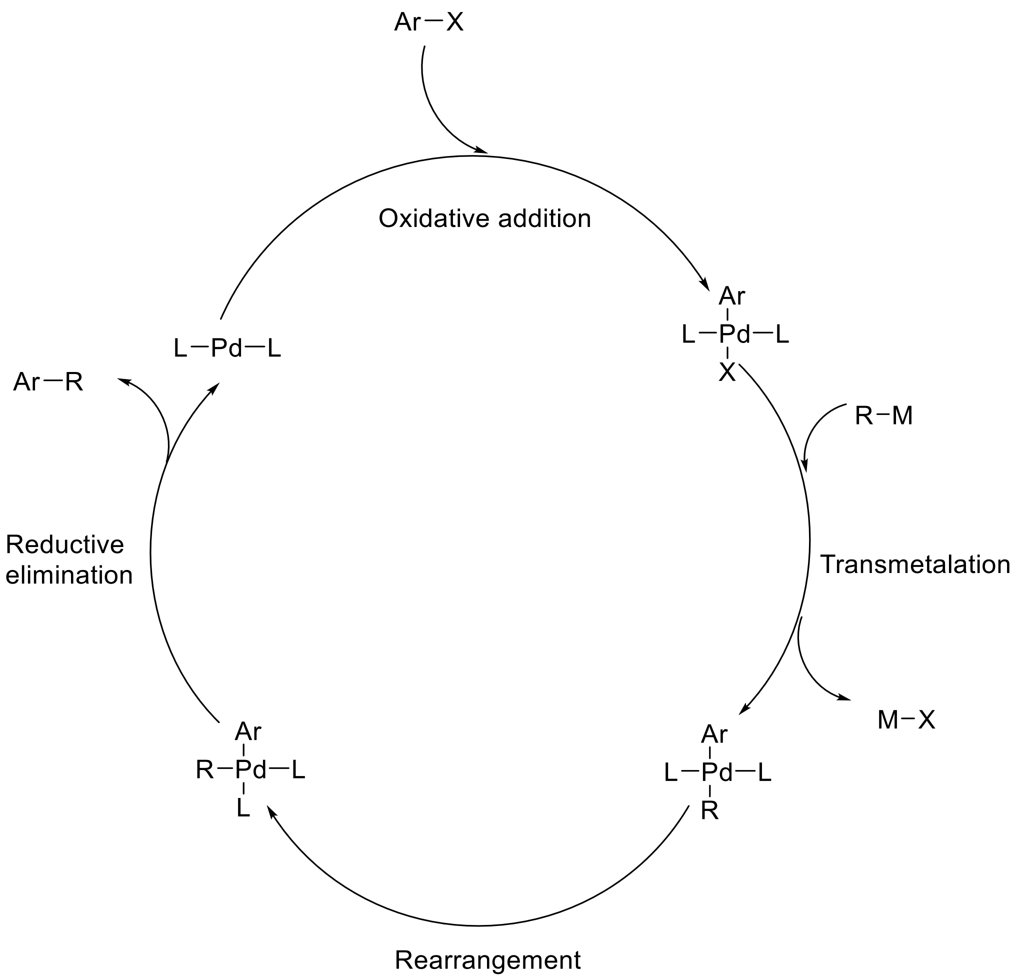

Scheme 4.2: General catalytic cycle for palladium catalysed coupling reactions

The oxidative addition of arylhalides (Ar–X) to Pd(0) complex is the initial step to give a Pd(II) species (organopalladium complex). It is favoured by electron poor aromatics (Ar) as the bond dissociation energy for the Ar–X bond is reduced. The order of reactivity for X is usually I>Br~OTf>>Cl.

The Pd(II) species will subsequently react with the nucleophilic coupling partner (olefins or organometallic compounds R–M of low reactivity, where M is typically zinc, boron, or tin) via a transmetalation process to afford an intermediate. Transmetalation is the transfer of an organic group from one (pseudo) metal to another and this step is favoured by electron-rich R groups and lack of steric hindrance on the Ar and R groups. This is followed by reductive elimination to give the desired product and regenerate the Pd(0) species. Coupling partners with opposite electronic properties favour the reductive elimination step.

Despite the initial lack of evidence, organopalladium(IV) species were tentatively suggested as intermediates in various cleavage reactions of organopalladium(II) complexes, usually with dihalogens or other simple inorganics. Yamamoto[209] reported that reactions of complexes [PdR_2L_2] (R = Me, Et; L = PEt_3, PPh_2Me) with iodine afforded [PdI_2L_2] and RI, and of [PdR_2(dppe)] with MeI gave CH_3H, CH_3CH_3, RH, RCH_3, R–R, R–I, and alkene products together with [PdI_2L_2], suggesting the presence of a six-coordinate intermediate Pd(IV) species (Scheme 4.3).[210] Interestingly, this was probably the first observation of transient organopalladium(IV) complexes supported by phosphine ligands.

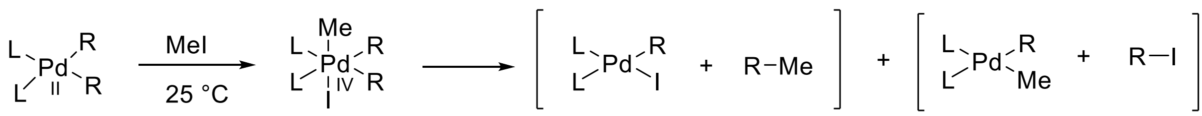

Scheme 4.3: Reaction of Pd(II) complexes with methyliodide and decomposition of the resulting transient Pd(IV) complex

The Negishi coupling utilises organozinc reagents to cross couple with organic halides. The organozinc reagent can be prepared *in situ* by transmetalation of the corresponding organolithium or Grignard reagent,[211] or via oxidative addition of activated Zn(0) to an organohalide.[212] With the demonstration of the reactivity of alternative organometallic derivatives, Negishi significantly broadened the concept of the cross-coupling approach and set the stage for the uncovering of milder, less electropositive-metal coupling species.

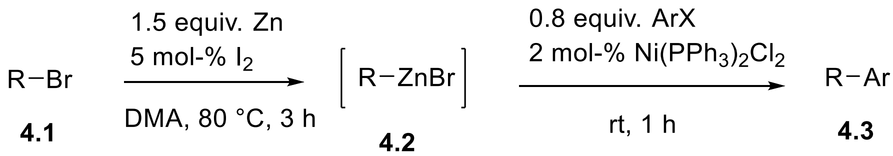

Scheme 4.4: Preparation of alkylzinc reagents from unactivated alkyl bromides[213]

The Hiyama coupling is a metal catalysed coupling reaction between organic halides and organosilanes. This reaction requires an activating agent such as fluoride ion or a base to activate the organosilane towards transmetalation by the formation of silicate intermediates (Scheme 4.5).[214] The Hiyama coupling approach provided a more environmentally friendly option than the organostannane (Stille) reagents.[215] This discovery has been pursued on other silicon derivatives, for example, siloxanes. The use of a silanol as the organosilane is one recent method that has managed to negate the requirement for the reaction to contain fluoride as an activator,[216] this has helped to enlarge the substrate scope of the reaction.

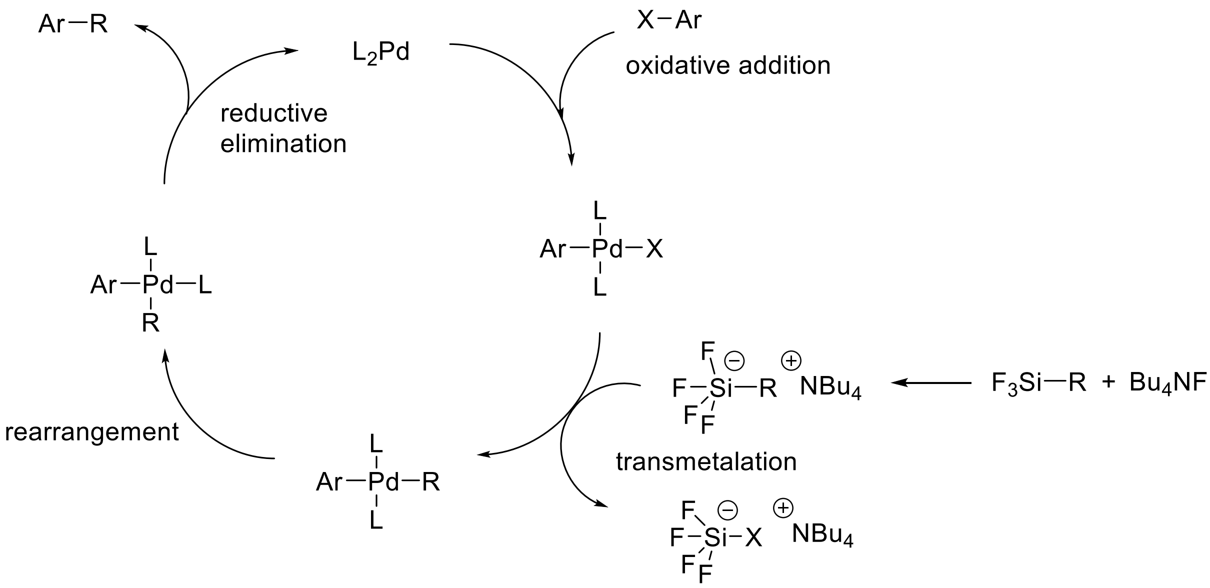

Scheme 4.5: Mechanism of the Hiyama coupling reaction

The palladium catalysed carbonylation is a very convenient method for the regioselective synthesis of carbonyl-containing compounds. The palladium catalysed carbonylation is compatible with a range of functional groups, which gives it significant advantage over standard organolithium and Grignard chemistry for the synthesis of aryl aldehydes, acids, esters and amides (Scheme 4.6). The reactions generally require added base to react with the acid generated in the reaction (by deprotonation of alcohols and amines, for example) and to promote the formation of the Pd(0) species which initiates the reaction.[217]

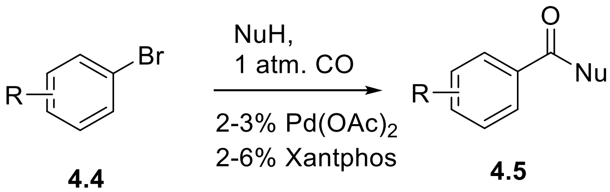

4.4 **4.5**

NuH = HN(OMe)Me, HNR_2, MeOH

Scheme 4.6: Palladium catalysed carbonylation reactions[218]

The palladium catalysed cyanation of aromatic halides allows for an efficient access towards aryl nitriles and offers a convenient alternative to the Rosemund-Von Braun reaction, which often employs harsh conditions and can have a labour-intensive work-up (Scheme 4.7). As the cyanide nucleophile is a strong σ-donor and can poison the catalyst, it is necessary to keep its concentration low during the reaction. The less poisonous cyanide source $K_4[Fe(CN)_6]$, in contrast to other cyanating agents, can be used in combination with palladium catalysts to synthesise aryl nitriles from their corresponding halides. Due to the slow release of cyanide ions, a significantly improved catalyst productivity is achieved.[219]

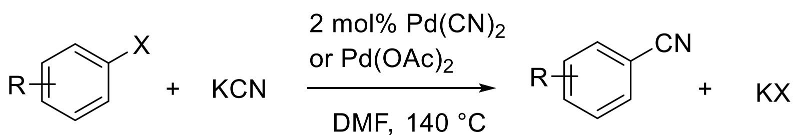

4.6 **4.7** **4.8** **4.9**

Scheme 4.7: First palladium-catalysed cyanation of aryl iodides and bromides[220]

Where the organometallic reactant (R–M) is replaced by a compound with a sp^2-hybridised carbon-hydrogen bond (Heck reaction), a sp-hybridised carbon-hydrogen bond (Sonogashira reaction), or an amine (Buchwald-Hartwig reaction), the cross-coupling follows a different path to the general mechanism.

The Heck reaction is the metal catalysed coupling between organic halides and activated alkenes in the presence of a base.[204] It can be regarded as the "father" of Pd-catalysed coupling processes.[221] The reaction tolerates electron-withdrawing groups and electron-donating groups on both reactants. One of the benefits of the Heck reaction is its outstanding *trans* selectivity. After the oxidative addition, a Heck reaction proceeds via π-coordination of the alkene reactant, then a migratory insertion of the alkene into the Pd–C bond previously formed during oxidative addition of the organohalide. The intermediate formed then undergoes β-hydride elimination under thermodynamically controlled conditions, leading to preferential formation of the *E*-product[222] (Scheme 4.8). For intermolecular reactions with mono-substituted alkenes, the alkene insertion step is usually directed by steric hindrance. The lack of an obligatory preformed organometallic species as one of the coupling partners makes the Heck reaction mechanistically different from most cross-coupling reactions, imparting freedom from the requirement of a transmetalation step.[215] Double-bond isomerisation in the Heck reaction is sometimes a problem. However, various additives can alleviate this; for example, the use of silver[223-226] or thallium[227] salts or the "greener" supercritical CO_2.[228]

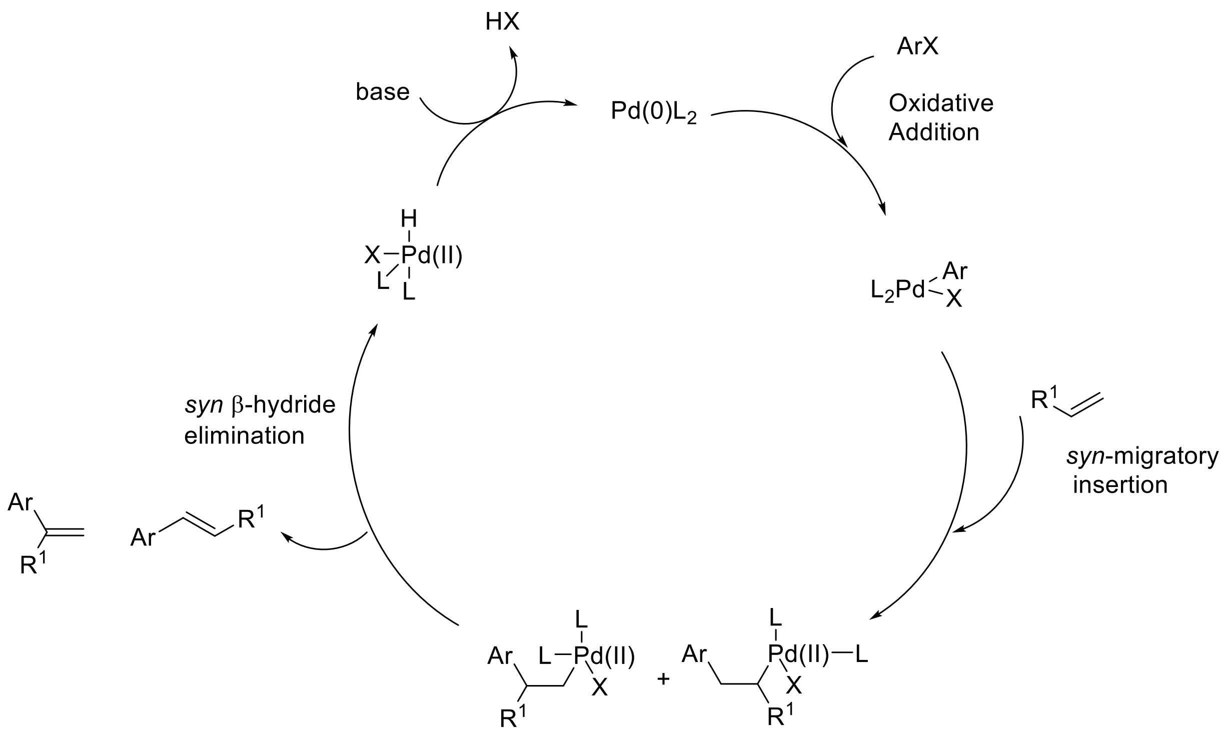

Scheme 4.8: Catalytic cycle for the Heck reaction

Since the halogenation of azaquinone was successful, it would be interesting to further elaborate the structure with some palladium catalysed cross-coupling reactions to enhance structural diversity and to determine the selectivity of the reactions. 3-Bromoazaquinone, **4.11** and 3-chloroazaquinone, **4.13** were considered as substrates for the reactions (Scheme 4.9).

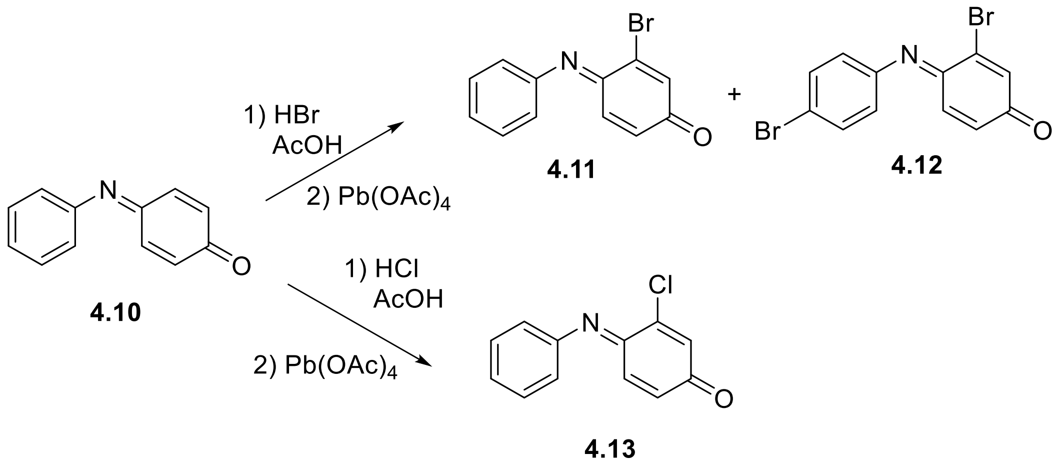

Scheme 4.9: Halogenation of azaquinone, **4.10**

3-Chloroazaquinone was found to be unreactive towards Suzuki coupling reactions under the conditions explored while 3-bromoazaquinone gave the expected result (13–66% **4.14**). 3-Bromoazaquinone was therefore used to investigate the rest of the coupling reactions. The palladium catalysed cross-coupling reactions investigated are the Suzuki, Stille, Sonogashira, Kumada and Buchwald-Hartwig reactions (Scheme 4.10).

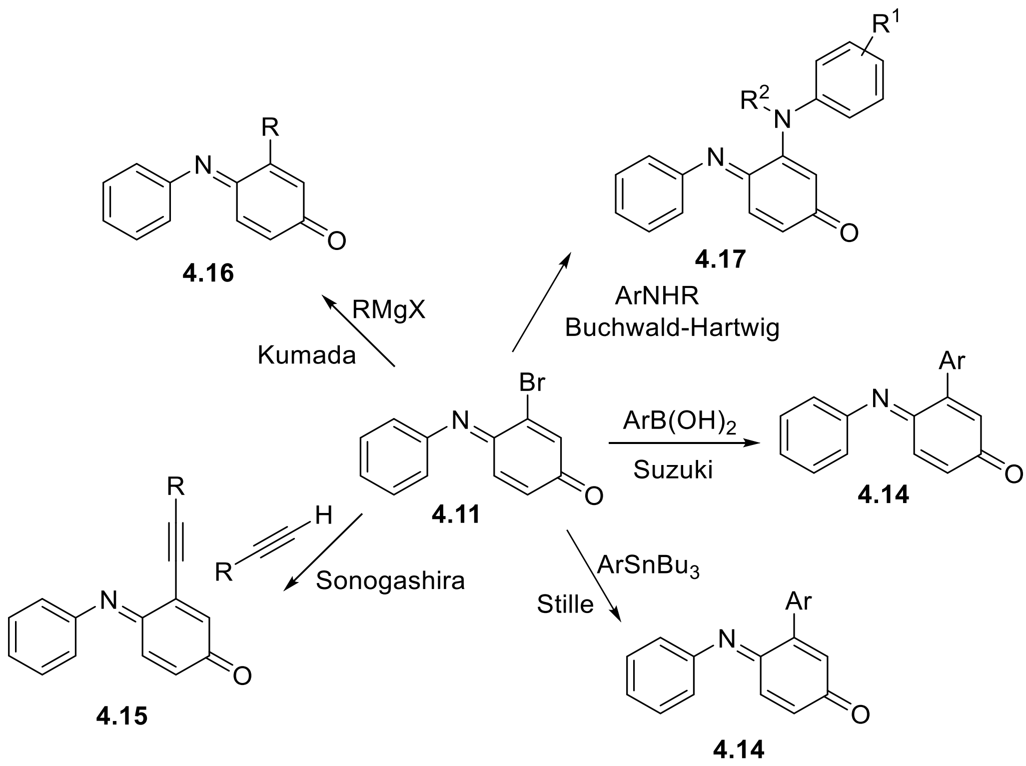

Scheme 4.10: Some cross-coupling reactions of 3-bromoazaquinone, **4.11**

4.2 Suzuki coupling

Suzuki coupling is a metal catalysed reaction, typically by palladium, between a vinyl, aryl, or alkynyl organoborane (boronic acid or boronate ester, or in special cases an aryl trifluoroborate) and organohalides or triflates under basic conditions (Scheme 4.11). The Suzuki reaction is undoubtedly the most intensively investigated C–C coupling reaction, particularly in the 21st century.[184,229] The organoboranes are usually air and moisture tolerant, are often commercially available and generally non-toxic and environmentally safer than the other organometallic reagents which may contain metals and the reaction can be run under very mild conditions. The reaction is generally carried out at a temperature range of 60–80 °C, is highly tolerant of many different functional groups, is highly chemoselective, and boron containing by-products are easily removed by a simple alkali work-up.[230] The Suzuki reaction has the advantage of high regio- and stereoselectivity, the use of a small amount of catalyst, and application in one-pot synthesis.[229] The Suzuki reaction is highly efficient for the synthesis of highly substituted styrenes, conjugated systems of alkenes, or biaryl compounds.[230]

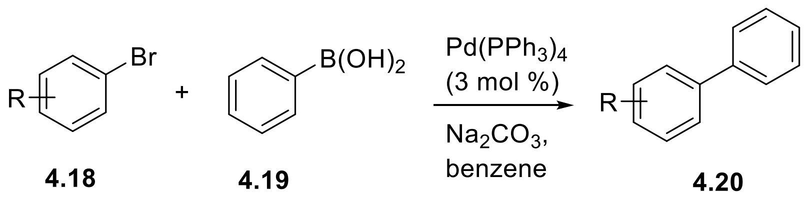

Scheme 4.11: Suzuki cross-coupling reaction of phenylboronic acid and haloarenes[198]

4.2.1 Suzuki Coupling of 3-bromoazaquinone with arylboronic acids

The Suzuki coupling was carried out using 3-bromoazaquinone and a range of aryl boronic acids. Two equivalents of the boronic acids were used.[231,232] The results are given in Table 4.1.

The coupled products, **4.14** were obtained in average to good yields (best yields reported) with the biaryl products, **4.21** obtained as by-products, resulting from the homocoupling of the arylboronic acid. There is no significant change with the use of palladium acetate with triphenylphosphine as the catalyst (Entry 2), so tetrakis(triphenylphosphine)palladium(0) was used for the rest of the studies. A much lower yield is observed when electron-deficient boronic acids are used, and the substitution of silver carbonate for cesium carbonate does not lead to any significant change.

The reaction was also carried out using one equivalent of the phenylboronic acid, **4.19a** to determine the stoichiometric effect on the products formed, in an attempt to reduce the symmetrical biaryl product formed and so increase the yield of the coupled product (Entry 3). This biaryl product is still observed with the yield of the coupled product not being significantly different from the reaction using two equivalents of the phenylboronic acid meaning that the reaction pathway is not affected by the change in the equivalents of arylboronic acid.

Table 4.1: Suzuki Reaction of 3-bromoazaquinone with arylboronic acids

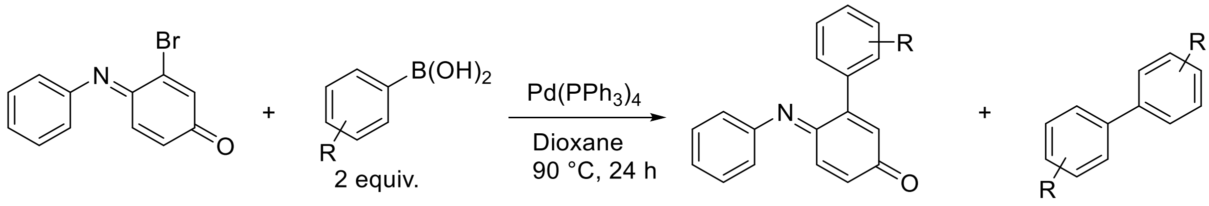

4.11 **4.19** **4.14** **4.21**

Entry	**Boronic acid 4.19**	**R**	**Coupled product 4.14 (%)**		**Biaryl product 4.21 (%)**	
			Cs_2CO_3	Ag_2CO_3	Cs_2CO_3	Ag_2CO_3
1	**a**	H	66	58	31	39
2[a]	**a**	H	58	n	30	n
3[b]	**a**	H	37	17	29	38
4	**b**	4-Cl	48	nd	32	35
5	**c**	4-Br	n	13	n	26
6	**d**	4-OMe	20	35	32	21[c]
7	**e**	2-Me	t	t	18	24
8	**f**	4-CHO	nd	13	49	23
9	**g**	2-naphthyl	34	30	30	38

[a]$Pd(OAc)_2/PPh_3$, [b]1 equiv. boronic acid, [c]4-methoxy-1,1'-biphenyl also observed (4%), t = trace amount, n = not done (because results from using Cs_2CO_3 were similar to Ag_2CO_3), nd = not detected

4.2.2 Suzuki Coupling of 3-bromo(4-bromophenyl)azaquinone, 4.12 with phenylboronic acid

The Suzuki coupling of 3-bromo(4-bromophenyl)azaquinone was carried out to determine the selectivity of the reaction between the two different bromo groups. There are two coupled products formed in the reaction, compounds **4.22** and **4.14a** (Scheme 4.12). Compound **4.22** is as a result of coupling only to the carbon attached to the bromine atom on the phenyl ring while the bromine on the quinoid ring remained intact. Compound **4.14a**, however, is a product from coupling to the carbon bearing the bromine atom on the quinoid ring only although it is surprising that the bromine atom is not residual on the phenyl ring in **4.14a** which could result from the hydrodehalogenation of the phenyl ring.[233,234] The higher yield of compound **4.22** in the reaction suggests that the bromine on the phenyl ring is more reactive than the bromine on the quinoid ring however the difference is small suggesting it may be possible for compound **4.22** to be formed selectively.

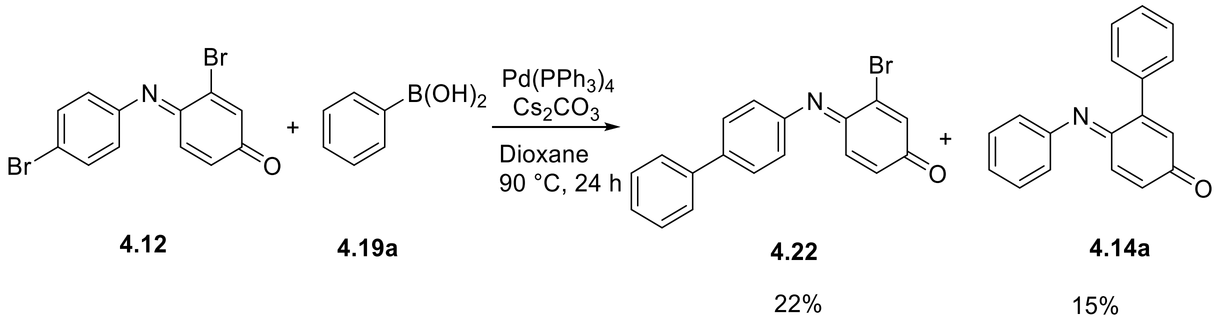

Scheme 4.12: Suzuki coupling of 3-bromo(4-bromophenyl)azaquinone, **4.12**

4.3 Stille coupling

The Stille reaction is an extremely versatile alternative to the Suzuki reaction in organic synthesis. It replaces the organoborane with an organotin compound (also known as an organostannane) such as $ArSnR_3$ or $vinylSnR_3$ (Scheme 4.13). Organostannanes with R=Bu are preferred to those with R=Me because they have lower toxicity, are cheaper and more readily available but are less reactive.

The relative rate of transmetalation of Sn to Pd is alkynyl>vinyl>aryl~benzyl>>alkyl. The Stille Coupling is useful for constructing new carbon-carbon bonds because organotin compounds are easy to synthesize, and some are commercially available. The reaction also has the advantage that it is run under neutral conditions making it even more tolerant of different functional groups than the Suzuki reaction. However, the main disadvantage of the Stille reaction is the toxicity of the organostannanes and also removal of the by-products. Compared with boron or zinc derivatives, the lower polarity (hence lower basicity) and higher steric demand of tin derivatives makes them less nucleophilic and less reactive.[235] However, nucleophilicity is not the only virtue sought for in a nucleophilic reagent: reactivity and selectivity are often in conflict and selectivity is a must in many areas of synthesis.

$$\underset{\substack{\text{X:Br, Cl}\\ \textbf{4.23}}}{\text{Ar—X}} + \underset{\substack{\text{1.1 equiv.}\\ \textbf{4.24}}}{RSnBu_3} \xrightarrow[\substack{\text{DMF}\\ \text{45 °C (-Br) or 100 °C (-Cl), 15 h}}]{\substack{\text{2 mol\% } PdCl_2\text{, 4 mol\% } P^tBu_3\\ \text{4 mol\% CuI, 2 eq. CsF}}} \underset{\substack{\text{R: Ar, vinyl}\\ \textbf{4.25}}}{\text{Ar—R}}$$

Scheme 4.13: An example of Stille coupling. [185]

Side reactions of the Stille reaction include homocoupling, transfer of “non-transferable” ligands (e.g. Bu), destannylation, cine substitution and aryl migration. Undoubtedly, the most common side-products are those involving a homocoupling event as observed in the Suzuki reaction. Reaction of a Pd(II) precatalyst with two equivalents of the organostannane mostly accounts for this observation. In other cases such as when Pd(0) is used, the homocoupling products can be formed in the presence of air which could facilitate insertion of the Pd(0) into the C–Sn bond.[234,236]

4.3.1 Stille coupling of 3-bromoazaquinone with organostannanes

The reaction of 3-bromoazaquinone, **4.11** with tributyl(phenyl)stannane, **4.26a** was carried out using one equivalent of the arylstannane in THF, with LiCl as the base, and heated at 100 °C for 24 h,[237] both the coupled product and biaryl product were obtained in low yields. The reaction was repeated with the base changed to Ag_2CO_3 and the solvent to dioxane and an increase in yield was observed for the coupled product while the biaryl product was not formed (Scheme 4.14). This demonstrates that the solvent/base combination is critical in the optimisation of the palladium catalysed Stille reaction. The reaction with tributyl(thiophen-2-yl)stannane, **4.26h** was therefore only carried out using Ag_2CO_3 in dioxane and the coupled product was obtained in good yield while the biaryl product was not formed. This selectivity could also result from the use of one equivalent of the organostannane since the reaction of a Pd(II) precatalyst with two equivalents of the organostannane mostly accounts for the homocoupling side-products.[234] Other organostannanes such as tributyl(vinyl)tin and tributyl(phenylethynyl)tin were also investigated but surprisingly no positive reaction was observed. The reaction with tributyl(vinyl)tin only gave unreacted starting material while the reaction with tributyl(phenylethynyl)tin gave several unidentified products.

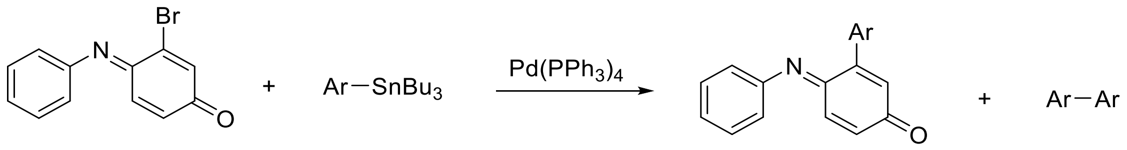

4.11 **4.26** **4.14** **4.21**

Ar = Ph (**a**)

Ar = 2-thienyl (**h**)

4.14a 7% **4.21a** 11% (LiCl/THF)
4.14a 63% **4.21a** not detected (Ag_2CO_3/Dioxane)
4.14h 55% **4.21h** not detected (Ag_2CO_3/Dioxane)

Scheme 4.14: Stille Coupling of 3-bromoazaquinone, **4.11** with organostannanes, **4.26**

4.4 Sonogashira coupling

The Sonogashira reaction is the palladium catalysed cross coupling reaction between aryl or vinyl halides and terminal alkynes. The reaction offers an extremely useful route to aryl- and alkenyl-alkynes. Sonogashira reaction is one of the most popular cross-coupling reactions for the formation of C(sp^2)—C(sp) bonds, with its use extending to applications in pharmaceuticals, nanomaterials, and natural products.[238-240] The alkyne moiety is usually introduced *via* its copper salt which is generated *in situ* from a Cu(I) salt, such as CuI or CuCN, and a terminal alkyne in the presence of an amine base (Scheme 4.15).[241] The copper (I) acetylide which is formed subsequently transmetalates to palladium, as in other cross-coupling reactions with preformed organometallic reagents. Despite the popularity of the reaction, Sonogashira coupling exhibits several important limitations. The copper salts used in the co-catalysed reaction are environmentally unfriendly and difficult to recover from the reaction mixture. Additionally, upon exposure to air, the copper acetylide will undergo a homocoupling side reaction, decreasing the overall efficiency of the reaction.[242] Thus, efficient variants for these reactions that do not employ copper co-catalysts (copper-free Sonogashira reactions) are much sought after and have been increasingly reported.[243-245]

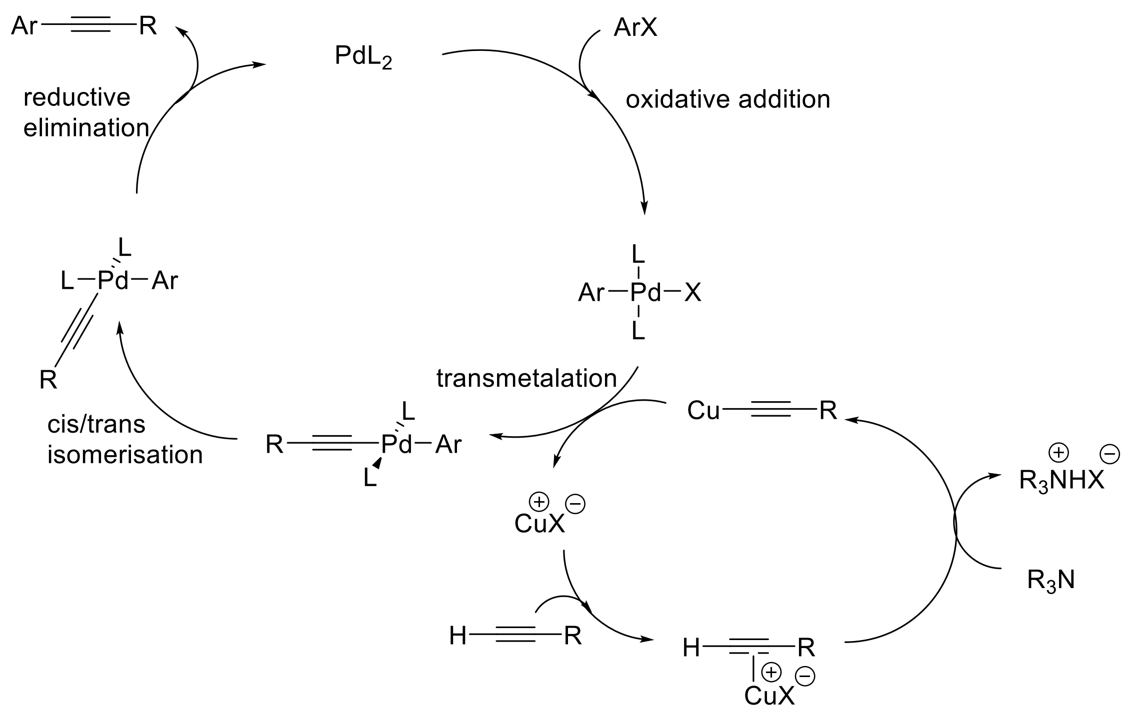

Scheme 4.15: Catalytic cycle of palladium and copper co-catalysed Sonogashira reaction

4.4.1 Sonogashira coupling of 3-bromoazaquinone with terminal alkynes

It was observed that the Sonogashira coupling reaction of 3-bromoazaquinone with 4-ethynyltoluene is not as successful as the Suzuki and Stille reaction as it gives only the dialkynyl product **4.28**. This is due to the homocoupling side reaction of the copper acetylide.

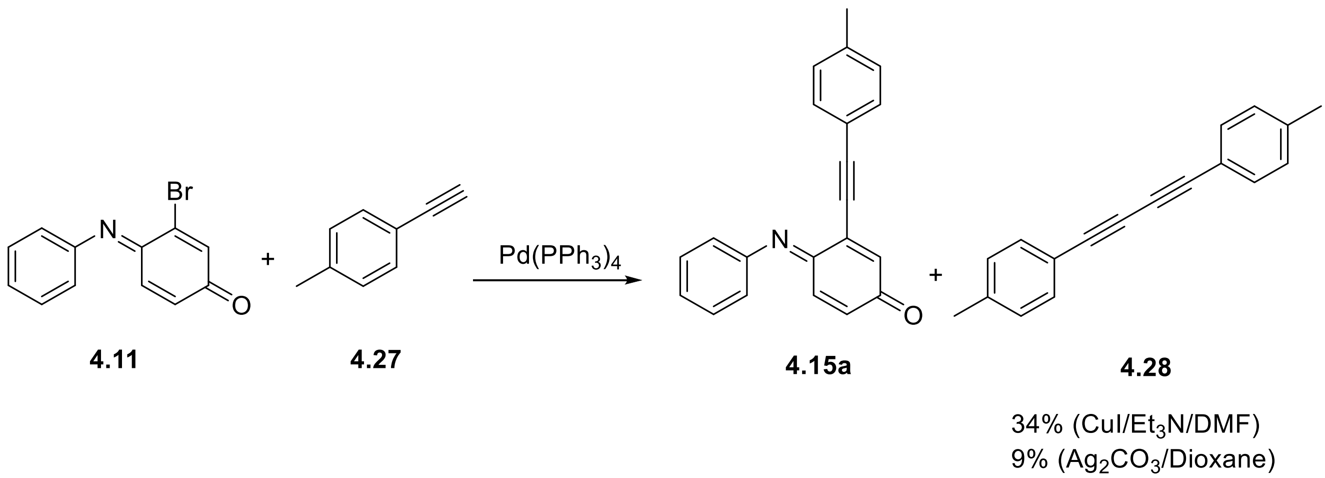

Scheme 4.16: Sonogashira coupling of 3-bromoazaquinone, **4.11** with 4-ethynyltoluene, **4.27**

4.5 Buchwald-Hartwig amination reaction

The Buchwald-Hartwig amination is a chemical reaction used for the synthesis of carbon-nitrogen bonds via the palladium-catalysed coupling reactions of amines with aryl halides. This reaction is significant as all other coupling reactions considered make C–C bonds. The reaction's synthetic utility stems primarily from the shortcomings of typical methods (nucleophilic substitution, reductive amination, the Goldberg reaction) for the synthesis of aromatic C–N bonds, with most suffering from limited substrate scope and functional group tolerance. These reactions are mechanistically strictly related to classical cross-coupling reactions (Scheme 4.2) in that they involve oxidative addition of the aryl halide, coordination and deprotonation of the amine, and finally reductive elimination of the product with formation of the C–N bond. However, in these reactions the reductive elimination step is often critical, being the rate-determining step of the whole process; consequently, in order to promote this step, Pd complexes with suitable ligands such as P(*o*-tolyl)$_3$, DPPF, BINAP and xantphos have to be employed as catalysts.[246,247] The reaction has gained wide use in synthetic organic chemistry because of the ubiquity of aryl C–N bonds in pharmaceuticals and natural products, with application in many total syntheses and the industrial preparation of numerous pharmaceuticals.[248,249] Bulky tri- and di-alkyl phosphine ligands have been shown to be remarkably active catalysts, allowing the coupling of a wide range of amines (primary, secondary, electron-withdrawing, heterocyclic) with aryl halides and triflates. The activity of these ligands is attributed to their propensity to sterically favour the monoligated palladium species at all stages of the catalytic cycle, dramatically increasing the rate of oxidative addition, amide formation, and reductive elimination.[102,186]

The preparation of enantiomerically enriched aniline derivatives by coupling enantiomerically enriched amines with aryl bromides has been reported.[250] Due to the importance of amino alcohols in the pharmaceutical industry, the methodology was extended to the selective *N*-arylation of enantiomerically enriched amino alcohols. However, protection of the hydroxyl group was required in order to obtain the desired product in good yield. Amino alcohols protected as their *tert*-butyl ethers were found to undergo efficient coupling (Scheme 4.17).

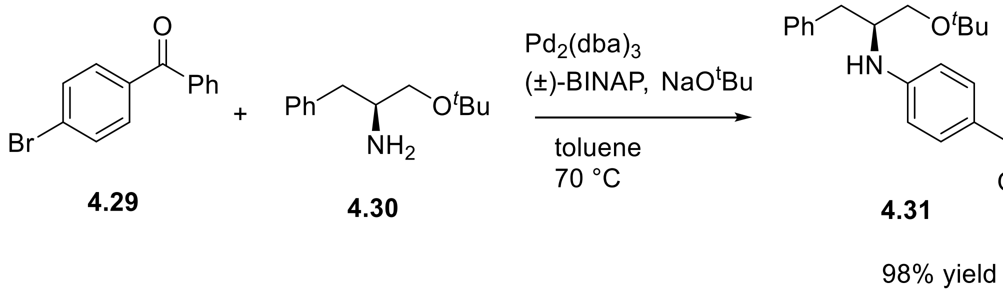

Scheme 4.17: An example of Buchwald-Hartwig amination

4.5.1 Buchwald Hartwig coupling of 3-bromoazaquinone with arylamines

The Buchwald-Hartwig amination reaction was investigated by coupling 3-bromoazaquinone with arylamines as a means of forming new C–N bonds. The results are presented in Table 4.2.

Table 4.2: Reaction of 3-bromoazaquinone with aniline derivatives

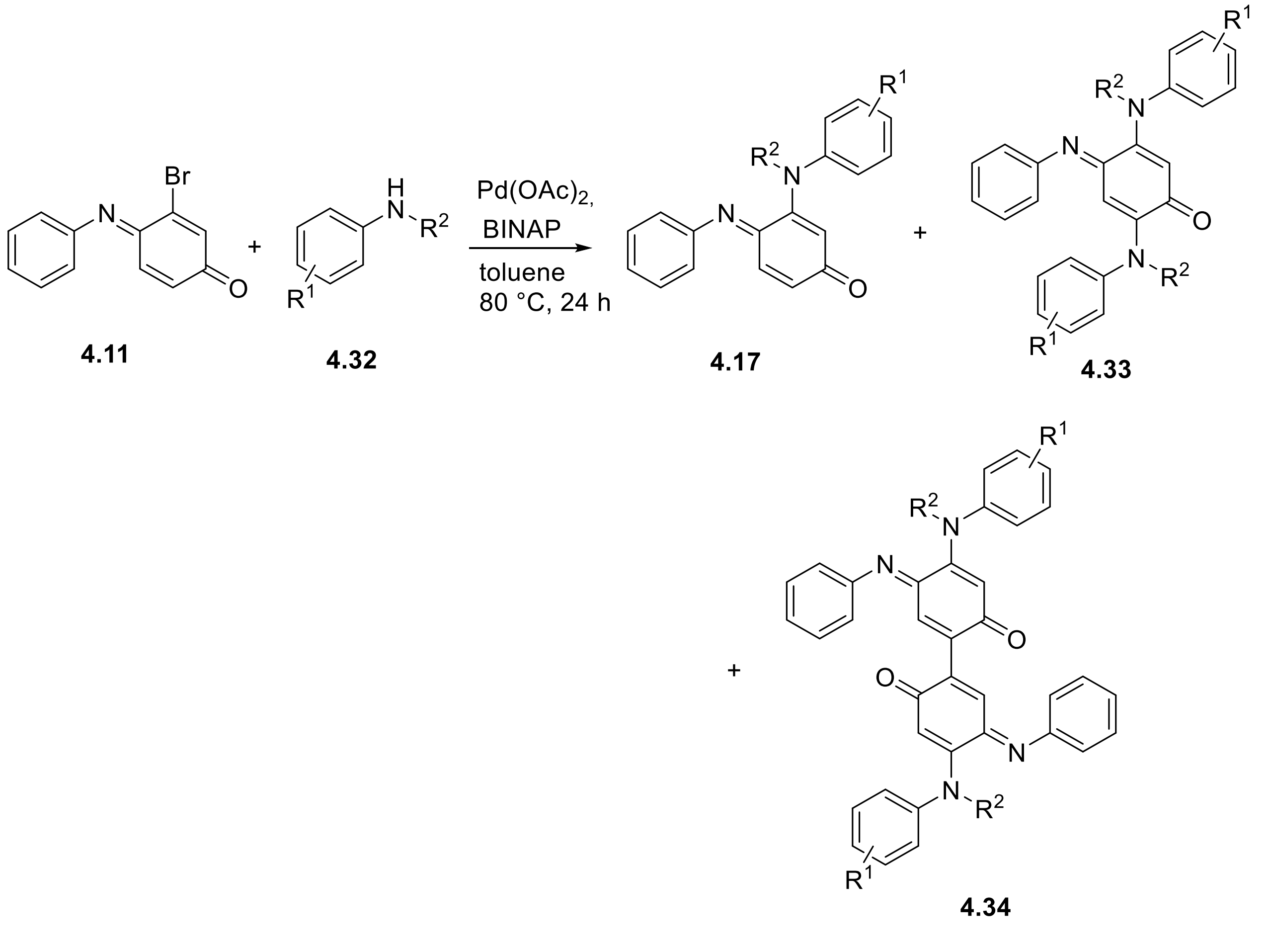

Entry	Aniline 4.32	R1	R2	4.17 (%)	4.33 (%)	4.34 (%)
1	**a**	H	H	79	13	nd
2	**b**	4-OMe	H	66	17	nd
3	**c**	4-Cl	H	29	15	nd
4	**d**	4-CF_3	H	29	3	nd
5	**e**	2-Me	H	72	t	5
6	**f**	H	Me	59	8	3

nd = not detected, t = trace amount

The reaction, which may also occur by addition to the α,β-unsaturated ketone, gives the expected coupled product **4.17** in good yields. The anilines with electron-deficient groups (entries 3 and 4) were observed to give lower yields. The structural assignment was confirmed by X-ray analysis of single crystals of **4.17e** (Fig. 4.1). The product of diaddition to the α,β-unsaturated ketone and α,β-unsaturated imine, **4.33** was also observed.

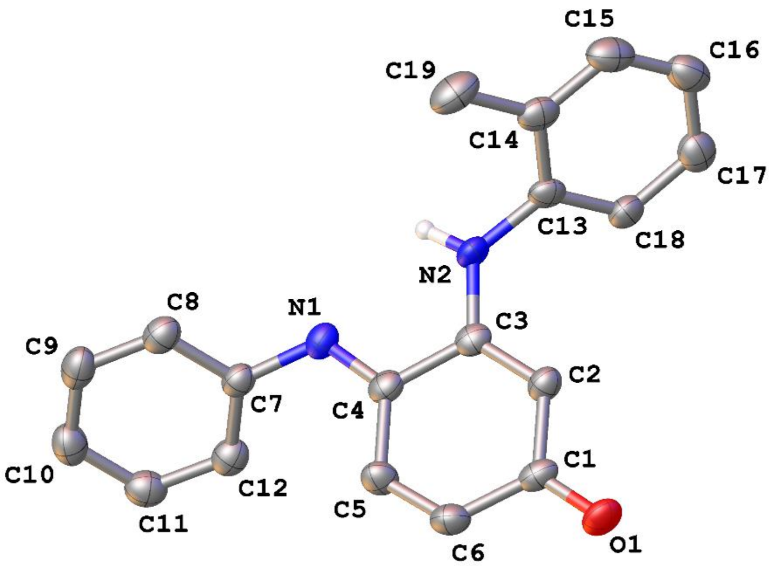

Figure 4.1: Crystal structure of compound **4.17e**

Interestingly, this reaction also offers insight into the possible mechanism of the direct addition of aromatic amines to azaquinone (see Section 2.1.1) as the mono-addition product resulting from the α,β-keto attack has now been independently made. Also, the diaddition product formed from the addition of aromatic amines to azaquinone was observed in the Buchwald-Hartwig amination as a by-product **4.33** again suggesting that compound **4.17** may be an intermediate in forming the diaddition product. To confirm this, compound **4.17a** was then reacted with aniline (1 equiv.) under the same reaction conditions for the reaction of azaquinone with aniline derivatives (Scheme 4.18).

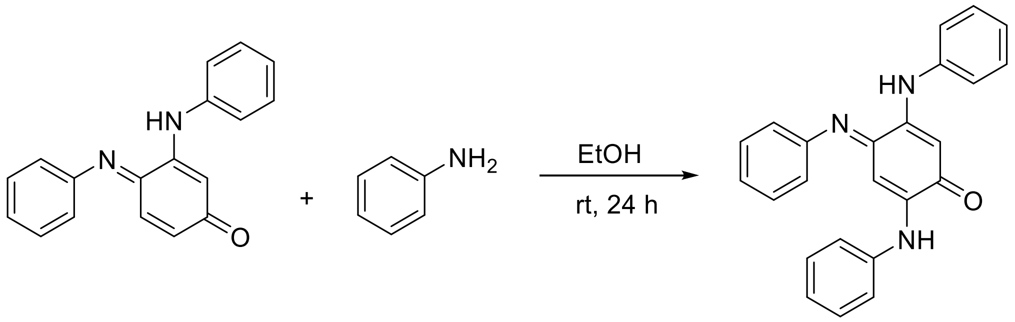

4.17a **4.32a** **4.33a**

Scheme 4.18: Addition of aniline to mono-addition product, **4.17a**

At the completion of the reaction, it was observed that although the di-addition product, **4.33a** was formed, compound **4.17a** was still present in the reaction mixture suggesting that it may be an intermediate for the reaction, but it may not be the major intermediate as this result would suggest it would be possible to isolate this material from the aniline addition reaction and therefore it is likely that there may be multiple processes taking place (Fig. 4.2).

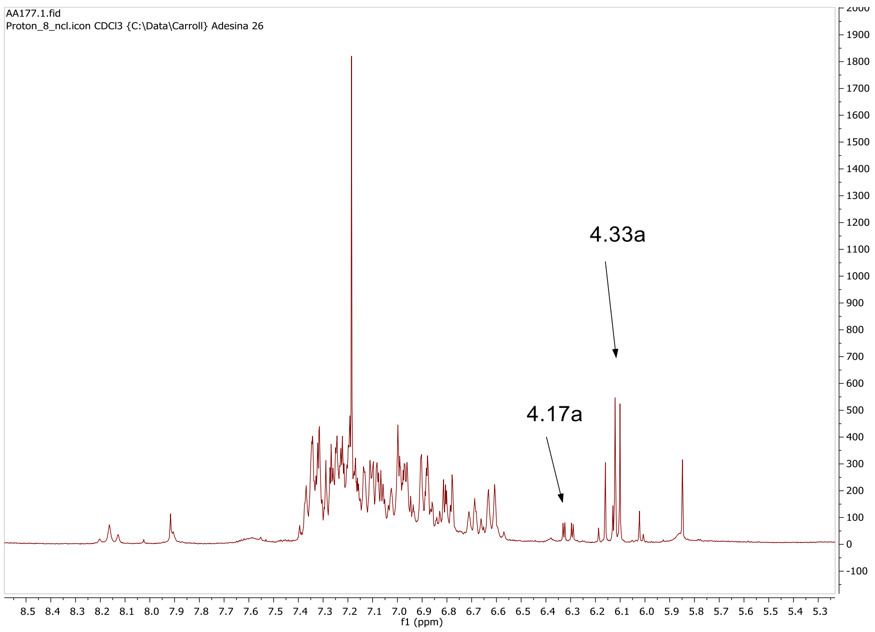

Figure 4.2: ^{1}H NMR spectrum of the reaction mixture of compound **4.17a** with aniline

A product of dimerization was observed with entries 5 and 6, giving compound **4.34** as by-product resulting from oxidative coupling between two molecules (Table 4.2). The absence of the double doublet corresponding to H6 (6.28ppm) and the replacement of the doublet for H5 (6.68ppm) with a singlet (6.82ppm) in the ^{1}H NMR spectrum of compound **4.34f** suggests dimerised product. The X-ray analysis of **4.34f** confirms the structural assignment (Fig. 4.3).

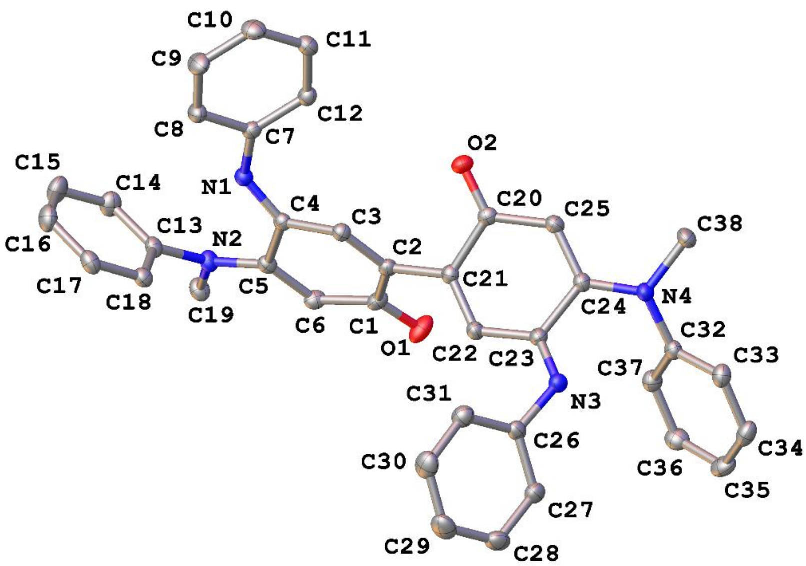

Figure 4.3: Crystal structure of compound **4.34f**

The formation of the dimerised product **4.34** is not surprising as it has been reported that unexpected observations, new transformations or unusual side reactions often occur in Pd-catalysed reactions and these stem from poor catalytic turnover, unusual reactivity or selectivity, or the presence of unwanted side-products.[234]

A naphthoquinoneimine dimer **4.37** has been reported as a by-product in the reaction of naphthoquinoneimine **4.35** with thiols suggesting that this type of dimerization is not limited to cross-coupling reactions only (Scheme 4.19)[251].

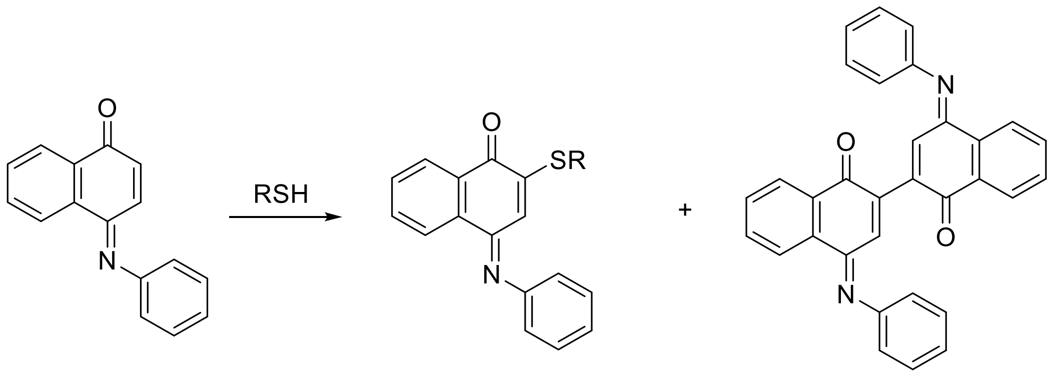

4.35 **4.36** **4.37**

R = $C_{10}H_{21}$ (a), 4-$CH_3C_6H_4$ (b)

Scheme 4.19: Reaction of naphthoquinoneimine with thiols

Compound **4.37** has been reportedly synthesised from the oxidative coupling of *N*-phenylnaphtho-1,4-quinoneimine, **4.35** (Scheme 4.20).[252] A mixture of naphthoquinoneimine **4.35** and potassium hexacyanoferrate(III) were treated in a basic aqueous medium giving the dimeric compound **4.37** in 80% yield.

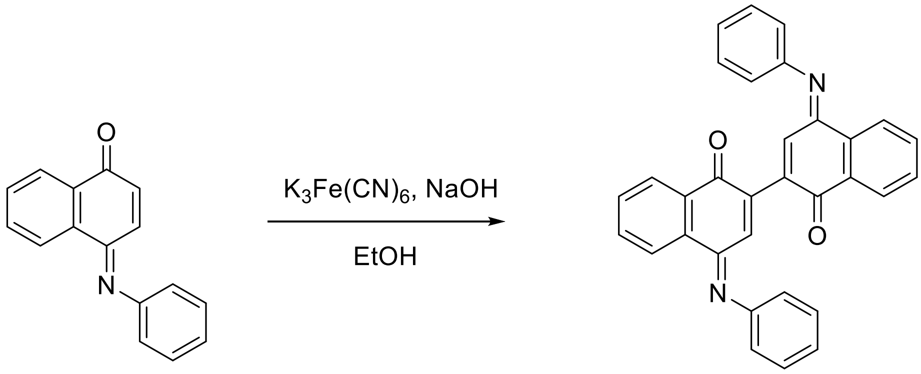

4.35 4.37

Scheme 4.20: Oxidative coupling of *N*-phenylnaphtho-1,4-quinoneimine

4.6 Kumada Coupling

The reaction of an organohalide substrate with a Grignard reagent to produce the corresponding coupled product is known as the Kumada coupling (Scheme 4.21). The procedure uses transition metal catalysts, typically nickel or palladium, to couple a combination of two alkyl, aryl or vinyl groups. Although it suffers from a limited tolerance of different functional groups, the higher reactivity and basicity of the Grignard reagent allows viable reactions to take place under mild conditions.[253] The advantage of this reaction is the direct use of Grignard reagents, which avoids additional reaction steps such as the conversion of Grignard reagents to zinc compounds for the starting materials in the Negishi coupling.

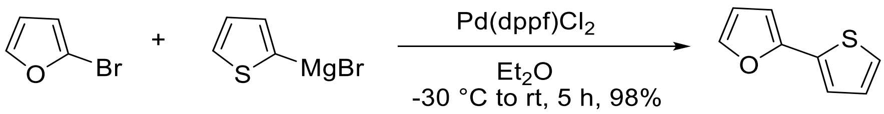

4.38 4.39 4.40

Scheme 4.21: An example of Kumada coupling reaction[254]

4.6.1 Kumada coupling of 3-bromoazaquinone with Grignard reagents

The reaction of 3-bromoazaquinone, **4.11** with isopropylmagnesium chloride **4.41** was done in THF at 60 °C for 2 h (Scheme 4.22).[255] The crude reaction mixture was purified by chromatography (SiO_2 1:4 ethylacetate-petrol) to give the coupled product **4.16a** as a red oil. The Kumada coupling, although it only gives a low yield of the product, is important and different from the other coupling reactions investigated as it allows the introduction of alkyl as well as aryl groups.

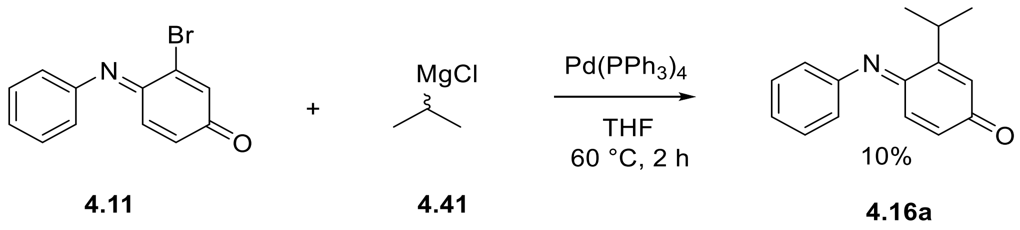

Scheme 4.22: Reaction of 3-bromoazaquinone with isopropylmagnesium chloride

The lack of reactivity and low yields observed in some of the palladium catalysed coupling reactions considered may result from the oxidation of Pd(0) to Pd(II) by the azaquinone in the oxidative addition step of the catalytic cycle since it also acts as an oxidising agent.

4.7 Summary

The introduction of halogens into the azaquinone offers the possibility of further elaboration of the structure. 3-Bromoazauinone has been used as a substrate for Suzuki, Stille, Kumada and Buchwald-Hartwig cross-coupling reactions. The mono-addition product derived from the Buchwald-Hartwig reaction has been used to investigate the order of addition in the formation of the diarylamino products which resulted from the direct addition of aromatic amines to azaquinone. A novel dimerised product was also observed as a by-product in the Buchwald-Hartwig amination resulting from oxidative coupling between two molecules of the amination mono-addition product.

Chapter 5. Conclusion and Future Work

5.1 Conclusion

Azaquinone is an unexplored yet versatile building block with all six carbon atoms in the quinoid ring being different. It can be prepared on a large scale and is compatible with automation e.g. flow chemistry. Azaquinone has potential for building complex structures as part of tandem processes, scaffold diversity and drug discovery.

The multiple products formed by the arylation of 4-hydroxyaniline **5.2** with diphenyliodonium trifluoroacetate **5.1** have been identified. Good yields of the desired products – 4-hydroxydiphenylamine **5.3** and iodobenzene are obtained in DMF at 130 °C for 24 h, the effect of the counter-ion on the reactions of diphenyliodonium salts with 4-hydroxyaniline has also been studied and the reaction proceeds as expected giving **5.3** in good yields where the counter-ion is less nucleophilic in nature than the aniline. Azaquinone **5.4** has also been observed as a product resulting from the in-situ oxidation of **5.3** during these reactions (Scheme 5.1).

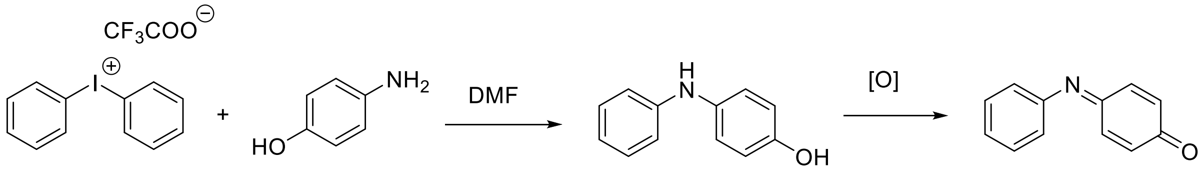

5.1 **5.2** **5.3** **5.4**

Scheme 5.1: *N*-arylation of 4-hydroxyaniline with diphenyliodonium trifluoroacetate

The nucleophilic addition of amines to azaquinone has been successfully studied with aliphatic amines being 1,2-selective giving diaminoarenes **5.5** following a reductive work-up while aromatic amines were 1,4-selective and resulted in double addition, with the regiochemistry of the products **5.6** being confirmed for the first time (Scheme 5.2). The α,β-keto mono-addition product of aromatic amines was independently prepared as a search for the intermediate. Computational studies has shown that the reaction intermediate results from single addition to the α,β-ketone (before oxidation) which the second nucleophile then adds to.

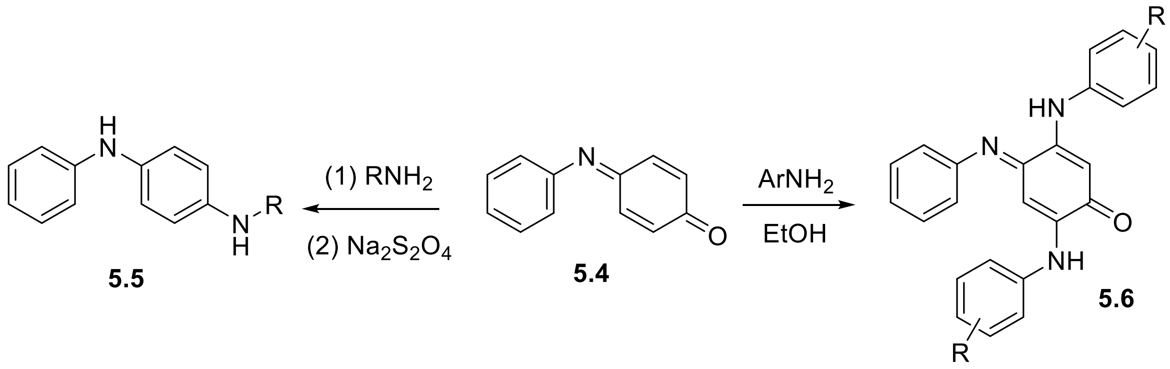

Scheme 5.2: Nucleophilic addition of amines to azaquinone

The reaction of azaquinone with arenesulfinates gives 1,4-addition products (mono only) **5.8** and has served as a new route to making phenoxathiin-10,10-dioxide **5.9** as part of tandem processes (Scheme 5.3).

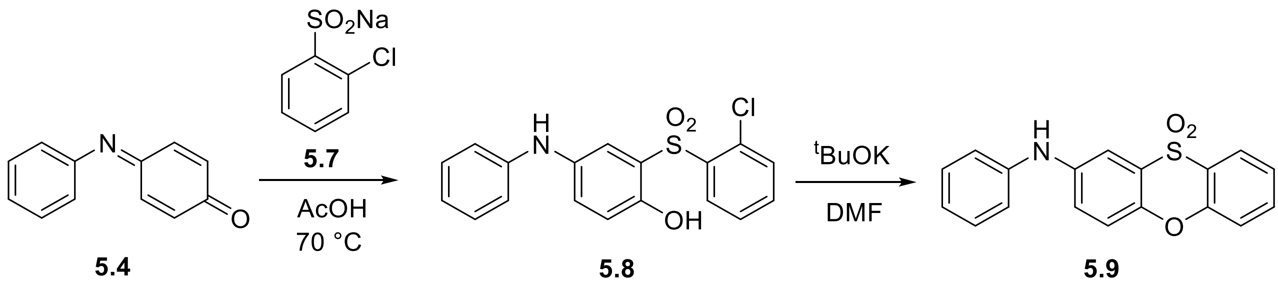

Scheme 5.3: Reaction of azaquinone with arenesulfinates

The halogenation of azaquinone **5.1** is selective allowing targeted functionalisation while azaquinone *N*-oxide **5.12** gives direct halogenation to the phenyl ring, changing the selectivity of the reaction (Scheme 5.4).

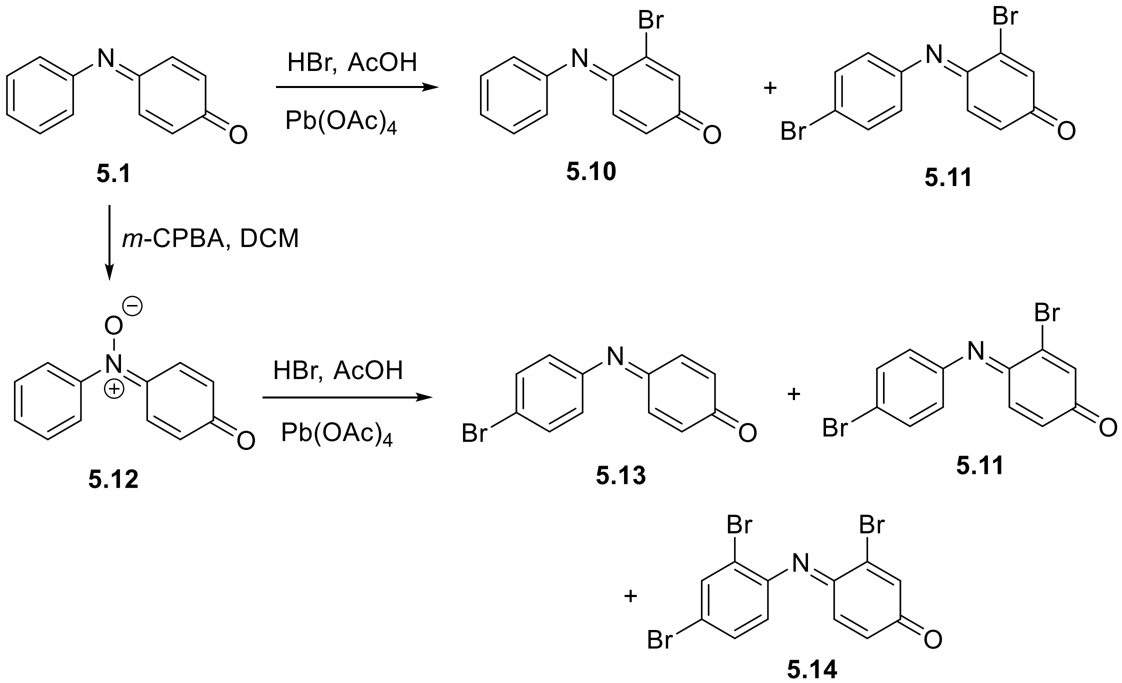

Scheme 5.4: Halogenation of azaquinone **5.1** and azaquinone *N*-oxide **5.12**

3-Bromoazaquinone **5.10** has been used as a substrate for Suzuki, Stille, Kumada and Buchwald-Hartwig cross-coupling reactions (Scheme 5.5). The Sonogashira coupling was also considered although it gave only the homocoupling product.

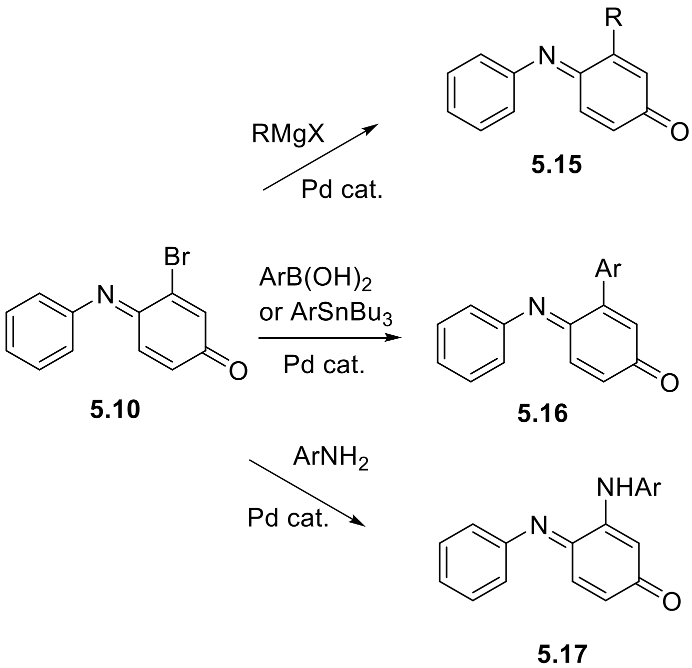

Scheme 5.5: Cross-coupling reactions of 3-bromoazaquinone **5.10**

These coupling reactions have served as a means of incorporating both new R and Ar groups into the quinoid ring of the azaquinone, and so elaborating the structure.

5.2 Future Work

Metal-halogen exchange to generate a Grignard or organolithium reagent from 3-bromoazaquinone **5.10** offers additional reactivity and scope as the electrophile can also be varied (an example is shown in Scheme 5.6 of a derived Grignard reagent reacting with an aldehyde).

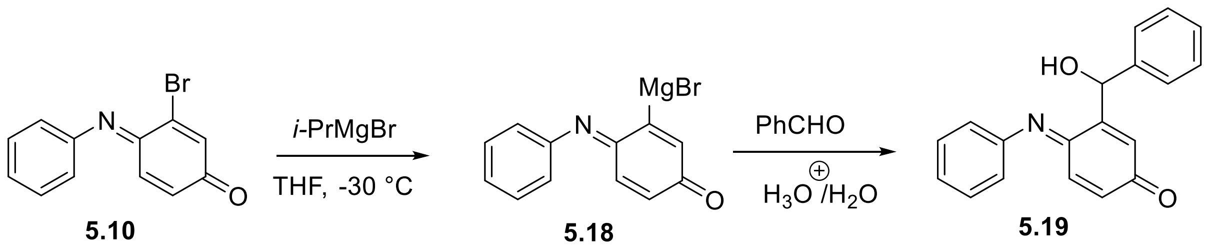

Scheme 5.6: Grignard reaction of 3-bromoazaquinone

The addition of nucleophiles (e.g. sodium arenesulfinates) to substituted azaquinones can be investigated (Scheme 5.7) to see the influence of electron-withdrawing/donating and bulky groups on the position of nucleophilic attack and selectivity of the reaction. These substituted azaquinones **5.20** could be prepared from substituted or asymmetric iodonium salts. A 2-pyridyl unit (*N*-aryl ring) could also be used as this would remove the steric twist and allow full conjugation throughout the ring.

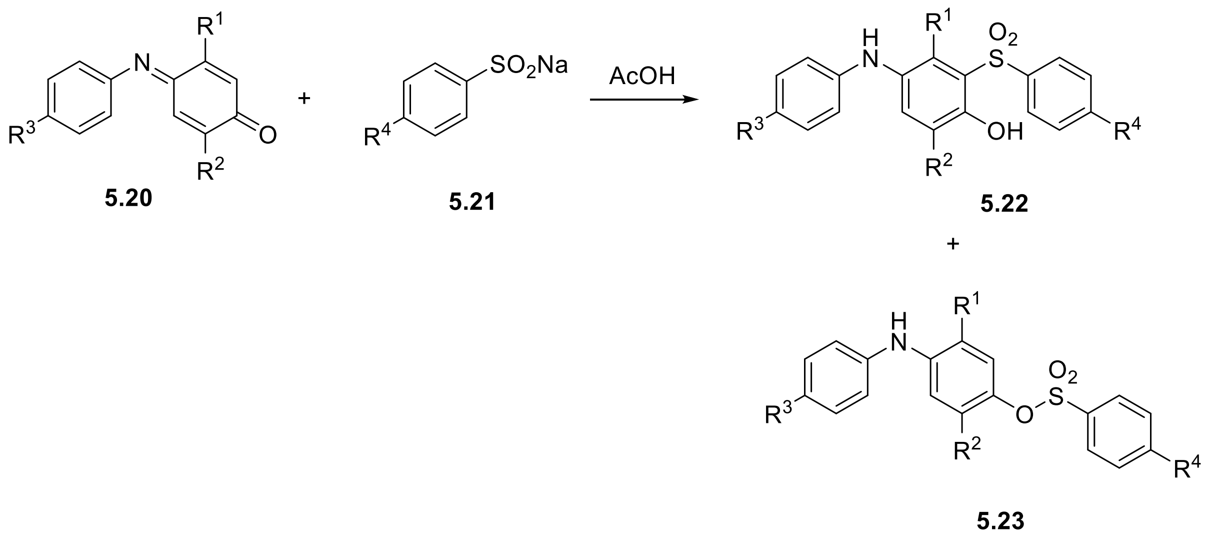

Scheme 5.7: Nucleophilic addition to substituted azaquinones

The selectivity of arylhalide versus quinoidhalide in di-substituted and tri-substituted azaquinone for cross-coupling reactions will be investigated in addition to using substrates where X = Cl (**5.24** and **5.25**). Some computational studies will also be done to ascertain selectivity of azaquinone *N*-oxide halogenation (Scheme 5.8).

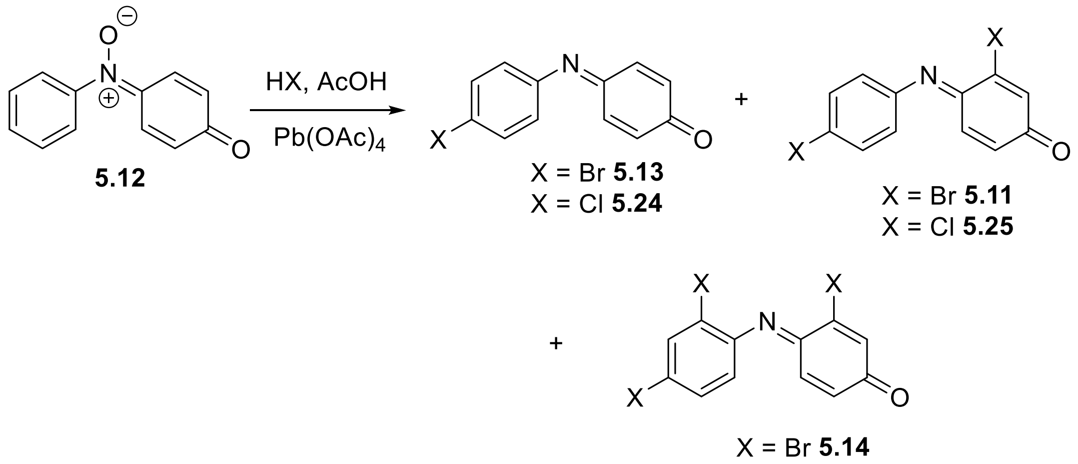

Scheme 5.8: Halogenation of azaquinone *N*-oxide **5.12**

Optimisation of the palladium catalysed reactions will be considered in terms of ligands, additives and solvents. Other cross-coupling reactions like cyanation and carbonylation will also be investigated as these extend the structural diversity of the products still further (Scheme 5.9).

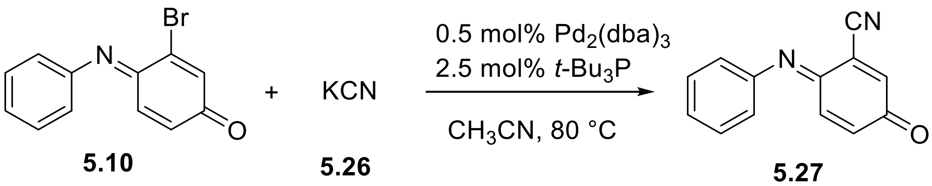

Scheme 5.9 Palladium-catalysed carbonylation[256] of 3-bromoazaquinone **5.10**

The spectral and luminescent properties of some azaquinone products such as the diarylamino compounds **5.6** and the dimers **5.28** (Fig. 5.1) would be useful.

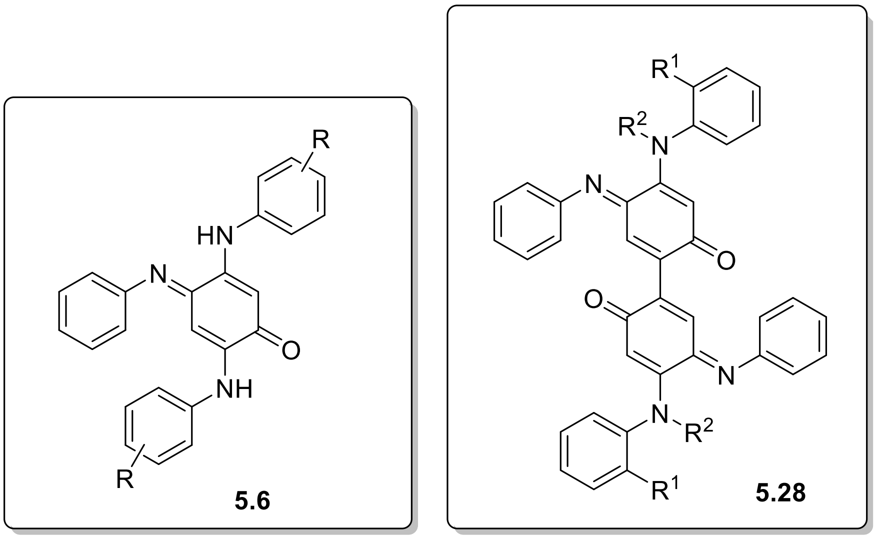

Figure 5.1: Diarylamino compounds and Dimers for UV-vis and fluorescence studies

Combination of reaction types could be used to generate real tandem processes and translation of processes to automated reaction systems and, in particular, flow chemistry processes would be a major goal to demonstrate the versatility of azaquinone as a building block.

Chapter 6. Experimental

6.1 General Procedures

Reactions requiring anhydrous conditions were performed using oven-dried glassware and conducted under a positive pressure of nitrogen. Anhydrous solvents were prepared in accordance with standard protocols. A Mettler PB 303-L analytical balance was used to weigh all reagents. Infrared spectra were recorded on a Nicolet Avatar 370DTGS FT-IR spectrometer with internal calibration. ^{1}H NMR and ^{13}C NMR spectra were recorded on a Bruker Avance 300 MHz and 700 MHz spectrometers with residual protic solvent as an internal reference. ^{19}F NMR were recorded on a Bruker λ 300 MHz spectrometer with $CFCl_3$ as an external reference. Elemental analyses were carried out at London Metropolitan University and are reported as the average of two runs. Mass Spectra and accurate masses were recorded using the SAgE Mass Spectrometry Facility (Newcastle University). Melting points were recorded on a Gallenkamp MF-370 melting point apparatus and are uncorrected. Diaryliodonium salt **2.1** was prepared according to a reported procedure.[149] Other diaryliodonium salts such as Ph_2ICl, Ph_2IOTf, Ph_2IOTs and Ph_2IPF_6 are commercially available.

6.2 HPLC Method[155]

Instrumentation and Equipment

HPLC Analysis was performed using a Varian Prostar 325 HPLC setup consisting of

1) Varian Prostar 210/SD-1 pump
2) A 20 µL sample injector loop
3) A Fluophase PFP column (Dimensions:150 × 4.6 mm, particle size: 5 µm)
4) An ultraviolet detector operating at 254 nm

Data Collection and Analysis

A mixture of 90% H_2O:10%MeCN from 0 to 2 mins, and 28% H_2O:72% MeCN from 2 to 30 mins was used as the mobile phase. This solution was degassed with nitrogen prior to being used. A flow rate of 1.00 mL/min was employed during both the equilibration and the subsequent injections of the sample.

HPLC Gradient

	A: H_2O	B: MeCN
0 to 2 min	90	10
2 to 30 min	28	72

6.3 Computational Modelling

Initial calculations were carried out using Gaussian software 09 and visualised with Gaussview 5, calculation type FOPT (full optimisation), calculation method RHF (Restricted Hartree-Fock), and basis set 6-31G. Final geometry optimisation study was performed with Austin Model one (AM1) using ArgusLab 3.0 software.

6.4 (Diacetoxyiodo)benzene, 2.9

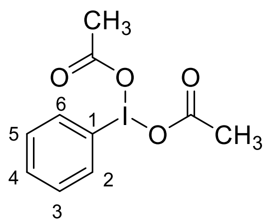

Iodobenzene (2.04 g, 10 mmol) was added to acetic acid (100 mL) at 45 °C. Sodium perborate tetrahydrate (15.39 g, 100 mmol) was added portion-wise to the solution over 1 hour and the solution stirred for a further 3.5 hours. Water (100 mL) was added to the solution and the reaction mixture was extracted with chloroform (3 × 100 mL). The combined chloroform layers were concentrated in *vacuo* to give the crude product. Subsequent crystallization gave the product as a white crystalline solid (0.88 g, 2.73 mmol, 27%); Mp 156–158 °C from dichloromethane-petrol (lit.,[257] mp 157–159 °C from acetic acid); IR (neat) 1641, 1445, 1364, 1267 cm^{-1}; ^{1}H NMR (DMSO-d_6) δ 8.24 (2H, d, H2/H6 J 9.1 Hz), 7.84 (1H, t, H4 J 7.2 Hz), 7.40 (2H, t, H3/H5 J 7.0 Hz), 1.92 (6H, s, OCH_3), ^{13}C NMR (DMSO-d_6) δ 175.8 (CO), 134.1 (C2/C6), 131.5 (C4), 130.8 (C3/C5), 122.6 (C1), 20.7 (OCH_3).

6.5 Diphenyliodonium trifluoroacetate, 2.1

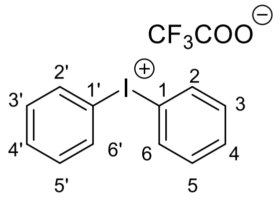

Trifluoroacetic acid (7.7 mL, 100 mmol) was added dropwise at –30 °C, to a stirred suspension of (diacetoxyiodo)benzene **2.9** (16.1 g, 50 mmol) in DCM (500 mL). After 30 min, the mixture was allowed to warm to room temperature and stirred for a further hour when it was recooled (–30 °C) and benzeneboronic acid (6.1 g, 50 mmol) was added. The resulting mixture was allowed to warm to room temperature overnight and the solvent was removed in vacuo to give the crude product as a golden yellow oil. Subsequent crystallization gave the product as an off-white crystalline solid (11.37 g, 28.9 mmol, 58%). Mp 186–188 °C from DCM-acetone-petrol (lit.,[258] mp 186–190 °C from acetone-ether); IR (neat) 1651, 1440, 1411, 1190, 1120 cm^{-1}; ^{1}H NMR (DMSO-d_6) δ 8.25 (4H, d, H2/H2'/H6/H6' *J* 8 Hz), 7.66 (2H, t, H4/H4' *J* 7 Hz), 7.54 (4H, t, H3/H3'/H5/H5' *J* 7 Hz); ^{13}C NMR (DMSO-d_6) δ 159.3 (CO), 135.6 (C2/C2'/C6/C6'), 132.5 (C4/C4'), 132.2 (C3/C3'/C5/C5'), 127.8 (CF_3), 117.0 (C1/C1').

6.6 4-Hydroxydiphenylamine, 2.5

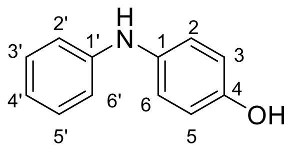

4-Hydroxyaniline (0.54 g, 5 mmol) was added to diphenyliodonium trifluoroacetate (1.97 g, 5 mmol) in DMF (50 mL) and the resulting mixture was heated at 130 °C for 24 h. After cooling, water (50 mL) was added and the mixture was extracted with ether (3 × 50 mL). The organic extracts were combined and washed with more water (200 mL), dried ($MgSO_4$) and the solvents removed in vacuo to give the product as a brown oil. Purification by chromatography (SiO_2, 1:1 ether-petrol) gave the product as a solid. Mp 72–74 °C from ether-petrol (lit.,[156] mp 70 °C) R_f = 0.46 (1:1 ether-petrol); IR (neat) 1597, 1492, 1313, 1238, 1173, 822, 746, 692 cm^{-1}; ^{1}H NMR ($CDCl_3$) δ 7.19 (2H, m, H3'/H5'), 7.05 (2H, m, H2/H6), 6.92 (2H, m, H3/H5), 6.86 (1H, m, H4'), 6.69 (2H, d, H2'/H6', *J* 7Hz), 5.30 (1H, s, NH), 4.94 (1H, s, OH); ^{13}C NMR ($CDCl_3$) δ 172.6 (C4), 144.1 (C1'), 129.4 (C1), 120.7 (C3'/C5'), 120.2 (C2/C6), 119.8 (C4'), 117.1 (C2'/C6'), 115.9 (C3/C5).

6.7 Ag_2CO_3 on Celite (Oxidizing Agent)[163]

Celite (30 g) was added to a mechanically stirred solution of silver nitrate (34 g, 200 mmol) in distilled water (200 mL). A solution of $Na_2CO_3 \cdot 10H_2O$ (30 g, 105 mmol) in distilled water was then added slowly to the resulting homogeneous suspension. When the addition was complete, stirring was continued for a further 10 min at RT. The yellow-green precipitate which was formed was then filtered off and finally dried in vacuo over a period of several hours. The silver carbonate/Celite reagent contains about 1 mmol of Ag_2CO_3 in 0.57 g of the mixture (total product 92.47 g).

6.8 4-(Phenylimino)cyclohexa-2,5-dien-1-one, 2.6

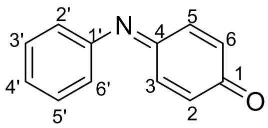

To a solution of 4-hydroxydiphenylamine (3.7 g, 20 mmol) in toluene (800 mL) was added Ag_2CO_3/Celite (12.0 g, 21.1 mmol) in one portion. The resulting mixture was vigorously stirred for 24 h at RT. The reaction mixture was then filtered through a 1 cm thick pad of Celite, washing with toluene (100 mL). The filtrate was evaporated under reduced pressure to give the crude product. Purification by chromatography (SiO_2 1:4 ether-petrol) gave the azaquinone as an orange solid (2.81 g, 15.4 mmol, 77%). R_f = 0.37 (SiO_2 1:4 ether-petrol); Mp 98–100 °C from DCM (lit.,[159] 101–102 °C from toluene); IR (neat) 1643, 1319, 1168, 873, 794, 700 cm^{-1}; ^{1}H NMR ($CDCl_3$) δ 7.35 (2H, t, *J* 8.8 Hz, H3', H5'), 7.24 (1H, dd, *J* 10.0, 2.7 Hz, H5), 7.18 (1H, t, *J* 8.0 Hz, H4'), 7.02 (1H, dd, *J* 10.3, 2.6 Hz, H3), 6.82 (2H, d, *J* 7.6 Hz, H2', H6'), 6.63 (1H, dd, *J* 10.1, 2.2 Hz, H6), 6.47 (1H, dd, *J* 10.3, 2.2 Hz, H2); ^{13}C NMR ($CDCl_3$) δ 187.7 (C1), 157.4 (C4), 149.4 (C1') 141.9 (C5), 133.5 (C2), 132.9 (C6), 129.1(C3', C5'), 128.3 (C3), 126.2 (C4'), 120.6 (C2', C6'); *m/z* (ESI+) 185 (M+2, 15%), 184 (M+H^{+}, 100). Found: M+H^{+}, 184.1019. $C_{12}H_{10}NO$

requires 184.0762. Anal Calcd for $C_{12}H_9NO$: C, 78.67; H, 4.95; N, 7.65. Found: C, 78.76; H, 4.74; N, 7.57. Crystal structure determined (see Appendix).

6.9 2-Amino-3*H*-phenoxazin-3-one, 2.19

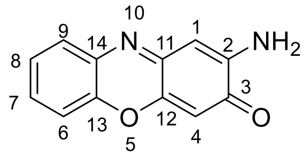

A solution of 2-aminophenol (0.54 g, 5 mmol) in ethanol (15 mL) was added to azaquinone (0.46 g, 2.5 mmol) in ethanol (15 mL) at RT. At the end of the reaction (30 min), the solvent was removed in vacuo to give the crude product. Purification by chromatography (1:4 ethylacetate-petrol) gave the pure product. (0.2 g, 0.94 mmol, 48%), R_f =0.15 (SiO_2 1:4 ethylacetate-petrol); ^{1}H NMR 300 MHz (DMSO-d_6) δ 7.70 (1H, d, *J* 7.8 Hz, H9), 7.49 (1H, d, *J* 8.0 Hz, H6), 7.46 (1H, t, *J* 8.8 Hz, H8), 7.41 (1H, t, *J* 8.8 Hz, H7), 6.81 (2H, s, NH_2), 6.37 (1H, s, H1), 6.36 (1H, s, H4); ^{13}C NMR (DMSO-d_6) δ 180.7 (C3), 149.3 (C2), 148.6 (C11), 147.8 (C12), 142.4 (C13), 134.2 (C14), 129.3 (C8), 128.4 (C9), 125.7 (C7), 116.4 (C6), 103.9 (C1), 98.8 (C4).

Typical procedure for the preparation of 2,5-diarylamino-1,4-benzoquinone-4-phenylimines **2.27**

A solution of the aniline (10 mmol) in ethanol (25 mL) was added to a solution of azaquinone **2.6** (5 mmol) in ethanol (25 mL) and the mixture stirred at RT for 24 h when the solvent was removed in *vacuo* to give the crude product as a red solid. The crude product was dissolved in minimum amount of chloroform and purified by chromatography (1:9 ethylacetate-petrol + 1% v/v triethylamine). The regiochemistry of the 2,5-diarylamino derivatives was not confirmed by the literature data.

6.10 *(E)*-2,5-Bis(phenylamino)-4-(phenylimino)cyclohexa-2,5-dien-1-one, 2.27a, (Table 2.7, Entry 1)

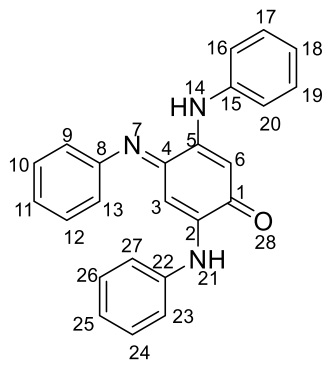

Using aniline **2.26a** (0.93 g, 10 mmol) and azaquinone **2.6** (0.92 g, 5 mmol). Red solid (1.0 g, 2.74 mmol, 56%). R_f = 0.38 (SiO_2 1:9 ethylacetate-petrol + 1% v/v triethylamine); Mp 198–200 °C from chloroform-ethanol (lit.,[5] 203–204 °C from chloroform-ethanol); IR (neat) υ_{max} 3260, 1633, 1574, 1501, 1443, 1341 cm^{-1}; ^1H NMR 700 MHz ($CDCl_3$) δ 8.69 (1H, s, NH, H14), 7.67 (1H, s, NH, H21), 7.45 (2H, t, *J* 8.1 Hz, H17, H19), 7.41 (2H, t, *J* 8.1 Hz, H10, H12), 7.35 (2H, d, *J* 8.1 Hz, H16, H20), 7.29 (2H, t, *J* 8.1 Hz, H24, H26), 7.24 (1H, tt, *J* 7.4, 1.2 Hz, H18), 7.17 (1H, tt, *J* 7.5, 1.2 Hz, H11), 7.08 (2H, d, *J* 8.1 Hz, H23, H27), 7.06 (1H, tt, *J* 7.5, 1.2 Hz, H25), 6.98 (2H, d, *J* 8.1 Hz, H9, H13), 6.22 (1H, s, H3), 6.20 (1H, s, H6); ^{13}C NMR ($CDCl_3$) δ 181.1 (C1), 153.9 (C5), 149.6 (C4), 149.3 (C8), 140.6 (C2), 138.6 (C22), 137.9 (C15),129.6 (C17, C19), 129.4 (C24, C26), 129.0 (C10, C12), 125.4 (C18), 124.7 (C11), 124.0 (C25), 123.1 (C16, C20), 120.9 (C23, C27), 120.8 (C9, C13), 97.1 (C6), 90.5 (C3). *m/z* (ESI+) 367 ($M+H^+$, 34%), 366 ($M+H^+$, 100). Found: $M+H^+$, 366.1850. $C_{24}H_{20}N_3O$ requires 366.1606.

6.11 *(E)*-2,5-Bis((4-methoxyphenyl)amino)-4-(phenylimino)cyclohexa-2,5-dien-1-one, 2.27b, (Table 2.7, Entry 2)

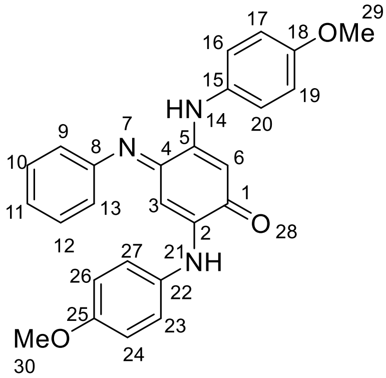

Using 4-methoxyaniline **2.26b** (1.23 g, 10 mmol) and azaquinone **2.6** (0.92 g, 5 mmol). Green crystalline solid (1.28 g, 3.0 mmol, 60%). R_f = 0.13 (SiO_2 1:9 ethylacetate-petrol + 1% v/v triethylamine); Mp 192–194 °C from chloroform-ethanol (lit.,[5] 199–201 °C from chloroform-ethanol); IR (neat) υ_{max} 3245, 2924, 1720, 1634, 1578, 1497, 1415, 1372, 1339 cm^{-1}; ^1H NMR 700 MHz ($CDCl_3$) δ 8.56 (1H, s, NH, H14), 7.56 (1H, s, NH, H21), 7.38 (2H, t, *J* 7.7 Hz, H10, H12), 7.27 (2H, d, *J* 8.3 Hz, H16, H20), 7.14 (1H, t, *J* 7.4 Hz, H11), 7.02 (2H, d, *J* 8.3 Hz, H23, H27), 6.96 (4H, d, *J* 8.3 Hz, H9, H13; H17, H19), 6.82 (2H, d, *J* 8.3 Hz, H24, H26), 6.00 (1H, s, H3), 5.98 (1H, s, H6), 3.85 (3H, s, H29), 3.69 (3H, s, H30); ^{13}C NMR ($CDCl_3$) δ 180.8 (C1), 157.5 (C18), 156.4 (C25), 153.8 (C5), 150.8 (C4), 149.5 (C8), 141.7 (C2), 131.5 (C15), 130.7 (C22), 128.9 (C10, C12), 125.2(C16, C20), 124.5 (C11), 122.9 (C23, C27), 121.0 (C9, C13), 114.7 (C17, C19), 114.6 (C24, C26), 96.2 (C6), 89.0 (C3), 55.6 (C29), 55.5 (C30). *m/z* (ESI+) 426 ($M+H^+$, 100%), 345 (82), 270 (20). Found: $M+H^+$, 426.1934. $C_{26}H_{24}N_3O_3$ requires 426.1818.

6.12 *(E)*-2,5-Bis((4-chlorophenyl)amino)-4-(phenylimino)cyclohexa-2,5-dien-1-one, 2.27c, (Table 2.7, Entry 3)

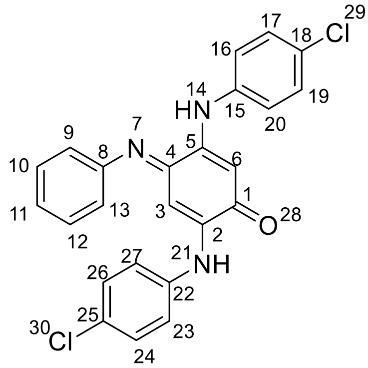

Using 4-chloroaniline **2.26c** (1.27 g, 10 mmol) and azaquinone **2.6** (0.92 g, 5 mmol). Red solid (1.34 g, 3.1 mmol, 62%). R_f = 0.42 (SiO_2 1:9 ethylacetate-petrol + 1% v/v triethylamine); Mp 192–194 °C from chloroform-ethanol (lit.,[5] 200–201 °C from chloroform-ethanol); IR (neat) υ_{max} 3251, 3078, 2923, 1901, 1673, 1626, 1485, 1403, 1338, cm^{-1}; ^{1}H NMR 700 MHz ($CDCl_3$) δ 8.63 (1H, s, NH, H14), 7.62 (1H, s, NH, H21), 7.42 (2H, t, *J* 7.6 Hz, H10, H12), 7.41 (2H, d, *J* 8.0 Hz, H17, H19), 7.28 (2H, d, *J* 8.0 Hz, H16, H20), 7.24 (2H, d, *J* 8.3 Hz, H24, H26), 7.20 (1H, t, *J* 7.5 Hz, H11), 6.99 (2H, d, *J* 8.3 Hz, H23, H27), 6.96 (2H, d, *J* 7.7 Hz, H9, H13), 6.15 (1H, s, H3), 6.13 (1H, s, H6); ^{13}C NMR ($CDCl_3$) δ 180.9 (C1), 153.5 (C5), 149.2 (C4), 149.1 (C8), 140.3 (C2), 137.2 (C15), 136.5 (C22), 130.7 (C18), 129.7 (C17, C19), 129.5 (C24, C26), 129.1 (C10, C12), 129.1 (C25), 125.1 (C11), 124.2 (C16, C20), 122.0 (C23, C27), 120.8 (C9, C13), 97.4 (C6), 90.8 (C3). *m/z* (ESI+) 436 ([$^{35}Cl^{37}Cl$]M+H$^+$, 52%), 434 ([$^{35}Cl_2$]M+H$^+$, 78%). Found: M+H$^+$, 434.1223. $C_{24}H_{18}{}^{35/35}Cl_2N_3O$ requires 434.0827. Anal Calcd for $C_{24}H_{17}Cl_2N_3O$: C, 66.37; H, 3.95; N, 9.68. Found: C, 66.21; H, 4.12; N, 9.83. Crystal structure determined (see Appendix).

6.13 *(E)*-4-(Phenylimino)-2,5-bis((4-trifluoromethyl)phenyl)amino)cyclohexa-2,5-dien-1-one, 2.27d,[5] (Table 2.7, Entry 4)

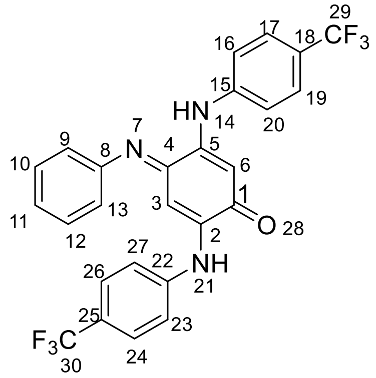

Using 4-(trifluoromethyl)aniline **2.26d** (1.61 g, 10 mmol) and azaquinone **2.6** (0.92 g, 5 mmol). Red solid (1.70 g, 3.4 mmol, 68%). R_f = 0.47 (SiO_2 1:9 ethylacetate-petrol + 1% v/v triethylamine); Mp 188–190 °C from chloroform-ethanol; IR (neat) υ_{max} 3263, 3086, 1580, 1522, 1497, 1413, 1320 cm^{-1}; ^1H NMR 700 MHz ($CDCl_3$) δ 8.78 (1H, s, NH, H14), 7.79 (1H, s, NH, H21), 7.70 (2H, d, *J* 8.3 Hz, H17, H19), 7.54 (2H, d, *J* 8.4 Hz, H24, H26), 7.47 (2H, t, *J* 8.3 Hz, H10, H12), 7.45 (2H, d, *J* 3.2 Hz, H16, H20), 7.25 (1H, tt, *J* 7.4, 1.2 Hz, H11), 7.14 (2H, d, *J* 8.3 Hz, H23, H27), 6.99 (2H, d, *J* 8.3 Hz, H9, H13), 6.35 (1H, s, H3), 6.32 (1H, s, H6); ^{13}C NMR ($CDCl_3$) δ 181.0 (C1), 153.3 (C5), 148.8 (C4), 148.1 (C8), 141.8 (C15), 141.3 (C22), 139.4 (C2), 129.2 (C10, C12), 126.9 (C17, C19), 126.8 (C18), 126.7 (C24, C26), 126.7 (C25), 125.4 (C11), 123.95 (C29/C30),[a] 123.91 (C29/C30),[a] 122.1 (C16, C20), 120.8 (C9, C13), 119.7 (C23, C27), 98.6 (C6), 92.5 (C3); *m/z* (ESI+) 502 ($M+H^+$, 100%). Found: $M+H^+$, 502.1635. $C_{26}H_{18}F_6N_3O$ requires 502.1309. Anal Calcd for $C_{26}H_{17}F_6N_3O$: C, 62.28; H, 3.42; N, 8.38. Found: C, 62.39; H, 3.24; N, 8.27. Crystal structure determined (see Appendix). [a]C29/C30 cannot be distinguished

6.14 *(E)*-4-(Phenylimino)-2,5-bis(o-tolylamino)cyclohexa-2,5-dien-1-one, 2.27e,[5] (Table 2.7, Entry 5)

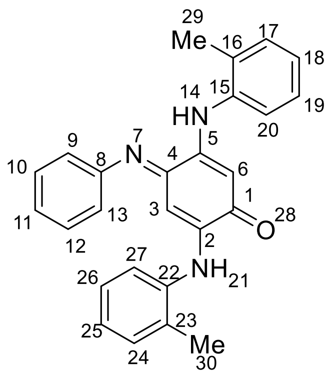

Using 2-methylaniline **2.26e** (1.07 g, 10 mmol) and azaquinone **2.6** (0.92 g, 5 mmol). Red solid (1.32 g, 3.35 mmol, 67%). R_f = 0.46 (SiO_2 1:9 ethylacetate-petrol + 1% v/v triethylamine); Mp 156–158 °C from chloroform-ethanol; IR (neat) υ_{max} 3333, 1738, 1568, 1503, 1456, 1340 cm^{-1}; ^{1}H NMR 700 MHz ($CDCl_3$) δ 8.51 (1H, s, NH, H14), 7.47 (1H, s, NH, H21), 7.38 (2H, t, *J* 7.1 Hz, H10, H12), 7.36 (1H, d, *J* 8.0 Hz, H27), 7.31 (1H, t, *J* 7.7 Hz, H11), 7.29 (1H, d, *J* 7.7 Hz, H20), 7.22 (1H, t, *J* 7.5 Hz, H19), 7.20 (1H, d, *J* 7.7 Hz, H24), 7.14 (1H, t, *J* 7.1 Hz, H26), 7.13 (1H, d, *J* 7.7 Hz, H17), 7.12 (1H, t, *J* 7.1 Hz, H18), 7.03 (1H, t, *J* 8.1 Hz, H25), 6.97 (2H, d, *J* 7.7 Hz, H9, H13), 5.91 (1H, s, H3), 5.78 (1H, s, H6), 2.35 (3H, s, CH_3, H29), 2.27 (3H, s, CH_3, H30); ^{13}C NMR ($CDCl_3$) δ 181.0 (C1), 153.7 (C5), 150.9 (C4), 149.2 (C8), 141.6 (C2), 136.7 (C15), 136.2 (C22), 133.4 (C20), 131.4 (C18), 131.2 (C11), 131.1 (C24), 128.9 (C27), 126.9 (C19), 126.6 (C16), 126.5 (C23), 125.0 (C10, C12), 124.9 (C25), 124.6 (C17), 122.1 (C26), 121.1 (C9, C13), 96.6 (C6), 87.8 (C3), 29.7 (C29), 17.9 (C30). *m/z* (ESI+) 394 (M+H$^+$, 100%), 392 (30). Found: M+H$^+$, 394.2256. $C_{26}H_{24}N_3O$ requires 394.1919. Crystal structure determined (see Appendix).

6.15 *(E)*-2,5-Bis(methyl(phenyl)amino)-4-(phenylimino)cyclohexa-2,5-dien-1-one, 2.27f,[5] (Table 2.7, Entry 6)

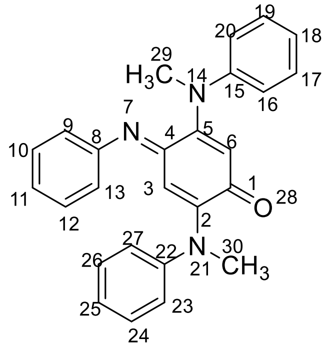

Using *N*-methylaniline **2.27f** (1.07 g, 10 mmol) and azaquinone **2.6** (0.92 g, 5 mmol). Red solid (1.29 g, 3.3 mmol, 66%). R_f = 0.15 (SiO_2 1:9 ethylacetate-petrol + 1% v/v triethylamine); Mp 164–166 °C from chloroform-ethanol; IR (neat) υ_{max} 2934, 2499, 1629, 1548, 1480, 1443, 1390, 1336 cm^{-1}; ^{1}H NMR ($CDCl_3$) δ 7.26 (2H, t, *J* 8.2 Hz, H24, H26), 7.20 (2H, t, *J* 8.2 Hz, H10, H12), 7.12 (2H, t, *J* 7.7 Hz, H17, H19), 7.10 (1H, t, *J* 7.3 Hz, H25), 7.07 (2H, d, *J* 8.0 Hz, H23, H27), 7.01 (1H, t, J 7.3 Hz, H11), 6.94 (2H, d, *J* 7.3 Hz, H9, H13), 6.92 (1H, t, *J* 7.3 Hz, H18), 6.34 (2H, d, *J* 8.2 Hz, H16, H20), 5.80 (1H, s, H3), 5.75 (1H, s, H6), 3.31 (3H, s, H30), 3.04 (3H, s, H29); ^{13}C NMR ($CDCl_3$) δ 182.3 (C1), 155.6 (C2), 154.8 (C4), 150.3 (C22), 149.5 (C15), 148.7 (C8), 147.6 (C5), 129.08 (C24, C26), 129.04 (C10, C12), 128.5 (C17, C19), 125.2 (C23, C27), 124.7 (C25), 124.3 (C11), 124.2 (C18), 123.6 (C9, C13), 119.7 (C16, C20), 110.4 (C3), 104.7 (C6), 43.1 (C30), 41.9 (C29); Crystal structure determined (see Appendix).

Typical Procedure for the preparation of phenylenediamines **2.37**[6]

Into a two neck 100 mL flask, which was equipped with a thermometer, stirrer, condenser and Dean Stark trap was added azaquinone **2.6** (10 mmol), the primary amine (20 mmol), toluene (50 mL) and methanesulfonic acid (1 drop). The mixture was heated to 110 °C and the reaction was stopped after 6 hours of reaction by cooling. The mixture was then washed with sodium hydrosulfite (1.0 g) in water (200 mL), decanted and the solvent was removed in vacuo to give the crude product. The crude mixture was purified by RP C18 chromatography (Gradient 1:4

MeOH/H_2O + 1% formic acid to 4:1 MeOH/H_2O + 1% formic acid) to give the title compound.

6.16 Attempted synthesis of *N*1-benzyl-*N*4-phenylbenzene-1,4-diamine, 2.37a, (Table 2.9, Entry 1)

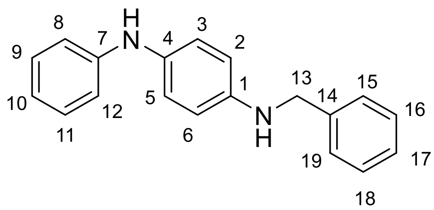

Using benzylamine **2.35a** (2.89 g, 27 mmol) and azaquinone **2.6** (1.83 g, 10 mmol), xylene (50 mL), toluenesulfonic acid (0.05 g), sodium hydrosulfite (3.5 g).

Brown oil (1.64 g, 6.0 mmol, 60%), ^{1}H NMR ($CDCl_3$) δ 8.00 (1H, s, NH), 7.28-6.69 (14H, m, ArH), 4.96 (1H, s, NH), 3.42 (2H, s, CH_2).

6.17 Attempted synthesis of *N*1-octyl-*N*4-phenylbenzene-1,4-diamine, 2.37b, (Table 2.9, Entry 2)

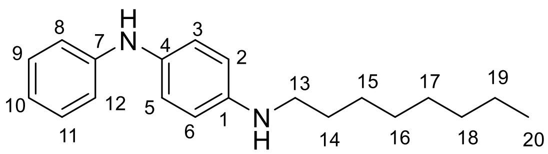

Using octylamine **2.35b** (2.58g, 20 mmol) and azaquinone **2.6** (1.83 g, 10 mmol).[6] The crude product was further purified by acid-base extraction using 5M aq. HCl (50 mL) and ethylacetate (3 × 50 mL), the aqueous layer was basified with NaOH pellets in an ice bath and extracted with ethylacetate (50 mL). The solvent was removed in vacuo to give the pure product.

Brown oil (1.84 g, 6.2 mmol, 62%), R_f = 0.69 (4:1 MeOH/H_2O + 1% formic acid), ^{1}H NMR ($CDCl_3$) δ 7.19 (1H, s, NH), 7.10 (2H, t, H9/H11), 6.93 (2H, d, H3/H5), 6.75 (2H, d, H8/H12), 6.69 (1H, t, H10), 6.52 (2H, d, H2/H6), 3.02 (2H, t, H13), 1.55 (2H, q, H14), 1.27 (2H, m, H15), 1.21 (8H, m, H16/H17/H18/H19), 0.82 (3H, t, H20); ^{13}C NMR ($CDCl_3$) δ 144.9, 129.2, 123.9, 118.6, 115.5, 114.7, 113.6, 110.0, 44.6, 29.5, 27.2, 22.7, 14.1.

6.18 Attempted synthesis of *N*[1]-cyclohexyl-*N*[4]-phenylbenzene-1,4-diamine, 2.37c, Crude mixture (2.23 g), *N*[1]-isopropyl-*N*[4]-phenylbenzene-1,4-diamine, 2.37d, Crude mixture (1.76 g), *N*-phenyl-4-(piperidin-1-yl)aniline, 2.39a, Crude mixture (2.07 g), and 4-morpholino-*N*-phenylaniline, 2.39b, Crude mixture (2.03 g) Table 2.9, Entries 3, 4, 5 and 6.

6.19 4-(Phenylamino)-2-tosylphenol, 2.47a

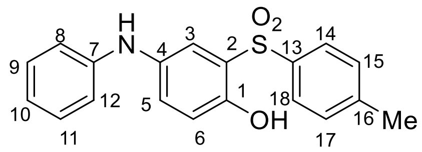

Sodium 4-methylbenzenesulfinate **2.46a** (0.71 g, 4 mmol) was added in one portion to a solution of azaquinone **2.6** (0.37 g, 2 mmol) in glacial acetic acid (20 mL) and heated to 70 °C. When the mixture turned colourless, it was cooled to room temperature and water was added until complete precipitation. The solid was filtered to give the crude product which was recrystallized from THF-petrol to give a colourless solid (0.67 g, 1.97 mmol, 98%), R_f = 0.43 (SiO_2 1:4 ethylacetate-petrol); Mp 104–106 °C (THF-petrol), lit.,[7] 82–84 °C (acetic acid); IR (neat) 3550, 3487, 3375, 2759, 1598, 1507, 1447, 1403 cm^{-1}; ^1H NMR 300 MHz (DMSO-d_6) δ 10.20 (1H, s, OH), 8.10 (1H, s, NH), 7.81 (2H, d, *J* 8.1 Hz, H14, H18), 7.67 (1H, d, *J* 2.8 Hz, H3), 7.39 (2H, d, *J* 8.1 Hz, H15, H17), 7.26 (1H, dd, *J* 8.0, 2.3 Hz, H5), 7.22 (2H, t, *J* 8.0 Hz, H9, H11), 6.97 (2H, d, *J* 8.1 Hz, H8, H12), 6.84 (1H, d, *J* 8.8 Hz, H6), 6.79 (1H, td, *J* 7.2, 1.2 Hz, H10), 2.37 (3H, s, CH_3); ^{13}C NMR (DMSO-d_6) δ 149.9 (C1), 144.7 (C7), 144.1 (C16), 138.9 (C13), 135.5 (C4), 129.7 (C9, C11), 128.4 (C14, C18), 127.1 (C2), 126.4 (C5), 119.6 (C10), 118.9 (C6), 118.1 (C3), 116.6 (C15, C17), 115.9 (C8, C12), 21.5 (CH_3); *m/z* (ESI+) 340 ($M+H^+$, 100). Found: $M+H^+$, 340.1261. $C_{19}H_{18}NO_3S$ requires 340.1007. Crystal structure determined (see Appendix).

6.20 2-((2-Chlorophenyl)sulfonyl)-4-(phenylamino)phenol, 2.47b

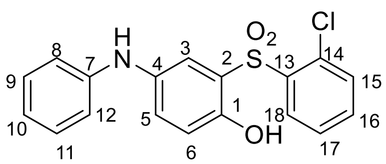

Sodium 2-chlorobenzenesulfinate **2.46b** (1.19 g, 6 mmol) was added in one portion to a solution of azaquinone **2.6** (0.55 g, 3 mmol) in glacial acetic acid (30 mL) and heated to 70 °C. When the mixture turned colourless, it was cooled and water was added until complete precipitation. The solid was filtered to give the crude product which was recrystallized from THF-petrol to give a colourless solid (1.02 g, 2.84 mmol, 94%), R_f = 0.36 (SiO_2 1:4 ethylacetate-petrol); Mp 176–178 °C (THF-Petrol); IR (neat) 3375, 1596, 1515, 1486, 1449, 1402 cm^{-1}; ^1H NMR 700 MHz (DMSO-d_6) δ 10.20 (1H, s, OH), 8.27 (1H, dd, *J* 7.9, 1.8 Hz, H18), 8.11 (1H, s, NH), 7.74 (1H, d, *J* 2.9 Hz, H15), 7.69 (1H, td, *J* 7.7, 1.8 Hz, H17), 7.64 (1H, td, *J* 7.7, 1.3 Hz, H16), 7.59 (1H, dd, *J* 7.9, 1.3 Hz, H5), 7.29 (1H, dd, *J* 8.7, 2.9 Hz, H3), 7.22 (2H, t, *J* 7.7 Hz, H9, H11), 6.96 (2H, d, *J* 8.7 Hz, H8, H12), 6.84 (1H, d, *J* 8.7 Hz, H6), 6.78 (1H, tt, *J* 7.3, 1.1 Hz, H10); ^{13}C NMR (DMSO-d_6) δ 150.1 (C1), 144.9 (C7), 138.8 (C13), 135.4 (C17), 135.2 (C4), 132.5 (C18), 131.9 (C5), 131.3 (C14), 129.7 (C9, C11), 127.9 (C16), 127.4 (C3), 125.5 (C2), 119.8 (C15), 119.5 (C10), 118.7 (C6), 115.7 (C8, C12); *m/z* (ESI+) 362 ([^{37}Cl]M+H^+, 42%), 360 ([^{35}Cl]M+H^+, 100). Found: M+H^+, 360.0433. $C_{18}H_{15}{}^{35}ClNO_3S$ requires 360.0461. Anal Calcd for $C_{18}H_{14}ClNO_3S$: C, 60.08; H, 3.92; N, 3.89. Found: C, 59.89; H, 3.89; N, 3.70. Crystal structure determined (see Appendix).

6.21 2-(Phenylamino)phenoxathiine-10,10-dioxide, 2.58

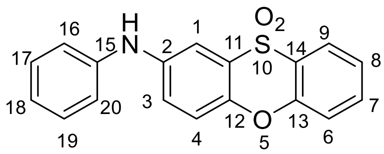

Potassium tert-butoxide (0.67 g, 6 mmol) was added to a solution of **2.47b** (1.0 g, 2.79 mmol) in DMF (20 mL) and heated to 90 °C for 24 h. The reaction mixture was diluted with water (200 mL) and extracted with ethylacetate (3 × 150 mL). The organic products were combined, dried with $MgSO_4$ and the solvent removed in vacuo. Recrystallisation from THF gave **2.58** as colourless crystals (0.8 g, 2.46 mmol, 88%); R_f = 0.31 (1:4 ethylacetate-petrol); Mp 160–162 °C (THF); IR (neat) 3345, 2954, 1768, 1661, 1616, 1598, 1514, 1492, 1469, 1442, 1398, 1337 cm^{-1}; ^1H NMR 300 MHz (DMSO-d_6) δ 8.54 (1H, s, NH), 7.95 (1H, dd, *J* 8.2, 1.6 Hz, H9), 7.62 (1H, td, *J* 7.8, 7.4, 1.6 Hz, H8), 7.49 (1H, d, *J* 2.5 Hz, H1), 7.36 (1H, m, H3), 7.35 (1H, m, H7), 7.35 (1H, m, H6), 7.32 (1H, m, H4), 7.20 (2H, t, *J* 8.4 Hz, H3', H5'), 7.06 (2H, d, *J* 8.2 Hz, H2', H6'), 6.83 (1H, t, *J* 7.8 Hz, H4'); ^{13}C NMR (DMSO-d_6) δ 151.7 (C14), 144.2 (C11), 142.6 (C1'), 141.9 (C12), 135.0 (C8), 129.8 (C3', C5'), 125.3 (C7), 125.2 (C13), 124.3 (C2), 123.4 (C9), 123.3 (C6), 121.7 (C4'), 120.6 (C4), 119.3 (C3), 118.4 (C2', C6'), 106.9 (C1). *m/z* (ESI+) 324 ($M+H^+$, 42%). Found: $M+H^+$, 324.0694. $C_{18}H_{14}NO_3S$ requires 324.0689. Crystal structure determined (see Appendix).

Typical procedure for the addition of HBr to azaquinone, **3.1** or azaquinone *N*-oxide, **3.23**

Aqueous hydrobromic acid (48%, 8.8 mmol, 1 mL) was added dropwise to a solution of azaquinone, **3.1** (1.0 g, 5.46 mmol) in acetic acid (75 mL). The solution was stirred at RT for 30 min and its colour changed from orange to blue. The reaction mixture was diluted with water (200 mL) and extracted with DCM (3 × 150 mL). The organic extracts were washed with water (3 × 100 mL), dried over sodium sulfate and stirred with lead (IV) acetate (8.0 g, 18 mmol) at RT for 1 h. The reaction mixture was then filtered to remove the oxidising agent and the solvent removed in vacuo to give the crude product.

Azaquinone, **3.1** reaction with HBr

Purification by chromatography (1:4 ethylacetate-petrol) and further purification by RP C18 (1:1 MeCN-H_2O) gave **3.2** and **3.3** as the two major products.

6.22 *(E)*-3-Bromo-4-(phenylimino)cyclohexa-2,5-dien-1-one, 3.2

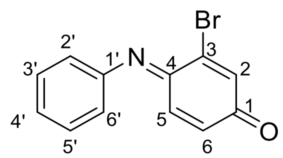

An orange oil, (0.46 g, 1.76 mmol, 32%), R_f = 0.29 (RP C18 1:1 MeCN-H_2O); IR υ_{max}/cm^{-1} (neat) 3199, 2918, 1596, 1492, 1467, 1227; ^1H NMR 300 MHz ($CDCl_3$) δ 7.32 (2H, t, *J* 8.6 Hz, H3', H5'), 7.15 (1H, ddt, *J* 8.6, 7.4, 1.2 Hz, H4'), 7.13 (1H, d, *J* 2.2 Hz, H2), 7.02 (1H, d, *J* 10.2 Hz, H5), 6.79 (2H, d, *J* 8.6 Hz, H2', H6'), 6.42 (1H, dd, *J* 10.2, 2.1 Hz, H6); ^{13}C NMR ($CDCl_3$) δ 185.3 (C1), 153.1 (C4), 148.9 (C1'), 140.6 (C3), 136.0 (C2), 132.4 (C6), 129.2 (C3', C5'), 128.5 (C5), 126.6 (C4'), 120.4 (C2', C6'); *m/z* (ESI+) 261 ([^{79}Br]$M+H^+$, 34%), 264 ([^{81}Br]$M+H^+$, 20%). Found:

M+H$^+$, 261.9771. $C_{12}H_9{}^{79}BrNO$ requires 261.9868. Anal Calcd for $C_{12}H_8BrNO$: C, 54.99; H, 3.08; N, 5.34. Found: C, 54.83; H, 3.16; N, 5.24.

6.23 *(E)*-3-Bromo-4-((4-bromophenyl)imino)cyclohexa-2,5-dien-1-one, 3.3

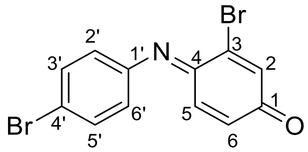

An orange solid, (0.67 g, 1.96 mmol, 36%), R_f = 0.21 (RP C18 1:1 MeCN-H_2O); Mp 100–102 °C (THF), lit.,[8] 113-114 °C (benzene); IR υ_{max}/cm^{-1} (neat) 3059, 2952, 1773, 1661, 1636, 1573, 1560, 1473, 1399, 1380, 1326; ^{1}H NMR 300 MHz ($CDCl_3$) δ 7.45 (2H, d, *J* 8.6 Hz, H3', H5'), 7.14 (1H, d, *J* 2.1 Hz, H2), 7.00 (1H, d, *J* 10.2 Hz, H5), 6.69 (2H, d, *J* 8.6 Hz, H2', H6'), 6.46 (1H, dd, *J* 10.2, 2.1 Hz, H6); ^{13}C NMR ($CDCl_3$) δ 185.0 (C1), 153.5 (C4), 147.7 (C1'), 140.2 (C3), 136.2 (C2), 132.7 (C6), 132.3 (C3', C5'), 128.1 (C5), 122.0 (C2', C6'), 120.1 (C4'); *m/z* (ESI+) 343 ([$^{81}Br_2$]M+H$^+$, 20%), 341 ([$^{79}Br^{81}Br$]M+H$^+$, 40), 339 ([$^{79}Br_2$]M+H$^+$, 20). Found: M+H$^+$, 339.8847. $C_{12}H_8{}^{79/79}Br_2NO$ requires 339.8973. Anal Calcd for $C_{12}H_7Br_2NO$: C, 42.27; H, 2.07; N, 4.11. Found: C, 42.06; H, 1.93; N, 3.98. Crystal structure determined (see Appendix).

6.24 4-Oxo-*N*-phenylcyclohexa-2,5-dien-1-imine oxide, 3.23

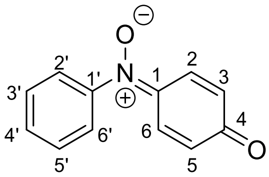

m-CPBA (0.94 g, 5.46 mmol) was added in small portions to a solution of azaquinone (0.5 g, 2.73 mmol) in dichloromethane (100 mL) over a 5 min period and stirred for 24 h at RT. The solvent was removed in vacuo to give the crude product which was recrystallized with ether-petrol to give **3.23** as a yellow solid (0.40 g, 2.0 mmol, 74%); R_f = 0.27 (SiO_2 1:4 ethylacetate-petrol + 1% v/v triethylamine); Mp 136–138 °C (ether-petrol), lit.,[196] 141–142 °C(petrol-benzene); IR υ_{max}/cm^{-1} (neat) 3048, 1617, 1592, 1488, 1465, 1438, 1377; ^{1}H NMR 700MHz ($CDCl_3$) δ 8.06 (1H, dd, *J* 10.2, 2.9 Hz, H2), 7.61 (1H, ddt, *J* 8.6, 7.4, 1.2 Hz, H4'), 7.57 (2H, t, *J* 8.6 Hz, H3', H5'), 7.49 (2H, d, *J* 8.6 Hz, H2', H6'), 7.20 (1H, dd, *J*

10.2, 2.9 Hz, H6), 6.68 (1H, dd, J 10.2, 2.0 Hz, H3), 6.27 (1H, dd, J 10.2, 2.0 Hz, H5); ^{13}C NMR ($CDCl_3$) δ 186.4 (C4), 171.2 (C1), 145.5 (C1'), 143.5 (C3', C5'), 132.0 (C3), 131.4 (C4'), 129.6 (C6), 128.5(C2), 126.5 (C5), 124.5 (C2', C6'); *m/z* (ESI+) 200 (M+H$^+$, 100). Found: M+H$^+$, 200.0823. $C_{12}H_{10}NO_2$ requires 200.0712. Anal Calcd for $C_{12}H_9NO_2$: C, 72.35; H, 4.55; N, 7.03. Found: C, 72.24; H, 4.42; N, 6.91. Crystal structure determined (see Appendix).

Azaquinone *N*-oxide, **3.23** with HBr

Using azaquinone *N*-oxide (1.0 g, 5.0 mmol). Purification by chromatography (SiO_2 1:8 ethylacetate-petrol) and RP (C18) (7:3 MeCN-H_2O) gave three products **3.24**, **3.3** and **3.25**.

6.25 *(E)*-3-Bromo-4-((2,4-dibromophenyl)imino)cyclohexa-2,5-dien-1-one, 3.24

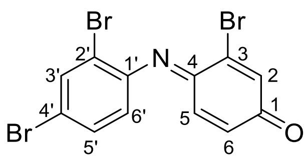

An orange solid, (0.63 g, 1.5 mmol, 30%), R_f = 0.48 (RP 9:1 MeCN-H_2O); IR υ_{max}/cm^{-1} (neat) 3328, 2957, 2885, 1721, 1642, 1457, 1441, 1367, 1342, 1320, 1284; ^{1}H NMR 300 MHz ($CDCl_3$) δ 7.76 (1H, d, J 2.0 Hz, H3'), 7.42 (1H, dd, J 8.4, 2.1 Hz, H5'), 7.21 (1H, d, J 2.1 Hz, H2), 6.86 (1H, d, J 10.2 Hz, H5), 6.58 (1H, d, J 8.4 Hz, H6'), 6.49 (1H, dd, J 10.2, 2.1 Hz, H6); ^{13}C NMR ($CDCl_3$) δ 184.9 (C1), 154.7 (C4), 146.5 (C1'), 139.8 (C3), 136.5 (C2), 135.7 (C3'), 133.0 (C6), 131.0 (C5'), 128.2 (C5), 121.2 (C6'), 119.4 (C4'), 115.3 (C2'); *m/z* (ESI+) 423 ([$^{81}Br_3$]M+H$^+$, 58%), 422 (65), 421 (100), 419 (92), 417 ([$^{79}Br_3$]M+H$^+$, 36). Found 418.62. $C_{12}H_6{}^{79/79/79}Br_3NO$ requires 418.7979.

6.26 *(E)*-3-Bromo-4-((4-bromophenyl)imino)cyclohexa-2,5-dien-1-one, 3.3

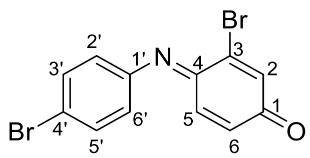

An orange solid, (0.63 g, 1.85 mmol, 37%), R_f = 0.58 (RP 9:1 MeCN-H_2O); Mp 100–102 °C (THF), lit.,[8] 113-114 °C (benzene); IR υ_{max}/cm^{-1} (neat) 3059, 2952, 1773, 1661, 1636, 1573, 1560, 1473, 1399, 1380, 1326; ^{1}H NMR 300 MHz ($CDCl_3$) δ 7.45 (2H, d, *J* 8.6 Hz, H3', H5'), 7.14 (1H, d, *J* 2.1 Hz, H2), 7.00 (1H, d, *J* 10.2 Hz, H5), 6.69 (2H, d, *J* 8.6 Hz, H2', H6'), 6.46 (1H, dd, *J* 10.2, 2.1 Hz, H6); ^{13}C NMR ($CDCl_3$) δ 185.0 (C1), 153.5 (C4), 147.7 (C1'), 140.2 (C3), 136.2 (C2), 132.7 (C6), 132.3 (C3', C5'), 128.1 (C5), 122.0 (C2', C6'), 120.1 (C4'); *m/z* (ESI+) 343 ([$^{81}Br_2$]M+H$^+$, 20%), 341 ([$^{79}Br^{81}Br$]M+H$^+$, 40), 339 ([$^{79}Br_2$]M+H$^+$, 20), 282 (12). Found: M+H$^+$, 339.8847. $C_{12}H_8{}^{79/79}Br_2NO$ requires 339.8973. Anal Calcd for $C_{12}H_7Br_2NO$: C, 42.27; H, 2.07; N, 4.11. Found: C, 42.06; H, 1.93; N, 3.98. Crystal structure determined (see Appendix).

6.27 4-((4-Bromophenyl)imino)cyclohexa-2,5-dien-1-one, 3.25

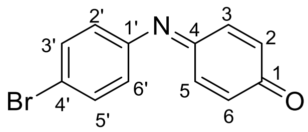

An orange oil, (0.09 g, 0.35 mmol, 7%), R_f = 0.54 (SiO_2 1:9 ethylacetate-petrol); IR υ_{max}/cm^{-1} (neat) 3312, 2959, 2931, 2872, 1779, 1713, 1654, 1591, 1476, 1373, 1304; ^{1}H NMR 300 MHz ($CDCl_3$) δ 7.46 (2H, d, *J* 8.6 Hz, H3', H5'), 7.23 (1H, dd, *J* 10.1, 2.7 Hz, H3), 6.98 (1H, dd, *J* 10.3, 2.7 Hz, H5), 6.71 (2H, d, *J* 8.6 Hz, H2', H6'), 6.64 (1H, dd, *J* 10.1, 2.2 Hz, H2), 6.50 (1H, dd, *J* 10.3, 2.2 Hz, H6); ^{13}C NMR ($CDCl_3$) δ 187.5 (C1), 157.8 (C4), 148.1 (C1'), 141.2 (C3), 133.9 (C6), 133.1 (C2), 132.2 (C3', C5'), 127.9 (C5), 122.4 (C2', C6'), 119.9 (C4'). *m/z* (ESI+) 264 ([^{81}Br]M+H$^+$, 55%), 262 ([^{79}Br]M+H$^+$, 48), 261 ([^{79}Br]M+H$^+$, 100).

Typical procedure for the addition of HCl to **3.1** or **3.23**

Conc. hydrochloric acid (37%, 1 mL) was added dropwise to a solution of azaquinone (1.0 g, 5.46 mmol) in acetic acid (75 mL). The solution was heated at reflux for 24 h when its colour changed from orange to blue. The reaction mixture was diluted with water (200 mL) and extracted with DCM (3 × 150 mL). The organic extracts were washed with water (3 × 50 mL), dried over sodium sulfate and stirred with lead (IV) acetate (8.0 g, 18 mmol) at RT for 1 h. The reaction mixture was then filtered to remove the oxidising agent and the solvent removed in vacuo to give the crude product.

Azaquinone, **3.1** reaction with HCl

Purification by chromatography (SiO_2 1:9 ethylacetate-petrol) gave one major product, **3.12** with unreacted azaquinone as the second product.

6.28 *(E)*-3-Chloro-4-(phenylimino)cyclohexa-2,5-dien-1-one, 3.12

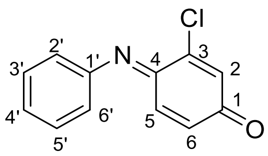

An orange oil, (0.71 g, 3.28 mmol, 60%), R_f = 0.69 (SiO_2 1:9 ethylacetate-petrol); IR υ_{max}/cm^{-1} (neat) 3201, 1677, 1640, 1577, 1497, 1479, 1447, 1383, 1309; ^{1}H NMR 400 MHz (DMSO-d_6) δ 7.48 (2H, t, *J* 7.4 Hz, H3', H5'), 7.30 (1H, t, *J* 7.4 Hz, H4'), 7.14 (1H, d, *J* 2.1 Hz, H2), 7.09 (1H, d, *J* 10.2 Hz, H5), 6.97 (2H, d, *J* 8.6 Hz, H2', H6'), 6.62 (1H, dd, *J* 10.2, 2.1 Hz, H6); ^{13}C NMR (DMSO-d_6) δ 185.9 (C1), 153.1 (C4), 149.1 (C1'), 146.7 (C3), 132.9 (C6), 132.1 (C2), 129.7 (C3', C5'), 129.2 (C5), 126.8 (C4'), 120.8 (C2', C6'); *m/z* (ESI+) 220 ([^{37}Cl]M+H$^+$, 100%), 219 (42), 218 ([^{35}Cl]M+H$^+$, 45). Found: M+H$^+$, 218.0355. $C_{12}H_9{}^{35}ClNO$ requires 218.0367.

Azaquinone *N*-oxide, **3.23** reaction with HCl

Using azaquinone *N*-oxide (1.0 g, 5.0 mmol). Purification by chromatography (SiO_2 1:9 ethylacetate-petrol) gave two products **3.26** and **3.27**.

6.29 *(E)*-3-Chloro-4-((4-chlorophenyl)imino)cyclohexa-2,5-dien-1-one, 3.26

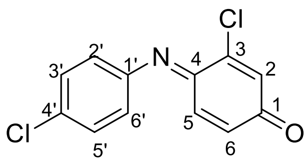

An orange solid, (0.88 g, 3.5 mmol, 70%), R_f = 0.64 (SiO_2 1:4 ethylacetate-petrol); Mp 80–82 °C (petrol-ethylacetate); IR υ_{max}/cm^{-1} (neat) 3372, 3058, 2960, 2872, 1701, 1640, 1575, 1479, 1383, 1364; ^{1}H NMR 300 MHz ($CDCl_3$) δ 7.30 (2H, d, *J* 8.6 Hz, H3', H5'), 7.00 (1H, d, *J* 10.3 Hz, H5), 6.86 (1H, d, *J* 2.2 Hz, H2), 6.76 (2H, d, *J* 8.6 Hz, H2', H6'), 6.46 (1H, dd, *J* 10.2, 2.1 Hz, H6); ^{13}C NMR ($CDCl_3$) δ 185.7 (C1), 153.3 (C4), 147.0 (C1'), 132.6 (C6), 132.4 (C3), 131.7 (C2), 129.3 (C3', C5'), 128.3 (C5), 121.8 (C2', C6'), 120.4 (C4'); *m/z* (ESI+) 253 ([^{37}Cl^{35}Cl]M$^+$, 85%), 251

($[^{35}Cl_2]M^+$, 100). Found: $M+H^+$, 251.9997. $C_{12}H_8{}^{35/35}Cl_2NO$ requires 251.9977. Crystal structure determined (see Appendix).

6.30 4-((4-Chlorophenyl)imino)cyclohexa-2,5-dien-1-one, 3.27

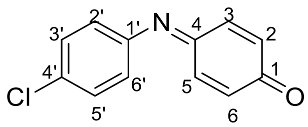

An orange oil, (0.13 g, 0.6 mmol, 12%), R_f = 0.51 (SiO_2 1:4 ethylacetate-petrol); IR υ_{max}/cm^{-1} (neat) 3365, 2961, 2935, 2874, 1645, 1595, 1491, 1458, 1364,1313; ^1H NMR 300 MHz ($CDCl_3$) δ 7.31 (2H, d, *J* 8.6 Hz, H3', H5'), 7.25 (1H, dd, *J* 10.1, 2.6 Hz, H3), 6.99 (1H, dd, *J* 10.1, 2.6 Hz, H5), 6.78 (2H, d, *J* 8.6 Hz, H2', H6'), 6.64 (1H, dd, *J* 10.0, 2.2 Hz, H2), 6.50 (1H, dd, *J* 10.0, 2.2 Hz, H6); ^{13}C NMR ($CDCl_3$) δ 187.5 (C1), 157.9 (C4), 147.4 (C1'), 141.5 (C3), 133.8 (C6), 133.0 (C2), 132.2 (C4'), 129.3 (C3', C5'), 127.9 (C5), 122.2 (C2', C6').*m/z* (ESI+) 220 ($[^{37}Cl]M+H^+$, 96%), 219 (52), 218 ($[^{35}Cl]M+H^+$, 45), 217 (20). Found 217.03. $C_{12}H_8{}^{35}ClNO$ requires 217.0294.

Typical procedure for the Suzuki and Stille coupling reactions

A mixture of 3-bromoazaquinone **4.11** (1 mmol), arylboronic acid **4.20** (2 mmol) or arylstannane **4.26** (1 mmol), $Pd(PPh_3)_4$ (0.1 mmol, 10mol%) and Cs_2CO_3/Ag_2CO_3 (2 mmol) were suspended in dioxane (10 mL) and heated at 90 °C for 24 h. The reaction mixture was diluted with water (100 mL) and extracted with ethylacetate (3 × 100 mL). The solvent was removed in vacuo to give the crude product. Purification by chromatography (SiO_2 1:9 ethylacetate-petrol and/or RP (C18) $MeCN-H_2O$) gave the expected product, **4.14** with the biaryl product, **4.21** as a by-product.

6.31 *(E)*-6-(Phenylimino)-[1,1'-biphenyl]-3(6*H*)-one, 4.14a (Table 1, Entry 1)

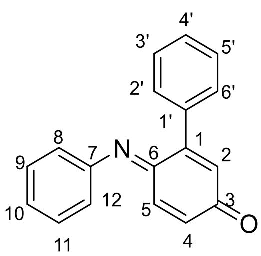

Using phenylboronic acid (0.244 g, 2 mmol) gave the title compound as a red oil, (171 mg, 0.66 mmol, 66%), R_f = 0.4 (SiO_2 1:9 ethylacetate-petrol); IR (neat) 3341, 3054, 1920, 1797, 1688, 1640 cm^{-1}; ^1H NMR 300 MHz ($CDCl_3$) δ 7.45 (2H, d, *J* 8.0 Hz, H2', H6'), 7.33 (2H, t, J = 8.0 Hz, H3', H5'), 7.31 (1H, t, *J* 8.0 Hz, H4'), 7.29 (2H, t, *J* 8.0 Hz, H9, H11), 7.10 (1H, t, *J* 7.6 Hz, H10), 7.06 (1H, d, *J* 10.3 Hz, H5), 6.74 (2H, d, *J* 8.0 Hz, H8, H12), 6.69 (1H, d, *J* 2.3Hz, H2), 6.51 (1H, dd, *J* 10.3, 2.3 Hz, H4); ^{13}C NMR ($CDCl_3$) δ 188.2 (C3), 156.9 (C6), 151.2 (C1), 149.7 (C7), 135.5 (C1'), 132.7 (C4), 131.1 (C2), 129.9 (C2', C6'), 129.2 (C5), 129.0 (C4'), 128.9 (C3', C5'), 128.0 (C9, C11), 125.8 (C10), 120.0 (C8, C12); *m/z* (ESI+) 282 ([M+Na^+], 100%), 260 (M+H^+, 72). Found: M+H^+, 260.1114. $C_{18}H_{14}NO$ requires 260.1075.

6.32 1,1'-Biphenyl, 4.21a (Table 1, Entry 1)

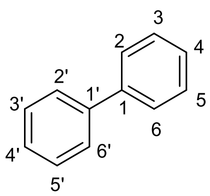

White solid (67 mg, 0.39 mmol, 39%); R_f = 0.94 (SiO_2 5% ethylacetate-petrol); Mp 70–72 °C (DCM), lit.,[259] 71–72 °C (EtOAc-cyclohexane); IR (neat) 3030, 2922, 2853, 1881, 1568, 1468, 1428, 1377 cm^{-1}; ^1H NMR 300 MHz ($CDCl_3$) δ 7.48 (4H, d, *J* 7.4 Hz, H2, H6, H2', H6'), 7.31 (4H, t, *J* 7.6 Hz, H3, H5, H3', H5'), 7.22 (2H, t, *J* 7.4 Hz, H4, H4'); ^{13}C NMR ($CDCl_3$) δ 141.3 (C1, C1'), 128.8 (C3, C5, C3', C5'), 127.3 (C4, C4'), 127.2 (C2, C6, C2', C6').

6.33 *(E)*-4'-Chloro-6-(phenylimino)-[1,1'-biphenyl]-3(6*H*)-one, 4.14b (Table 1, Entry 4)

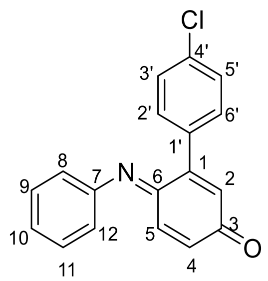

Using 4-chlorophenylboronic acid (0.312 g, 2 mmol) gave the title compound as a red oil, (140 mg, 0.5 mmol, 48%), R_f = 0.44 (SiO_2 1:9 ethylacetate-petrol); IR (neat)

3332, 2961, 2873, 1638 cm^{-1}; ^{1}H NMR 300 MHz ($CDCl_3$) δ 7.41 (2H, d, *J* 8.0 Hz, H3', H5'), 7.33 (2H, d, *J* 8.0 Hz, H2', H6'), 7.30 (2H, t, *J* 7.8 Hz, H9, H11), 7.16 (1H, t, *J* 7.6 Hz, H10), 7.09 (1H, d, *J* 10.3 Hz, H5), 6.76 (2H, dt, *J* 7.7, 1.2 Hz, H8, H12), 6.69 (1H, d, *J* 2.3 Hz, H2), 6.52 (1H, dd, *J* 10.3, 2.3 Hz, H4); ^{13}C NMR ($CDCl_3$) δ 187.9 (C3), 156.7 (C6), 150.0 (C1), 149.5 (C7), 135.5 (C4'), 133.9 (C1'), 132.8 (C4), 131.2 (C3', C5'), 129.3 (C5), 129.0 (C9, C11), 128.3 (C2', C6'), 126.1 (C10), 120.1 (C8, C12), 116.8 (C2); *m/z* (ESI+) 296 ([^{37}Cl]M+H$^+$, 78%), 294 ([^{35}Cl]M+H$^+$, 95). Found: M+H$^+$, 294.0676. $C_{18}H_{13}{}^{35}ClNO$ requires 294.068.

6.34 4,4'-Dichloro-1,1'-biphenyl, 4.21b Table 1, Entry 4

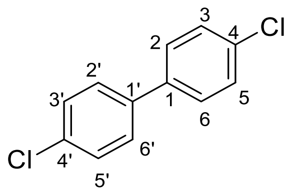

White solid, (84 mg, 0.35 mmol, 35%); R_f = 0.78 (SiO_2 1:9 ethylacetate-petrol); Mp 140–142 °C (EtOAc), lit.,[260] 141–142 °C (*n*-hexane-EtOAc); IR (neat) 2922, 2854, 1904, 1782, 1587 cm^{-1}; ^{1}H NMR 300 MHz ($CDCl_3$) δ 7.35 (4H, d, *J* 8.8 Hz, H2, H6, H2', H6'), 7.29 (4H, d, *J* 8.8 Hz, H3, H5, H3', H5'); ^{13}C NMR ($CDCl_3$) δ 138.4 (C1, C1'), 133.7 (C4, C4'), 129.0 (C2, C6, C2', C6'), 128.2 (C3, C5, C3', C5').

6.35 *(E)*-4'-Bromo-6-(phenylimino)-[1,1'-biphenyl]-3(6*H*)-one, 4.14c (Table 1, Entry 5)

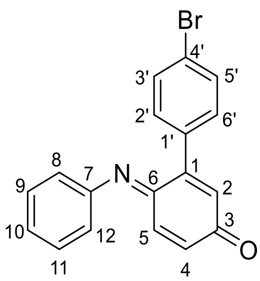

Using 4-bromophenylboronic acid (0.402 g, 2 mmol) gave the title compound as a red oil, (42 mg, 0.13 mmol, 13%); R_f = 0.45 (SiO_2 1:9 ethylacetate-petrol); IR (neat) 3278, 3058, 2960, 1733, 1637, 1585 cm^{-1}; ^{1}H NMR 300 MHz ($CDCl_3$) δ 7.48 (2H, d, *J* 8.6 Hz, H3', H5'), 7.34 (2H, d, *J* 8.6 Hz, H2', H6'), 7.30 (2H, t, *J* 8.2 Hz, H9, H11), 7.13 (1H, t, *J* 7.6 Hz, H10), 7.07 (1H, d, *J* 10.3 Hz, H5), 6.75 (2H, d, *J* 7.8

Hz, H8, H12), 6.66 (1H, d, *J* 2.2 Hz, H2), 6.50 (1H, dd, *J* 10.3, 2.3 Hz, H4); ^{13}C NMR ($CDCl_3$) δ 187.5 (C3), 156.7 (C6), 149.8 (C1), 149.5 (C7), 134.5 (C4'), 132.9 (C4), 132.4 (C1'), 131.5 (C2', C6'), 131.3 (C3', C5'), 129.0 (C9, C11), 128.8 (C5), 126.0 (C10), 120.0 (C8, C12), 117.3 (C2); *m/z* (ESI+) 339 ([^{81}Br]M+H$^+$, 100), 337 ([^{79}Br]M+H$^+$, 88). Found: 338.0157. $C_{18}H_{13}{}^{79}BrNO$ requires 338.0175.

6.36 4,4'-Dibromo-1,1'-biphenyl, 4.21c (Table1, Entry 5)

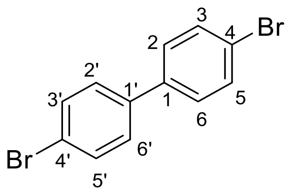

Red solid (89 mg, 0.26 mmol, 26%); R_f =0.91 (SiO_2 1:4 ethylacetate-petrol); Mp 168–170 °C (EtOAc), lit.,[260] 168–171 °C (*n*-hexane-EtOAc); IR (neat) 1640, 1470, 1381, 1067 cm^{-1}; ^1H NMR 300 MHz ($CDCl_3$) δ 7.48 (4H, d, *J* 8.5 Hz, H2, H6, H2', H6'), 7.33 (4H, d, *J* 8.5 Hz, H3, H5, H3', H5'); ^{13}C NMR ($CDCl_3$) δ 138.9 (C1, C1'), 132.0 (C2, C6, C2', C6'), 128.5 (C3, C5, C3', C5'), 121.9 (C4, C4').

6.37 *(E)*-4'-Methoxy-6-(phenylimino)-[1,1'-biphenyl]-3(6*H*)-one, 4.14d (Table1, Entry 6)

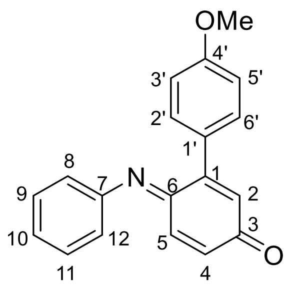

Using 4-methoxyphenylboronic acid (0.304 g, 2 mmol) gave the title compound as a red oil, (100 mg, 0.35 mmol, 35%), R_f = 0.35 (SiO_2 1:9 ethylacetate-petrol); IR (neat) 3350, 3057, 2959, 2836, 1634, 1601, 1578, cm^{-1}; ^1H NMR 300 MHz ($CDCl_3$) δ 7.44 (2H, d, *J* 8.8 Hz, H2', H6'), 7.30 (2H, t, *J* 7.5 Hz, H9, H11), 7.11 (1H, t, *J* 7.5 Hz, H10), 7.03 (1H, d, *J* 10.3 Hz, H5), 6.86 (2H, d, *J* 8.8 Hz, H3', H5'), 6.74 (2H, d, *J* 8.0 Hz, H8, H12), 6.66 (1H, d, *J* 2.3 Hz, H2), 6.47 (1H, dd, *J* 10.3, 2.3 Hz, H4), 3.75 (3H, s, OMe); ^{13}C NMR ($CDCl_3$) δ 187.9 (C3), 160.6 (C6), 157.2 (C4'), 150.3 (C1), 149.8 (C7), 132.8 (C4), 131.4 (C2', C6'), 130.2 (C2), 128.9 (C9, C11), 128.9 (C5), 127.9 (C1'), 125.7 (C10), 119.9 (C8, C12), 113.6 (C3', C5'), 55.3 (OCH_3). *m/z* (ESI+) 290 ($M+H^+$, 100%), 289 (M^+, 64). Found 290.05. $C_{19}H_{16}NO_2$ requires 290.1136.

6.38 4,4'-Dimethoxy-1,1'-biphenyl, 4.21d (Table1, Entry 6)

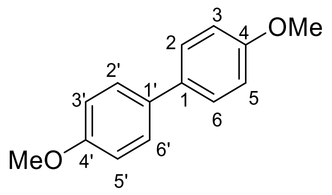

White solid (49 mg, 0.21 mmol, 21%); R_f = 0.42 (SiO_2 5% ethylacetate-petrol); Mp 176–178 °C EtOAc), lit.[260] 178–181 °C (*n*-hexane-EtOAc); IR (neat) 3014, 2955, 2839, 2530, 2065, 1893, 1601 cm^{-1}; ^{1}H NMR 300 MHz ($CDCl_3$) δ 7.39 (4H, d, *J* 8.8 Hz, H2, H6, H2', H6'), 6.87 (4H, d, *J* 8.8 Hz, H3, H5, H3', H5'), 3.75 (6H, s, OMe); ^{13}C NMR ($CDCl_3$) δ 158.7 (C4, C4'), 133.5 (C1, C1'), 127.7 (C2, C6, C2', C6'), 114.2 (C3, C5, C3', C5'), 55.3 (OMe).

6.39 4-Methoxy-1,1'-biphenyl (Table 1, Entry 6)

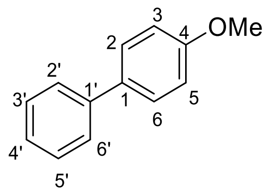

Orange solid (8 mg, 0.04 mmol, 4%); R_f = 0.69 (SiO_2 5% ethylacetate-petrol); Mp 86–88 °C (EtOAc), lit.[260] 85–87 °C (*n*-hexane-EtOAc); IR (neat) 3000, 2959, 2836, 1729, 1603 cm^{-1}; ^{1}H NMR 300 MHz ($CDCl_3$) δ 7.48 (2H, d, *J* 7.4 Hz, H2', H6'), 7.45 (2H, d, *J* 8.8 Hz, H2, H6), 7.34 (2H, t, *J* 7.6 Hz, H3', H5'), 7.22 (1H, t, *J* 7.4 Hz, H4'), 6.90 (2H, d, *J* 8.8 Hz, H3, H5), 3.77 (3H, s, OMe); ^{13}C NMR ($CDCl_3$) δ 159.1 (C4), 140.8 (C1'), 133.8 (C1), 128.7 (C2, C6), 128.1 (C3', C5'), 126.7 (C2', C6'), 126.6 (C4'), 114.2 (C3, C5), 55.3 (OMe). *m/z* (ESI+) 186 ($M+H^+$, 12), 185 ($M+H^+$, 100).

6.40 2,2'-Dimethyl-1,1'-biphenyl, 4.21e (Table 1, Entry 7)

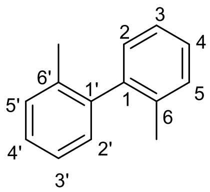

Colourless oil (36 mg, 0.18 mmol, 18%); R_f = 0.91 (SiO_2 1:4 ethylacetate-petrol); IR (neat) 3058, 3017, 2922, 1914, 1476 cm^{-1}; ^1H NMR 300 MHz ($CDCl_3$) δ 7.17 (4H, m H2, H3, H2', H3'), 7.12 (2H, m, H4, H4'), 7.02 (2H, m, H5, H5'), 1.97 (6H, s, CH_3); ^{13}C NMR ($CDCl_3$) δ 141.6 (C1, C1'), 135.8 (C6, C6'), 129.8 (C5, C5'), 129.3 (C4, C4'), 127.1 (C3, C3'), 125.5 (C2, C2'), 19.8 (CH_3). *m/z* (ESI+) 183 ($M+H^+$, 35), 182 (24).

6.41 *(E)*-5-Oxo-2-(phenylimino)-2,5-dihydro-[1,1'-biphenyl]-4'-carbaldehyde, 4.14f (Table 1, Entry 8)

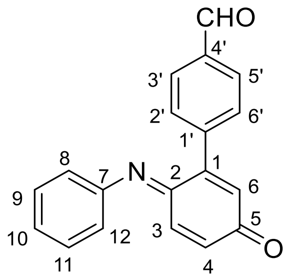

Using 4-formylphenylboronic acid (0.30 g, 2 mmol). Further purification by chromatography RP C18 (9:1 MeOH-H_2O) gave the title compound as a red oil, (36 mg, 0.13 mmol, 13%); R_f = 0.21 (SiO_2 1:9 ethylacetate-petrol); IR (neat) 3355, 2923, 2852, 1697, 1638, 1602, 1587 cm^{-1}; ^1H NMR 300 MHz ($CDCl_3$) δ 10.00 (1H, s, CHO), 7.87 (2H, d, *J* 8.0 Hz, H3', H5'), 7.64 (2H, d, *J* 8.0 Hz, H2', H6'), 7.33 (2H, t, *J* 8.0 Hz, H9, H11), 7.15 (1H, t, *J* 7.4 Hz, H10), 7.12 (1H, d, *J* 10.3 Hz, H3), 6.77 (2H, d, *J* 8.5 Hz, H8, H12), 6.72 (1H, d, *J* 2.3 Hz, H6), 6.54 (1H, dd, *J* 10.3, 2.2 Hz, H4); ^{13}C NMR ($CDCl_3$) δ 191.8 (CHO), 187.2 (C5), 156.5 (C2), 149.7 (C1), 149.2 (C7), 141.7 (C1'), 136.4 (C4'), 133.0 (C4), 131.9 (C6), 130.6 (C2', C6'), 129.2 (C3', C5'), 129.0 (C9, C11), 128.8 (C3), 126.1 (C10), 120.0 (C8, C12). *m/z* (ESI+) 290 ($M+H^+$, 90%).

6.42 [1,1'-Biphenyl]-4,4'-dicarboxaldehyde, 4.21f (Table 1, Entry 8)

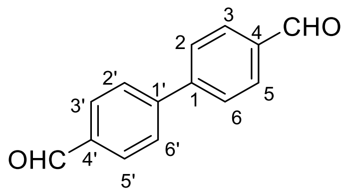

Brown solid (52 mg, 0.23 mmol, 23%); R_f = 0.27 (SiO_2 1:9 ethylacetate-petrol); Mp 142–144 °C (EtOAc), lit.,[261] 146–148 °C (DCM-MeCN); IR (neat) 1693, 1599, 1387, 1299, 1206 cm^{-1}; ^1H NMR 300 MHz ($CDCl_3$) δ 9.98 (2H, s, CHO), 7.90 (4H, d, *J* 8.3 Hz, H3, H5, H3', H5'), 7.70 (4H, d, *J* 8.3 Hz, H2, H6, H2', H6'); ^{13}C NMR ($CDCl_3$) δ 191.7 (CHO), 145.4 (C1, C1'), 135.9 (C4, C4'), 130.3 (C3, C5, C3', C5'), 128.0 (C2, C6, C2', C6'). *m/z* (ESI+) 212 (M+2, 16), 211 ($M+H^+$, 100).

6.43 *(E)*-3-(Naphthalene-1-yl)-4-(phenylimino)cyclohexa-2,5-dien-1-one, 4.14g (Table 1, Entry 9)

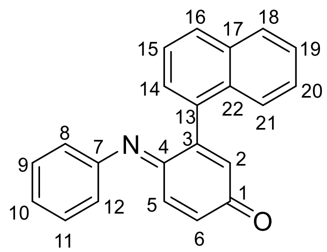

Using 1-naphthaleneboronic acid (0.344 g, 2 mmol)gave the title compound as a red oil, (105 mg, 0.34 mmol, 34%), R_f = 0.59 (SiO_2 1:9 ethylacetate-petrol); IR (neat) 3055, 1733, 1636, 1587, 1505, 1479, 1446, 1388, 1371, 1337, 1285 cm^{-1}; ^1H NMR 300 MHz ($CDCl_3$) δ 7.81 (1H, d, *J* 8.0 Hz, H16), 7.78 (1H, t, *J* 7.5 Hz, H20), 7.67 (1H, ddt, *J* 6.4, 3.5, 0.8 Hz, H18), 7.43 (1H, t, *J* 7.5 Hz, H15), 7.39 (1H, d, *J* 8.0 Hz, H21), 7.37 (1H, t, *J* 7.5 Hz, H19), 7.21 (2H, t, *J* 8.1 Hz, H9, H11), 7.11 (1H, d, *J* 10.3 Hz, H5), 7.03 (1H, t, *J* 7.2 Hz, H10), 6.72 (1H, d, *J* 2.3 Hz, H2), 6.60 (2H, d, *J* 8.0 Hz, H8, H12), 6.56 (1H, dd, *J* 10.3, 2.3 Hz, H6); ^{13}C NMR ($CDCl_3$) δ 187.8 (C1), 157.6 (C4), 151.7 (C3), 149.7 (C7), 141.9 (C17), 134.2 (C13), 133.3 (C2), 132.9 (C6), 131.9 (C22), 129.2 (C18), 128.8 (C9, C11), 128.4 (C5), 127.1 (C16), 126.2 (C21), 126.0 (C20), 125.9 (C15), 125.7 (C10), 125.1 (C19), 120.7 (C14), 119.9 (C8, C12). *m/z* (ESI+) 310 ($M+H^+$, 88%). Found: $M+H^+$ 310.1227. $C_{22}H_{16}NO$ requires 310.1226.

6.44 1,1'-Binaphthalene, 4.21g Table 1, Entry 9

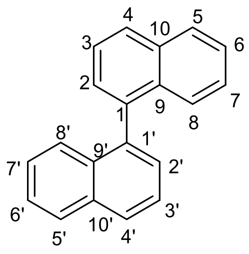

White solid (82 mg, 0.3 mmol, 30%); R_f = 0.86 (SiO_2 5% ethylacetate-petrol); Mp 142–144 °C (EtOAc), lit.,[262] 142–144 °C (hexane); IR (neat) 3039, 1585, 1501, 1375 cm^{-1}; ^{1}H NMR 300 MHz ($CDCl_3$) δ 7.83 (2H, d, *J* 8.2Hz, H8, H8'), 7.82 (2H, d, *J* 8.2 Hz, H2, H2'), 7.46 (2H, dd, *J* 8.2, 7.0 Hz, H5, H5'), 7.38 (2H, dd, *J* 7.0, 1.3 Hz, H4, H4'), 7.35 (2H, dd, *J* 8.2, 1.3 Hz, H3, H3'), 7.29 (2H, d, *J* 8.2 Hz, H7, H7'), 7.15 (2H, ddd, *J* 8.4, 6.7, 1.3 Hz, H6, H6'); ^{13}C NMR ($CDCl_3$) δ 138.5 (C1, C1'), 133.6 (C10, C10'), 132.9 (C9, C9'), 128.2, 127.97, 127.91, 126.6, 126.0, 125.8, 125.4. *m/z* (ESI+) 256 ($M+H^+$, 25%), 255 ($M+H^+$, 100).

6.45 1,4-Bis(4-methylphenyl)-1,3-butadiyne, 4.28

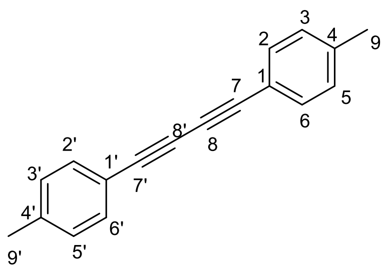

White solid (100 mg, 0.34 mmol, 34%); R_f = 0.78 (SiO_2 1:9 ethylacetate-petrol); Mp 182–184 °C (EtOAc), lit.,[263] 182–184 °C (hexane); IR (neat) 2915, 1596, 1498 cm^{-1}; ^{1}H NMR 300 MHz ($CDCl_3$) δ 7.34 (4H, d, *J* 8.5 Hz, H2, H6, H2', H6'), 7.06 (4H, d, *J* 8.5 Hz, H3, H5, H3', H5'), 2.29 (6H, s, H9, H9'); ^{13}C NMR ($CDCl_3$) δ 139.5 (C4, C4'), 132.4 (C2, C6, C2', C6'), 129.2 (C3, C5, C3', C5'), 118.7 (C1, C1'), 81.5 (C7, C7'), 73.4 (C8, C8'), 21.6 (C9, C9'). *m/z* (ESI+) 231 ($M+H^+$, 100%).

6.46 *(E)*-4-(Phenylimino)-3-(thiophen-2-yl)cyclohexa-2,5-dien-1-one, 4.14h (Table 3, Entry 2)

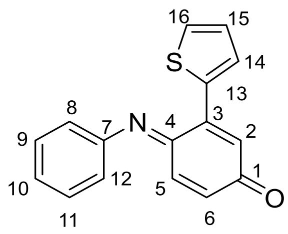

Using tributyl(thiophen-2-yl)stannane (0.373 g, 1 mmol). Purification by chromatography RP C18 (7:3 MeCN-H_2O) gave the title compound as a red oil, (146 mg, 0.55 mmol, 55%), R_f = 0.27 RP C18 (7:3 MeCN-H_2O); IR (neat) 2920, 1639, 1614, 1586, 1573, 1556 cm^{-1}; ^1H NMR 300 MHz ($CDCl_3$) δ 7.62 (1H, dd, *J* 3.8, 1.2 Hz, H14), 7.50 (1H, dd, *J* 5.1, 1.2 Hz, H16), 7.35 (2H, t, *J* 8.0 Hz, H9, H11), 7.17 (1H, t, *J* 7.5 Hz, H10), 7.04 (1H, t, *J* 5.3 Hz, H15), 7.02 (1H, d, *J* 10.3 Hz, H5), 6.96 (1H, d, *J* 2.2 Hz, H2), 6.85 (2H, d, *J* 8.2 Hz, H8, H12), 6.44 (1H, dd, *J* 10.3, 2.2 Hz, H6); ^{13}C NMR ($CDCl_3$) δ 187.5 (C1), 155.6 (C4), 148.5 (C7), 142.5 (C3), 135.3 (C13), 133.1 (C16), 132.8 (C6), 129.1 (C9, C11), 128.9 (C14), 128.3 (C5), 126.9 (C15), 126.5 (C2), 126.1 (C10), 120.3 (C8, C12); *m/z* (ESI+) 266 (M+H^+, 100%). Found: M+H^+, 266.063. $C_{16}H_{12}NOS$ requires 266.0634.

6.47 *(E)*-4-([1,1'-Biphenyl]-4-ylimino)-3-bromocyclohexa-2,5-dien-1-one, 4.22

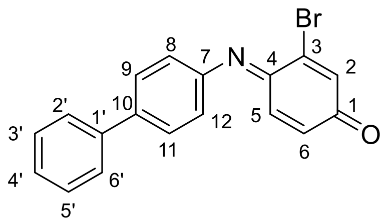

Using 3-bromo(4-bromophenyl)azaquinone, **4.12** (0.341 g, 1 mmol) and phenylboronic acid (0.244 g, 2 mmol). Further purification by chromatography RP C18 (7:3 MeCN-H_2O) gave the title compound as a red oil (74 mg, 0.22 mmol, 22%); R_f = 0.27 RP C18 (7:3 MeCN-H_2O); IR (neat) 3278, 3055, 2923, 2852, 1889, 1638 cm^{-1}; ^1H NMR 300 MHz ($CDCl_3$) δ 7.45 (2H, t, *J* 7.8 Hz, H3', H5'), 7.43 (2H, d, *J* 8.6 Hz, H9, H11), 7.37 (2H, d, *J* 8.0 Hz, H2', H6'), 7.35 (1H, t, *J* 7.5 Hz, H4'), 7.04 (1H, d, *J* 10.3 Hz, H5), 6.69 (1H, d, *J* 2.3 Hz, H2), 6.65 (2H, d, *J* 8.6 Hz, H8, H12), 6.52 (1H, dd, *J* 10.3, 2.3 Hz, H6); ^{13}C NMR ($CDCl_3$) δ 187.5 (C1), 157.4 (C4), 150.7 (C7), 148.6 (C1'), 135.4 (C3), 133.2 (C6), 132.0 (C9, C11), 131.4 (C2), 129.8 (C3', C5'), 129.3 (C10), 128.5 (C5), 128.1 (C2', C6'), 121.6 (C8, C12), 119.2 (C4'); *m/z* (ESI+) 339 ([^{81}Br]M+H^{+}, 48%), 337 ([^{79}Br]M+H^{+}, 74), 336 (85). Found: 338.0197. $C_{18}H_{13}{}^{79}BrNO$ requires 338.0175.

6.48 *(E)*-3-Isopropyl-4-(phenylimino)cyclohexa-2,5-dien-1-one, 4.16a

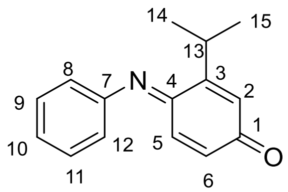

To a solution of 3-bromoazaquinone (0.262 g, 1 mmol) and $Pd(PPh_3)_4$ (0.116 g, 0.1 mmol) in anhydrous THF (10 mL) was added dropwise a solution of iPrMgCl (2.0 M in THF, 1.0 mL, 2 mmol) under nitrogen. The mixture was stirred for 2 h at 60 °C. After completion of reaction, the mixture was quenched with water (25 mL) and extracted with ethylacetate (3 × 10 mL). The organic extracts were washed with water, dried over $MgSO_4$, filtered and concentrated under vacuum. The crude reaction mixture was purified by chromatography (SiO_2 1:4 ethylacetate-petrol) to give the product as a red oil (22.5 mg, 0.1 mmol, 10%); R_f = 0.67 (SiO_2 1:4 ethylacetate-petrol); IR (neat) 3383, 2967, 2871, 1703, 1594 cm^{-1}; ^{1}H NMR 500 MHz ($CDCl_3$) δ 7.24 (1H, d, *J* 2.8 Hz, H2), 7.18 (2H, t, *J* 8.2 Hz, H9, H11), 7.07 (1H, d, *J* 8.5 Hz, H5), 6.87 (1H, dd, *J* 8.5, 2.9 Hz, H6), 6.70 (1H, tt, *J* 7.3, 1.0 Hz, H10), 6.50 (2H, dt, *J* 7.3, 1.1 Hz, H8, H12), 4.33 (1H, hept, *J* 6.5 Hz, H13), 1.22 (6H, d, *J* 6.5 Hz, H14, H15); ^{13}C NMR ($CDCl_3$) δ 185.8 (C1), 171.8 (C4), 155.5 (C3), 147.8 (C7), 133.7 (C5), 128.9 (C9, C11), 120.6 (C2), 116.5 (C10), 115.8 (C6), 113.0 (C8, C12), 48.5 (C13), 20.7 (C14, C15).

Typical procedure for Buchwald-Hartwig amination reactions

A mixture of 3-bromoazaquinone (0.262 g, 1 mmol), arylamine (1.2 mmol), $Pd(OAc)_2$ (0.034 g, 0.15 mmol), (+/-)-BINAP (0.093 g, 0.15 mmol) and Cs_2CO_3 (0.456 g, 1.4 mmol) were suspended in anhydrous toluene (5 mL) under nitrogen and heated to 80 °C for 24 h. The mixture was filtered and washed with ethylacetate (100 mL) to give the crude product which was purified by chromatography (SiO_2 1:4 ethylacetate-petrol) to give the pure product.

6.49 *(E)*-3-(Phenylamino)-4-(phenylimino)cyclohexa-2,5-dien-1-one, 4.17a (Table 2, Entry 1)

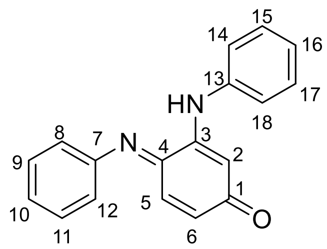

Using aniline (0.112 g, 1.2 mmol) gave the title compound as a red solid (217 mg, 0.79 mmol, 79%); R_f = 0.48 (SiO_2 1:4 ethylacetate-petrol); Mp 134–136 °C (EtOAc); IR (neat) 3241, 3051, 2922, 1716, 1559 cm^{-1}; ^1H NMR 300 MHz ($CDCl_3$) δ 7.90 (1H, s, NH), 7.37 (2H, t, *J* 7.8 Hz, H9, H11), 7.32 (2H, t, *J* 7.6 Hz, H15, H17), 7.22 (2H, d, *J* 7.8 Hz, H14, H18), 7.18 (1H, t, *J* 7.9 Hz, H10), 7.11 (1H, t, *J* 7.3 Hz, H16), 6.87 (2H, d, *J* 7.9 Hz, H8, H12), 6.79 (1H, d, *J* 10.3 Hz, H5), 6.31 (1H, dd, *J* 10.2, 2.2 Hz, H6), 6.12 (1H, d, *J* 2.2 Hz, H2); ^{13}C NMR ($CDCl_3$) δ 186.8 (C1), 153.0 (C3), 147.8 (C4), 146.8 (C7), 138.1 (C13), 134.6 (C6), 129.6 (C9, C11), 129.2 (C15, C17), 126.1 (C10), 125.1 (C16), 125.0 (C5), 122.8 (C14, C18), 120.6 (C8, C12), 100.6 (C2); *m/z* (ESI+) 274 ($M+H^+$, 100%), 275 ($M+H^+$, 38). Found 274.04. $C_{18}H_{14}N_2O$ requires 274.1106.

6.50 *(E)*-3-((4-Methoxyphenyl)amino)-4-(phenylimino)cyclohexa-2,5-dien-1-one, 4.17b (Table 2, Entry 2)

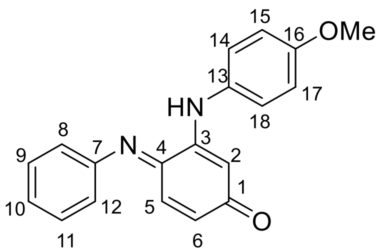

Using methoxyaniline (0.147 g, 1.2 mmol) gave the title as a red oil (201 mg, 0.66 mmol, 66%); R_f = 0.23 (SiO_2 1:4 ethylacetate-petrol); ^1H NMR 300 MHz ($CDCl_3$) δ 7.83 (1H, s, NH), 7.33 (2H, t, H9, H11), 7.16 (1H, t, H10), 6.86 (2H, d, H8, H12), 6.75 (1H, d, H5), 6.67 (2H, d, H14, H18), 6.59 (2H, d, H15, H17), 6.31 (1H, dd, H6), 5.90 (1H, d, H2), 3.66 (3H, s, OMe); ^{13}C NMR ($CDCl_3$) δ 186.8 (C1), 156.4 (C16), 152.8 (C3), 151.1 (C4), 142.3 (C7), 141.6 (C13), 131.5 (C6), 128.5 (C9, C11), 125.1 (C10), 124.6 (C5), 123.0 (C8, C12), 114.6 (C14, C18), 114.2 (C15, C17), 96.0 (C2), 55.5 (OMe).

6.51 *(E)*-3-((4-Chlorophenyl)amino)-4-(phenylimino)cyclohexa-2,5-dien-1-one, 4.17c (Table 2, Entry 3)

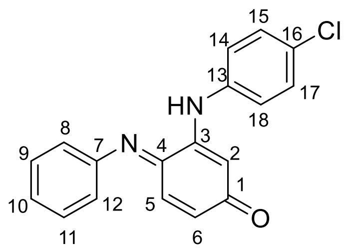

Using 4-chloroaniline (0.153 g, 1.2 mmol) gave the title compound as a red solid (90 mg, 0.29 mmol, 29%); R_f = 0.63 (SiO_2 1:4 ethylacetate-petrol); IR (neat) 3318, 2958, 2889, 1720, 1633, 1440, 1345 cm^{-1}; ^1H NMR 500 MHz ($CDCl_3$) δ 7.93 (1H, s, NH), 7.44 (2H, t, *J* 8.3 Hz, H9, H11), 7.36 (2H, d, *J* 8.7 Hz, H15, H17), 7.27 (1H, t, *J* 8.0 Hz, H10), 7.23 (2H, d, *J* 8.8 Hz, H14, H18), 6.93 (2H, d, *J* 8.2 Hz, H8, H12), 6.88 (1H, d, *J* 10.2 Hz, H5), 6.39 (1H, dd, *J* 10.2, 2.1 Hz, H6), 6.13 (1H, d, *J* 2.1 Hz, H2); ^{13}C NMR ($CDCl_3$) δ 186.7 (C1), 152.8 (C3), 147.7 (C4), 146.5 (C7), 136.8 (C13), 134.6 (C6), 130.2 (C16), 129.6 (C15, C17), 129.2 (C9, C11), 126.2 (C10), 125.1 (C5), 123.9 (C14, C18), 120.6 (C8, C12), 100.9 (C2); *m/z* (ESI+) Found: $M+H^+$ 309.1, $C_{18}H_{14}{}^{35}ClN_2O$ requires 309.2

6.52 *(E)*-4-(Phenylimino)-3-((4-(trifluoromethyl)phenyl)amino)cyclohexa-2,5-dien-1-one, 4.17d (Table 2, Entry 4)

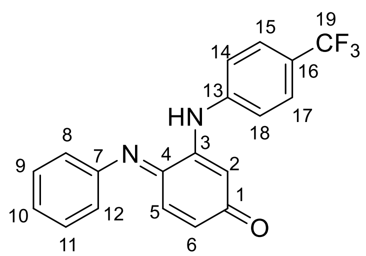

Using 4-trifluoromethylaniline (0.193 g, 1.2 mmol) gave the title compound as a red solid (98 mg, 0.29 mmol, 29%); R_f = 0.63 (SiO_2 1:4 ethylacetate-petrol); ^1H NMR 500 MHz ($CDCl_3$) δ 8.13 (1H, s, NH), 7.64 (2H, d, *J* 8.4 Hz, H15, H17), 7.44 (2H, t, *J* 8.4 Hz, H9, H11), 7.38 (2H, d, *J* 8.4 Hz, H14, H18), 7.27 (1H, t, *J* 8.4 Hz, H10), 6.93 (2H, d, *J* 8.4 Hz, H8, H12), 6.91 (1H, d, *J* 10.2 Hz, H5), 6.40 (1H, dd, *J* 10.2, 2.1 Hz, H6), 6.29 (1H, d, *J* 2.2 Hz, H2); ^{13}C NMR ($CDCl_3$) δ 186.9 (C1), 152.6 (C3), 147.6 (C4), 145.5 (C7), 141.6 (C13), 134.3 (C6), 129.2 (C9, C11), 126.8 (C16), 126.7 (C15, C17), 126.3 (C10), 125.4 (C5), 123.97 (C19), 121.5 (C14, C18), 120.6 (C8, C12), 102.1 (C2).

6.53 *(E)*-4-(Phenylimino)-3-(*o*-tolylamino)cyclohexa-2,5-dien-1-one, 4.17e (Table 2, Entry 5)

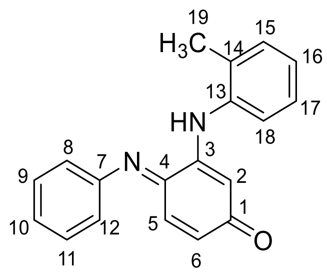

Using 2-methylaniline (0.128 g, 1.2 mmol) gave the title compound as a red solid (207 mg, 0.72 mmol, 72%); R_f = 0.56 RP C18 (9:1 MeCN-H_2O); IR (neat) 3245, 3050, 2922, 1920, 1599 cm^{-1}; ^{1}H NMR 500 MHz ($CDCl_3$) δ 7.79 (1H, d, *J* 8.7 Hz, H15), 7.75 (1H, s, NH), 7.43 (2H, t, *J* 8.5 Hz, H9, H11), 7.33 (1H, m, H17), 7.26 (1H, m, H18), 7.24 (1H, m, H10), 7.15 (1H, t, *J* 7.5 Hz, H16), 6.95 (2H, d, *J* 8.6 Hz, H8, H12), 6.85 (1H, d, *J* 10.3 Hz, H5), 6.35 (1H, dd, *J* 10.2, 2.2 Hz, H6), 5.74 (1H, d, *J* 2.2 Hz, H2), 2.29 (3H, s, CH_3); ^{13}C NMR ($CDCl_3$) δ 186.7 (C1), 153.0 (C3), 148.0 (C4), 147.9 (C7), 136.2 (C13), 134.7 (C6), 133.1 (C14), 131.2 (C18), 129.9 (C17), 129.2 (C9, C11), 127.9 (C15), 126.3 (C10), 126.1 (C16), 124.9 (C5), 120.7 (C8, C12), 100.1 (C2), 17.8 (C19); *m/z* (ESI+) 289 (M+H$^+$, 100%). Crystal structure determined (see appendix).

6.54 *(E)*-3-(Methyl(phenyl)amino)-4-(phenylimino)cyclohexa-2,5-dien-1-one, 4.17f (Table 2, Entry 6)

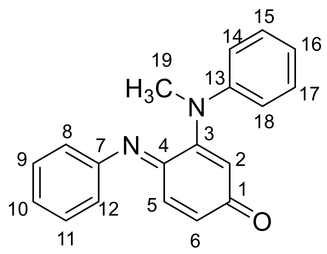

Using *N*-methylaniline (0.128 g, 1.2 mmol) gave the title compound as a red oil (170 mg, 0.59 mmol, 59%); R_f = 0.59 RP C18 (9:1 MeCN-H_2O); IR (neat) 3056, 2953, 1949, 1869, 1728 cm^{-1}; ^{1}H NMR 300 MHz ($CDCl_3$) δ 7.26 (2H, t, *J* 8.1Hz, H15, H17), 7.16 (2H, t, *J* 8.4 Hz, H9, H11), 7.09 (1H, t, *J* 7.6 Hz, H10), 7.04 (2H, d, *J* 8.4 Hz, H14, H18), 7.00 (1H, t, *J* 7.6 Hz, H16), 6.68 (1H, d, *J* 10.2 Hz, H5), 6.30 (2H, d, *J* 8.4 Hz, H8, H12), 6.28 (1H, dd, *J* 10.2, 2.1 Hz, H6), 5.95 (1H, d, *J* 2.1 Hz, H2), 3.32 (3H, s, CH_3); ^{13}C NMR ($CDCl_3$) δ 184.8 (C1), 153.5 (C3), 152.3 (C4), 147.9 (C13), 146.4 (C7), 131.2 (C6), 127.3 (C15, C17), 126.8 (C9, C11), 125.4 (C5), 123.4 (C16), 123.3 (C14, C18), 123.1 (C10), 117.6 (C8, C12), 108.9 (C2), 41.2 (C19). *m/z* (ESI+) 289 (M+H$^+$, 100).

6.55 *(5E,5'E)*-5,5'-(Phenylimino)-4,4'-bis(*o*-tolylamino)-[1,1'-bi(cyclohexane)]-3,3',6,6'-tetraene-2,2'-dione, 4.34e (Table 2, Entry 5)

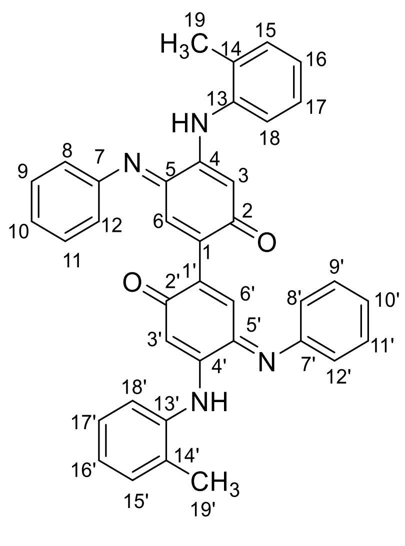

Using 2-methylaniline (0.128 g, 1.2 mmol) gave the title compound as a red oil (15 mg, 0.026 mmol, 5%); R_f = 0.52 RP C18 (9:1 MeCN-H_2O); IR (neat) 3310, 3059, 2960, 2922, 1572 cm^{-1}; ^{1}H NMR 500 MHz ($CDCl_3$) δ 7.76 (2H, s, NH), 7.45 (4H, t, *J* 7.9 Hz, H9, H11, H9', H11'), 7.31 (2H, m, H18, H18'), 7.29 (2H, m, H17, H17'), 7.27 (2H, m, H10, H10'), 7.25 (2H, m, H15, H15'), 7.17 (2H, t, *J* 7.3 Hz, H16, H16'), 7.05 (4H, d, *J* 8.3 Hz, H8, H12, H8', H12'), 7.00 (2H, s, H3, H3'), 5.75 (2H, s, H6, H6'), 2.30 (6H, s, CH_3); ^{13}C NMR ($CDCl_3$) δ 184.1 (C2, C2'), 152.5 (C4, C4'), 147.8 (C5, C5'), 147.7 (C7, C7'), 137.0 (C1, C1'), 136.2 (C13, C13'), 133.3 (C14, C14'), 131.1 (C15, C15'), 129.1 (C9, C11, C9', C11'), 126.9 (C3, C3'), 126.36 (C17, C17'), 126.33 (C10, C10'), 126.0 (C16, C16'), 125.0 (C18, C18'), 121.3 (C8, C12, C8', C12'), 100.3 (C6, C6'), 17.8 (C19, C19').

6.56 *(5E,5'E)*-4,4'-Bis(methyl(phenyl)amino)-5,5'-(phenylimino)-[1,1'-bi(cyclohexane)]-3,3',6,6'-tetraene-2,2'-dione, 4.34f (Table 2, Entry 6)

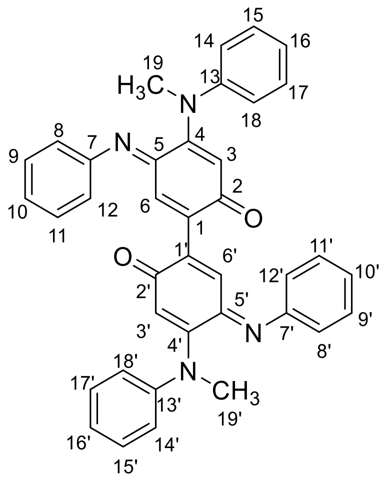

Using *N*-methylaniline (0.128 g, 1.2 mmol) gave the title compound as a red solid (10 mg, 0.017 mmol, 3%); R_f = 0.50 RP C18 (9:1 MeCN-H_2O); ^{1}H NMR 500 MHz ($CDCl_3$) δ 7.24 (4H, t, *J* 8.0 Hz, H15, H17, H15', H17'), 7.16 (4H, t, *J* 8.0 Hz, H9, H11, H9', H11'), 7.08 (2H, t, *J* 8.0 Hz, H16, H16'), 7.05 (4H, d, *J* 8.0 Hz, H14, H18, H14', H18'), 7.01 (2H, t, *J* 8.0 Hz, H10, H10'), 6.82 (2H, s, H6, H6'), 6.38 (4H, d, *J* 8.0 Hz, H8, H12, H8', H12'), 5.91 (2H, s, H3, H3'), 3.30 (6H, s, H19, H19'); ^{13}C NMR ($CDCl_3$) δ 184.2 (C2, C2'), 154.8 (C4, C4'), 153.6 (C5, C5'), 149.6 (C13, C13'), 148.1 (C7, C7'), 135.6 (C1, C1'), 129.1 (C15, C17, C15', C17'), 128.6 (C9, C11, C9', C11'), 128.1 (C6, C6'), 125.6 (C10, C10'), 125.3 (C14, C18, C14', C18'), 125.0 (C16, C16'), 120.2 (C8, C12, C8', C12'), 110.6 (C3, C3'), 43.0 (C19, C19'). Crystal structure determined (see appendix).

Chapter 7. References

1. J. D. Sunderhaus and S. F. Martin, *Chem. Eur. J.*, 2009, **15**, 1300-1308.
2. M. D. Burke and S. L. Schreiber, *Angew. Chem. Int. Ed.*, 2004, **43**, 46-58.
3. D. R. Spring, *Org. Biomol. Chem.*, 2003, **1**, 3867-3870.
4. R. A. Bunce, *Tetrahedron*, 1995, **51**, 13103-13159.
5. E. V. Tsoi, G. B. Afanas'eva and O. N. Chupakhin, *Chem. Heterocycl. Compd.*, 1984, **20**, 263-267.
6. K. S. Cottman, U. S. Patent 4968843A, 1990.
7. S. A. Konovalova, A. P. Avdeenko, A. A. Santalova, V. V. D'Yakonenko, G. V. Palamarchuk and O. V. Shishkin, *Russ. J. Org. Chem.*, 2014, **50**, 1757-1762.
8. K. S. Burmistrov, N. V. Toropin and S. I. Burmistrov, *Zh. Org. Khim.*, 1993, **29**, 1170-1174.
9. K. S. Burmistrov and A. G. Yurchenko, *Zh. Org. Khim.*, 1985, **21**, 575-578.
10. K. C. Nicolaou, *Angew. Chem. Int. Ed.*, 2013, **52**, 131-146.
11. K. C. Nicolaou, *Proc. R. Soc. London Ser. A*, 2014, **470**.
12. C. J. O'connor, L. Laraia and D. R. Spring, *Chem. Soc. Rev.*, 2011, **40**, 4332-4345.
13. E. Lenci, A. Guarna and A. Trabocchi, *Molecules*, 2014, **19**, 16506-16528.
14. D. J. Newman, G. M. Cragg and K. M. Snader, *J. Nat. Prod.*, 2003, **66**, 1022-1037.
15. L. M. Mayr and P. Fuerst, *J. Biomol. Screening*, 2008, **13**, 443-448.
16. P. Ertl, S. Jelfs, J. Muehlbacher, A. Schuffenhauer and P. Selzer, *J. Med. Chem.*, 2006, **49**, 4568-4573.
17. M. Garcia-Castro, S. Zimmermann, M. G. Sankar and K. Kumar, *Angew. Chem. Int. Ed.*, 2016, **55**, 7586-7605.
18. S. L. Schreiber, *Science*, 2000, **287**, 1964-1969.
19. E. J. Corey and X.-M. Cheng, *The Logic of Chemical Synthesis*, Wiley, New York, 1989.
20. L. F. Tietze and U. Beifuss, *Angew. Chem., Int. Ed. Engl.*, 1993, **32**, 131-163.
21. A. Dömling, *Chem. Rev.*, 2006, **106**, 17-89.
22. T. E. Nielsen and S. L. Schreiber, *Angew. Chem. Int. Ed.*, 2008, **47**, 48-56.
23. D. A. Spiegel, F. C. Schroeder, J. R. Duvall and S. L. Schreiber, *J. Am. Chem. Soc.*, 2006, **128**, 14766-14767.
24. E. Comer, E. Rohan, L. Deng and J. A. Porco Jr, *Org. Lett.*, 2007, **9**, 2123-2126.
25. R. J. Spandl, A. Bender and D. R. Spring, *Org. Biomol. Chem.*, 2008, **6**, 1149-1158.
26. A. Dömling and I. Ugi, *Angew. Chem. Int. Ed.*, 2000, **39**, 3168-3210.
27. P. A. Tempest, *Curr. Opin. Drug Discovery Dev.*, 2005, **8**, 776-788.
28. I. Akritopoulou-Zanze and S. W. Djuric, *Heterocycles*, 2007, **73**, 125-147.
29. M. C. Pirrung, *Molecular diversity and combinatorial chemistry : principles and applications*, Oxford : Elsevier, Oxford, 2004.
30. Y. A. Amador-Sánchez, E. Hernández-Vázquez, N. González-Mojica, M. T. Ramírez-Apan and L. D. Miranda, *Tetrahedron*, 2020, **76**.
31. S. M. Yang, C. Y. Wang, C. K. Lin, P. Karanam, G. M. Reddy, Y. L. Tsai and W. Lin, *Angew. Chem. Int. Ed.*, 2018, **57**, 1668-1672.
32. I. A. Khan, M. V. Kulkarni, M. Gopal, M. S. Shahabuddin and C. M. Sun, *Bioorg. Med. Chem. Lett.*, 2005, **15**, 3584-3587.
33. B. M. Chougala, S. L. Shastri, M. Holiyachi, L. A. Shastri, S. S. More and K. V. Ramesh, *Med. Chem. Res.*, 2015, **24**, 4128-4138.

34. J. D. Sunderhaus, C. Dockendorff and S. F. Martin, *Org. Lett.*, 2007, **9**, 4223-4226.
35. A. Shavnya, S. B. Coffey, K. D. Hesp, S. C. Ross and A. S. Tsai, *Org. Lett.*, 2016, **18**, 5848-5851.
36. S. Tai, N. J. Williams and J. D. Carrick, *J. Heterocycl. Chem.*, 2016, **53**, 307-312.
37. N. Hsueh, G. J. Clarkson and M. Shipman, *Org. Lett.*, 2016, **18**, 4908-4911.
38. R. A. Bunce, *Tetrahedron*, 1995, **51**, 13103-13159.
39. R. J. Robinson, *J. Chem. Soc., Perkin Trans. 1*, 1917, **111**, 762.
40. C. Schopf, G. Lehmann and W. Arnold, *Angew. Chem.*, 1937, **50**, 779.
41. L. F. Tietze, *Chem. Rev.*, 1996, **96**, 115-136.
42. A. Padwa and S. K. Bur, *Tetrahedron*, 2007, **63**, 5341-5378.
43. H. Pellissier, *Tetrahedron*, 2006, **62**, 1619-1665.
44. K. C. Nicolaou, D. J. Edmonds and P. G. Bulger, *Angew. Chem. Int. Ed.*, 2006, **45**, 7134-7186.
45. J. C. Wasilke, S. J. Obrey, R. T. Baker and G. C. Bazan, *Chem. Rev.*, 2005, **105**, 1001-1020.
46. C. J. Chapman and C. G. Frost, *Synthesis*, 2007, 1-21.
47. D. Enders, C. Grondal and M. R. M. Hüttl, *Angew. Chem. Int. Ed.*, 2007, **46**, 1570-1581.
48. G. Bhaskar, V. Satish Kumar and B. Venkateswara Rao, *Tetrahedron: Asymmetry*, 2004, **15**, 1279-1283.
49. L. M. Stark, K. Pekari and E. J. Sorensen, *Proc. Natl. Acad. Sci. U.S.A.*, 2004, **101**, 12064-12066.
50. M. S. Lee, G. W. Qin, K. Nakanishi and M. G. Zagorski, *J. Am. Chem. Soc.*, 1989, **111**, 6234-6241.
51. A. V. K. Prasad and Y. Shimizu, *J. Am. Chem. Soc.*, 1989, **111**, 6476-6477.
52. D. E. Cane, W. D. Celmer and J. W. Westley, *J. Am. Chem. Soc.*, 1983, **105**, 3594-3600.
53. A. Zakarian, A. Batch and R. A. Holton, *J. Am. Chem. Soc.*, 2003, **125**, 7822-7824.
54. T. Nakata, *Chem. Rev.*, 2005, **105**, 4314-4347.
55. M. Inoue, *Chem. Rev.*, 2005, **105**, 4379-4405.
56. M. Albert, L. Fensterbank, E. Lacôte and M. Malacria, *Top. Curr. Chem.*, 2006, **264**, 1-62.
57. A. J. McCarroll and J. C. Walton, *J. Chem. Soc., Perkin Trans. 1*, 2001, 3215-3229.
58. D. P. Curran and M. H. Chen, *Tetrahedron Lett.*, 1985, **26**, 4991-4994.
59. K. A. Parker and D. Fokas, *J. Am. Chem. Soc.*, 1992, **114**, 9688-9689.
60. K. A. Parker and D. Fokas, *J. Org. Chem.*, 2006, **71**, 449-455.
61. L. M. Mascavage, M. L. Wilson and D. R. Dalton, *Curr. Org. Synth.*, 2006, **3**, 99-120.
62. J. Zezula and T. Hudlicky, *Synlett*, 2005, 388-405.
63. D. A. Barrera-Adame, J. M. Álvarez-Caballero and E. D. Coy-Barrera, *Rev. Fac. Cienc. Bas.*, 2016, **8**, 292-309.
64. K. C. Nicolaou, N. A. Petasis, R. E. Zipkin and J. Uenishi, *J. Am. Chem. Soc.*, 1982, **104**, 5555-5557.
65. O. Reiser, M. Weber and A. de Meijere, *Angew. Chem. Int. Ed. Engl.*, 1989, **28**, 1037-1038.
66. S. P. Watson, G. R. Knox and N. M. Heron, *Tetrahedron Lett.*, 1994, **35**, 9763-9766.
67. R. Grigg, P. Kennewell, A. Teasdale and V. Sridharan, *Tetrahedron Lett.*, 1993, **34**, 153-156.

68. R. Grigg and V. Sridharan, *Tetrahedron Lett.*, 1992, **33**, 7965-7968.
69. G. D. Harris, R. J. Herr and S. M. Weinreb, *J. Org. Chem.*, 1993, **58**, 5452-5464.
70. L. F. Tietze and J. R. Wunsch, *Angew. Chem. Int. Ed. Engl.*, 1991, **30**, 1697-1699.
71. M. C. Pirrung, W. L. Brown, S. Rege and P. Laughton, *J. Am. Chem. Soc.*, 1991, **113**, 8561-8562.
72. M. C. Pirrung and J. A. Werner, *J. Am. Chem. Soc.*, 1986, **108**, 6060-6062.
73. J. Stephen Clark and P. B. Hodgson, *Tetrahedron Lett.*, 1995, **36**, 2519-2522.
74. T. H. Eberlein, F. G. West and R. W. Tester, *J. Org. Chem.*, 1992, **57**, 3479-3482.
75. F. G. West, K. W. Glaeske and B. N. Naidu, *Synthesis*, 1993, 977-980.
76. F. G. West and B. N. Naidu, *J. Am. Chem. Soc.*, 1993, **115**, 1177-1178.
77. F. G. West and B. N. Naidu, *J. Org. Chem.*, 1994, **59**, 6051-6056.
78. F. G. West and B. N. Naidu, *J. Am. Chem. Soc.*, 1994, **116**, 8420-8421.
79. F. G. West, B. N. Naidu and R. W. Tester, *J. Org. Chem.*, 1994, **59**, 6892-6894.
80. A. Padwa, D. L. Hertzog, W. R. Nadler, M. H. Osterhout and A. T. Price, *J. Org. Chem.*, 1994, **59**, 1418-1427.
81. A. Padwa, S. F. Hornbuckle, G. E. Fryxell and Z. J. Zhang, *J. Org. Chem.*, 1992, **57**, 5747-5757.
82. A. Padwa, J. M. Kassir, M. A. Semones and M. D. Weingarten, *J. Org. Chem.*, 1995, **60**, 53-62.
83. J. P. Marino Jr, M. H. Osterhout, A. T. Price, M. A. Semones and A. Padwa, *J. Org. Chem.*, 1994, **59**, 5518-5520.
84. H. Koyama, R. G. Ball and G. D. Berger, *Tetrahedron Lett.*, 1994, **35**, 9185-9188.
85. D. Fleece, J. P. Gaughan and S. C. Aronoff, *Pediatrics*, 2004, **114**, 1312-1315.
86. M. Matsuoka, in *Infrared Absorbing Dyes*, Springer, 1990, pp. 35-43.
87. A. A. Kutyrev, *Tetrahedron*, 1991, **47**, 8043-8065.
88. M. Adachi, Y. Murata and S. Nakamura, *J. Org. Chem.*, 1993, **58**, 5238-5244.
89. W. Tao and M. Barra, *J. Org. Chem.*, 2001, **66**, 2158-2160.
90. M. Barra, A. Tan and S. Wong, *Dyes Pigm.*, 2004, **61**, 63-67.
91. P. W. Vittum and G. H. Brown, *J. Am. Chem. Soc.*, 1946, **68**, 2235-2239.
92. P. D. Josephy, R. P. Mason and T. Eling, *Carcinogenesis*, 1982, **3**, 1227-1230.
93. S. Imai, T. Noguchi and H. Seto, *J. Antibiot.*, 1993, **46**, 1232-1238.
94. S. Imai, A. Shimazu, K. Furihata, K. Furihata, Y. Hayakawa and H. Seto, *J. Antibiot.*, 1990, **43**, 1606-1607.
95. A. Bolognese, G. Correale, M. Manfra, A. Lavecchia, O. Mazzoni, E. Novellino, V. Barone, A. Pani, E. Tramontano, P. La Colla, C. Murgioni, I. Serra, G. Setzu and R. Loddo, *J. Med. Chem.*, 2002, **45**, 5205-5216.
96. F. Cortés-Salazar, S. Beggah, J. R. van der Meer and H. H. Girault, *Biosens. Bioelectron.*, 2013, **47**, 237-242.
97. S. Bhattacharya, S. R. Boone and C. G. Pierpont, *J. Am. Chem. Soc.*, 1990, **112**, 4561-4562.
98. S. Bhattacharya and C. G. Pierpont, *Inorg. Chem.*, 1992, **31**, 2020-2029.
99. P. Ghosh, G. Han, M. De, C. K. Kim and V. M. Rotello, *Adv. Drug Delivery Rev.*, 2008, **60**, 1307-1315.
100. N. Stephanopoulos, Z. M. Carrico and M. B. Francis, *Angew. Chem. Int. Ed.*, 2009, **48**, 9498-9502.
101. S. Chandrasekar and G. Sekar, *Org. Biomol. Chem.*, 2016, **14**, 3053-3060.
102. D. S. Surry and S. L. Buchwald, *Angew. Chem. Int. Ed.*, 2008, **47**, 6338-6361.

103. J. Clayden, N. Greeves and S. Warren, in *Organic Chemistry*, Oxford University Press Inc., New York, Second edn., 2012, ch. 22, pp. 498-527.
104. A. L. De Sousa and I. S. Resck, *J. Braz. Chem. Soc.*, 2002, **13**, 233-237.
105. C. W. Bird, *J. Chem. Soc.*, 1965, 3016.
106. G. B. Afanaseva, E. V. Tsoi, O. N. Chupakhin, E. O. Sidorov and S. V. Konovalov, *Zh. Org. Khim.*, 1985, **21**, 1926-1932.
107. S. J. Blanksby and G. B. Ellison, *Acc. Chem. Res.*, 2003, **36**, 255-263.
108. P. J. Stang, *J. Org. Chem.*, 2003, **68**, 2997-3008.
109. A. Varvoglis, in *Hypervalent Iodine in Organic Synthesis*, Academic Press, London, 1997, pp. 1-223.
110. T. Wirth, M. Ochiai, A. Varvoglis, V. V. Zhdankin, G. F. Koser, H. Tohma and Y. Kita, in *Topics in Current Chemistry: Hypervalent Iodine Chemistry -/- Modern Developments in Organic Synthesis*, Springer-Verlag, Berlin, 2002, pp. 1-248.
111. P. Stang and V. V. Zhdankin, *Chem. Rev.*, 1996, **96**, 1123-1178.
112. V. V. Zhdankin, *J. Org. Chem.*, 2011, **76**, 1185-1197.
113. A. Duschek and S. F. Kirsch, *Angew. Chem. Int. Ed.*, 2011, **50**, 1524-1552.
114. K. C. Nicolaou, P. S. Baran, Y. L. Zhong and K. Sugita, *J. Am. Chem. Soc.*, 2002, **124**, 2212-2220.
115. K. C. Nicolaou, K. Sugita, P. S. Baran and Y. L. Zhong, *J. Am. Chem. Soc.*, 2002, **124**, 2221-2232.
116. K. C. Nicolaou, P. S. Baran, Y. L. Zhong, S. Barluenga, K. W. Hunt, R. Kranich and J. A. Vega, *J. Am. Chem. Soc.*, 2002, **124**, 2233-2244.
117. E. A. Merritt and B. Olofsson, *Synthesis-Stuttgart*, 2011, 517-538.
118. M. Bielawski, *Diaryliodonium Salts: development of Synthetic methodologies and alpha-Arylation of Enolates,* PhD, Stockholm University, 2011.
119. A. Pacheco-Benichou, T. Besson and C. Fruit, *Catalysts*, 2020, **10**.
120. The Chemistry of Hypervalent Iodine, https://www.princeton.edu/chemistry/macmillan group).
121. C. Hartmann and V. Meyer, *Chem. Ber.*, 1894, **27**, 426-432.
122. J. Malmgren, *Iodonium Salts: Preparation, Chemoselectivity and Metal-Catalysed Applications,* PhD, Stockholm University, 2014.
123. M. Ochiai, *Top. Curr. Chem.*, 2003, **224**, 5-68.
124. K. Aradi, B. L. Tóth, G. L. Tolnai and Z. Novák, *Synlett*, 2016, **27**, A-AD.
125. F. M. Beringer, R. A. Falk, M. Karniol, I. Lillien, G. Masullo, M. Mausner and E. Sommer, *J. Am. Chem. Soc.*, 1959, **81**, 342-351.
126. G. F. Koser, R. H. Wettach and C. S. Smith, *J. Org. Chem.*, 1980, **45**, 1543-1544.
127. C. S. Carman and G. F. Koser, *J. Org. Chem.*, 1983, **48**, 2534-2539.
128. A. J. Margida and G. F. Koser, *J. Org. Chem.*, 1984, **49**, 3643-3646.
129. M. Bielawski, D. Aili and B. Olofsson, *J. Org. Chem.*, 2008, **73**, 4602-4607.
130. E. A. Merritt and B. Olofsson, *Angew. Chem. Int. Ed.*, 2009, **48**, 9052-9070.
131. N. R. Deprez and M. S. Sanford, *Inorg. Chem.*, 2007, **46**, 1924-1935.
132. V. K. Aggarwal and B. Olofsson, *Angew. Chem. Int. Ed.*, 2005, **44**, 5516-5519.
133. J. H. Ryan and P. J. Stang, *Tetrahedron Lett.*, 1997, **38**, 5061-5064.
134. P. Gao and P. S. Portoghese, *J. Org. Chem.*, 1995, **60**, 2276-2278.
135. F. M. Beringer, W. J. Daniel, S. A. Galton and G. Rubin, *J. Org. Chem.*, 1966, **31**, 4315-4318.

136. T. Kitamura, M. Yamane, K. Inoue, M. Todaka, N. Fukatsu, Z. H. Meng and Y. Fujiwara, *J. Am. Chem. Soc.*, 1999, **121**, 11674-11679.
137. M.-R. Zhang, K. Kumata and K. Suzuki, *Tetrahedron Lett.*, 2007, **48**, 8632-8635.
138. E. J. C. Goldstein, D. M. Citron, Y. Warren, C. V. Merriam, K. Tyrrell, H. Fernandez, U. Radhakrishnan, P. J. Stang and G. Conrads, *Antimicrob. Agents Chemother.*, 2004, **48**, 2766-2770.
139. N. R. Deprez, D. Kalyani, A. Krause and M. S. Sanford, *J. Am. Chem. Soc.*, 2006, **128**, 4972-4973.
140. A. M. Wagner and M. S. Sanford, *Org. Lett.*, 2011, **13**, 288-291.
141. A. Ozanne-Beaudenon and S. Quideau, *Angew. Chem. Int. Ed.*, 2005, **44**, 7065-7069.
142. N. Jalalian and B. Olofsson, *Tetrahedron*, 2010, **66**, 5793-5800.
143. M. Ochiai, Y. Kitagawa, N. Takayama, Y. Takaoka and M. Shiro, *J. Am. Chem. Soc.*, 1999, **121**, 9233-9234.
144. J. V. Crivello, *J. Polym. Sci., Part A: Polym. Chem.*, 1999, **37**, 4241-4254.
145. Y. Toba, *J. Photopolym. Sci. Technol.*, 2003, **16**, 115-118.
146. F. M. Beringer, A. Brierley, M. Drexler, E. M. Gindler and C. C. Lumpkin, *J. Am. Chem. Soc.*, 1953, **75**, 2708-2712.
147. J. R. Crowder, E. E. Glover, M. F. Grundon and H. X. Kaempfen, *J. Chem. Soc.*, 1963, 4614-4616.
148. T. B. Petersen, R. Khan and B. Olofsson, *Org. Lett.*, 2011, **13**, 3462-3465.
149. M. A. Carroll and R. A. Wood, *Tetrahedron*, 2007, **63**, 11349-11354.
150. L. Wang and Z. C. Chen, *Synth. Commun.*, 2001, **31**, 1227-1232.
151. S. M. Omar, *N-, O- Arylation using Diaryliodonium Salts in Continuous Flow,* PhD, Newcastle University, 2018.
152. M.-S. Wang, H.-C. Xu, Y. Gong, R.-Y. Qu, L.-S. Zhuo and W. Huang, *ACS Comb. Sci.*, 2020, **22**, 457-467.
153. M. D. Hossain and T. Kitamura, *J. Org. Chem.*, 2005, **70**, 6984-6986.
154. T. L. Ross, J. Ermert, C. Hocke and H. H. Coenen, *J. Am. Chem. Soc.*, 2007, **129**, 8018-8025.
155. M. A. Carroll and S. M. Omar, *Unpublished results*.
156. D. Maiti and S. L. Buchwald, *J. Am. Chem. Soc.*, 2009, **131**, 17423-17429.
157. V. V. Zhdankin and P. J. Stang, *Chem. Rev.*, 2008, **108**, 5299-5358.
158. K. S. Burmistrov and S. I. Burmistrov, *Ukr. Khim. Zh. (Russ. Ed.)*, 1978, **44**, 832-835.
159. F. Baragona, T. Lomberget, C. Duchamp, N. Henriques, E. Lo Piccolo, P. Diana, A. Montalbano and R. Barret, *Tetrahedron*, 2011, **67**, 8731-8739.
160. D. L. Fields Jr. and J. S. Lodaya, WO9952860A1, 1999.
161. D. L. Fields Jr. and R. Lohr, WO9952859A1, 1999.
162. D. L. Fields Jr., M. K. Stern and J. S. Lodaya, WO9936395A2, 1999.
163. V. Balogh, M. Fétizon and M. Golfier, *J. Org. Chem.*, 1971, **36**, 1339-1341.
164. M. K. Abou-Elregal, A. S. A. Youssef, M. M. Hemdan and S. S. Samir, *Synth. Commun.*, 2019, **49**, 2369-2378.
165. K. S. Cottman and J. A. Kuczkowski, EP617004A1, 1994.
166. J. A. Kuczkowski, K. S. Cottman and F. H. Hoppstock, *Polym. Prepr. (Am. Chem. Soc., Div. Polym. Chem.)*, 1993, **34**, 162-163.
167. A. M. Bayoumy, M. Ibrahim and A. Omar, *Opt. Quant. Electron.*, 2020, **52**.

168. S. A. Konovalova, A. P. Avdeenko, A. A. Santalova, V. V. D'Yakonenko, G. V. Palamarchuk and O. V. Shishkin, *Russ. J. Org. Chem.*, 2014, **50**, 1757-1762.
169. I. E. Otuokere, *Acta. Sci. Pharm. Sci.*, 2017, **1**, 18-22.
170. A. S. Christensen, T. Kubař, Q. Cui and M. Elstner, *Chem. Rev.*, 2016, **116**, 5301-5337.
171. P. Geerlings, P. W. Ayers, A. Toro-Labbé, P. K. Chattaraj and F. De Proft, *Acc. Chem. Res.*, 2012, **45**, 683-695.
172. T. C. Allison and Y. J. Tong, *Electrochim. Acta*, 2013, **101**, 334-340.
173. J. K. Fink, *High Performance Polymers*, William Andrew, 2008.
174. V. A. Drill and J. R. DiPalma, *Drill's Pharmacology in Medicine*, McGraw-Hill, New York, 1971.
175. C. L. Deasy, *Chem. Rev.*, 1943, **32**, 173-194.
176. H. D. K. Drew, *J. Chem. Soc.*, 1928, 511-524.
177. F. Mauthner, *Ber. Dtsch. Chem. Ges.*, 1906, **39**, 1340-1347.
178. C. M. Suter and F. O. Green, *J. Am. Chem. Soc.*, 1937, **59**, 2578-2580.
179. M. Ueda, T. Aizawa and Y. Imai, *J. Polym. Sci., Part A: Polym. Chem.*, 1977, **15**, 2739-2747.
180. V. Kuznetsov, S. Gorohovsky, A. Levy, S. Meir, V. Shkoulev, N. Menashe, M. Greenwald, A. Aizikovich, D. Ofer, G. Byk and G. Gellerman, *Molecular Diversity*, 2004, **8**, 437-448.
181. M. Feng, B. Tang, S. H. Liang and X. Jiang, *Curr. Top. Med. Chem.*, 2016, **16**, 1200-1216.
182. H. W. Van Hamersvelt, H. J. Kloke, D. J. De Jong, R. A. P. Koene and F. T. M. Huysmans, *J. Hypertens.*, 1996, **14**, 1041-1045.
183. A. A. Peshkov, V. A. Peshkov, O. P. Pereshivko, K. Van Hecke, R. Kumar and E. V. Van der Eycken, *J. Org. Chem.*, 2015, **80**, 6598-6608.
184. I. Maluenda and O. Navarro, *Molecules*, 2015, **20**, 7528-7557.
185. S. P. H. Mee, V. Lee and J. E. Baldwin, *Angew. Chem. Int. Ed.*, 2004, **43**, 1132-1136.
186. J. F. Hartwig, *Acc. Chem. Res.*, 2008, **41**, 1534-1544.
187. D. Maiti, *Chem. Commun.*, 2011, **47**, 8340-8342.
188. J. Zýka, *Pure Appl. Chem.*, 1966, **13**, 569-581.
189. V. Glezer, B. Turovska, J. Stradins and J. Freimanis, *Electrochim. Acta*, 1990, **35**, 1933-1940.
190. J. Stradins, V. Glezer, B. Turovska, E. Markava and J. Freimanis, *Electrochim. Acta*, 1991, **36**, 1219-1225.
191. N. V. Toropin, K. S. Burmistrov, S. I. Burmistrov and N. L. Zaichenko, *Zh. Org. Khim.*, 1986, **22**, 999-1005.
192. V. Thavasi, L. P. Leong and R. P. A. Bettens, *J. Phys. Chem. A*, 2006, **110**, 4918-4923.
193. N. V. Toropin and K. S. Burmistrov, *Zh. Org. Khim.*, 1983, **19**, 1546-1546.
194. E. A. Titov and A. P. Avdeenko, *Zh. Org. Khim.*, 1972, **8**, 616-620.
195. E. Y. Markava, D. V. Kanepe, E. E. Liepinsh and Y. F. Freimanis, *Zh. Org. Khim.*, 1980, **16**, 2362-2368.
196. C. J. Pedersen, *J. Am. Chem. Soc.*, 1957, **79**, 5014-5019.
197. R. Jana, T. P. Pathak and M. S. Sigman, *Chem. Rev.*, 2011, **111**, 1417-1492.
198. N. Miyaura, T. Yanagi and A. Suzuki, *Synth. Commun.*, 1981, **11**, 513-519.
199. J. K. Stille, *Angew. Chem., Int. Ed. Engl.*, 1986, **25**, 508-524.
200. E. I. Negishi and S. Baba, *J. Chem. Soc. Chem. Comm.*, 1976, 596-597.

201. K. Tamao, K. Sumitani and M. Kumada, *J. Am. Chem. Soc.*, 1972, **94**, 4374-4376.
202. Y. Hatanaka and T. Hiyama, *J. Org. Chem.*, 1988, **53**, 918-920.
203. K. Sonogashira, Y. Tohda and N. Hagihara, *Tetrahedron Lett.*, 1975, **16**, 4467-4470.
204. R. F. Heck and J. P. Nolley, *J. Org. Chem.*, 1972, **37**, 2320-2322.
205. A. S. Guram and S. L. Buchwald, *J. Am. Chem. Soc.*, 1994, **116**, 7901-7902.
206. D. T. Cohen and S. L. Buchwald, *Org. Lett.*, 2015, **17**, 202-205.
207. A. Brennführer, H. Neumann and M. Beller, *Angew. Chem. Int. Ed.*, 2009, **48**, 4114-4133.
208. E. Galardon, S. Ramdeehul, J. M. Brown, A. Cowley, K. K. Hii and A. Jutand, *Angew. Chem. Int. Ed.*, 2002, **41**, 1760-1763.
209. T. Ito, H. Tsuchiya and A. Yamamoto, *Bull. Chem. Soc. Jpn.*, 1977, **50**, 1319-1327.
210. P. Sehnal, R. J. K. Taylor and I. J. S. Fairlamb, *Chem. Rev.*, 2010, **110**, 824-889.
211. A. Krasovskiy, V. Krasovskaya and P. Knochel, *Angew. Chem. Int. Ed.*, 2006, **45**, 2958-2961.
212. A. S. B. Prasad, T. M. Stevenson, J. R. Citineni, V. Nyzam and P. Knochel, *Tetrahedron*, 1997, **53**, 7237-7254.
213. S. Huo, *Org. Lett.*, 2003, **5**, 423-425.
214. J. H. Li, C. L. Deng, W. J. Liu and Y. X. Xie, *Synthesis*, 2005, 3039-3044.
215. C. C. C. Johansson Seechurn, M. O. Kitching, T. J. Colacot and V. Snieckus, *Angew. Chem. Int. Ed.*, 2012, **51**, 5062-5085.
216. S. E. Denmark and C. S. Regens, *Acc. Chem. Res.*, 2008, **41**, 1486-1499.
217. C. F. J. Barnard, *Organometallics*, 2008, **27**, 5402-5422.
218. J. R. Martinelli, D. A. Watson, D. M. M. Freckmann, T. E. Barder and S. L. Buchwald, *J. Org. Chem.*, 2008, **73**, 7102-7107.
219. T. Schareina, A. Zapf and M. Beller, *Chem. Commun.*, 2004, 1388-1389.
220. K. Takagi, T. Okamoto, Y. Sakakibara and S. Oka, *Chem. Lett.*, 1973, 471-474.
221. R. F. Heck, *J. Am. Chem. Soc.*, 1968, **90**, 5518-5526.
222. J. Sherwood, J. H. Clark, I. J. S. Fairlamb and J. M. Slattery, *Green Chem.*, 2019, **21**, 2164-2213.
223. K. Nilsson and A. Hallberg, *J. Org. Chem.*, 1992, **57**, 4015-4017.
224. K. Nilsson and A. Hallberg, *J. Org. Chem.*, 1990, **55**, 2464-2470.
225. T. Jeffery, *Tetrahedron Lett.*, 1993, **34**, 1133-1136.
226. M. M. Abelman, T. Oh and L. E. Overman, *J. Org. Chem.*, 1987, **52**, 4130-4133.
227. C. Carfagna, A. Musco, G. Sallese, R. Santi and T. Fiorani, *J. Org. Chem.*, 1991, **56**, 261-263.
228. N. Shezad, A. A. Clifford and C. M. Rayner, *Tetrahedron Lett.*, 2001, **42**, 323-325.
229. A. Suzuki, *Angew. Chem. Int. Ed.*, 2011, **50**, 6723-6733.
230. S. Gujral, S. Khatri and P. Riyal, *Indo Global J. Pharm. Sci.*, 2012, **2**, 351-367.
231. I. Kondolff, H. Doucet and M. Santelli, *Tetrahedron*, 2004, **60**, 3813-3818.
232. T. Fujihara, S. Yoshida, J. Terao and Y. Tsuji, *Org. Lett.*, 2009, **11**, 2121-2124.
233. L. Ghosez, C. Franc, F. Denonne, C. Cuisinier and R. Touillaux, *Can. J. Chem.*, 2001, **79**, 1827-1839.
234. G. P. McGlacken and I. J. S. Fairlamb, *Eur. J. Org. Chem.*, 2009, 4011-4029.
235. C. Cordovilla, C. Bartolomé, J. M. Martínez-Ilarduya and P. Espinet, *ACS Catal.*, 2015, **5**, 3040-3053.
236. V. Farina, V. Krishnamurthy and W. J. Scott, *The Stille Reaction*, John Wiley & Sons Inc., New York, 1998.

237. T. R. Bailey, *Tetrahedron Lett.*, 1986, **27**, 4407-4410.
238. D. Wang and S. H. Gao, *Org. Chem. Front.*, 2014, **1**, 556-566.
239. A. F. P. Biajoli, C. S. Schwalm, J. Limberger, T. S. Claudino and A. L. Monteiro, *J. Braz. Chem. Soc.*, 2014, **25**, 2186-2214.
240. S. U. Son, Y. Jang, J. Park, H. B. Na, H. M. Park, H. J. Yun, J. Lee and T. Hyeon, *J. Am. Chem. Soc.*, 2004, **126**, 5026-5027.
241. S. Thorand and N. Krause, *J. Org. Chem.*, 1998, **63**, 8551-8553.
242. A. Elangovan, Y. H. Wang and T. I. Ho, *Org. Lett.*, 2003, **5**, 1841-1844.
243. A. Sapegin and M. Krasavin, *J. Org. Chem.*, 2019, **84**, 8788-8795.
244. N. Touj, S. Yasar, N. Ozdemir, N. Hamdi and I. Ozdemir, *J. Organomet. Chem.*, 2018, **860**, 59-71.
245. S. Handa, J. D. Smith, Y. T. Zhang, B. S. Takale, F. Gallou and B. H. Lipshute, *Org. Lett.*, 2018, **20**, 542-545.
246. A. Biffis, P. Centomo, A. Del Zotto and M. Zecca, *Chem. Rev.*, 2018, **118**, 2249-2295.
247. J. F. Hartwig, *Nature*, 2008, **455**, 314-322.
248. P. Ruiz-Castillo and S. L. Buchwald, *Chem. Rev.*, 2016, **116**, 12564-12649.
249. P. Yaseneva, P. Hodgson, J. Zakrzewski, S. Falss, R. E. Meadows and A. A. Lapkin, *React. Chem. Eng.*, 2016, **1**, 229-238.
250. S. Wagaw, R. A. Rennels and S. L. Buchwald, *J. Am. Chem. Soc.*, 1997, **119**, 8451-8458.
251. E. Coj, G. B. Afanas'eva, O. N. Chupakhin and E. O. Sidorov, *Zh. Org. Khim.*, 1989, **25**, 2409-2416.
252. M. C. Carreno and M. Ribagorda, *Sci. Synth.*, 2006, **28**, 629-734.
253. V. Bonnet, F. Mongin, F. Trécourt, G. Quéguiner and P. Knochel, *Tetrahedron*, 2002, **58**, 4429-4438.
254. A. Carpita, R. Rossi and C. A. Veracini, *Tetrahedron*, 1985, **41**, 1919-1929.
255. L. Iffland, A. Petuker, M. van Gastel and U. P. Apfel, *Inorganics*, 2017, **5**.
256. C. H. Yang and J. M. Williams, *Org. Lett.*, 2004, **6**, 2837-2840.
257. M. S. Yusubov, G. A. Zholobova, I. L. Filimonova and K. W. Chi, *Russ. Chem. Bull., Int. Ed.*, 2004, **53**, 1735-1742.
258. P. Kazmierczak and L. Skulski, *Synthesis*, 1995, 1027-1032.
259. S. Schweizer, J. M. Becht and C. Le Drian, *Tetrahedron*, 2010, **66**, 765-772.
260. L. Wang and W. Lu, *Org. Lett.*, 2009, **11**, 1079-1082.
261. R. Bernard, D. Cornu, J. P. Scharff, R. Chiriac, P. Miele, P. L. Baldeck and J. Čáslavský, *Inorg. Chem.*, 2006, **45**, 8743-8748.
262. Y. Yu and B. Yubo, *Appl. Organomet. Chem.*, 2008, **22**, 15-18.
263. F. V. Singh, M. F. Z. J. Amaral and H. A. Stefani, *Tetrahedron Lett.*, 2009, **50**, 2636-2639.

Chapter 8. Appendix

4-(Phenylimino)cyclohexa-2,5-dien-1-one, 2.11

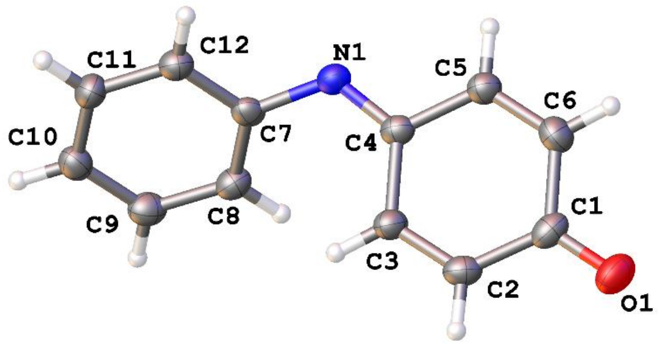

Table 1: Crystal data and structure refinement for mac180045_fa.

Identification code	mac180045_fa
Empirical formula	$C_{12}H_9NO$
Formula weight	183.20
Temperature/K	150.0(2)
Crystal system	orthorhombic
Space group	$Pca2_1$
a/Å	20.3710(9)
b/Å	6.7890(2)
c/Å	13.5265(4)
α/°	90
β/°	90
γ/°	90
Volume/Å^3	1870.70(11)
Z	8
ρ_{calc}g/cm^3	1.301
μ/mm^{-1}	0.668
F(000)	768.0
Crystal size/mm^3	0.27 × 0.1 × 0.04
Radiation	CuKα (λ = 1.54184)
2Θ range for data collection/°	8.682 to 133.542
Index ranges	$-22 \le h \le 24$, $-4 \le k \le 8$, $-16 \le l \le 15$

Reflections collected	7216
Independent reflections	3080 [R_{int} = 0.0374, R_{sigma} = 0.0381]
Data/restraints/parameters	3080/1/253
Goodness-of-fit on F^2	1.044
Final R indexes [I>=2σ (I)]	R_1 = 0.0393, wR_2 = 0.0924
Final R indexes [all data]	R_1 = 0.0513, wR_2 = 0.1014
Largest diff. peak/hole / e $Å^{-3}$	0.14/-0.19
Flack parameter	-0.2(3)

Table 2 Fractional Atomic Coordinates (×10⁴) and Equivalent Isotropic Displacement Parameters (Å²×10³) for mac180045_fa. U_{eq} is defined as 1/3 of of the trace of the orthogonalised U_{IJ} tensor.

Atom	*x*	*y*	*z*	U(eq)
O1	5547.1(13)	6774(3)	3886(2)	43.3(7)
O2	5932.8(12)	12165(3)	6357(3)	45.8(6)
N1	3909.1(13)	553(3)	3855(2)	28.1(6)
N2	4376.6(13)	5769(4)	6304(2)	29.2(6)
C1	5167.4(17)	5373(5)	3853(3)	31.3(8)
C2	4469.4(17)	5643(5)	3653(2)	30.5(7)
C3	4046.1(16)	4127(4)	3639(2)	28.1(7)
C4	4271.8(16)	2117(4)	3831(2)	26.2(7)
C5	4976.5(17)	1828(5)	3975(2)	29.4(7)
C6	5399.1(16)	3344(5)	3999(3)	33.1(8)
C7	3217.2(16)	627(4)	3788(2)	25.8(7)
C8	2833.4(17)	1839(4)	4397(3)	29.7(7)
C9	2154.1(18)	1762(5)	4324(3)	33.5(8)
C10	1851.1(18)	465(4)	3677(3)	32.1(8)
C11	2233.3(17)	-760(5)	3090(3)	32.4(8)
C12	2911.8(17)	-699(5)	3150(3)	29.0(8)
C13	5569.3(17)	10722(5)	6376(3)	31.1(7)
C14	4855.3(17)	10932(5)	6481(3)	32.2(8)
C15	4455.6(17)	9391(5)	6465(3)	30.6(7)
C16	4715.3(16)	7380(4)	6340(3)	26.4(6)
C17	5428.6(16)	7164(4)	6282(3)	29.6(7)
C18	5828.7(16)	8717(5)	6296(3)	31.6(7)
C19	3681.4(15)	5758(4)	6289(3)	26.8(7)
C20	3311.7(16)	6877(4)	5631(3)	29.7(7)
C21	2630.5(17)	6712(5)	5625(3)	33.5(8)
C22	2319.7(16)	5448(4)	6262(3)	33.3(7)
C23	2687.5(18)	4286(5)	6908(3)	32.9(8)
C24	3363.9(17)	4421(5)	6914(3)	30.1(7)

Table 3 Anisotropic Displacement Parameters (Å^2×10^3) for mac180045_fa. The Anisotropic displacement factor exponent takes the form: -2π^2[$h^2a^{*2}U_{11}$+2hka*b*U_{12}+…].

Atom	U_{11}	U_{22}	U_{33}	U_{23}	U_{13}	U_{12}
O1	40.9(15)	33.3(12)	55.6(16)	-5.4(12)	6.6(13)	-10.6(12)
O2	40.7(14)	32.2(11)	64.4(16)	4.1(13)	-9.7(14)	-10.5(11)
N1	30.3(14)	22.7(13)	31.4(15)	0.3(13)	-1.2(12)	-0.5(11)
N2	28.0(13)	25.4(12)	34.2(14)	0.5(13)	-0.2(13)	0.7(11)
C1	36(2)	27.7(17)	29.9(18)	-3.5(16)	4.0(16)	-6.7(15)
C2	34.6(19)	23.9(15)	32.9(18)	0.9(14)	3.9(15)	2.8(14)
C3	28.4(16)	22.8(14)	33.1(18)	-1.4(13)	2.2(14)	0.8(13)
C4	30.8(17)	21.9(14)	26.1(16)	0.5(14)	-0.4(14)	0.2(13)
C5	30.5(17)	24.9(15)	32.8(17)	1.0(14)	0.4(14)	0.9(13)
C6	26.6(17)	35.0(17)	37.8(19)	-0.4(16)	0.3(14)	3.3(14)
C7	26.3(16)	19.2(14)	31.9(18)	5.4(14)	0.6(15)	0.7(12)
C8	33.2(19)	24.3(15)	31.6(17)	-1.7(15)	1.3(14)	-1.9(14)
C9	33.9(19)	28.7(16)	37.9(19)	-0.2(16)	6.3(15)	1.3(14)
C10	27.8(16)	30.2(16)	38(2)	4.4(16)	-1.5(15)	0.2(14)
C11	28.9(18)	28.4(16)	40.0(19)	-3.4(16)	-5.0(15)	-2.7(15)
C12	30.6(19)	23.9(15)	32.6(19)	-0.3(14)	-0.5(14)	0.7(14)
C13	37.1(18)	27.1(15)	29.1(16)	3.0(15)	-6.8(15)	-5.1(14)
C14	36.1(18)	22.5(14)	38(2)	-1.2(14)	-2.9(15)	2.9(13)
C15	30.3(17)	27.4(16)	34.1(19)	-0.8(15)	2.8(14)	4.3(13)
C16	28.6(16)	22.7(14)	27.9(15)	0.8(14)	0.1(15)	1.6(12)
C17	30.9(16)	26.9(15)	30.9(16)	0.4(16)	0.8(15)	4.1(13)
C18	29.1(17)	33.7(15)	31.9(18)	-0.8(17)	1.2(15)	0.2(14)
C19	29.7(16)	19.9(13)	30.8(16)	-2.9(14)	2.6(16)	2.0(13)
C20	35.3(18)	20.5(15)	33.3(17)	1.7(14)	-0.4(15)	0.4(13)
C21	35.2(19)	27.5(16)	37.8(18)	-1.6(16)	-8.6(15)	6.6(15)
C22	30.5(18)	28.7(15)	40.8(19)	-5.1(17)	-0.4(17)	2.1(14)
C23	36(2)	26.5(16)	36.6(18)	0.5(15)	5.0(15)	-2.7(14)
C24	33.3(19)	24.4(15)	32.6(17)	3.7(14)	-2.7(14)	1.6(13)

Table 4 Bond Lengths for mac180045_fa.

Atom	Atom	Length/Å	Atom	Atom	Length/Å
O1	C1	1.227(4)	C9	C10	1.387(5)
O2	C13	1.228(4)	C10	C11	1.388(5)
N1	C4	1.294(4)	C11	C12	1.385(5)
N1	C7	1.413(4)	C13	C14	1.468(5)
N2	C16	1.294(4)	C13	C18	1.464(5)
N2	C19	1.416(4)	C14	C15	1.326(5)
C1	C2	1.459(5)	C15	C16	1.474(4)
C1	C6	1.469(5)	C16	C17	1.463(4)

C2	C3	1.343(5)	C17	C18	1.333(4)
C3	C4	1.463(4)	C19	C20	1.391(5)
C4	C5	1.462(5)	C19	C24	1.399(5)
C5	C6	1.342(5)	C20	C21	1.392(5)
C7	C8	1.402(5)	C21	C22	1.371(5)
C7	C12	1.394(5)	C22	C23	1.395(5)
C8	C9	1.388(5)	C23	C24	1.381(5)

Table 5 Bond Angles for mac180045_fa.

Atom	Atom	Atom	Angle/°	Atom	Atom	Atom	Angle/°
C4	N1	C7	122.6(3)	C11	C12	C7	120.0(3)
C16	N2	C19	122.6(3)	O2	C13	C14	121.4(3)
O1	C1	C2	121.5(3)	O2	C13	C18	121.5(3)
O1	C1	C6	121.3(3)	C18	C13	C14	117.1(3)
C2	C1	C6	117.1(3)	C15	C14	C13	122.0(3)
C3	C2	C1	122.1(3)	C14	C15	C16	120.8(3)
C2	C3	C4	120.7(3)	N2	C16	C15	126.6(3)
N1	C4	C3	126.2(3)	N2	C16	C17	116.3(3)
N1	C4	C5	116.6(3)	C17	C16	C15	117.1(3)
C5	C4	C3	117.2(3)	C18	C17	C16	121.8(3)
C6	C5	C4	122.0(3)	C17	C18	C13	121.1(3)
C5	C6	C1	120.6(3)	C20	C19	N2	123.2(3)
C8	C7	N1	122.6(3)	C20	C19	C24	119.4(3)
C12	C7	N1	117.5(3)	C24	C19	N2	117.2(3)
C12	C7	C8	119.6(3)	C19	C20	C21	120.0(3)
C9	C8	C7	119.5(3)	C22	C21	C20	120.5(3)
C10	C9	C8	120.8(3)	C21	C22	C23	120.0(3)
C9	C10	C11	119.5(3)	C24	C23	C22	120.2(3)
C12	C11	C10	120.6(3)	C23	C24	C19	120.0(3)

Table 6 Hydrogen Atom Coordinates (Å×10^4) and Isotropic Displacement Parameters (Å^2×10^3) for mac180045_fa.

Atom	*x*	*y*	*z*	U(eq)
H2	4309	6934	3527	37
H3	3595	4362	3504	34
H5	5140	527	4054	35
H6	5852	3103	4110	40
H8	3037	2705	4855	36
H9	1894	2609	4723	40
H10	1386	416	3635	39
H11	2028	-1648	2645	39
H12	3169	-1562	2756	35
H14	4674	12211	6563	39

H15	3996	9586	6535	37
H17	5612	5881	6234	35
H18	6290	8520	6253	38
H20	3524	7752	5186	36
H21	2379	7482	5177	40
H22	1854	5363	6263	40
H23	2472	3400	7344	39
H24	3614	3605	7343	36

(*E*)-2,5-Bis((4-chlorophenyl)amino)-4-(phenylimino)cyclohexa-2,5-dien-1-one, 2.59c

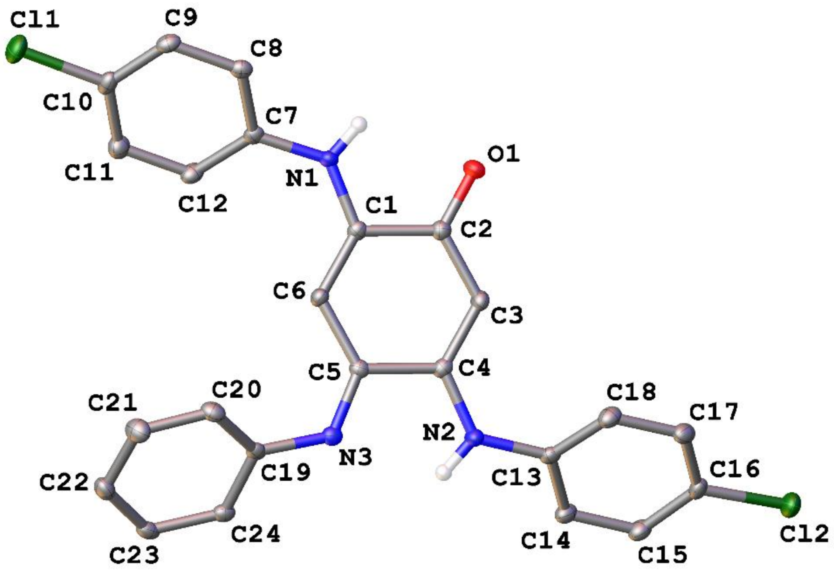

Table 1: Crystal data and structure refinement for mac180020.

Identification code	mac180020
Empirical formula	$C_{24}H_{17}Cl_2N_3O$
Formula weight	434.30
Temperature/K	100.0(2)
Crystal system	monoclinic
Space group	$P2_1/n$
a/Å	9.7627(4)
b/Å	21.0105(9)
c/Å	20.3998(8)
α/°	90
β/°	102.5060(10)
γ/°	90
Volume/Å^3	4085.1(3)
Z	8

ρ_{calc}g/cm^3	1.412
μ/mm^{-1}	0.314
F(000)	1792.0
Crystal size/mm^3	0.3 × 0.02 × 0.017
Radiation	Synchrotron (λ = 0.6889)
2Θ range for data collection/°	2.732 to 53.142
Index ranges	-12 ≤ h ≤ 12, -27 ≤ k ≤ 27, -26 ≤ l ≤ 26
Reflections collected	57280
Independent reflections	9366 [R_{int} = 0.0623, R_{sigma} = 0.0444]
Data/restraints/parameters	9366/0/553
Goodness-of-fit on F^2	1.134
Final R indexes [I>=2σ (I)]	R_1 = 0.0605, wR_2 = 0.1814
Final R indexes [all data]	R_1 = 0.0632, wR_2 = 0.1835
Largest diff. peak/hole / e Å^{-3}	1.16/-0.40

Table 2 Fractional Atomic Coordinates (×10^4) and Equivalent Isotropic Displacement Parameters (Å^2×10^3) for mac180020. U_{eq} is defined as 1/3 of of the trace of the orthogonalised U_{IJ} tensor.

Atom	*x*	*y*	*z*	U(eq)
Cl1	6124.7(7)	7894.7(3)	7319.0(3)	24.36(16)
Cl2	-595.6(7)	1131.6(3)	4589.1(3)	25.69(17)
Cl3	-992.4(8)	2108.1(3)	2632.6(4)	28.34(17)
Cl4	4978.9(7)	8979.8(3)	5203.4(3)	25.20(17)
O1	3901.8(19)	4502.1(9)	5086.6(9)	19.6(4)
O2	988(2)	5523.1(9)	4884.0(9)	20.8(4)
N1	4320(2)	5460.1(9)	5925.8(10)	13.8(4)
N2	1313(2)	3314.5(10)	6385.3(10)	15.0(4)
N3	1765(2)	4191.4(9)	7288.7(10)	13.2(4)
N4	490(2)	4566.4(9)	4032.7(10)	13.7(4)
N5	3898(2)	6593.7(9)	3649.2(10)	14.1(4)
N6	3350(2)	5727.8(9)	2740.2(10)	13.3(4)
C1	3558(2)	4965.5(10)	6096.6(11)	12.5(4)
C2	3393(2)	4437.8(11)	5586.4(11)	13.8(4)
C3	2632(2)	3882.3(11)	5692.9(11)	13.8(4)
C4	2083(2)	3815.0(11)	6250.0(11)	12.6(4)
C5	2289(2)	4328.5(11)	6774.6(11)	12.1(4)
C6	3013(2)	4903.4(11)	6652.4(11)	12.5(4)
C7	4698(2)	6037.6(11)	6260.2(11)	12.7(4)
C8	6015(2)	6296.2(11)	6242.8(11)	13.6(4)
C9	6458(2)	6860.4(11)	6573.7(11)	14.9(4)
C10	5574(3)	7175.8(11)	6917.8(12)	16.5(5)
C11	4265(3)	6937.7(12)	6930.3(12)	18.9(5)
C12	3816(2)	6368.9(11)	6598.7(12)	16.4(5)
C13	917(2)	2770.1(11)	5987.9(11)	13.6(4)
C14	-453(2)	2548.7(11)	5906.1(12)	16.6(5)

C15	-919(3)	2036.2(12)	5488.2(13)	18.4(5)
C16	7(3)	1740.0(11)	5156.4(12)	16.5(5)
C17	1394(3)	1931.5(12)	5259.1(13)	18.0(5)
C18	1854(2)	2443.7(11)	5680.1(12)	17.4(5)
C19	1855(2)	4588.5(11)	7849.8(11)	12.6(4)
C20	3079(2)	4902.2(12)	8179.5(12)	16.6(5)
C21	3052(3)	5291.3(13)	8725.7(12)	20.1(5)
C22	1821(3)	5371.8(12)	8954.9(12)	18.1(5)
C23	620(3)	5039.5(11)	8648.9(12)	16.1(5)
C24	643(2)	4637.0(11)	8110.9(11)	14.3(4)
C25	1325(2)	5038.9(10)	3881.9(11)	12.0(4)
C26	1573(2)	5554.6(11)	4407.0(11)	13.4(4)
C27	2479(2)	6069.6(11)	4328.6(12)	13.8(4)
C28	3071(2)	6112.2(10)	3783.3(11)	11.9(4)
C29	2797(2)	5608.5(10)	3249.2(11)	10.9(4)
C30	1917(2)	5079.4(10)	3337.1(11)	11.8(4)
C31	113(2)	3995.3(11)	3681.0(11)	12.1(4)
C32	58(2)	3439.1(11)	4051.1(12)	15.5(4)
C33	-290(3)	2862.2(11)	3729.7(13)	19.1(5)
C34	-588(3)	2837.8(11)	3033.6(12)	17.1(5)
C35	-602(2)	3387.3(12)	2655.3(12)	15.9(4)
C36	-255(2)	3966.5(11)	2978.5(11)	13.9(4)
C37	4221(2)	7155.2(11)	4024.8(11)	12.8(4)
C38	4099(2)	7738.0(11)	3689.0(11)	13.8(4)
C39	4374(2)	8302.6(11)	4046.1(12)	15.4(4)
C40	4759(2)	8279.3(11)	4743.4(12)	15.7(5)
C41	4931(2)	7704.6(12)	5082.3(12)	16.8(5)
C42	4687(2)	7138.5(11)	4721.7(12)	15.9(5)
C43	3267(2)	5315.5(11)	2190.6(11)	12.2(4)
C44	3515(2)	4659.3(11)	2251.7(12)	15.0(4)
C45	3491(3)	4287.2(12)	1687.8(13)	18.9(5)
C46	3213(3)	4564.5(13)	1051.1(12)	19.0(5)
C47	3002(2)	5216.5(13)	990.6(12)	18.9(5)
C48	3041(2)	5594.7(12)	1551.1(12)	16.6(5)

Table 3 Anisotropic Displacement Parameters (Å^2×10^3) for mac180020. The Anisotropic displacement factor exponent takes the form: -2π^2[h^{2}a*^{2}U$_{11}$+2hka*b*U$_{12}$+…].

Atom	U_{11}	U_{22}	U_{33}	U_{23}	U_{13}	U_{12}
Cl1	28.2(3)	17.2(3)	26.2(3)	-6.3(2)	2.8(3)	-5.6(2)
Cl2	33.8(4)	20.6(3)	24.6(3)	-8.4(2)	10.7(3)	-9.7(2)
Cl3	38.5(4)	15.9(3)	30.4(4)	-8.5(2)	6.8(3)	-8.2(2)
Cl4	31.5(4)	21.3(3)	23.6(3)	-10.6(2)	7.7(3)	-8.4(2)
O1	24.8(9)	20.5(9)	16.4(8)	-2.5(7)	11.0(7)	-6.1(7)

O2	26.9(10)	20.4(9)	19.1(9)	-5.2(7)	13.4(7)	-8.2(7)
N1	16.8(10)	13.5(9)	12.5(9)	0.0(7)	6.3(7)	-2.7(7)
N2	16.7(10)	14.8(10)	14.9(9)	-2.2(7)	6.5(8)	-4.4(7)
N3	12.0(9)	13.5(9)	14.1(9)	1.6(7)	2.8(7)	1.1(7)
N4	15.3(9)	14.4(9)	13.0(9)	-1.8(7)	6.5(7)	-4.5(7)
N5	17.8(10)	14.0(9)	11.0(9)	0.2(7)	4.3(7)	-5.3(7)
N6	12.0(9)	14.3(9)	13.4(9)	1.9(7)	2.2(7)	-0.8(7)
C1	12.5(10)	12.1(10)	11.9(10)	1.5(8)	0.3(8)	0.4(8)
C2	12.9(10)	14.4(10)	13.8(10)	-0.1(8)	2.1(8)	0.1(8)
C3	13.0(10)	13.9(11)	14.1(10)	-2.5(8)	2.4(8)	-1.9(8)
C4	10.5(10)	11.9(10)	14.4(10)	0.9(8)	0.3(8)	-0.1(8)
C5	10.0(10)	14.0(10)	11.9(10)	1.0(8)	1.5(8)	0.6(8)
C6	13.6(10)	11.2(10)	12.5(10)	-0.2(8)	2.1(8)	-1.4(8)
C7	14.0(11)	12.1(10)	11.1(10)	3.2(8)	1.0(8)	0.0(8)
C8	12.2(10)	15.6(11)	12.7(10)	3.6(8)	2.0(8)	0.9(8)
C9	10.4(10)	16.1(11)	17.0(11)	3.8(8)	0.3(8)	-2.2(8)
C10	21.7(12)	12.4(10)	13.5(10)	0.2(8)	-0.3(9)	-1.9(9)
C11	19.0(12)	17.0(11)	21.0(12)	-1.2(9)	4.9(9)	0.7(9)
C12	11.6(10)	15.5(11)	21.7(11)	0.8(9)	3.0(8)	-1.5(8)
C13	14.5(11)	12.4(10)	13.9(10)	2.4(8)	3.2(8)	-1.7(8)
C14	15.1(11)	13.8(11)	22.0(11)	0.3(9)	6.6(9)	-1.0(8)
C15	15.5(11)	16.2(11)	23.8(12)	-0.4(9)	5.0(9)	-3.7(9)
C16	22.7(12)	10.8(10)	16.0(11)	-0.9(8)	4.1(9)	-3.0(9)
C17	17.4(11)	15.3(11)	23.7(12)	0.2(9)	9.6(9)	0.8(9)
C18	12.9(11)	15.6(11)	23.8(12)	0.1(9)	4.2(9)	-1.7(8)
C19	15.2(11)	11.4(10)	11.5(10)	3.7(8)	3.9(8)	1.5(8)
C20	12.3(11)	22.4(12)	15.7(11)	1.8(9)	4.3(8)	0.6(9)
C21	16.1(11)	26.6(13)	16.5(11)	-2.1(9)	1.0(9)	-3.3(9)
C22	22.3(12)	19.1(11)	13.9(10)	-1.0(9)	6.2(9)	1.4(9)
C23	17.2(11)	16.6(11)	16.5(11)	4.3(8)	8.2(9)	2.7(9)
C24	13.4(10)	14.4(10)	15.3(10)	3.9(8)	3.6(8)	0.2(8)
C25	11.5(10)	10.6(10)	13.2(10)	1.1(8)	1.2(8)	-0.6(8)
C26	13.8(10)	12.3(10)	14.3(10)	0.2(8)	3.9(8)	-0.7(8)
C27	14.1(11)	12.6(10)	14.7(10)	-1.5(8)	3.5(8)	-3.5(8)
C28	10.4(10)	10.0(10)	14.9(10)	1.5(8)	1.6(8)	-0.3(8)
C29	8.9(9)	11.6(10)	11.7(10)	1.5(8)	0.9(7)	1.1(7)
C30	12.1(10)	11.0(10)	12.3(10)	-0.4(8)	2.4(8)	-1.9(8)
C31	8.6(10)	13.4(10)	14.5(10)	-0.6(8)	3.0(8)	-2.4(8)
C32	14.0(11)	18.2(11)	13.4(10)	2.3(8)	1.2(8)	-4.2(8)
C33	19.8(12)	13.3(11)	22.5(12)	4.7(9)	0.8(9)	-3.3(9)
C34	18.7(12)	12.0(11)	20.2(11)	-3.6(9)	3.2(9)	-3.1(8)
C35	13.3(11)	19.8(11)	14.1(10)	-2.1(9)	2.2(8)	-1.6(9)
C36	14.1(11)	13.3(10)	14.5(10)	3.0(8)	3.5(8)	-0.6(8)
C37	10.0(10)	13.2(11)	15.2(10)	0.4(8)	2.6(8)	-3.6(8)
C38	11.4(10)	16.1(11)	13.4(10)	2.4(8)	1.7(8)	-2.6(8)

C39	14.8(11)	14.1(11)	17.2(11)	2.3(8)	3.2(8)	-1.9(8)
C40	11.8(10)	17.5(11)	17.7(11)	-5.3(9)	3.1(8)	-4.7(8)
C41	12.3(10)	24.7(12)	12.7(10)	-0.7(9)	1.2(8)	-5.1(9)
C42	13.6(11)	17.6(11)	15.6(11)	3.4(8)	1.2(8)	-4.2(8)
C43	7.5(9)	16.5(11)	12.8(10)	1.5(8)	2.6(8)	-1.2(8)
C44	13.3(10)	16.6(11)	15.4(10)	3.2(8)	3.8(8)	1.1(8)
C45	15.7(11)	18.4(12)	23.6(12)	-1.4(9)	6.3(9)	1.4(9)
C46	15.2(11)	26.5(13)	15.7(11)	-5.5(9)	4.3(9)	-0.5(9)
C47	14.0(11)	29.5(13)	13.1(10)	2.9(9)	2.4(8)	1.6(9)
C48	15.3(11)	18.7(11)	16.7(11)	4.7(9)	5.1(8)	1.8(9)

Table 4 Bond Lengths for mac180020.

Atom	Atom	Length/Å	Atom	Atom	Length/Å
Cl1	C10	1.746(2)	C15	C16	1.389(3)
Cl2	C16	1.739(2)	C16	C17	1.384(3)
Cl3	C34	1.742(2)	C17	C18	1.389(3)
Cl4	C40	1.734(2)	C19	C20	1.402(3)
O1	C2	1.235(3)	C19	C24	1.403(3)
O2	C26	1.232(3)	C20	C21	1.387(3)
N1	C1	1.367(3)	C21	C22	1.390(3)
N1	C7	1.402(3)	C22	C23	1.391(4)
N2	C4	1.355(3)	C23	C24	1.389(3)
N2	C13	1.407(3)	C25	C26	1.506(3)
N3	C5	1.295(3)	C25	C30	1.362(3)
N3	C19	1.404(3)	C26	C27	1.429(3)
N4	C25	1.362(3)	C27	C28	1.363(3)
N4	C31	1.405(3)	C28	C29	1.501(3)
N5	C28	1.359(3)	C29	C30	1.440(3)
N5	C37	1.405(3)	C31	C32	1.399(3)
N6	C29	1.294(3)	C31	C36	1.401(3)
N6	C43	1.405(3)	C32	C33	1.385(3)
C1	C2	1.505(3)	C33	C34	1.387(3)
C1	C6	1.359(3)	C34	C35	1.387(3)
C2	C3	1.425(3)	C35	C36	1.391(3)
C3	C4	1.365(3)	C37	C38	1.396(3)
C4	C5	1.502(3)	C37	C42	1.396(3)
C5	C6	1.448(3)	C38	C39	1.388(3)
C7	C8	1.403(3)	C39	C40	1.391(3)
C7	C12	1.400(3)	C40	C41	1.383(3)
C8	C9	1.386(3)	C41	C42	1.392(3)
C9	C10	1.392(3)	C43	C44	1.401(3)
C10	C11	1.378(4)	C43	C48	1.403(3)
C11	C12	1.396(3)	C44	C45	1.387(3)

C13	C14	1.391(3)	C45	C46	1.396(4)
C13	C18	1.397(3)	C46	C47	1.387(4)
C14	C15	1.388(3)	C47	C48	1.386(3)

Table 5 Bond Angles for mac180020.

Atom	Atom	Atom	Angle/°	Atom	Atom	Atom	Angle/°
C1	N1	C7	129.4(2)	C21	C22	C23	119.6(2)
C4	N2	C13	127.5(2)	C24	C23	C22	120.2(2)
C5	N3	C19	124.2(2)	C23	C24	C19	120.2(2)
C25	N4	C31	127.6(2)	N4	C25	C26	112.07(19)
C28	N5	C37	126.1(2)	N4	C25	C30	127.6(2)
C29	N6	C43	124.0(2)	C30	C25	C26	120.3(2)
N1	C1	C2	111.51(19)	O2	C26	C25	119.5(2)
C6	C1	N1	128.2(2)	O2	C26	C27	122.2(2)
C6	C1	C2	120.2(2)	C27	C26	C25	118.3(2)
O1	C2	C1	119.2(2)	C28	C27	C26	121.6(2)
O1	C2	C3	122.1(2)	N5	C28	C27	126.0(2)
C3	C2	C1	118.6(2)	N5	C28	C29	113.5(2)
C4	C3	C2	121.6(2)	C27	C28	C29	120.4(2)
N2	C4	C3	125.8(2)	N6	C29	C28	114.0(2)
N2	C4	C5	114.0(2)	N6	C29	C30	127.8(2)
C3	C4	C5	120.2(2)	C30	C29	C28	118.10(19)
N3	C5	C4	113.7(2)	C25	C30	C29	121.3(2)
N3	C5	C6	128.2(2)	C32	C31	N4	118.3(2)
C6	C5	C4	118.15(19)	C32	C31	C36	119.0(2)
C1	C6	C5	121.2(2)	C36	C31	N4	122.7(2)
N1	C7	C8	117.9(2)	C33	C32	C31	120.7(2)
C12	C7	N1	123.1(2)	C32	C33	C34	119.5(2)
C12	C7	C8	119.0(2)	C33	C34	Cl3	119.27(19)
C9	C8	C7	120.6(2)	C35	C34	Cl3	119.82(19)
C8	C9	C10	119.4(2)	C35	C34	C33	120.9(2)
C9	C10	Cl1	119.10(19)	C34	C35	C36	119.5(2)
C11	C10	Cl1	119.9(2)	C35	C36	C31	120.3(2)
C11	C10	C9	121.0(2)	C38	C37	N5	118.9(2)
C10	C11	C12	119.8(2)	C38	C37	C42	119.8(2)
C11	C12	C7	120.2(2)	C42	C37	N5	121.3(2)
C14	C13	N2	118.6(2)	C39	C38	C37	120.4(2)
C14	C13	C18	119.2(2)	C38	C39	C40	119.0(2)
C18	C13	N2	122.2(2)	C39	C40	Cl4	119.86(19)
C15	C14	C13	120.8(2)	C41	C40	Cl4	118.88(18)
C14	C15	C16	119.1(2)	C41	C40	C39	121.2(2)
C15	C16	Cl2	119.45(19)	C40	C41	C42	119.6(2)
C17	C16	Cl2	119.55(19)	C41	C42	C37	119.8(2)

C17	C16	C15	121.0(2)	C44	C43	N6	123.8(2)
C16	C17	C18	119.6(2)	C44	C43	C48	118.9(2)
C17	C18	C13	120.2(2)	C48	C43	N6	117.0(2)
C20	C19	N3	124.5(2)	C45	C44	C43	120.6(2)
C20	C19	C24	119.0(2)	C44	C45	C46	120.1(2)
C24	C19	N3	116.3(2)	C47	C46	C45	119.4(2)
C21	C20	C19	120.0(2)	C48	C47	C46	121.1(2)
C20	C21	C22	120.7(2)	C47	C48	C43	119.9(2)

Table 6 Hydrogen Atom Coordinates (Å×10[4]) and Isotropic Displacement Parameters (Å[2]×10[3]) for mac180020.

Atom	*x*	*y*	*z*	U(eq)
H1	4670(30)	5408(15)	5604(16)	17
H2	970(30)	3365(15)	6716(17)	18
H4	270(30)	4603(15)	4403(16)	16
H5	4070(30)	6577(15)	3285(17)	17
H3	2504	3551	5368	17
H6	3108	5243	6966	15
H8	6608	6083	6002	16
H9	7356	7030	6566	18
H11	3670	7160	7164	23
H12	2910	6206	6603	20
H14	-1077	2751	6139	20
H15	-1859	1890	5430	22
H17	2027	1714	5043	22
H18	2808	2572	5759	21
H20	3926	4848	8029	20
H21	3882	5505	8946	24
H22	1801	5652	9318	22
H23	-219	5088	8808	19
H24	-165	4394	7919	17
H27	2674	6390	4665	17
H30	1745	4752	3008	14
H32	260	3457	4528	19
H33	-324	2486	3984	23
H35	-848	3368	2179	19
H36	-268	4345	2722	17
H38	3826	7748	3213	17
H39	4301	8699	3818	18
H41	5214	7696	5558	20
H42	4837	6742	4949	19
H44	3700	4467	2684	18
H45	3664	3843	1735	23

H46	3169	4309	663	23
H47	2828	5407	558	23
H48	2915	6042	1503	20

(*E*)-4-(Phenylimino)-2,5-bis((4-trifluoromethyl)phenyl)amino)cyclohexa-2,5-dien-1-one, 2.59d

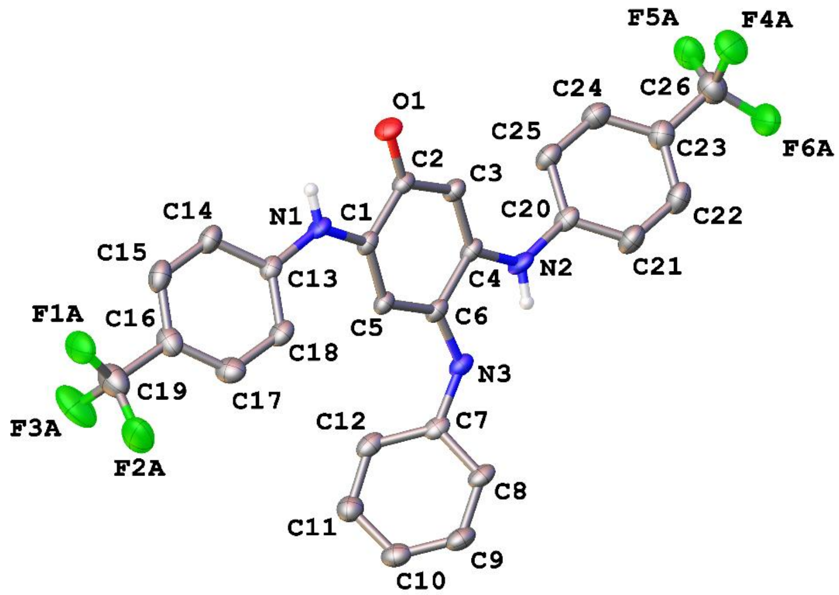

Table 1: Crystal data and structure refinement for mac180028.

Identification code	mac180028
Empirical formula	$C_{27}H_{18}Cl_3F_6N_3O$
Formula weight	620.79
Temperature/K	100.0(2)
Crystal system	triclinic
Space group	P-1
a/Å	9.9547(13)
b/Å	16.415(2)
c/Å	17.900(2)
α/°	65.818(2)
β/°	87.680(2)
γ/°	81.170(3)
Volume/Å^3	2636.0(6)
Z	4
ρ_{calc}g/cm^3	1.564
μ/mm^{-1}	0.403

F(000)	1256.0
Crystal size/mm^3	0.156 × 0.014 × 0.012
Radiation	Synchrotron (λ = 0.6889)
2Θ range for data collection/°	2.418 to 53.322
Index ranges	$-12 \leq h \leq 12$, $-21 \leq k \leq 21$, $-23 \leq l \leq 23$
Reflections collected	33117
Independent reflections	12044 [R_{int} = 0.0747, R_{sigma} = 0.1135]
Data/restraints/parameters	12044/2149/1120
Goodness-of-fit on F^2	1.064
Final R indexes [I>=2σ (I)]	R_1 = 0.0765, wR_2 = 0.2064
Final R indexes [all data]	R_1 = 0.1043, wR_2 = 0.2261
Largest diff. peak/hole / e Å^{-3}	0.67/-0.58

Table 2 Fractional Atomic Coordinates (×10^4) and Equivalent Isotropic Displacement Parameters (Å^2×10^3) for mac180028. U_{eq} is defined as 1/3 of of the trace of the orthogonalised U_{IJ} tensor.

Atom	*x*	*y*	*z*	U(eq)
O1	8778(2)	5582.5(15)	4422.0(13)	30.0(5)
O2	3811(2)	5598.6(15)	4407.3(13)	30.4(5)
N1	9370(2)	3882.2(17)	4679.3(15)	23.1(5)
N2	5361(3)	6204.8(18)	2393.3(15)	26.7(5)
N3	5961(2)	4568.7(17)	2522.0(14)	23.1(5)
N4	4264(2)	3889.3(17)	4699.7(14)	22.6(5)
N5	369(3)	6311.5(18)	2380.0(15)	24.4(5)
N6	910(2)	4654.5(17)	2492.9(14)	23.3(5)
C1	8381(3)	4381(2)	4097.3(16)	20.4(6)
C2	8100(3)	5339(2)	4008.3(17)	21.9(6)
C3	7057(3)	5946(2)	3443.0(17)	23.3(6)
C4	6340(3)	5673(2)	2975.2(17)	22.0(6)
C5	6642(3)	4723(2)	3046.6(17)	21.4(6)
C6	7659(3)	4103(2)	3638.6(16)	20.3(6)
C10	6220(3)	2116.7(18)	2281(2)	31.2(7)
C9B	7408(3)	2405(9)	2394(16)	30(6)
C8B	7342(3)	3208(9)	2491(16)	28(6)
C7	6088(3)	3722.0(17)	2476.3(18)	22.7(6)
C12B	4901(3)	3434(9)	2364(16)	27(6)
C11B	4966(3)	2631(9)	2266(16)	25(6)
C13	9844(3)	2948.3(15)	5005.8(16)	22.0(6)
C18B	8967(7)	2338(2)	5083(12)	26(5)
C17B	9425(7)	1414.8(18)	5453(12)	28(5)
C16	10760(3)	1102.5(15)	5746(2)	33.8(7)
C15B	11637(7)	1713(2)	5670(12)	20(5)
C14B	11179(7)	2635.9(19)	5299(12)	18(4)
C19	11224(4)	106(3)	6164(3)	48.9(9)
C23	4152(3)	8997.9(16)	1496(2)	32.5(7)
C22B	3195(4)	8430(2)	1593(13)	21(6)

C21B	3594(4)	7501(2)	1902(13)	21(6)
C20	4951(3)	7139.0(16)	2113.5(17)	24.8(6)
C25B	5909(4)	7706(2)	2016(13)	25(6)
C24B	5509(5)	8636(2)	1708(13)	30(6)
C26	3774(4)	10003(3)	1171(2)	42.7(8)
C27	3296(3)	4407(2)	4109.8(16)	20.5(6)
C28	3111(3)	5376(2)	3986.6(17)	22.4(6)
C29	2124(3)	6013(2)	3398.4(18)	24.1(6)
C30	1360(3)	5757(2)	2941.3(16)	21.2(6)
C31	1609(3)	4797(2)	3014.9(17)	21.0(6)
C32	2551(3)	4150(2)	3642.0(16)	21.2(6)
C33	1070(3)	3819(2)	2418.2(17)	22.2(6)
C38B	980(30)	3037(8)	3118(6)	23(5)
C37B	1100(40)	2209(4)	3062(17)	24(4)
C36B	1310(50)	2163(12)	2310(20)	25(5)
C35B	1400(40)	2945(18)	1608(16)	26(4)
C34B	1280(30)	3773(13)	1663(6)	23(4)
C45	6289(4)	130(3)	6069(2)	41.9(8)
C46	-7(3)	7256.9(16)	2089.7(16)	24.3(6)
C47B	-260(30)	7740(3)	1253(3)	26(6)
C48B	-670(30)	8670(3)	935(2)	26(6)
C49	-817(3)	9115.6(16)	1453.9(19)	32.1(7)
C50B	-560(30)	8632(3)	2291(3)	37(8)
C51B	-160(30)	7703(3)	2608(2)	31(7)
C52	-1246(4)	10122(3)	1115(2)	44.0(8)
Cl1A	3509.4(13)	5507.5(10)	1070.1(10)	42.8(3)
Cl2A	1388.3(10)	5699.2(8)	-81.5(6)	40.9(3)
Cl3A	1736.6(12)	7207.5(7)	301.8(6)	46.5(3)
Cl4A	6216.2(11)	6467.7(10)	-247.3(8)	56.1(3)
Cl5A	7925.9(14)	7685.4(8)	-141.0(7)	53.6(3)
Cl6A	8282.6(13)	5822.6(9)	1026.8(6)	38.2(3)
F1A	12283(9)	-86(12)	6660(7)	51(2)
F2A	11764(7)	-235(4)	5575(3)	63.6(15)
F3A	10326(6)	-374(4)	6511(5)	69.4(18)
F4A	4858(9)	10402(8)	1108(6)	52.1(16)
F5A	2881(10)	10233(10)	1662(6)	47.6(19)
F6A	3167(11)	10345(8)	423(4)	59(2)
F7A	7551(11)	-89(13)	6352(10)	46(3)
F8A	5551(16)	-311(13)	6749(8)	55(3)
F9A	6120(20)	-294(13)	5597(11)	65(4)
F10A	-302(8)	10579(6)	1174(5)	48(2)
F11A	-1622(12)	10469(7)	316(5)	63(3)
F12A	-2348(8)	10362(8)	1482(7)	60(3)
C8A	6222(3)	3710(2)	1707.2(19)	26.7(7)
C9A	6318(3)	2902(2)	1619(2)	31.2(7)

C11A	6037(3)	2110(2)	3059(2)	31.2(7)
C12A	5978(3)	2906(2)	3161.3(19)	27.0(7)
C14A	10254(3)	2534(2)	5830.9(19)	28.8(7)
C15A	10693(3)	1621(3)	6194(2)	33.5(8)
C17A	10415(3)	1506(2)	4915(2)	34.3(8)
C18A	9970(3)	2430(2)	4544(2)	27.6(7)
C21A	4736(4)	7640(3)	1273(2)	33.1(7)
C22A	4335(4)	8558(3)	968(2)	34.7(8)
C24A	4340(3)	8487(2)	2335(2)	32.8(7)
C25A	4723(3)	7567(2)	2650(2)	28.6(7)
C34A	-122(3)	3541(2)	2278.9(19)	25.8(7)
C35A	-65(3)	2732(2)	2204(2)	31.2(7)
C36A	1167(4)	2206(3)	2224(2)	32.4(8)
C37A	2359(3)	2515(3)	2311(2)	33.2(7)
C38A	2314(3)	3316(2)	2407(2)	29.3(7)
C40A	6066(3)	2657(2)	5298.4(18)	23.2(6)
C41A	6584(3)	1754(2)	5622.5(19)	26.6(7)
C43A	4403(3)	1407(2)	5420(2)	30.2(7)
C44A	3868(3)	2317(2)	5096.5(19)	26.3(7)
C47A	-1355(3)	7633(2)	1861.1(19)	29.8(7)
C48A	-1761(4)	8546(3)	1545(2)	33.5(8)
C50A	538(4)	8764(3)	1664(2)	34.0(8)
C51A	956(3)	7850(2)	1974(2)	29.1(7)
C53A	1854(4)	6029(3)	683(2)	33.3(8)
C54A	7839(4)	6582(3)	-7(2)	35.4(8)
Cl1B	3110(18)	5820(11)	1043(10)	48(4)
Cl2B	1167(12)	6467(7)	-255(7)	48(3)
Cl3B	2846(13)	7679(6)	-145(7)	48(3)
Cl4B	6415(12)	5684(5)	-95(7)	61(3)
Cl5B	6693(14)	7215(5)	288(7)	67(3)
Cl6B	8530(20)	5458(10)	1121(15)	114(8)
F1B	12459(10)	-109(15)	6481(9)	63(4)
F2B	10975(8)	-372(4)	5810(5)	70.0(19)
F3B	10440(7)	-241(5)	6906(4)	64.1(18)
F4B	4686(19)	10428(16)	1338(12)	75(5)
F5B	2652(17)	10303(19)	1465(12)	62(5)
F6B	3600(20)	10417(16)	367(8)	79(5)
F7B	7084(14)	-73(9)	6697(8)	41(3)
F8B	5409(13)	-390(9)	6161(12)	52(3)
F9B	7150(14)	-32(7)	5471(7)	50(3)
F10B	-706(14)	10515(8)	1531(7)	59(3)
F11B	-873(16)	10543(8)	324(6)	65(3)
F12B	-2581(9)	10400(9)	1085(8)	59(3)
C40B	5190(20)	2524(4)	5836(4)	20(6)
C41B	5700(20)	1607(4)	6165(4)	23(6)

C42	5748(3)	1120.8(15)	5683.4(18)	29.3(7)
C43B	5280(20)	1550(4)	4873(5)	37(8)
C44B	4770(20)	2467(4)	4544(4)	38(8)
C39	4723(3)	2953.2(15)	5025.1(16)	22.2(6)
C53B	2800(30)	6570(13)	-4(15)	38(5)
C54B	6920(30)	6030(13)	662(17)	62(7)
F7C	7628(9)	-50(14)	6097(9)	58(4)
F8C	5867(15)	-253(12)	6875(5)	57(3)
F9C	5766(15)	-362(10)	5745(8)	41(2)
F10C	-188(15)	10568(11)	822(11)	59(4)
F11C	-2165(14)	10400(14)	507(9)	52(4)
F12C	-1946(18)	10322(17)	1694(10)	60(5)

Table 3 Anisotropic Displacement Parameters ($Å^2 \times 10^3$) for mac180028. The Anisotropic displacement factor exponent takes the form: -$2\pi^2[h^2a^{*2}U_{11}+2hka^*b^*U_{12}+…]$.

Atom	U_{11}	U_{22}	U_{33}	U_{23}	U_{13}	U_{12}
O1	25.4(11)	37.2(13)	31.2(11)	-17.3(10)	-10.6(9)	-3.7(9)
O2	31.7(12)	33.4(12)	30.6(11)	-16.4(10)	-13.4(9)	-4.6(10)
N1	19.6(12)	31.8(13)	20.3(11)	-12.7(10)	-6.8(9)	-2.9(10)
N2	24.9(13)	35.6(14)	22.7(12)	-16.8(11)	-10.5(10)	3.4(11)
N3	17.0(12)	34.5(14)	20.4(11)	-13.8(11)	-2.2(9)	-3.0(10)
N4	21.0(12)	30.5(13)	19.7(11)	-12.3(10)	-5.3(9)	-5.6(10)
N5	19.4(12)	33.8(14)	23.0(12)	-13.8(11)	-5.4(10)	-4.8(10)
N6	18.0(12)	33.8(14)	19.9(11)	-11.6(10)	-1.4(9)	-6.8(10)
C1	12.6(12)	29.6(15)	17.4(12)	-8.7(11)	-1.3(10)	-0.9(11)
C2	16.4(13)	31.1(15)	19.7(12)	-11.4(12)	-2.2(10)	-4.1(11)
C3	19.8(14)	28.3(15)	21.6(13)	-11.0(12)	-4.1(11)	0.2(11)
C4	15.0(13)	32.5(15)	18.1(12)	-11.0(12)	-3.2(10)	-0.1(11)
C5	14.4(13)	32.9(15)	17.8(12)	-11.5(12)	-0.4(10)	-2.6(11)
C6	15.4(13)	27.9(15)	17.2(12)	-8.8(11)	-1.5(10)	-2.7(11)
C10	23.6(15)	38.6(18)	37.2(16)	-21.3(14)	-6.7(13)	-2.9(13)
C9B	19(7)	40(9)	40(17)	-25(10)	-6(7)	0(5)
C8B	16(6)	40(8)	33(17)	-22(10)	-6(6)	0(5)
C7	10.4(12)	36.3(16)	25.0(13)	-16.1(12)	-3.6(10)	-2.3(11)
C12B	14(7)	38(8)	35(17)	-21(10)	-8(6)	-1(5)
C11B	24(7)	35(8)	22(15)	-16(9)	-7(6)	-3(5)
C13	12.8(13)	30.2(15)	21.2(13)	-8.5(11)	-3.0(10)	-3.1(11)
C18B	16(7)	30(5)	27(11)	-8(5)	-7(7)	-1(4)
C17B	22(6)	30(6)	30(11)	-9(6)	-6(6)	-2(4)
C16	22.2(15)	31.8(16)	40.8(17)	-7.4(14)	-9.7(13)	-3.3(12)
C15B	15(6)	34(5)	14(10)	-12(5)	1(6)	0(4)
C14B	13(5)	34(6)	9(9)	-13(5)	-1(5)	0(4)

C19	41(2)	35.6(19)	61(2)	-9.0(17)	-17.7(17)	-4.0(15)
C23	23.2(16)	37.1(17)	33.2(16)	-11.1(14)	-2.9(13)	-1.2(13)
C22B	20(7)	31(6)	7(13)	-6(6)	-4(7)	3(5)
C21B	17(6)	32(6)	11(13)	-7(6)	-6(6)	2(4)
C20	14.5(13)	35.4(16)	24.2(13)	-13.8(12)	-6.3(11)	3.2(11)
C25B	22(7)	40(6)	19(14)	-18(6)	-6(7)	0(5)
C24B	28(6)	40(7)	26(15)	-19(7)	-5(6)	1(5)
C26	40.2(19)	37.6(19)	45.8(19)	-13.4(16)	-2.4(15)	-2.8(15)
C27	15.7(13)	28.4(15)	16.4(12)	-7.5(11)	-1.3(10)	-5.0(11)
C28	19.3(14)	30.5(15)	19.5(12)	-11.7(12)	-1.0(10)	-5.2(11)
C29	21.5(14)	28.1(15)	24.8(14)	-13.3(12)	-4.0(11)	-1.6(12)
C30	13.9(13)	32.8(15)	18.4(12)	-12.3(12)	-2.3(10)	-1.8(11)
C31	15.7(13)	30.8(15)	18.6(12)	-10.7(11)	-0.8(10)	-7.5(11)
C32	17.9(13)	27.1(15)	17.9(12)	-8.0(11)	-2.6(10)	-4.2(11)
C33	20.9(14)	31.4(15)	17.1(12)	-11.1(11)	-3.2(10)	-7.3(11)
C38B	26(11)	31(5)	19(6)	-14(4)	-4(6)	-10(5)
C37B	25(9)	31(6)	23(6)	-17(5)	-8(6)	-9(6)
C36B	25(9)	35(7)	25(6)	-19(5)	-10(7)	-6(7)
C35B	26(9)	35(6)	25(6)	-19(5)	-5(6)	-3(6)
C34B	20(11)	34(7)	21(5)	-16(5)	-3(6)	-6(7)
C45	38.8(18)	35.0(18)	53(2)	-18.5(16)	-11.7(15)	-2.3(14)
C46	20.2(14)	36.5(16)	17.2(12)	-12.3(12)	-1.5(10)	-2.8(12)
C47B	20(16)	39(6)	17(5)	-10(4)	-2(6)	0(7)
C48B	14(16)	37(7)	24(7)	-10(5)	-6(7)	0(7)
C49	29.0(16)	39.4(17)	25.5(14)	-12.0(13)	-4.7(12)	-0.2(13)
C50B	50(20)	38(7)	26(6)	-14(5)	-6(6)	7(7)
C51B	38(19)	36(7)	18(7)	-14(5)	-10(7)	6(7)
C52	43.4(19)	40.5(19)	43.6(18)	-14.4(16)	-10.0(15)	1.4(15)
Cl1A	23.3(6)	52.8(9)	52.6(7)	-21.6(7)	-7.6(5)	-4.3(6)
Cl2A	36.8(5)	63.2(7)	33.1(5)	-28.6(5)	1.5(4)	-11.8(5)
Cl3A	58.0(7)	45.5(6)	37.5(5)	-21.5(5)	-0.4(5)	1.3(5)
Cl4A	31.5(6)	93.8(10)	57.6(7)	-45.0(7)	-9.3(5)	-7.7(6)
Cl5A	81.3(9)	40.5(6)	37.8(5)	-13.6(5)	-8.8(5)	-10.0(6)
Cl6A	46.5(7)	45.2(8)	23.7(4)	-11.3(5)	-4.3(4)	-15.4(6)
F1A	56(4)	32(4)	54(4)	-8(3)	-27(3)	6(3)
F2A	91(5)	34(3)	58(3)	-16(2)	-1(3)	8(3)
F3A	49(3)	42(3)	108(5)	-16(3)	8(3)	-21(2)
F4A	51(3)	47(3)	58(4)	-17(3)	7(2)	-18(2)
F5A	53(4)	34(3)	49(3)	-15(3)	2(3)	5(3)
F6A	83(5)	38(3)	47(3)	-9(2)	-27(3)	-2(3)
F7A	39(4)	28(5)	54(8)	0(6)	-15(4)	-2(4)
F8A	53(6)	32(4)	70(6)	-7(5)	4(5)	-17(4)
F9A	78(11)	51(7)	77(8)	-42(7)	-18(6)	6(6)
F10A	44(4)	42(3)	58(6)	-17(5)	-8(4)	-9(3)
F11A	83(8)	41(4)	52(3)	-5(3)	-26(4)	0(6)

F12A	47(4)	50(5)	79(7)	-29(6)	-7(4)	12(4)
C8A	18.3(15)	42.4(19)	24.9(14)	-18.1(14)	-3.1(12)	-6.8(13)
C9A	25.3(17)	47(2)	30.0(16)	-23.1(15)	-1.8(13)	-7.5(14)
C11A	25.8(17)	36.4(18)	32.2(16)	-13.4(15)	-3.7(13)	-7.4(14)
C12A	15.7(15)	45.1(19)	24.4(14)	-17.9(14)	-1.1(12)	-5.9(13)
C14A	20.8(16)	40.6(18)	21.9(14)	-10.2(14)	-1.8(12)	-2.9(13)
C15A	23.6(17)	43.6(19)	24.5(15)	-4.5(14)	-3.4(13)	-5.5(14)
C17A	25.3(17)	37.5(18)	42.8(18)	-19.0(16)	-10.4(14)	-1.8(14)
C18A	18.5(15)	39.4(18)	24.8(14)	-12.9(14)	-5.2(12)	-3.2(13)
C21A	28.9(18)	44(2)	25.2(15)	-15.2(15)	-3.5(13)	1.2(15)
C22A	27.7(18)	45(2)	24.9(15)	-10.0(15)	-2.2(14)	0.0(15)
C24A	27.0(17)	42.6(19)	32.5(16)	-20.0(15)	-1.0(14)	-1.6(14)
C25A	21.1(16)	41.7(18)	23.9(15)	-15.6(14)	-2.0(12)	-0.2(13)
C34A	18.0(15)	38.2(18)	22.6(14)	-13.1(13)	-4.2(12)	-5.1(13)
C35A	24.1(16)	41.7(19)	32.0(17)	-16.6(15)	-4.7(13)	-11.4(14)
C36A	32.4(19)	34.6(18)	33.9(18)	-16.2(15)	-6.7(15)	-7.4(14)
C37A	22.6(16)	44(2)	35.8(17)	-19.8(16)	-2.0(14)	-3.7(14)
C38A	19.2(15)	43.2(19)	29.9(16)	-18.1(15)	-1.6(12)	-8.4(13)
C40A	17.9(14)	37.7(17)	18.1(13)	-14.2(13)	0.0(11)	-7.9(12)
C41A	18.0(15)	41.3(18)	24.6(15)	-16.6(14)	-0.4(12)	-7.3(13)
C43A	22.6(16)	37.1(18)	30.8(16)	-11.8(14)	-3.9(13)	-9.0(13)
C44A	15.1(14)	38.7(18)	24.3(15)	-11.1(14)	-1.8(12)	-6.8(13)
C47A	21.0(15)	43.7(19)	23.2(15)	-11.7(14)	-0.8(12)	-6.0(13)
C48A	21.3(16)	47(2)	28.5(16)	-12.4(15)	-2.2(13)	-1.3(14)
C50A	27.9(17)	41.1(19)	34.7(18)	-15.7(15)	-4.4(14)	-8.1(14)
C51A	18.5(15)	41.1(18)	30.0(16)	-16.0(15)	-2.8(13)	-5.5(13)
C53A	28.8(18)	49(2)	25.5(16)	-18.2(16)	-0.8(14)	-7.4(16)
C54A	34(2)	45(2)	25.9(17)	-13.7(16)	-3.9(15)	-2.5(17)
Cl1B	54(10)	42(8)	37(5)	-12(5)	-18(6)	23(6)
Cl2B	55(6)	28(5)	49(6)	-7(5)	-31(5)	17(4)
Cl3B	80(8)	13(4)	42(5)	-6(4)	-27(5)	11(4)
Cl4B	98(8)	16(4)	73(6)	-25(4)	-33(5)	13(4)
Cl5B	113(9)	19(4)	59(6)	-12(4)	-25(6)	10(4)
Cl6B	122(12)	45(9)	160(16)	-26(9)	-78(11)	9(7)
F1B	35(3)	43(5)	86(8)	-1(5)	-22(4)	0(3)
F2B	90(5)	30(3)	80(5)	-11(3)	-34(4)	-4(3)
F3B	60(4)	36(3)	76(4)	3(3)	-8(3)	-18(3)
F4B	70(7)	50(6)	105(12)	-28(8)	-4(6)	-19(5)
F5B	53(6)	42(7)	87(11)	-23(9)	10(6)	-6(5)
F6B	106(13)	51(7)	56(4)	-5(4)	2(4)	6(7)
F7B	45(7)	30(6)	44(5)	-14(5)	-13(5)	8(5)
F8B	46(6)	35(6)	69(9)	-10(6)	-9(6)	-15(5)
F9B	53(6)	33(6)	62(6)	-22(5)	1(5)	8(5)
F10B	77(8)	38(5)	58(6)	-20(5)	-25(5)	5(5)
F11B	90(9)	37(5)	48(4)	0(4)	7(5)	0(6)

F12B	48(4)	54(6)	58(7)	-10(6)	-11(4)	8(3)
C40B	21(14)	24(6)	16(6)	-8(4)	-3(7)	-12(6)
C41B	22(15)	25(6)	21(7)	-5(5)	-1(7)	-12(6)
C42	28.3(16)	32.8(16)	28.0(14)	-12.5(13)	-2.8(12)	-6.9(12)
C43B	54(19)	28(7)	32(6)	-15(5)	-11(8)	0(8)
C44B	70(20)	29(7)	23(7)	-15(6)	-13(9)	2(8)
C39	23.8(14)	29.6(15)	15.3(12)	-10.1(11)	-0.1(10)	-7.2(11)
C53B	54(11)	18(8)	35(9)	-10(7)	-23(8)	16(7)
C54B	105(14)	20(8)	60(11)	-16(7)	-32(10)	2(8)
F7C	36(3)	51(6)	82(9)	-24(7)	-13(3)	4(3)
F8C	94(9)	41(5)	30(3)	-9(3)	-9(3)	-7(5)
F9C	49(6)	34(3)	41(4)	-13(3)	-5(3)	-15(4)
F10C	49(5)	38(6)	80(10)	-14(7)	-7(6)	-7(4)
F11C	42(7)	48(7)	54(6)	-10(6)	-20(5)	6(6)
F12C	72(10)	46(7)	55(6)	-24(6)	-13(6)	22(8)

Table 4 Bond Lengths for mac180028.

Atom	Atom	Length/Å	Atom	Atom	Length/Å
O1	C2	1.237(3)	C33	C34A	1.401(4)
O2	C28	1.239(3)	C33	C38A	1.384(5)
N1	C1	1.365(4)	C38B	C37B	1.3900
N1	C13	1.407(3)	C37B	C36B	1.3900
N2	C4	1.369(4)	C36B	C35B	1.3900
N2	C20	1.401(4)	C35B	C34B	1.3900
N3	C5	1.306(4)	C45	F7A	1.314(10)
N3	C7	1.411(3)	C45	F8A	1.383(10)
N4	C27	1.364(4)	C45	F9A	1.326(10)
N4	C39	1.408(3)	C45	F7B	1.299(10)
N5	C30	1.367(4)	C45	F8B	1.275(10)
N5	C46	1.412(4)	C45	F9B	1.427(10)
N6	C31	1.301(4)	C45	C42	1.501(4)
N6	C33	1.416(4)	C45	F7C	1.319(10)
C1	C2	1.497(4)	C45	F8C	1.394(9)
C1	C6	1.362(4)	C45	F9C	1.341(9)
C2	C3	1.427(4)	C46	C47B	1.3900
C3	C4	1.366(4)	C46	C51B	1.3900
C4	C5	1.495(4)	C46	C47A	1.390(4)
C5	C6	1.439(4)	C46	C51A	1.420(4)
C10	C9B	1.3900	C47B	C48B	1.3900
C10	C11B	1.3900	C48B	C49	1.3900
C10	C9A	1.362(5)	C49	C50B	1.3900
C10	C11A	1.392(5)	C49	C52	1.505(5)
C9B	C8B	1.3900	C49	C48A	1.385(5)

C8B	C7	1.3900
C7	C12B	1.3900
C7	C8A	1.386(4)
C7	C12A	1.414(4)
C12B	C11B	1.3900
C13	C18B	1.3900
C13	C14B	1.3900
C13	C14A	1.397(4)
C13	C18A	1.399(4)
C18B	C17B	1.3900
C17B	C16	1.3900
C16	C15B	1.3900
C16	C19	1.497(5)
C16	C15A	1.381(5)
C16	C17A	1.392(5)
C15B	C14B	1.3900
C19	F1A	1.320(8)
C19	F2A	1.434(6)
C19	F3A	1.256(6)
C19	F1B	1.310(9)
C19	F2B	1.248(7)
C19	F3B	1.460(7)
C23	C22B	1.3900
C23	C24B	1.3900
C23	C26	1.497(4)
C23	C22A	1.398(5)
C23	C24A	1.391(5)
C22B	C21B	1.3900
C21B	C20	1.3900
C20	C25B	1.3900
C20	C21A	1.394(4)
C20	C25A	1.397(4)
C25B	C24B	1.3900
C26	F4A	1.324(7)
C26	F5A	1.345(7)
C26	F6A	1.348(7)
C26	F4B	1.337(12)
C26	F5B	1.328(12)
C26	F6B	1.320(12)
C27	C28	1.496(4)
C27	C32	1.365(4)
C28	C29	1.426(4)
C29	C30	1.362(4)
C30	C31	1.508(4)
C31	C32	1.439(4)
C49	C50A	1.385(5)
C50B	C51B	1.3900
C52	F10A	1.321(7)
C52	F11A	1.349(8)
C52	F12A	1.345(8)
C52	F10B	1.338(9)
C52	F11B	1.362(9)
C52	F12B	1.332(9)
C52	F10C	1.341(11)
C52	F11C	1.333(11)
C52	F12C	1.349(12)
Cl1A	C53A	1.761(4)
Cl2A	C53A	1.766(4)
Cl3A	C53A	1.754(4)
Cl4A	C54A	1.744(4)
Cl5A	C54A	1.743(4)
Cl6A	C54A	1.784(4)
C8A	C9A	1.387(5)
C11A	C12A	1.385(5)
C14A	C15A	1.373(5)
C17A	C18A	1.389(5)
C21A	C22A	1.374(5)
C24A	C25A	1.374(5)
C34A	C35A	1.381(5)
C35A	C36A	1.380(5)
C36A	C37A	1.398(5)
C37A	C38A	1.388(5)
C40A	C41A	1.373(5)
C40A	C39	1.386(4)
C41A	C42	1.397(4)
C43A	C44A	1.387(5)
C43A	C42	1.383(4)
C44A	C39	1.409(4)
C47A	C48A	1.367(5)
C50A	C51A	1.370(5)
Cl1B	C53B	1.779(19)
Cl2B	C53B	1.756(19)
Cl3B	C53B	1.741(18)
Cl4B	C54B	1.786(18)
Cl5B	C54B	1.758(18)
Cl6B	C54B	1.775(19)
C40B	C41B	1.3900
C40B	C39	1.3900
C41B	C42	1.3900
C42	C43B	1.3900

C33	C38B	1.3900		C43B	C44B	1.3900
C33	C34B	1.3900		C44B	C39	1.3900

Table 5 Bond Angles for mac180028.

Atom	Atom	Atom	Angle/°	Atom	Atom	Atom	Angle/°
C1	N1	C13	129.8(2)	C36B	C37B	C38B	120.0
C4	N2	C20	127.8(3)	C37B	C36B	C35B	120.0
C5	N3	C7	123.7(3)	C34B	C35B	C36B	120.0
C27	N4	C39	130.5(2)	C35B	C34B	C33	120.0
C30	N5	C46	129.2(2)	F7A	C45	F8A	103.6(10)
C31	N6	C33	123.3(3)	F7A	C45	F9A	109.5(14)
N1	C1	C2	111.5(2)	F7A	C45	C42	116.3(9)
C6	C1	N1	128.2(3)	F8A	C45	C42	110.7(9)
C6	C1	C2	120.2(3)	F9A	C45	F8A	102.1(10)
O1	C2	C1	119.3(3)	F9A	C45	C42	113.3(10)
O1	C2	C3	122.0(3)	F7B	C45	F9B	105.1(9)
C3	C2	C1	118.7(2)	F7B	C45	C42	111.7(6)
C4	C3	C2	121.3(3)	F8B	C45	F7B	116.3(11)
N2	C4	C5	113.6(2)	F8B	C45	F9B	102.0(10)
C3	C4	N2	126.2(3)	F8B	C45	C42	114.9(7)
C3	C4	C5	120.2(3)	F9B	C45	C42	105.1(5)
N3	C5	C4	114.0(3)	F7C	C45	C42	113.8(10)
N3	C5	C6	127.5(3)	F7C	C45	F8C	106.5(10)
C6	C5	C4	118.5(2)	F7C	C45	F9C	110.0(12)
C1	C6	C5	121.1(3)	F8C	C45	C42	110.3(8)
C9B	C10	C11B	120.0	F9C	C45	C42	114.2(8)
C9A	C10	C11A	120.5(3)	F9C	C45	F8C	101.0(8)
C10	C9B	C8B	120.0	N5	C46	C51A	122.5(3)
C9B	C8B	C7	120.0	C47B	C46	N5	117.5(2)
N3	C7	C12A	123.4(2)	C47B	C46	C51B	120.0
C8B	C7	N3	122.6(2)	C51B	C46	N5	122.5(2)
C8B	C7	C12B	120.0	C47A	C46	N5	119.3(3)
C12B	C7	N3	117.3(2)	C47A	C46	C51A	118.2(3)
C8A	C7	N3	117.6(3)	C48B	C47B	C46	120.0
C8A	C7	C12A	118.8(2)	C47B	C48B	C49	120.0
C11B	C12B	C7	120.0	C48B	C49	C52	120.4(2)
C12B	C11B	C10	120.0	C50B	C49	C48B	120.0
C18B	C13	N1	120.5(2)	C50B	C49	C52	119.6(2)
C18B	C13	C14B	120.0	C48A	C49	C52	120.5(3)
C14B	C13	N1	119.3(2)	C48A	C49	C50A	120.2(3)
C14A	C13	N1	117.3(3)	C50A	C49	C52	119.3(3)
C14A	C13	C18A	119.0(3)	C51B	C50B	C49	120.0
C18A	C13	N1	123.7(3)	C50B	C51B	C46	120.0

C17B	C18B	C13	120.0
C18B	C17B	C16	120.0
C17B	C16	C19	119.2(2)
C15B	C16	C17B	120.0
C15B	C16	C19	120.7(2)
C15A	C16	C19	119.2(3)
C15A	C16	C17A	120.2(3)
C17A	C16	C19	120.6(3)
C16	C15B	C14B	120.0
C15B	C14B	C13	120.0
F1A	C19	C16	111.9(8)
F1A	C19	F2A	102.3(6)
F2A	C19	C16	109.9(4)
F3A	C19	C16	116.4(4)
F3A	C19	F1A	111.1(8)
F3A	C19	F2A	103.9(5)
F1B	C19	C16	113.9(10)
F1B	C19	F3B	100.4(7)
F2B	C19	C16	117.6(4)
F2B	C19	F1B	113.4(9)
F2B	C19	F3B	101.3(5)
F3B	C19	C16	107.5(4)
C22B	C23	C24B	120.0
C22B	C23	C26	122.1(2)
C24B	C23	C26	117.9(2)
C22A	C23	C26	121.0(3)
C24A	C23	C26	120.1(3)
C24A	C23	C22A	118.9(3)
C21B	C22B	C23	120.0
C20	C21B	C22B	120.0
C21B	C20	N2	119.9(2)
C21B	C20	C25B	120.0
C25B	C20	N2	120.1(2)
C21A	C20	N2	117.9(3)
C21A	C20	C25A	120.0(3)
C25A	C20	N2	122.0(3)
C20	C25B	C24B	120.0
C25B	C24B	C23	120.0
F4A	C26	C23	111.3(6)
F4A	C26	F5A	108.9(8)
F4A	C26	F6A	107.7(7)
F5A	C26	C23	110.6(7)
F5A	C26	F6A	106.6(7)
F6A	C26	C23	111.6(6)
F4B	C26	C23	114.6(12)
F10A	C52	C49	114.5(5)
F10A	C52	F11A	106.5(6)
F10A	C52	F12A	106.3(7)
F11A	C52	C49	112.0(6)
F12A	C52	C49	112.6(6)
F12A	C52	F11A	104.2(7)
F10B	C52	C49	113.3(6)
F10B	C52	F11B	105.9(8)
F11B	C52	C49	112.2(6)
F12B	C52	C49	115.7(6)
F12B	C52	F10B	105.3(9)
F12B	C52	F11B	103.4(8)
F10C	C52	C49	111.6(9)
F10C	C52	F12C	115.0(13)
F11C	C52	C49	111.4(10)
F11C	C52	F10C	107.6(11)
F11C	C52	F12C	102.8(11)
F12C	C52	C49	108.2(11)
C7	C8A	C9A	120.4(3)
C10	C9A	C8A	120.5(3)
C12A	C11A	C10	119.7(3)
C11A	C12A	C7	119.9(3)
C15A	C14A	C13	120.3(3)
C14A	C15A	C16	120.6(3)
C18A	C17A	C16	119.5(3)
C17A	C18A	C13	120.4(3)
C22A	C21A	C20	120.2(3)
C21A	C22A	C23	120.3(3)
C25A	C24A	C23	121.5(3)
C24A	C25A	C20	119.1(3)
C35A	C34A	C33	120.4(3)
C36A	C35A	C34A	120.7(3)
C35A	C36A	C37A	118.6(3)
C38A	C37A	C36A	121.1(3)
C33	C38A	C37A	119.6(3)
C41A	C40A	C39	121.0(3)
C40A	C41A	C42	119.7(3)
C42	C43A	C44A	120.8(3)
C43A	C44A	C39	119.1(3)
C48A	C47A	C46	121.6(3)
C47A	C48A	C49	119.7(3)
C51A	C50A	C49	120.5(3)
C50A	C51A	C46	119.9(3)
Cl1A	C53A	Cl2A	110.8(2)
Cl3A	C53A	Cl1A	110.4(2)

F5B	C26	C23	116.0(13)	Cl3A	C53A	Cl2A	110.8(2)
F5B	C26	F4B	101.3(16)	Cl4A	C54A	Cl6A	109.4(2)
F6B	C26	C23	114.9(12)	Cl5A	C54A	Cl4A	111.5(2)
F6B	C26	F4B	103.6(13)	Cl5A	C54A	Cl6A	109.9(2)
F6B	C26	F5B	104.7(15)	C41B	C40B	C39	120.0
N4	C27	C28	111.7(2)	C42	C41B	C40B	120.0
N4	C27	C32	128.6(3)	C41A	C42	C45	120.1(3)
C32	C27	C28	119.7(3)	C43A	C42	C45	120.0(3)
O2	C28	C27	118.8(3)	C43A	C42	C41A	119.8(3)
O2	C28	C29	121.9(3)	C41B	C42	C45	118.1(2)
C29	C28	C27	119.3(2)	C41B	C42	C43B	120.0
C30	C29	C28	121.2(3)	C43B	C42	C45	121.9(2)
N5	C30	C31	114.5(2)	C44B	C43B	C42	120.0
C29	C30	N5	125.4(3)	C39	C44B	C43B	120.0
C29	C30	C31	120.0(3)	N4	C39	C44A	122.7(3)
N6	C31	C30	114.4(3)	C40A	C39	N4	117.8(3)
N6	C31	C32	127.6(3)	C40A	C39	C44A	119.5(2)
C32	C31	C30	118.0(2)	C40B	C39	N4	118.6(2)
C27	C32	C31	121.4(3)	C44B	C39	N4	121.3(2)
C38B	C33	N6	118.6(8)	C44B	C39	C40B	120.0
C38B	C33	C34B	120.0	Cl2B	C53B	Cl1B	106.1(14)
C34B	C33	N6	121.4(8)	Cl3B	C53B	Cl1B	110.8(14)
C34A	C33	N6	116.3(3)	Cl3B	C53B	Cl2B	109.6(13)
C38A	C33	N6	124.2(3)	Cl5B	C54B	Cl4B	110.7(12)
C38A	C33	C34A	119.2(3)	Cl5B	C54B	Cl6B	116.0(15)
C37B	C38B	C33	120.0	Cl6B	C54B	Cl4B	112.8(16)

Table 6 Hydrogen Atom Coordinates (Å×10^4) and Isotropic Displacement Parameters (Å^2×10^3) for mac180028.

Atom	***x***	***y***	***z***	**U(eq)**
H1	9670(30)	4100(20)	4954(19)	28
H2	5100(30)	5940(20)	2140(20)	32
H4	4680(30)	4160(20)	4880(20)	27
H5	-60(30)	6030(20)	2230(20)	29
H3	6857	6552	3391	28
H6	7830	3489	3711	24
H10	6276	1569	2212	37
H10A	6265	1568	2214	37
H9B	8265	2053	2404	36
H8B	8154	3404	2568	33
H12B	4044	3786	2353	32
H11B	4154	2434	2189	30
H18B	8054	2551	4882	31

H17B	8825	998	5505	34
H15B	12550	1500	5870	25
H14B	11779	3053	5247	21
H22B	2267	8678	1449	25
H21B	2940	7113	1968	26
H25B	6836	7459	2161	31
H24B	6163	9024	1642	36
H29	1998	6627	3324	29
H32	2657	3532	3732	25
H38B	842	3068	3634	28
H37B	1046	1674	3540	28
H36B	1396	1597	2269	31
H35B	1541	2913	1091	31
H34B	1337	4308	1185	27
H47B	-158	7436	899	31
H48B	-839	9000	363	32
H50B	-666	8937	2645	45
H51B	15	7372	3180	37
H8A	6248	4258	1238	32
H9A	6454	2897	1092	37
H11A	5954	1562	3517	37
H12A	5864	2904	3692	32
H14A	10228	2886	6142	35
H15A	10952	1343	6758	40
H17A	10485	1153	4603	41
H18A	9749	2711	3975	33
H21A	4868	7345	911	40
H22A	4181	8895	395	42
H24A	4202	8781	2697	39
H25A	4831	7226	3225	34
H34A	-974	3910	2236	31
H35A	-884	2535	2137	37
H36A	1204	1646	2180	39
H37A	3215	2170	2305	40
H38A	3133	3518	2463	35
H40A	6636	3086	5261	28
H41A	7508	1561	5805	32
H43A	3838	974	5461	36
H44A	2939	2508	4925	32
H47A	-2010	7246	1926	36
H48A	-2687	8789	1389	40
H50A	1182	9160	1592	41
H51A	1889	7614	2111	35
H53A	1208	5829	1143	40
H54A	8503	6420	-377	42

H40B	5153	2856	6165	23
H41B	6016	1314	6719	27
H43B	5318	1218	4544	44
H44B	4455	2760	3989	46
H53B	3491	6392	-354	45
H54B	6253	5832	1111	75

Table 7 Atomic Occupancy for mac180028.

Atom	***Occupancy***	**Atom**	***Occupancy***	**Atom**	***Occupancy***
H10	0.9433	H10A	0.0567	C9B	0.0567
H9B	0.0567	C8B	0.0567	H8B	0.0567
C12B	0.0567	H12B	0.0567	C11B	0.0567
H11B	0.0567	C18B	0.0567	H18B	0.0567
C17B	0.0567	H17B	0.0567	C15B	0.0567
H15B	0.0567	C14B	0.0567	H14B	0.0567
C22B	0.0567	H22B	0.0567	C21B	0.0567
H21B	0.0567	C25B	0.0567	H25B	0.0567
C24B	0.0567	H24B	0.0567	C38B	0.0567
H38B	0.0567	C37B	0.0567	H37B	0.0567
C36B	0.0567	H36B	0.0567	C35B	0.0567
H35B	0.0567	C34B	0.0567	H34B	0.0567
C47B	0.0567	H47B	0.0567	C48B	0.0567
H48B	0.0567	C50B	0.0567	H50B	0.0567
C51B	0.0567	H51B	0.0567	Cl1A	0.9145
Cl2A	0.9145	Cl3A	0.9145	Cl4A	0.8882
Cl5A	0.8882	Cl6A	0.8882	F1A	0.5356
F2A	0.5356	F3A	0.5356	F4A	0.6417
F5A	0.6417	F6A	0.6417	F7A	0.3708
F8A	0.3708	F9A	0.3708	F10A	0.4602
F11A	0.4602	F12A	0.4602	C8A	0.9433
H8A	0.9433	C9A	0.9433	H9A	0.9433
C11A	0.9433	H11A	0.9433	C12A	0.9433
H12A	0.9433	C14A	0.9433	H14A	0.9433
C15A	0.9433	H15A	0.9433	C17A	0.9433
H17A	0.9433	C18A	0.9433	H18A	0.9433
C21A	0.9433	H21A	0.9433	C22A	0.9433
H22A	0.9433	C24A	0.9433	H24A	0.9433
C25A	0.9433	H25A	0.9433	C34A	0.9433
H34A	0.9433	C35A	0.9433	H35A	0.9433
C36A	0.9433	H36A	0.9433	C37A	0.9433
H37A	0.9433	C38A	0.9433	H38A	0.9433
C40A	0.9433	H40A	0.9433	C41A	0.9433
H41A	0.9433	C43A	0.9433	H43A	0.9433
C44A	0.9433	H44A	0.9433	C47A	0.9433
H47A	0.9433	C48A	0.9433	H48A	0.9433

C50A	0.9433	H50A	0.9433	C51A	0.9433
H51A	0.9433	C53A	0.9145	H53A	0.9145
C54A	0.8882	H54A	0.8882	Cl1B	0.0855
Cl2B	0.0855	Cl3B	0.0855	Cl4B	0.1118
Cl5B	0.1118	Cl6B	0.1118	F1B	0.4644
F2B	0.4644	F3B	0.4644	F4B	0.3583
F5B	0.3583	F6B	0.3583	F7B	0.2006
F8B	0.2006	F9B	0.2006	F10B	0.297
F11B	0.297	F12B	0.297	C40B	0.0567
H40B	0.0567	C41B	0.0567	H41B	0.0567
C43B	0.0567	H43B	0.0567	C44B	0.0567
H44B	0.0567	C53B	0.0855	H53B	0.0855
C54B	0.1118	H54B	0.1118	F7C	0.4286
F8C	0.4286	F9C	0.4286	F10C	0.2434
F11C	0.2434	F12C	0.2434		

(*E*)-4-(Phenylimino)-2,5-bis(*o*-tolylamino)cyclohexa-2,5-dien-1-one, 2.59e

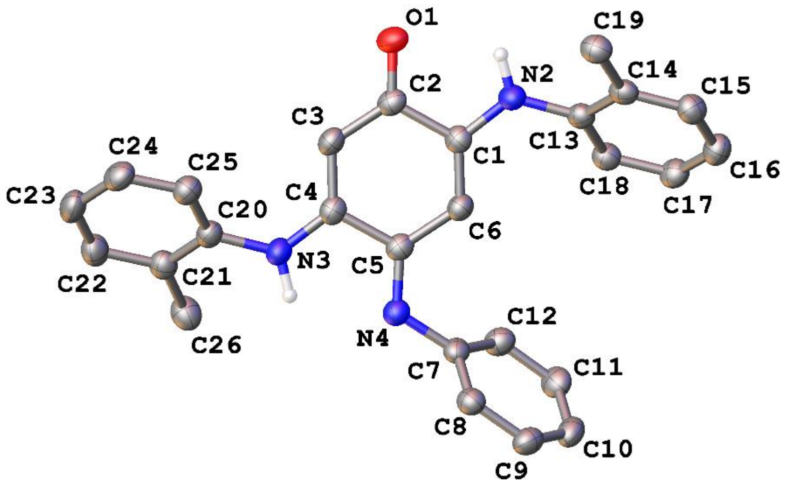

Table 1: Crystal data and structure refinement for mac180021_fa.

Identification code	mac180021_fa
Empirical formula	$C_{26}H_{23}N_3O$
Formula weight	393.47
Temperature/K	150.0(2)
Crystal system	triclinic
Space group	P-1
a/Å	9.5575(3)

b/Å	10.3543(4)
c/Å	11.4804(5)
α/°	64.821(4)
β/°	85.842(3)
γ/°	83.360(3)
Volume/Å^3	1020.92(7)
Z	2
ρ_{calc}g/cm^3	1.280
μ/mm^{-1}	0.622
F(000)	416.0
Crystal size/mm^3	0.33 × 0.05 × 0.04
Radiation	CuKα (λ = 1.54184)
2Θ range for data collection/°	8.514 to 133.68
Index ranges	-10 ≤ h ≤ 11, -12 ≤ k ≤ 12, -13 ≤ l ≤ 13
Reflections collected	14218
Independent reflections	3600 [R_{int} = 0.0452, R_{sigma} = 0.0333]
Data/restraints/parameters	3600/0/279
Goodness-of-fit on F^2	1.039
Final R indexes [I>=2σ (I)]	R_1 = 0.0435, wR_2 = 0.1167
Final R indexes [all data]	R_1 = 0.0551, wR_2 = 0.1266
Largest diff. peak/hole / e Å^{-3}	0.22/-0.21

Table 2 Fractional Atomic Coordinates (×10^4) and Equivalent Isotropic Displacement Parameters (Å^2×10^3) for mac180021_fa. U_{eq} is defined as 1/3 of of the trace of the orthogonalised U_{IJ} tensor.

Atom	*x*	*y*	*z*	U(eq)
O1	7274.4(12)	1718.4(11)	7685.7(10)	40.7(3)
N2	8425.5(13)	2294.0(14)	5391.9(13)	33.0(3)
N3	5338.0(14)	6551.7(14)	6467.5(12)	34.0(3)
N4	6493.0(13)	7219.3(13)	4168.1(11)	31.4(3)
C1	7731.1(14)	3418.4(15)	5569.0(14)	29.3(3)
C2	7084.2(15)	2989.7(16)	6901.9(14)	31.2(3)
C3	6273.5(15)	4072.5(16)	7185.2(14)	32.0(3)
C4	6075.6(15)	5458.4(16)	6285.1(13)	30.2(3)
C5	6748.2(15)	5886.7(15)	4962.7(13)	29.0(3)
C6	7573.8(15)	4797.2(15)	4686.6(13)	29.6(3)
C7	7156.7(15)	7740.3(15)	2934.1(14)	30.2(3)
C8	6327.2(16)	8385.9(15)	1844.4(14)	33.6(3)
C9	6951.8(18)	8951.9(17)	630.1(15)	38.4(4)
C10	8404.2(18)	8908.4(17)	475.4(15)	39.6(4)
C11	9230.9(17)	8284.7(17)	1548.3(16)	40.0(4)
C12	8616.9(16)	7702.8(17)	2771.5(15)	36.9(4)
C13	9174.7(15)	2347.1(15)	4264.3(14)	30.5(3)
C14	8938.5(15)	1357.8(15)	3783.0(14)	31.8(3)

C15	9714.7(17)	1399.4(17)	2697.3(15)	37.1(4)
C16	10683.5(17)	2395.2(18)	2096.8(16)	39.7(4)
C17	10904.4(16)	3370.7(17)	2578.4(15)	36.7(4)
C18	10154.6(16)	3346.7(16)	3662.9(14)	33.3(3)
C19	7873.0(16)	293.3(17)	4419.8(16)	37.5(4)
C20	4494.2(15)	6495.5(16)	7558.2(13)	31.7(3)
C21	4538.3(16)	7585.7(17)	7962.9(15)	34.4(3)
C22	3655.3(18)	7559.4(18)	8992.9(15)	40.6(4)
C23	2763.9(18)	6493.1(19)	9602.6(16)	43.5(4)
C24	2739.4(18)	5419.1(18)	9192.9(15)	41.6(4)
C25	3596.6(17)	5420.9(17)	8170.5(15)	36.5(4)
C26	5488.9(18)	8764.6(18)	7306.4(18)	42.9(4)

Table 3 Anisotropic Displacement Parameters (Å^2×10^3) for mac180021_fa. The Anisotropic displacement factor exponent takes the form: -2π^2[h^{2}a*^{2}U$_{11}$+2hka*b*U$_{12}$+…].

Atom	U_{11}	U_{22}	U_{33}	U_{23}	U_{13}	U_{12}
O1	37.9(6)	34.1(6)	36.8(6)	-3.4(5)	4.0(4)	-2.3(5)
N2	33.8(7)	27.4(6)	32.8(7)	-8.4(5)	4.4(5)	-4.5(5)
N3	38.8(7)	31.2(7)	30.2(6)	-11.7(6)	6.3(5)	-6.2(5)
N4	32.4(7)	29.6(6)	30.9(6)	-11.2(5)	2.6(5)	-6.3(5)
C1	22.7(7)	32.3(7)	33.4(7)	-13.7(6)	0.5(5)	-6.7(6)
C2	25.1(7)	33.5(8)	30.9(7)	-8.5(6)	-0.2(6)	-8.3(6)
C3	31.1(8)	36.6(8)	26.6(7)	-11.1(6)	1.9(6)	-6.8(6)
C4	27.6(7)	35.0(8)	30.2(7)	-14.8(6)	-0.3(6)	-8.0(6)
C5	26.0(7)	31.3(7)	30.2(7)	-11.9(6)	-1.1(5)	-8.7(6)
C6	29.2(7)	31.8(7)	27.7(7)	-11.7(6)	1.7(5)	-7.3(6)
C7	34.2(8)	24.2(7)	32.3(7)	-11.8(6)	3.8(6)	-6.9(6)
C8	31.3(8)	30.5(7)	37.3(8)	-12.4(6)	1.9(6)	-5.6(6)
C9	45.8(9)	34.9(8)	31.6(8)	-10.2(6)	-1.1(6)	-7.5(7)
C10	48.3(10)	35.8(8)	35.0(8)	-14.7(7)	11.9(7)	-13.5(7)
C11	32.9(8)	38.7(8)	45.9(9)	-14.8(7)	9.4(7)	-11.6(6)
C12	33.7(8)	36.2(8)	37.0(8)	-10.6(7)	-0.6(6)	-7.8(6)
C13	25.6(7)	29.7(7)	32.4(7)	-9.7(6)	-1.8(6)	-0.7(6)
C14	25.3(7)	28.9(7)	37.1(8)	-10.1(6)	-3.2(6)	-1.2(6)
C15	36.6(8)	37.0(8)	40.5(8)	-18.7(7)	-1.5(6)	-4.5(6)
C16	36.1(8)	45.0(9)	37.4(8)	-17.1(7)	5.0(6)	-6.4(7)
C17	30.3(8)	37.6(8)	38.6(8)	-11.9(7)	4.6(6)	-8.7(6)
C18	31.4(8)	31.4(7)	37.3(8)	-14.2(6)	-1.7(6)	-4.8(6)
C19	31.3(8)	34.1(8)	45.0(9)	-13.9(7)	-1.0(6)	-6.4(6)
C20	29.8(7)	34.9(8)	28.4(7)	-11.6(6)	-0.4(6)	-2.2(6)
C21	29.5(8)	37.6(8)	35.9(8)	-15.7(6)	-2.0(6)	-1.3(6)
C22	42.6(9)	44.3(9)	39.1(8)	-22.4(7)	0.1(7)	-0.9(7)

C23	41.7(9)	52.5(10)	33.2(8)	-17.0(7)	6.6(7)	-0.9(8)
C24	38.1(9)	42.5(9)	35.8(8)	-8.5(7)	6.2(6)	-8.5(7)
C25	37.2(8)	37.6(8)	34.3(8)	-14.3(6)	0.7(6)	-5.9(6)
C26	37.0(9)	43.4(9)	54.8(10)	-26.5(8)	3.0(7)	-7.8(7)

Table 4 Bond Lengths for mac180021_fa.

Atom	Atom	Length/Å	Atom	Atom	Length/Å
O1	C2	1.2394(18)	C10	C11	1.380(3)
N2	C1	1.357(2)	C11	C12	1.386(2)
N2	C13	1.416(2)	C13	C14	1.400(2)
N3	C4	1.348(2)	C13	C18	1.396(2)
N3	C20	1.4227(19)	C14	C15	1.391(2)
N4	C5	1.2958(19)	C14	C19	1.501(2)
N4	C7	1.4138(19)	C15	C16	1.385(2)
C1	C2	1.506(2)	C16	C17	1.383(2)
C1	C6	1.352(2)	C17	C18	1.383(2)
C2	C3	1.427(2)	C20	C21	1.397(2)
C3	C4	1.366(2)	C20	C25	1.391(2)
C4	C5	1.505(2)	C21	C22	1.394(2)
C5	C6	1.434(2)	C21	C26	1.503(2)
C7	C8	1.397(2)	C22	C23	1.381(3)
C7	C12	1.393(2)	C23	C24	1.382(3)
C8	C9	1.381(2)	C24	C25	1.381(2)
C9	C10	1.385(2)			

Table 5 Bond Angles for mac180021_fa.

Atom	Atom	Atom	Angle/°	Atom	Atom	Atom	Angle/°
C1	N2	C13	126.62(13)	C10	C11	C12	120.48(15)
C4	N3	C20	128.17(13)	C11	C12	C7	120.42(15)
C5	N4	C7	119.78(12)	C14	C13	N2	118.80(13)
N2	C1	C2	112.81(12)	C18	C13	N2	120.50(13)
C6	C1	N2	126.62(13)	C18	C13	C14	120.69(14)
C6	C1	C2	120.56(13)	C13	C14	C19	120.74(14)
O1	C2	C1	118.35(13)	C15	C14	C13	117.95(14)
O1	C2	C3	123.72(13)	C15	C14	C19	121.31(14)
C3	C2	C1	117.93(12)	C16	C15	C14	121.39(15)
C4	C3	C2	121.74(13)	C17	C16	C15	120.14(15)
N3	C4	C3	125.88(13)	C16	C17	C18	119.69(14)
N3	C4	C5	113.99(12)	C17	C18	C13	120.13(14)
C3	C4	C5	120.10(13)	C21	C20	N3	118.32(13)
N4	C5	C4	115.87(13)	C25	C20	N3	120.92(14)
N4	C5	C6	126.17(13)	C25	C20	C21	120.69(13)
C6	C5	C4	117.95(12)	C20	C21	C26	121.54(14)

C1	C6	C5	121.69(13)	C22	C21	C20	117.86(14)
C8	C7	N4	119.20(13)	C22	C21	C26	120.59(14)
C12	C7	N4	121.94(13)	C23	C22	C21	121.54(15)
C12	C7	C8	118.76(14)	C22	C23	C24	119.79(15)
C9	C8	C7	120.27(14)	C25	C24	C23	119.99(16)
C8	C9	C10	120.66(15)	C24	C25	C20	120.13(15)
C11	C10	C9	119.41(14)				

Table 6 Hydrogen Bonds for mac180021_fa.

D	H	A	d(D-H)/Å	d(H-A)/Å	d(D-A)/Å	D-H-A/°
N2	H2	O1	0.88(2)	2.170(18)	2.6261(16)	111.4(15)
N3	H3	N4	0.90(2)	2.143(19)	2.6203(17)	112.2(15)

Table 7 Hydrogen Atom Coordinates (Å×10^4) and Isotropic Displacement Parameters (Å^2×10^3) for mac180021_fa.

Atom	*x*	*y*	*z*	U(eq)
H2	8343(19)	1460(20)	6055(19)	40
H3	5380(20)	7410(20)	5786(19)	41
H3A	5869	3828	8004	38
H6	8012	5045	3880	35
H8	5350	8435	1937	40
H9	6391	9366	-91	46
H10	8819	9296	-344	48
H11	10207	8255	1450	48
H12	9184	7285	3488	44
H15	9581	745	2367	44
H16	11186	2408	1368	48
H17	11554	4040	2175	44
H18	10304	3998	3992	40
H19A	8227	-425	5223	56
H19B	7701	-153	3869	56
H19C	7010	776	4575	56
H22	3667	8277	9276	49
H23	2182	6498	10287	52
H24	2146	4696	9606	50
H25	3574	4702	7891	44
H26A	6412	8360	7181	64
H26B	5548	9270	7832	64
H26C	5114	9417	6487	64

(*E*)-2,5-Bis(methyl(phenyl)amino)-4-(phenylimino)cyclohexa-2,5-dien-1-one, 2.59f

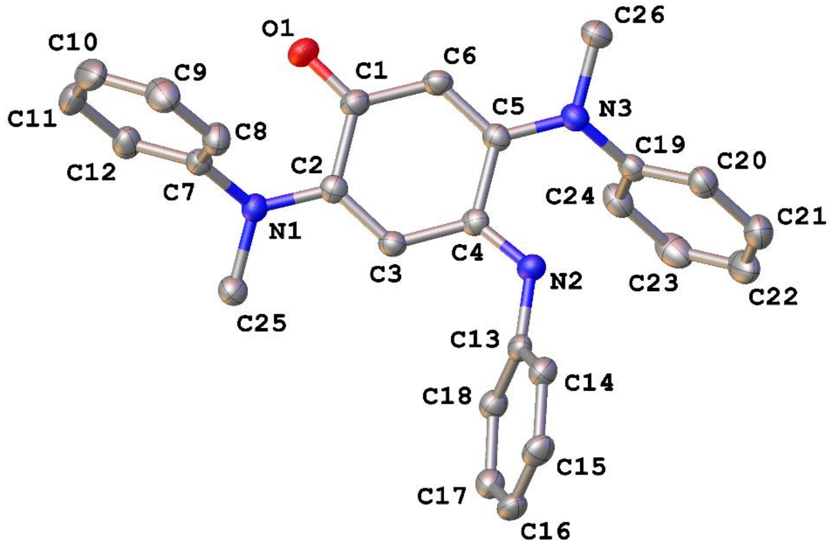

Table 1: Crystal data and structure refinement for mac190042_fa.

Identification code	mac190042_fa
Empirical formula	$C_{26}H_{23}N_3O$
Formula weight	393.47
Temperature/K	150.0(2)
Crystal system	monoclinic
Space group	Ia
a/Å	21.0681(3)
b/Å	5.96210(10)
c/Å	16.7646(3)
α/°	90
β/°	101.259(2)
γ/°	90
Volume/Å^3	2065.28(6)
Z	4
ρ_{calc}g/cm^3	1.265
μ/mm^{-1}	0.615
F(000)	832.0
Crystal size/mm^3	0.19 × 0.11 × 0.02
Radiation	CuKα (λ = 1.54184)
2Θ range for data collection/°	8.558 to 133.58
Index ranges	$-25 \leq h \leq 24$, $-6 \leq k \leq 7$, $-19 \leq l \leq 19$
Reflections collected	13687
Independent reflections	3441 [R_{int} = 0.0231, R_{sigma} = 0.0182]
Data/restraints/parameters	3441/2/274

Goodness-of-fit on F^2	1.078
Final R indexes [I>=2σ (I)]	$R_1 = 0.0269$, $wR_2 = 0.0693$
Final R indexes [all data]	$R_1 = 0.0276$, $wR_2 = 0.0703$
Largest diff. peak/hole / e Å^{-3}	0.14/-0.13
Flack parameter	0.48(10)

Table 2 Fractional Atomic Coordinates (×10^4) and Equivalent Isotropic Displacement Parameters (Å^2×10^3) for mac190042_fa. U_{eq} is defined as 1/3 of of the trace of the orthogonalised U_{IJ} tensor.

Atom	*x*	*y*	*z*	U(eq)
O1	3203.6(7)	8242(3)	4462.5(10)	39.0(4)
N1	4148.7(7)	10786(3)	3960.6(10)	25.3(4)
N2	5652.6(8)	5615(3)	5542.8(10)	26.6(4)
N3	4705.1(8)	3714(3)	6222.0(10)	26.5(4)
C1	3769.7(9)	7707(3)	4727.1(12)	26.5(4)
C2	4315.0(9)	8987(3)	4477.4(11)	23.8(4)
C3	4934.8(9)	8447(3)	4819.9(11)	23.7(4)
C4	5093.6(9)	6568(3)	5369.2(11)	22.8(4)
C5	4553.9(9)	5415(3)	5668.4(11)	23.7(4)
C6	3934.2(9)	5937(3)	5314.0(12)	26.1(4)
C7	3635.8(9)	10542(4)	3262.5(12)	26.2(4)
C8	3585.9(10)	8615(4)	2792.7(13)	32.4(5)
C9	3092.5(12)	8386(4)	2119.7(15)	40.6(5)
C10	2650.2(11)	10105(5)	1906.6(14)	43.6(6)
C11	2707.6(10)	12042(4)	2363.7(15)	40.3(6)
C12	3198.9(10)	12288(4)	3046.5(13)	32.7(5)
C13	6199.9(9)	6432(3)	5268.6(11)	24.8(4)
C14	6509.0(9)	4954(4)	4823.4(12)	28.3(4)
C15	7076.2(10)	5586(4)	4580.5(13)	31.8(5)
C16	7347.4(10)	7664(4)	4789.6(13)	31.6(5)
C17	7046.7(10)	9129(4)	5242.7(13)	30.5(4)
C18	6474.8(10)	8525(3)	5480.2(12)	27.6(4)
C19	5261.3(9)	3832(3)	6863.6(12)	25.2(4)
C20	5662.7(10)	1972(4)	7038.8(13)	30.6(4)
C21	6208.4(11)	2083(4)	7649.2(14)	39.4(5)
C22	6357.9(12)	4024(4)	8092.7(14)	42.8(6)
C23	5949.5(12)	5848(4)	7935.5(14)	41.1(6)
C24	5397.4(11)	5762(4)	7325.9(13)	32.5(5)
C25	4656.1(10)	12380(3)	3865.8(13)	28.5(4)
C26	4192.3(10)	2179(4)	6347.0(13)	30.9(5)

Table 3 Anisotropic Displacement Parameters ($Å^2 \times 10^3$) for mac190042_fa. The Anisotropic displacement factor exponent takes the form: -$2\pi^2[h^2a^{*2}U_{11}+2hka^*b^*U_{12}+\ldots]$.

Atom	U_{11}	U_{22}	U_{33}	U_{23}	U_{13}	U_{12}
O1	21.6(7)	44.9(9)	50.7(9)	15.0(7)	7.1(6)	3.9(6)
N1	23.7(8)	25.4(8)	26.0(9)	2.7(7)	3.2(6)	1.5(7)
N2	21.7(8)	32.5(9)	25.7(8)	3.4(7)	5.2(6)	-0.3(6)
N3	26.7(8)	28.1(8)	24.9(8)	3.3(7)	5.2(7)	-3.0(7)
C1	21.9(10)	29.6(10)	28.5(10)	-0.2(8)	6.1(8)	0.2(8)
C2	24.9(9)	25.5(9)	21.7(9)	-0.9(8)	6.0(7)	1.0(8)
C3	22.3(9)	26.6(10)	22.7(9)	0.6(7)	5.2(7)	-2.5(7)
C4	22.7(9)	27.4(10)	18.0(9)	-1.6(7)	3.3(7)	-1.1(8)
C5	26.2(10)	25.4(10)	20.3(9)	-0.3(7)	6.2(7)	-1.5(8)
C6	21.8(9)	31.4(10)	26.6(10)	0.4(8)	8.2(7)	-2.1(8)
C7	22.1(9)	30.4(10)	26.1(10)	6.4(8)	4.7(8)	0.0(8)
C8	32.9(11)	31.3(11)	30.9(11)	4.6(8)	0.8(8)	1.0(8)
C9	43.7(13)	40.5(13)	34.2(12)	1.7(10)	-0.8(9)	-10.2(10)
C10	31.3(11)	59.6(16)	34.8(12)	14.8(11)	-6.0(9)	-9.0(11)
C11	25.1(11)	54.0(15)	41.6(13)	19.0(11)	6.1(9)	9.0(10)
C12	29.7(10)	36.3(12)	33.9(12)	8.2(9)	10.7(8)	7.4(9)
C13	21.0(9)	30.6(10)	21.8(9)	6.4(7)	2.1(7)	2.4(7)
C14	24.9(9)	28.9(10)	30.2(10)	2.1(8)	3.2(7)	0.7(8)
C15	24.3(9)	40.3(12)	31.6(11)	-0.9(9)	7.6(8)	6.6(8)
C16	20.6(9)	41.3(12)	33.2(11)	7.4(9)	6.2(8)	1.2(8)
C17	28.1(10)	29.7(10)	31.9(11)	3.3(8)	1.6(8)	-1.3(8)
C18	24.3(9)	30.2(10)	27.9(10)	0.9(8)	4.4(7)	2.8(8)
C19	27.5(10)	27.6(10)	21.9(9)	4.1(7)	7.7(8)	-2.3(8)
C20	33.4(10)	28.9(10)	30.7(11)	3.9(8)	8.8(8)	1.3(8)
C21	36.5(12)	41.7(13)	38.7(13)	13.5(10)	4.3(9)	2.3(9)
C22	40.8(12)	51.1(14)	32.0(12)	12.6(10)	-4.1(10)	-12.2(11)
C23	53.4(14)	40.2(13)	28.1(11)	-1.5(9)	4.0(10)	-17.5(11)
C24	42.6(12)	26.6(10)	28.8(11)	2.8(8)	8.0(9)	-3.0(9)
C25	29.0(10)	25.9(10)	30.3(10)	1.4(8)	5.0(8)	-0.9(8)
C26	29.2(10)	29.4(11)	34.9(11)	3.4(8)	8.4(8)	-3.8(8)

Table 4 Bond Lengths for mac190042_fa.

Atom	Atom	Length/Å	Atom	Atom	Length/Å
O1	C1	1.231(2)	C8	C9	1.384(3)
N1	C2	1.380(2)	C9	C10	1.384(4)
N1	C7	1.437(2)	C10	C11	1.378(4)
N1	C25	1.462(3)	C11	C12	1.393(3)
N2	C4	1.289(3)	C13	C14	1.395(3)
N2	C13	1.409(2)	C13	C18	1.392(3)
N3	C5	1.370(3)	C14	C15	1.388(3)

N3	C19	1.429(3)	C15	C16	1.381(3)
N3	C26	1.462(3)	C16	C17	1.389(3)
C1	C2	1.505(3)	C17	C18	1.388(3)
C1	C6	1.438(3)	C19	C20	1.391(3)
C2	C3	1.359(3)	C19	C24	1.386(3)
C3	C4	1.448(3)	C20	C21	1.383(3)
C4	C5	1.496(3)	C21	C22	1.379(4)
C5	C6	1.361(3)	C22	C23	1.380(4)
C7	C8	1.386(3)	C23	C24	1.391(3)
C7	C12	1.390(3)			

Table 5 Bond Angles for mac190042_fa.

Atom	Atom	Atom	Angle/°	Atom	Atom	Atom	Angle/°
C2	N1	C7	119.42(16)	C12	C7	N1	119.42(19)
C2	N1	C25	118.16(15)	C9	C8	C7	120.4(2)
C7	N1	C25	115.26(16)	C8	C9	C10	119.9(2)
C4	N2	C13	122.98(17)	C11	C10	C9	119.7(2)
C5	N3	C19	121.42(16)	C10	C11	C12	121.0(2)
C5	N3	C26	118.70(16)	C7	C12	C11	118.9(2)
C19	N3	C26	116.31(16)	C14	C13	N2	116.97(17)
O1	C1	C2	120.45(18)	C18	C13	N2	123.55(18)
O1	C1	C6	121.60(17)	C18	C13	C14	119.21(17)
C6	C1	C2	117.86(16)	C15	C14	C13	120.26(19)
N1	C2	C1	117.04(16)	C16	C15	C14	120.43(19)
C3	C2	N1	123.70(17)	C15	C16	C17	119.54(19)
C3	C2	C1	119.01(17)	C18	C17	C16	120.5(2)
C2	C3	C4	122.41(17)	C17	C18	C13	120.04(19)
N2	C4	C3	124.91(17)	C20	C19	N3	119.67(19)
N2	C4	C5	116.29(17)	C24	C19	N3	120.77(19)
C3	C4	C5	118.19(15)	C24	C19	C20	119.55(19)
N3	C5	C4	118.40(16)	C21	C20	C19	120.1(2)
C6	C5	N3	122.80(17)	C22	C21	C20	120.6(2)
C6	C5	C4	118.40(17)	C21	C22	C23	119.4(2)
C5	C6	C1	123.30(17)	C22	C23	C24	120.8(2)
C8	C7	N1	120.55(18)	C19	C24	C23	119.6(2)
C8	C7	C12	120.01(19)				

Table 6 Hydrogen Atom Coordinates (Å×10^4) and Isotropic Displacement Parameters (Å^2×10^3) for mac190042_fa.

Atom	*x*	*y*	*z*	U(eq)
H3	5269	9317	4697	28
H6	3600	5108	5459	31

H8	3886	7467	2931	39
H9	3058	7080	1811	49
H10	2316	9953	1457	52
H11	2414	13203	2214	48
H12	3234	13599	3353	39
H14	6334	3539	4689	34
H15	7275	4603	4275	38
H16	7729	8080	4628	38
H17	7230	10526	5388	37
H18	6275	9519	5781	33
H20	5564	652	6745	37
H21	6477	837	7761	47
H22	6731	4104	8494	51
H23	6044	7151	8241	49
H24	5121	6991	7229	39
H25A	4912	12728	4390	43
H25B	4462	13729	3617	43
H25C	4927	11731	3529	43
H26A	3908	2934	6642	46
H26B	4381	900	6652	46
H26C	3952	1695	5829	46

4-(Phenylamino)-2-tosylphenol, 2.69a

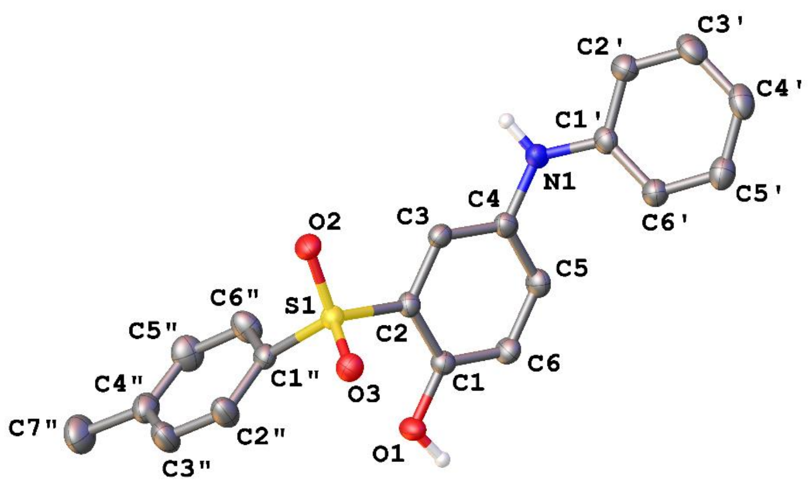

Table 1: Crystal data and structure refinement for mac180013_fa.

Identification code	mac180013_fa

Empirical formula	$C_{19}H_{19}NO_4S$
Formula weight	357.41
Temperature/K	150.0(2)
Crystal system	monoclinic
Space group	$P2_1/c$
a/Å	11.8423(2)
b/Å	7.75883(14)
c/Å	19.1121(4)
α/°	90
β/°	97.6413(18)
γ/°	90
Volume/Å^3	1740.47(6)
Z	4
ρ_{calc}g/cm^3	1.364
μ/mm^{-1}	1.857
F(000)	752.0
Crystal size/mm^3	0.24 × 0.18 × 0.13
Radiation	CuKα (λ = 1.54184)
2Θ range for data collection/°	7.532 to 133.722
Index ranges	$-13 \le h \le 14$, $-6 \le k \le 9$, $-21 \le l \le 22$
Reflections collected	12606
Independent reflections	3087 [R_{int} = 0.0301, R_{sigma} = 0.0230]
Data/restraints/parameters	3087/0/239
Goodness-of-fit on F^2	1.051
Final R indexes [I>=2σ (I)]	R_1 = 0.0321, wR_2 = 0.0769
Final R indexes [all data]	R_1 = 0.0400, wR_2 = 0.0822
Largest diff. peak/hole / e Å^{-3}	0.24/-0.34

Table 2 Fractional Atomic Coordinates (×10^4) and Equivalent Isotropic Displacement Parameters (Å^2×10^3) for mac180013_fa. U_{eq} is defined as 1/3 of of the trace of the orthogonalised U_{IJ} tensor.

Atom	*x*	*y*	*z*	U(eq)
S1	7604.4(3)	9166.5(5)	5390.0(2)	22.55(12)
O1	8474.5(9)	5582.2(15)	5331.4(6)	27.6(3)
O2	6798.9(9)	10574.5(14)	5354.2(6)	29.8(3)
O3	8617.8(9)	9446.1(14)	5056.9(6)	27.6(3)
O4	9357.0(11)	2841.8(16)	4805.7(7)	35.7(3)
N1	4163.5(12)	6643(2)	3819.3(7)	30.3(3)
C1	7413.4(13)	5783.9(19)	4976.1(8)	22.8(3)
C1"	8043.5(13)	8706(2)	6286.3(8)	25.0(3)
C1'	3897.6(13)	6389(2)	3089.8(8)	25.9(3)
C2	6873.1(13)	7377.9(19)	4991.7(7)	22.6(3)
C2"	9138.4(15)	9167(3)	6573.8(9)	36.4(4)
C2'	2846.4(14)	6997(2)	2761.5(9)	33.1(4)
C3	5797.0(13)	7663(2)	4610.6(8)	23.5(3)

C3''	9443.2(16)	9028(3)	7296.9(10)	42.5(5)
C3'	2540.1(16)	6782(2)	2042.5(10)	38.9(4)
C4	5246.3(13)	6349(2)	4207.2(8)	25.1(3)
C4''	8685.1(16)	8411(2)	7731.5(9)	36.3(4)
C4'	3254.3(17)	5949(2)	1637.2(9)	37.0(4)
C5	5770.4(14)	4738(2)	4217.0(8)	27.8(3)
C5''	7606.1(17)	7926(3)	7426.6(10)	40.9(4)
C5'	4298.8(16)	5366(2)	1958.6(9)	35.0(4)
C6	6832.8(13)	4458(2)	4590.8(8)	27.1(3)
C6''	7276.3(15)	8080(2)	6706.5(9)	35.5(4)
C6'	4625.3(14)	5581(2)	2677.0(9)	30.7(4)
C7''	9020(2)	8311(3)	8519.1(10)	54.5(6)

Table 3 Anisotropic Displacement Parameters (Å^2×10^3) for mac180013_fa. The Anisotropic displacement factor exponent takes the form: -2π^2[h^{2}a*^{2}U$_{11}$+2hka*b*U$_{12}$+…].

Atom	U_{11}	U_{22}	U_{33}	U_{23}	U_{13}	U_{12}
S1	24.38(19)	19.10(19)	23.6(2)	-1.02(14)	1.08(14)	1.30(14)
O1	24.8(5)	22.6(6)	33.5(6)	-2.3(5)	-3.6(4)	4.0(5)
O2	32.7(6)	22.6(6)	32.7(6)	-3.5(5)	-0.5(5)	6.2(5)
O3	29.2(6)	24.6(6)	29.6(6)	0.6(4)	5.6(4)	-2.5(5)
O4	26.4(6)	24.1(6)	56.9(8)	-1.5(6)	6.5(6)	1.6(5)
N1	24.4(7)	39.5(8)	26.0(7)	-9.1(6)	-0.5(5)	5.6(6)
C1	23.9(7)	22.3(7)	22.1(7)	1.7(6)	2.1(6)	1.0(6)
C1''	27.8(8)	22.1(8)	24.3(8)	-3.6(6)	0.9(6)	1.8(6)
C1'	27.8(8)	23.3(8)	25.9(8)	-2.3(6)	0.5(6)	-3.4(6)
C2	26.0(7)	21.7(8)	19.6(7)	-0.5(6)	1.7(6)	-0.4(6)
C2''	28.3(8)	52.4(11)	28.2(9)	-3.9(8)	2.9(7)	-3.3(8)
C2'	31.1(8)	33.0(9)	33.9(9)	-3.5(7)	-0.6(7)	3.4(7)
C3	25.3(7)	23.9(8)	21.2(7)	-0.4(6)	3.7(6)	3.8(6)
C3''	31.6(9)	61.2(13)	32.4(10)	-7.5(9)	-4.3(7)	-0.5(9)
C3'	40.1(10)	39.1(10)	33.5(9)	3.7(8)	-10.0(8)	2.4(8)
C4	23.8(7)	30.1(8)	21.4(7)	-1.2(6)	3.1(6)	0.0(6)
C4''	44.5(10)	36.9(10)	26.5(9)	-1.6(7)	1.1(7)	9.4(8)
C4'	52.6(11)	32.4(9)	23.7(8)	0.3(7)	-3.5(8)	-2.3(8)
C5	28.7(8)	25.8(8)	28.5(8)	-3.4(6)	1.9(6)	-4.0(7)
C5''	46.8(10)	44.9(11)	32.1(9)	6.0(8)	9.3(8)	-4.6(9)
C5'	45.9(10)	31.3(9)	28.2(9)	-3.2(7)	6.8(7)	-0.5(8)
C6	30.1(8)	20.3(8)	30.3(8)	-1.3(6)	2.5(6)	1.3(6)
C6''	32.1(9)	40.5(10)	32.9(9)	4.4(7)	0.5(7)	-9.2(8)
C6'	30.1(8)	32.1(9)	29.2(8)	-4.0(7)	1.8(6)	1.1(7)
C7''	68.4(14)	64.6(15)	28.5(10)	0.3(9)	-0.2(9)	10.2(12)

Table 4 Bond Lengths for mac180013_fa.

Atom	Atom	Length/Å	Atom	Atom	Length/Å
S1	O2	1.4460(11)	C2	C3	1.399(2)
S1	O3	1.4477(12)	C2"	C3"	1.385(3)
S1	C1"	1.7594(16)	C2'	C3'	1.384(2)
S1	C2	1.7550(15)	C3	C4	1.388(2)
O1	C1	1.3556(18)	C3"	C4"	1.387(3)
N1	C1'	1.402(2)	C3'	C4'	1.381(3)
N1	C4	1.412(2)	C4	C5	1.395(2)
C1	C2	1.395(2)	C4"	C5"	1.384(3)
C1	C6	1.392(2)	C4"	C7"	1.507(3)
C1"	C2"	1.386(2)	C4'	C5'	1.382(3)
C1"	C6"	1.378(2)	C5	C6	1.379(2)
C1'	C2'	1.399(2)	C5"	C6"	1.385(3)
C1'	C6'	1.392(2)	C5'	C6'	1.386(2)

Table 5 Bond Angles for mac180013_fa.

Atom	Atom	Atom	Angle/°	Atom	Atom	Atom	Angle/°
O2	S1	O3	116.50(7)	C3"	C2"	C1"	118.77(17)
O2	S1	C1"	107.88(7)	C3'	C2'	C1'	120.31(16)
O2	S1	C2	107.01(7)	C4	C3	C2	120.09(14)
O3	S1	C1"	107.68(7)	C2"	C3"	C4"	121.39(17)
O3	S1	C2	108.53(7)	C4'	C3'	C2'	120.94(16)
C2	S1	C1"	109.07(7)	C3	C4	N1	119.98(15)
C1'	N1	C4	124.58(14)	C3	C4	C5	118.41(14)
O1	C1	C2	119.28(13)	C5	C4	N1	121.57(14)
O1	C1	C6	122.65(14)	C3"	C4"	C7"	120.72(18)
C6	C1	C2	118.08(14)	C5"	C4"	C3"	118.45(16)
C2"	C1"	S1	118.25(13)	C5"	C4"	C7"	120.81(18)
C6"	C1"	S1	120.42(12)	C3'	C4'	C5'	118.86(16)
C6"	C1"	C2"	120.94(15)	C6	C5	C4	121.43(15)
C2'	C1'	N1	117.86(15)	C4"	C5"	C6"	121.16(17)
C6'	C1'	N1	123.56(14)	C4'	C5'	C6'	121.07(17)
C6'	C1'	C2'	118.58(15)	C5	C6	C1	120.70(15)
C1	C2	S1	120.61(11)	C1"	C6"	C5"	119.26(16)
C1	C2	C3	121.19(14)	C5'	C6'	C1'	120.22(15)
C3	C2	S1	117.63(12)				

Table 6 Hydrogen Bonds for mac180013_fa.

D	H	A	d(D-H)/Å	d(H-A)/Å	d(D-A)/Å	D-H-A/°
O1	H1	O4	0.83(2)	1.80(2)	2.6271(17)	170(2)

O4	H4A	O1[1]	0.83(3)	2.17(3)	2.8874(18)	146(2)
O4	H4A	O3[1]	0.83(3)	2.37(3)	2.9672(16)	130(2)
O4	H4B	O3[2]	0.86(3)	1.98(3)	2.8372(17)	173(2)
N1	H1A	O2[3]	0.87(2)	2.14(2)	2.9887(18)	164.1(18)

[1]2-X,1-Y,1-Z; [2]+X,-1+Y,+Z; [3]1-X,2-Y,1-Z

Table 7 Hydrogen Atom Coordinates (Å×10^4) and Isotropic Displacement Parameters (Å^2×10^3) for mac180013_fa.

Atom	*x*	*y*	*z*	U(eq)
H1	8740(19)	4650(30)	5210(11)	41
H4A	10060(20)	2860(30)	4815(12)	54
H4B	9190(20)	1800(30)	4906(12)	54
H1A	3765(17)	7430(30)	3998(10)	36
H2"	9659	9562	6287	44
H2'	2351	7548	3028	40
H3	5450	8735	4628	28
H3"	10172	9355	7495	51
H3'	1843	7204	1829	47
H4'	3036	5784	1156	44
H5	5395	3832	3966	33
H5"	7094	7488	7710	49
H5'	4791	4820	1688	42
H6	7165	3373	4586	32
H6"	6545	7766	6509	43
H6'	5333	5184	2884	37
H7"A	9826	8123	8621	82
H7"B	8623	7374	8706	82
H7"C	8824	9371	8732	82

2-((2-Chlorophenyl)sulfonyl)-4-(phenylamino)phenol, 2.69b

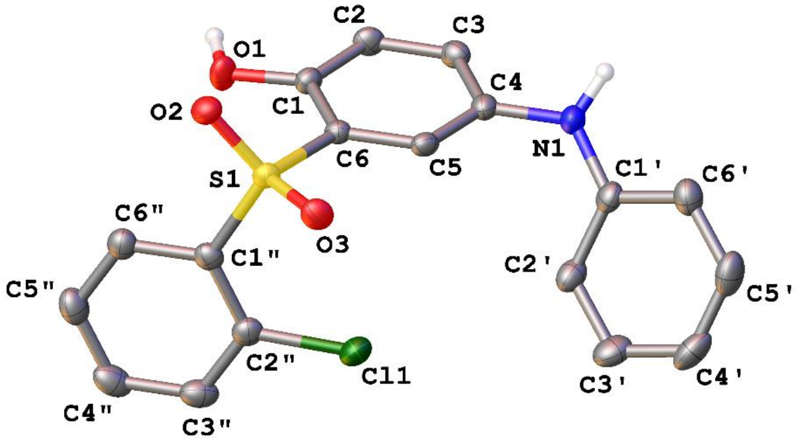

Table 1: Crystal data and structure refinement for mac180012_fa.

Identification code	mac180012_fa
Empirical formula	$C_{18}H_{14}ClNO_3S$
Formula weight	359.81
Temperature/K	150.0(2)
Crystal system	monoclinic
Space group	$P2_1/c$
a/Å	7.05994(14)
b/Å	12.0673(2)
c/Å	18.6213(4)
α/°	90
β/°	90.0639(18)
γ/°	90
Volume/Å^3	1586.43(5)
Z	4
ρ_{calc}g/cm^3	1.506
μ/mm^{-1}	3.510
F(000)	744.0
Crystal size/mm^3	0.28 × 0.06 × 0.04
Radiation	CuKα (λ = 1.54184)
2Θ range for data collection/°	8.732 to 133.85
Index ranges	$-8 \leq h \leq 8$, $-14 \leq k \leq 13$, $-19 \leq l \leq 22$
Reflections collected	12933
Independent reflections	2825 [R_{int} = 0.0390, R_{sigma} = 0.0285]
Data/restraints/parameters	2825/0/223
Goodness-of-fit on F^2	1.030

Final R indexes [I>=2σ (I)] R_1 = 0.0306, wR_2 = 0.0725
Final R indexes [all data] R_1 = 0.0407, wR_2 = 0.0790
Largest diff. peak/hole / e Å^{-3} 0.31/-0.31

Table 2 Fractional Atomic Coordinates (×10^4) and Equivalent Isotropic Displacement Parameters (Å^2×10^3) for mac180012_fa. U_{eq} is defined as 1/3 of of the trace of the orthogonalised U_{IJ} tensor.

Atom	*x*	*y*	*z*	U(eq)
Cl1	8282.5(7)	6112.1(4)	4803.3(3)	31.60(14)
S1	6609.5(6)	7726.9(4)	6068.8(2)	19.35(13)
O1	2403(2)	7626.2(12)	5932.8(8)	27.8(3)
O2	5805.8(19)	8155.7(11)	6721.2(7)	24.9(3)
O3	8547.7(18)	8015.0(11)	5910.1(7)	25.3(3)
N1	6049(3)	9567.2(15)	3588.6(9)	28.9(4)
C1	3242(3)	8138.8(15)	5367.8(10)	20.1(4)
C1"	6403(3)	6262.2(15)	6090.0(10)	21.4(4)
C1'	7712(3)	9153.3(16)	3282.8(10)	24.3(4)
C2	2229(3)	8610.2(15)	4803.3(10)	23.7(4)
C2"	7140(3)	5584.3(16)	5551.7(10)	24.2(4)
C2'	8176(3)	8031.7(17)	3317.4(11)	28.3(4)
C3	3154(3)	9074.7(15)	4221.1(10)	23.8(4)
C3"	6957(3)	4441.9(17)	5600.5(12)	30.5(5)
C3'	9742(3)	7629.3(19)	2959.8(12)	34.8(5)
C4	5122(3)	9089.1(15)	4185.6(10)	22.0(4)
C4"	6055(3)	3981.3(17)	6189.9(13)	32.7(5)
C4'	10861(3)	8327(2)	2549.1(12)	38.1(5)
C5	6141(3)	8651.5(14)	4754.0(10)	20.4(4)
C5"	5312(3)	4644.6(18)	6720.9(12)	30.9(5)
C5'	10423(3)	9436(2)	2521.6(12)	38.2(5)
C6	5222(2)	8177.4(14)	5337.0(10)	18.5(4)
C6"	5477(3)	5788.7(17)	6672.0(11)	25.4(4)
C6'	8887(3)	9861.7(18)	2894.8(11)	30.8(5)

Table 3 Anisotropic Displacement Parameters (Å^2×10^3) for mac180012_fa. The Anisotropic displacement factor exponent takes the form: -$2\pi^2[h^2a^{*2}U_{11}+2hka^*b^*U_{12}+\ldots]$.

Atom	U_{11}	U_{22}	U_{33}	U_{23}	U_{13}	U_{12}
Cl1	32.1(3)	32.8(3)	29.9(3)	0.18(19)	10.2(2)	7.32(19)
S1	15.5(2)	21.1(2)	21.4(2)	0.69(16)	0.16(16)	2.19(16)
O1	15.4(7)	38.7(8)	29.5(7)	11.7(6)	4.8(6)	1.3(6)
O2	26.3(7)	26.4(7)	22.0(7)	-1.5(5)	0.6(5)	4.2(5)
O3	15.8(6)	27.9(7)	32.1(7)	2.8(6)	-2.3(5)	-0.3(5)

N1	33.5(10)	27.2(9)	26.0(9)	7.9(7)	11.5(7)	7.5(7)
C1	17.3(9)	21.4(9)	21.8(9)	0.1(7)	2.5(7)	0.1(7)
C1"	16.3(9)	23.2(9)	24.7(9)	2.7(7)	-2.8(7)	2.0(7)
C1'	25.5(10)	29.8(10)	17.5(9)	0.2(7)	2.7(8)	0.2(8)
C2	15.7(9)	26.4(10)	29.0(10)	1.2(8)	-0.7(8)	1.1(7)
C2"	17.8(9)	27.6(10)	27.3(10)	1.2(8)	0.2(8)	2.8(7)
C2'	29.4(10)	28.8(10)	26.6(10)	-3.7(8)	7.5(8)	-4.5(8)
C3	25.8(10)	23.8(9)	21.7(9)	-0.2(7)	-1.9(8)	4.1(8)
C3"	23.5(10)	25.3(10)	42.6(12)	-4.1(9)	0.3(9)	2.8(8)
C3'	34.4(12)	34.2(11)	35.6(12)	-11.0(9)	6.7(9)	1.3(9)
C4	26.1(10)	18.9(9)	21.2(9)	0.5(7)	4.4(8)	1.8(7)
C4"	24.3(10)	22.9(10)	50.9(14)	4.1(9)	-3.0(9)	-2.1(8)
C4'	27.4(11)	56.0(15)	31.0(12)	-9.9(10)	10.1(9)	-1.5(10)
C5	17.7(9)	19.2(9)	24.3(9)	-0.4(7)	4.0(7)	2.2(7)
C5"	26.1(10)	31.9(11)	34.8(11)	10.0(9)	-0.5(9)	-4.1(8)
C5'	29.5(12)	54.4(15)	30.8(11)	9.3(10)	5.9(9)	-8.6(10)
C6	17.4(9)	18.5(8)	19.6(9)	0.0(7)	0.9(7)	2.3(7)
C6"	21.3(9)	29.6(10)	25.2(10)	3.9(8)	-0.4(8)	2.0(8)
C6'	30.4(11)	33.0(11)	29.1(11)	7.2(8)	1.0(9)	-3.1(9)

Table 4 Bond Lengths for mac180012_fa.

Atom	Atom	Length/Å	Atom	Atom	Length/Å
Cl1	C2"	1.7323(19)	C1'	C6'	1.393(3)
S1	O2	1.4377(13)	C2	C3	1.385(3)
S1	O3	1.4427(13)	C2"	C3"	1.388(3)
S1	C1"	1.7740(19)	C2'	C3'	1.379(3)
S1	C6	1.7633(19)	C3	C4	1.391(3)
O1	C1	1.357(2)	C3"	C4"	1.386(3)
N1	C1'	1.397(3)	C3'	C4'	1.385(3)
N1	C4	1.414(2)	C4	C5	1.384(3)
C1	C2	1.392(3)	C4"	C5"	1.376(3)
C1	C6	1.400(3)	C4'	C5'	1.374(4)
C1"	C2"	1.395(3)	C5	C6	1.389(2)
C1"	C6"	1.389(3)	C5"	C6"	1.389(3)
C1'	C2'	1.394(3)	C5'	C6'	1.388(3)

Table 5 Bond Angles for mac180012_fa.

Atom	Atom	Atom	Angle/°	Atom	Atom	Atom	Angle/°
O2	S1	O3	117.50(8)	C3"	C2"	C1"	120.05(18)
O2	S1	C1"	107.90(8)	C3'	C2'	C1'	120.53(19)
O2	S1	C6	108.83(8)	C2	C3	C4	120.96(18)

O3	S1	C1"	108.82(8)	C4"	C3"	C2"	119.55(19)
O3	S1	C6	107.08(8)	C2'	C3'	C4'	120.7(2)
C6	S1	C1"	106.19(9)	C3	C4	N1	120.40(17)
C1'	N1	C4	124.38(17)	C5	C4	N1	121.05(17)
O1	C1	C2	123.19(16)	C5	C4	C3	118.53(17)
O1	C1	C6	118.92(16)	C5"	C4"	C3"	120.77(19)
C2	C1	C6	117.88(16)	C5'	C4'	C3'	119.0(2)
C2"	C1"	S1	122.53(14)	C4	C5	C6	120.77(17)
C6"	C1"	S1	117.77(14)	C4"	C5"	C6"	119.93(19)
C6"	C1"	C2"	119.71(18)	C4'	C5'	C6'	121.2(2)
C2'	C1'	N1	121.72(17)	C1	C6	S1	120.79(13)
C6'	C1'	N1	119.52(18)	C5	C6	S1	118.12(14)
C6'	C1'	C2'	118.65(18)	C5	C6	C1	120.89(17)
C3	C2	C1	120.92(17)	C5"	C6"	C1"	119.99(19)
C1"	C2"	Cl1	122.47(15)	C5'	C6'	C1'	119.9(2)
C3"	C2"	Cl1	117.48(15)				

Table 6 Hydrogen Bonds for mac180012_fa.

D	H	A	d(D-H)/Å	d(H-A)/Å	d(D-A)/Å	D-H-A/°
O1	H1	O3[1]	0.87(3)	1.90(3)	2.7624(19)	172(3)
N1	H1A	O2[2]	0.90(3)	2.21(3)	3.098(2)	169(2)

[1]-1+X,+Y,+Z; [2]1-X,2-Y,1-Z

Table 7 Hydrogen Atom Coordinates (Å×10⁴) and Isotropic Displacement Parameters (Å²×10³) for mac180012_fa.

Atom	*x*	*y*	*z*	U(eq)
H1	1180(40)	7710(20)	5893(15)	42
H1A	5640(30)	10240(20)	3459(13)	35
H2	884	8613	4818	28
H2'	7408	7541	3589	34
H3	2435	9388	3841	29
H3"	7447	3979	5232	37
H3'	10057	6866	2996	42
H4"	5947	3199	6228	39
H4'	11914	8044	2290	46
H5	7486	8676	4745	24
H5"	4686	4320	7120	37
H5'	11186	9919	2242	46
H6"	4958	6248	7036	30
H6'	8636	10635	2886	37

2-(Phenylamino)phenoxathiine-10,10-dioxide, 2.77

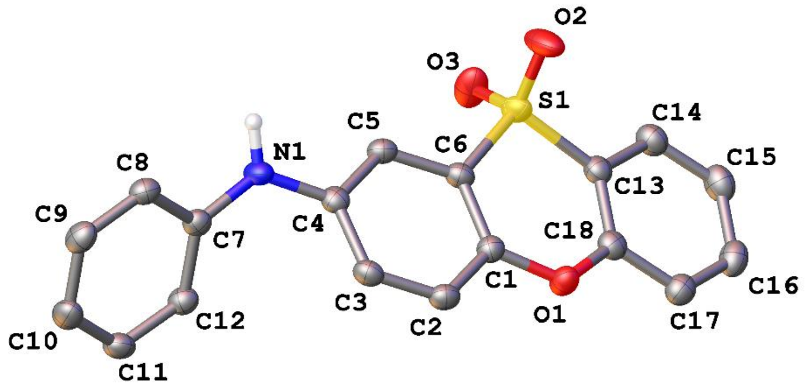

Table 1: Crystal data and structure refinement for mac180054.

Identification code	mac180054
Empirical formula	$C_{18}H_{13}NO_3S$
Formula weight	323.35
Temperature/K	150.0(2)
Crystal system	monoclinic
Space group	$P2_1/n$
a/Å	9.41475(17)
b/Å	10.8966(2)
c/Å	14.9344(3)
α/°	90
β/°	106.9572(18)
γ/°	90
Volume/$Å^3$	1465.49(5)
Z	4
ρ_{calc}g/cm^3	1.466
μ/mm^{-1}	2.097
F(000)	672.0
Crystal size/mm^3	0.32 × 0.23 × 0.12
Radiation	CuKα (λ = 1.54184)
2Θ range for data collection/°	9.966 to 133.786
Index ranges	$-10 \leq h \leq 11$, $-12 \leq k \leq 12$, $-17 \leq l \leq 16$
Reflections collected	10621
Independent reflections	2587 [R_{int} = 0.0259, R_{sigma} = 0.0205]

Data/restraints/parameters	2587/0/212
Goodness-of-fit on F^2	1.038
Final R indexes [I>=2σ (I)]	R_1 = 0.0318, wR_2 = 0.0792
Final R indexes [all data]	R_1 = 0.0378, wR_2 = 0.0838
Largest diff. peak/hole / e Å^{-3}	0.34/-0.32

Table 2 Fractional Atomic Coordinates (×10⁴) and Equivalent Isotropic Displacement Parameters (Å^2×10^3) for mac180054. U_{eq} is defined as 1/3 of of the trace of the orthogonalised U_{IJ} tensor.

Atom	*x*	*y*	*z*	U(eq)
S1	2316.0(4)	7848.3(4)	3777.1(3)	27.50(15)
O1	4928.8(12)	8184.9(11)	5616.9(8)	28.2(3)
O2	1134.2(13)	7075.3(13)	3869.1(11)	45.0(4)
O3	2131.9(15)	8361.9(13)	2857.2(8)	41.9(4)
N1	5757.3(15)	4520.8(13)	3217.3(10)	26.5(3)
C1	5030.7(17)	7284.6(15)	4995.9(11)	22.3(3)
C2	6306.7(17)	6567.5(15)	5271.7(11)	24.5(4)
C3	6559.5(17)	5668.2(15)	4694.9(11)	24.0(3)
C4	5540.7(17)	5446.3(15)	3811.1(11)	22.4(3)
C5	4252.2(17)	6143.4(15)	3546.1(11)	23.2(3)
C6	3995.5(17)	7054.9(15)	4138.3(11)	22.2(3)
C7	7125.7(17)	3978.5(15)	3257.5(10)	22.7(3)
C8	7162.0(18)	2736.7(15)	3034.1(11)	24.9(4)
C9	8485.1(19)	2187.5(16)	3025.8(12)	29.6(4)
C10	9784.6(19)	2865.9(17)	3230.7(12)	31.5(4)
C11	9751.8(18)	4101.6(17)	3447.7(11)	28.2(4)
C12	8442.5(18)	4658.0(16)	3462.9(11)	25.3(4)
C13	2616.4(17)	9035.3(15)	4594.5(11)	24.7(4)
C14	1559.4(19)	9971.1(16)	4449.2(12)	30.2(4)
C15	1697(2)	10889.6(17)	5098.6(13)	33.6(4)
C16	2910(2)	10891.7(16)	5901.8(12)	32.0(4)
C17	3973.7(19)	9990.9(16)	6047.3(12)	28.8(4)
C18	3827.1(18)	9047.1(15)	5396.3(11)	24.8(3)

Table 3 Anisotropic Displacement Parameters (Å^2×10^3) for mac180054. The Anisotropic displacement factor exponent takes the form: -$2\pi^2[h^2a^{*2}U_{11}+2hka^*b^*U_{12}+\ldots]$.

Atom	U_{11}	U_{22}	U_{33}	U_{23}	U_{13}	U_{12}
S1	20.3(2)	28.6(3)	29.4(2)	-3.45(16)	0.85(16)	4.25(16)
O1	27.2(6)	29.3(7)	24.7(6)	-4.0(5)	2.2(5)	5.4(5)
O2	21.0(6)	37.7(8)	73.7(10)	-16.2(7)	9.6(6)	-4.9(5)
O3	42.7(7)	49.9(9)	26.2(6)	1.6(6)	-0.9(5)	24.2(6)
N1	19.0(7)	26.3(8)	31.6(7)	-6.8(6)	3.2(5)	-1.7(6)
C1	23.2(8)	20.5(8)	23.1(8)	0.5(6)	6.3(6)	-0.7(6)

C2	22.2(8)	26.0(9)	22.6(8)	1.9(6)	2.2(6)	-1.2(6)
C3	18.9(7)	23.8(9)	27.6(8)	3.4(7)	4.0(6)	1.5(6)
C4	22.3(8)	19.7(8)	25.7(8)	1.4(6)	7.8(6)	-2.2(6)
C5	20.7(8)	23.8(9)	22.8(8)	1.5(6)	2.8(6)	-2.1(6)
C6	18.7(7)	22.5(8)	24.2(8)	3.1(6)	4.2(6)	0.5(6)
C7	22.4(8)	23.6(9)	20.5(7)	1.8(6)	3.5(6)	1.6(6)
C8	25.1(8)	23.9(9)	23.3(8)	0.4(6)	3.6(6)	-2.8(6)
C9	34.0(9)	23.0(9)	28.3(9)	-2.8(7)	3.8(7)	4.6(7)
C10	23.7(8)	36.7(10)	30.3(9)	-3.1(7)	2.1(7)	8.1(7)
C11	21.3(8)	33.2(10)	27.4(8)	-0.5(7)	2.6(6)	-2.0(7)
C12	25.8(8)	22.6(9)	25.5(8)	-0.1(6)	4.6(6)	-0.4(7)
C13	23.0(8)	24.9(9)	27.5(8)	0.5(7)	9.2(6)	-1.1(6)
C14	26.8(8)	29.0(9)	34.5(9)	2.3(7)	8.6(7)	3.5(7)
C15	34.5(9)	27.6(10)	42.1(10)	3.7(8)	16.4(8)	6.9(8)
C16	41.7(10)	24.6(9)	34.0(9)	-2.4(7)	17.8(8)	-1.5(8)
C17	32.0(9)	27.5(9)	27.6(8)	-0.2(7)	9.8(7)	-2.4(7)
C18	24.6(8)	23.9(9)	27.3(8)	2.9(7)	9.9(6)	-0.7(7)

Table 4 Bond Lengths for mac180054.

Atom	Atom	Length/Å	Atom	Atom	Length/Å
S1	O2	1.4337(14)	C5	C6	1.397(2)
S1	O3	1.4463(14)	C7	C8	1.397(2)
S1	C6	1.7439(16)	C7	C12	1.399(2)
S1	C13	1.7440(17)	C8	C9	1.385(2)
O1	C1	1.372(2)	C9	C10	1.385(2)
O1	C18	1.367(2)	C10	C11	1.387(3)
N1	C4	1.397(2)	C11	C12	1.380(2)
N1	C7	1.403(2)	C13	C14	1.397(2)
C1	C2	1.391(2)	C13	C18	1.392(2)
C1	C6	1.387(2)	C14	C15	1.373(3)
C2	C3	1.371(2)	C15	C16	1.394(3)
C3	C4	1.408(2)	C16	C17	1.373(3)
C4	C5	1.387(2)	C17	C18	1.394(2)

Table 5 Bond Angles for mac180054.

Atom	Atom	Atom	Angle/°	Atom	Atom	Atom	Angle/°
O2	S1	O3	115.91(9)	C5	C6	S1	117.73(12)
O2	S1	C6	109.76(8)	C8	C7	N1	118.95(14)
O2	S1	C13	109.92(8)	C8	C7	C12	118.90(15)
O3	S1	C6	109.41(7)	C12	C7	N1	122.04(15)
O3	S1	C13	109.14(8)	C9	C8	C7	120.36(15)

C6	S1	C13	101.76(8)	C10	C9	C8	120.40(16)
C18	O1	C1	121.75(12)	C9	C10	C11	119.42(15)
C4	N1	C7	125.41(13)	C12	C11	C10	120.74(16)
O1	C1	C2	115.22(14)	C11	C12	C7	120.17(16)
O1	C1	C6	125.74(14)	C14	C13	S1	118.03(13)
C6	C1	C2	119.04(15)	C18	C13	S1	122.27(13)
C3	C2	C1	120.59(14)	C18	C13	C14	119.63(15)
C2	C3	C4	121.08(15)	C15	C14	C13	120.40(16)
N1	C4	C3	122.24(14)	C14	C15	C16	119.59(16)
C5	C4	N1	119.45(14)	C17	C16	C15	120.75(16)
C5	C4	C3	118.25(14)	C16	C17	C18	119.84(16)
C4	C5	C6	120.46(14)	O1	C18	C13	125.07(15)
C1	C6	S1	121.71(13)	O1	C18	C17	115.16(14)
C1	C6	C5	120.54(14)	C13	C18	C17	119.76(15)

Table 6 Hydrogen Atom Coordinates (Å×10^4) and Isotropic Displacement Parameters (Å^2×10^3) for mac180054.

Atom	*x*	*y*	*z*	U(eq)
H1	4990(20)	4089(19)	2926(13)	32
H2	6994	6699	5853	29
H3	7418	5197	4891	29
H5	3555	6003	2970	28
H8	6293	2276	2890	30
H9	8501	1358	2882	35
H10	10671	2496	3223	38
H11	10622	4560	3585	34
H12	8435	5487	3610	30
H14	757	9972	3909	36
H15	986	11506	5003	40
H16	3001	11510	6344	38
H17	4790	10010	6579	35

(*E*)-3-Bromo-4-((4-bromophenyl)imino)cyclohexa-2,5-dien-1-one, 3.3

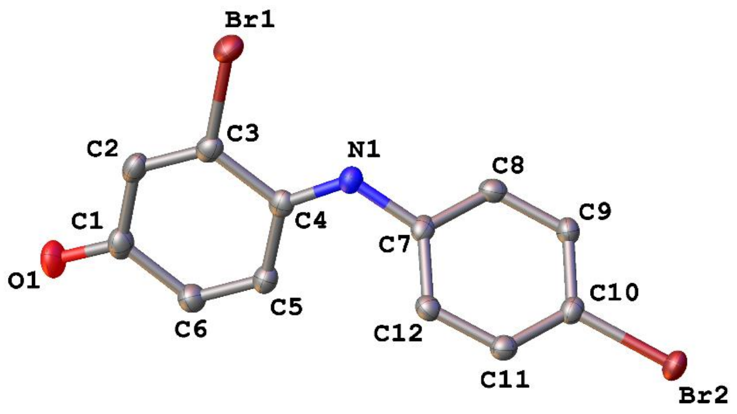

Table 1: Crystal data and structure refinement for mac180052.

Identification code	mac180052
Empirical formula	$C_{12}H_7Br_2NO$
Formula weight	341.01
Temperature/K	150.0(2)
Crystal system	monoclinic
Space group	$P2_1/c$
a/Å	10.5423(3)
b/Å	4.01735(12)
c/Å	26.7689(7)
α/°	90
β/°	93.229(3)
γ/°	90
Volume/Å^3	1131.93(6)
Z	4
ρ_{calc}g/cm^3	2.001
μ/mm^{-1}	8.891
F(000)	656.0
Crystal size/mm^3	0.26 × 0.19 × 0.04
Radiation	CuKα (λ = 1.54184)
2Θ range for data collection/°	8.4 to 133.534
Index ranges	$-12 \leq h \leq 12$, $-4 \leq k \leq 4$, $-31 \leq l \leq 31$
Reflections collected	8430
Independent reflections	2001 [R_{int} = 0.0244, R_{sigma} = 0.0185]
Data/restraints/parameters	2001/0/146
Goodness-of-fit on F^2	1.056

Final R indexes [I>=2σ (I)] R_1 = 0.0213, wR_2 = 0.0520
Final R indexes [all data] R_1 = 0.0258, wR_2 = 0.0545
Largest diff. peak/hole / e Å^{-3} 0.43/-0.34

Table 2 Fractional Atomic Coordinates (×10^4) and Equivalent Isotropic Displacement Parameters (Å^2×10^3) for mac180052. U_{eq} is defined as 1/3 of of the trace of the orthogonalised U_{IJ} tensor.

Atom	*x*	*y*	*z*	U(eq)
Br1	4980.0(2)	8134.1(7)	4222.5(2)	27.85(11)
Br2	8388.5(2)	2970.5(7)	1342.0(2)	25.71(11)
O1	8796.3(18)	3056(5)	5246.0(6)	36.1(5)
N1	6599.9(17)	5644(5)	3422.6(7)	20.7(4)
C1	8329(2)	3699(7)	4828.2(9)	25.7(5)
C2	7119(2)	5508(6)	4760.0(9)	25.0(5)
C3	6584(2)	6053(6)	4305.5(9)	22.0(5)
C4	7190(2)	5026(6)	3842.8(8)	19.5(5)
C5	8408(2)	3265(6)	3921.8(8)	21.7(5)
C6	8942(2)	2632(6)	4373.3(9)	25.2(5)
C7	7109(2)	4897(6)	2956.7(8)	19.0(5)
C8	6331(2)	3144(6)	2611.9(9)	21.6(5)
C9	6707(2)	2538(6)	2133.7(9)	21.0(5)
C10	7874(2)	3782(6)	1998.3(8)	20.4(5)
C11	8640(2)	5587(6)	2332.0(8)	20.7(5)
C12	8278(2)	6136(6)	2815.7(8)	20.0(5)

Table 3 Anisotropic Displacement Parameters (Å^2×10^3) for mac180052. The Anisotropic displacement factor exponent takes the form: -2π^2[h^{2}a*^{2}U$_{11}$+2hka*b*U$_{12}$+…].

Atom	U_{11}	U_{22}	U_{33}	U_{23}	U_{13}	U_{12}
Br1	24.66(15)	34.52(19)	24.91(16)	-2.90(10)	6.27(10)	3.76(10)
Br2	27.75(15)	32.87(18)	16.95(15)	-3.34(10)	5.06(10)	-0.29(10)
O1	39.4(10)	52.0(13)	16.5(9)	5.4(8)	-2.6(8)	-1.6(9)
N1	21.8(9)	24.3(11)	16.2(9)	-0.5(8)	1.8(7)	-0.4(8)
C1	29.8(12)	28.1(14)	19.0(12)	3.2(10)	0.8(10)	-5.6(10)
C2	28.0(11)	29.8(14)	17.9(11)	-1.8(10)	6.2(9)	-5.8(10)
C3	22.5(10)	21.8(13)	22.1(12)	-1.0(10)	4.5(9)	-4.5(10)
C4	22.3(10)	16.8(12)	19.4(11)	-1.2(9)	1.6(9)	-3.9(9)
C5	24.8(12)	22.9(13)	17.6(12)	-0.2(9)	2.5(9)	-0.1(9)
C6	23.8(11)	29.6(14)	22.2(13)	2.0(10)	0.1(10)	0.8(10)
C7	21.4(10)	19.8(12)	15.8(10)	2.0(9)	0.4(8)	6.0(9)
C8	16.4(10)	25.0(13)	23.2(12)	2.3(10)	1.0(9)	0.4(9)
C9	21.3(11)	24.8(13)	16.6(11)	-1.8(9)	-1.0(9)	-0.4(9)

C10	23.0(11)	22.3(12)	16.1(11)	0.8(9)	2.2(8)	3.6(10)
C11	18.7(10)	22.8(13)	20.6(11)	2.1(10)	1.6(9)	1.0(9)
C12	18.3(10)	21.9(13)	19.6(11)	0.8(9)	-1.7(8)	0.9(9)

Table 4 Bond Lengths for mac180052.

Atom	Atom	Length/Å	Atom	Atom	Length/Å
Br1	C3	1.888(2)	C4	C5	1.471(3)
Br2	C10	1.896(2)	C5	C6	1.329(3)
O1	C1	1.224(3)	C7	C8	1.391(3)
N1	C4	1.279(3)	C7	C12	1.400(3)
N1	C7	1.418(3)	C8	C9	1.383(3)
C1	C2	1.471(4)	C9	C10	1.395(3)
C1	C6	1.474(3)	C10	C11	1.377(3)
C2	C3	1.330(3)	C11	C12	1.388(3)
C3	C4	1.484(3)			

Table 5 Bond Angles for mac180052.

Atom	Atom	Atom	Angle/˚	Atom	Atom	Atom	Angle/˚
C4	N1	C7	122.91(19)	C5	C6	C1	120.9(2)
O1	C1	C2	121.3(2)	C8	C7	N1	116.9(2)
O1	C1	C6	121.4(2)	C8	C7	C12	119.7(2)
C2	C1	C6	117.3(2)	C12	C7	N1	123.0(2)
C3	C2	C1	121.0(2)	C9	C8	C7	121.0(2)
C2	C3	Br1	120.76(17)	C8	C9	C10	118.7(2)
C2	C3	C4	122.5(2)	C9	C10	Br2	118.79(18)
C4	C3	Br1	116.73(17)	C11	C10	Br2	120.25(17)
N1	C4	C3	118.0(2)	C11	C10	C9	121.0(2)
N1	C4	C5	126.7(2)	C10	C11	C12	120.4(2)
C5	C4	C3	115.3(2)	C11	C12	C7	119.2(2)
C6	C5	C4	123.0(2)				

Table 6 Hydrogen Atom Coordinates (Å×10^4) and Isotropic Displacement Parameters (Å^2×10^3) for mac180052.

Atom	*x*	*y*	*z*	U(eq)
H2	6721	6282	5039	30
H5	8824	2563	3643	26
H6	9712	1501	4403	30
H8	5547	2368	2704	26
H9	6191	1325	1907	25
H11	9406	6445	2233	25

H12	8805	7312	3043	24

4-Oxo-*N*-phenylcyclohexa-2,5-dien-1-imine oxide, 3.18

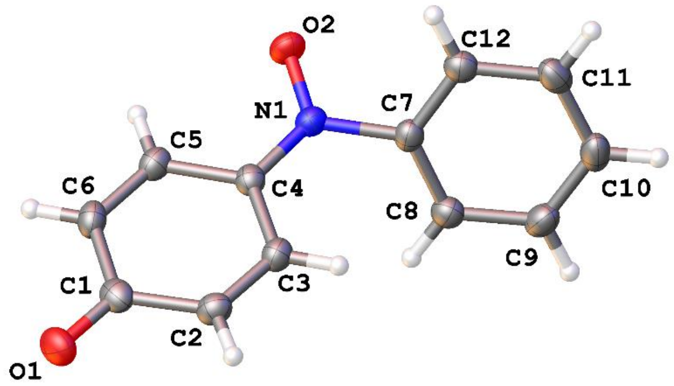

Table 1: Crystal data and structure refinement for mac180029_fa.

Identification code	mac180029_fa
Empirical formula	$C_{12}H_9NO_2$
Formula weight	199.20
Temperature/K	150.0(2)
Crystal system	monoclinic
Space group	$P2_1/c$
a/Å	10.2606(2)
b/Å	12.3811(3)
c/Å	7.4936(2)
α/°	90
β/°	100.965(2)
γ/°	90
Volume/Å^3	934.59(4)
Z	4
ρ_{calc}g/cm^3	1.416
μ/mm^{-1}	0.799
F(000)	416.0
Crystal size/mm^3	0.28 × 0.05 × 0.03
Radiation	CuKα (λ = 1.54184)
2Θ range for data collection/°	8.778 to 133.724
Index ranges	$-12 \leq h \leq 11$, $-14 \leq k \leq 14$, $-8 \leq l \leq 8$

Reflections collected	13038
Independent reflections	1659 [R_{int} = 0.0350, R_{sigma} = 0.0175]
Data/restraints/parameters	1659/0/136
Goodness-of-fit on F^2	1.031
Final R indexes [I>=2σ (I)]	R_1 = 0.0352, wR_2 = 0.0879
Final R indexes [all data]	R_1 = 0.0433, wR_2 = 0.0939
Largest diff. peak/hole / e $Å^{-3}$	0.16/-0.22

Table 2 Fractional Atomic Coordinates (×10^4) and Equivalent Isotropic Displacement Parameters (Å^2×10^3) for mac180029_fa. U_{eq} is defined as 1/3 of of the trace of the orthogonalised U_{IJ} tensor.

Atom	*x*	*y*	*z*	U(eq)
O1	3160.6(10)	6182.4(9)	599.5(14)	36.3(3)
O2	6751.9(10)	6316.0(8)	8203.0(13)	30.9(3)
N1	7038.4(11)	6290.6(9)	6610.4(15)	23.1(3)
C1	4056.3(14)	6202.9(11)	1959(2)	27.5(3)
C2	5456.0(14)	6052.4(11)	1844.5(19)	27.1(3)
C3	6421.4(13)	6109.5(11)	3331.7(19)	25.4(3)
C4	6102.7(13)	6290.3(10)	5092.3(18)	22.2(3)
C5	4738.8(13)	6424.2(11)	5257.4(19)	25.1(3)
C6	3772.3(14)	6394.7(11)	3769(2)	27.5(3)
C7	8455.4(13)	6265.0(11)	6595.9(18)	23.9(3)
C8	9029.0(14)	7088.2(12)	5761.5(18)	28.0(3)
C9	10398.7(15)	7083.5(13)	5895.0(19)	32.2(3)
C10	11158.5(14)	6271.8(13)	6852.6(19)	33.3(4)
C11	10561.4(15)	5455.6(13)	7677.0(19)	31.3(3)
C12	9195.4(14)	5446.5(12)	7563.8(18)	26.9(3)

Table 3 Anisotropic Displacement Parameters (Å^2×10^3) for mac180029_fa. The Anisotropic displacement factor exponent takes the form: -2π^2[h^{2}a*^{2}U$_{11}$+2hka*b*U$_{12}$+…].

Atom	U_{11}	U_{22}	U_{33}	U_{23}	U_{13}	U_{12}
O1	29.4(6)	44.0(6)	31.7(6)	1.6(4)	-3.9(4)	-5.2(5)
O2	30.1(5)	43.1(6)	21.2(5)	0.5(4)	9.2(4)	-2.0(4)
N1	24.0(6)	24.0(6)	22.1(6)	0.4(4)	6.6(4)	-0.7(4)
C1	26.9(7)	23.5(7)	30.2(7)	1.8(5)	1.0(6)	-4.2(5)
C2	29.7(8)	28.3(7)	24.0(7)	-1.3(5)	6.6(6)	-3.6(6)
C3	23.1(7)	26.1(7)	27.9(7)	-0.5(5)	7.2(5)	-0.4(5)
C4	21.4(7)	20.4(6)	24.6(7)	-0.2(5)	3.9(5)	-1.1(5)
C5	24.9(7)	24.2(7)	27.9(7)	-1.6(5)	9.2(5)	-0.7(5)
C6	19.9(7)	27.3(7)	35.9(8)	-0.4(6)	6.3(6)	-1.0(5)
C7	20.9(7)	30.4(7)	20.3(6)	-2.9(5)	3.7(5)	-1.0(5)

C8	26.7(7)	32.9(7)	23.6(7)	2.3(5)	3.2(5)	-1.2(6)
C9	28.5(8)	43.0(9)	25.8(7)	1.6(6)	7.1(6)	-7.2(6)
C10	21.5(7)	52.8(10)	25.1(7)	-3.8(7)	3.7(6)	-0.3(6)
C11	28.5(7)	40.4(8)	23.8(7)	0.1(6)	2.0(6)	8.0(6)
C12	27.9(7)	30.1(7)	22.6(7)	-0.1(5)	4.3(5)	0.1(6)

Table 4 Bond Lengths for mac180029_fa.

Atom	Atom	Length/Å	Atom	Atom	Length/Å
O1	C1	1.2358(17)	C4	C5	1.4378(19)
O2	N1	1.2826(15)	C5	C6	1.344(2)
N1	C4	1.3418(18)	C7	C8	1.384(2)
N1	C7	1.4564(17)	C7	C12	1.386(2)
C1	C2	1.467(2)	C8	C9	1.390(2)
C1	C6	1.460(2)	C9	C10	1.386(2)
C2	C3	1.345(2)	C10	C11	1.386(2)
C3	C4	1.4359(19)	C11	C12	1.388(2)

Table 5 Bond Angles for mac180029_fa.

Atom	Atom	Atom	Angle/°	Atom	Atom	Atom	Angle/°
O2	N1	C4	122.36(11)	C6	C5	C4	120.14(12)
O2	N1	C7	114.41(10)	C5	C6	C1	121.93(13)
C4	N1	C7	123.23(11)	C8	C7	N1	119.88(12)
O1	C1	C2	122.14(13)	C8	C7	C12	122.50(13)
O1	C1	C6	121.39(13)	C12	C7	N1	117.41(12)
C6	C1	C2	116.47(12)	C7	C8	C9	118.38(13)
C3	C2	C1	121.33(13)	C10	C9	C8	120.13(13)
C2	C3	C4	120.60(12)	C9	C10	C11	120.44(13)
N1	C4	C3	121.86(12)	C10	C11	C12	120.36(13)
N1	C4	C5	118.57(12)	C7	C12	C11	118.19(13)
C3	C4	C5	119.51(12)				

Table 6 Hydrogen Atom Coordinates (Å×10^4) and Isotropic Displacement Parameters (Å^2×10^3) for mac180029_fa.

Atom	*x*	*y*	*z*	U(eq)
H2	5680	5915	721	33
H3	7304	6031	3219	30
H5	4525	6532	6396	30
H6	2897	6500	3897	33
H8	8510	7631	5127	34
H9	10806	7626	5341	39

H10	12075	6275	6943	40
H11	11079	4911	8309	38
H12	8788	4906	8122	32

(*E*)-3-Chloro-4-((4-chlorophenyl)imino)cyclohexa-2,5-dien-1-one, 3.21

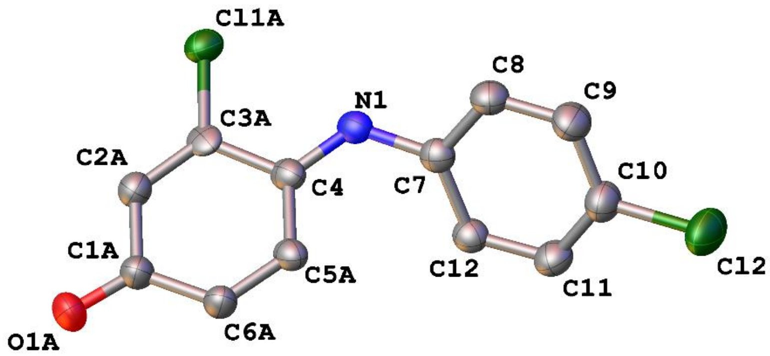

Table 1: Crystal data and structure refinement for mac180066_fa.

Identification code	mac180066_fa
Empirical formula	$C_{12}H_7Cl_2NO$
Formula weight	252.09
Temperature/K	150.0(2)
Crystal system	triclinic
Space group	P-1
a/Å	3.9115(2)
b/Å	7.1327(4)
c/Å	19.8384(10)
α/°	92.585(4)
β/°	92.771(4)
γ/°	98.729(4)
Volume/Å^3	545.65(5)
Z	2
ρ_{calc}g/cm^3	1.534
μ/mm^{-1}	5.146
F(000)	256.0
Crystal size/mm^3	0.46 × 0.03 × 0.02
Radiation	CuKα (λ = 1.54184)

2Θ range for data collection/°	8.938 to 133.348
Index ranges	$-4 \le h \le 4$, $-8 \le k \le 8$, $-23 \le l \le 23$
Reflections collected	14991
Independent reflections	1927 [R_{int} = 0.0623, R_{sigma} = 0.0289]
Data/restraints/parameters	1927/188/166
Goodness-of-fit on F^2	1.039
Final R indexes [I>=2σ (I)]	R_1 = 0.0432, wR_2 = 0.1030
Final R indexes [all data]	R_1 = 0.0534, wR_2 = 0.1087
Largest diff. peak/hole / e Å^{-3}	0.36/-0.46

Table 2 Fractional Atomic Coordinates (×10^4) and Equivalent Isotropic Displacement Parameters (Å^2×10^3) for mac180066_fa. U_{eq} is defined as 1/3 of of the trace of the orthogonalised U_{IJ} tensor.

Atom	*x*	*y*	*z*	U(eq)
Cl2	2052(3)	1687.6(11)	9533.8(4)	64.7(3)
N1	6421(5)	7618(3)	7627.8(10)	31.0(5)
C4	5714(7)	7444(3)	6987.0(12)	32.9(5)
C7	5326(6)	6154(4)	8059.9(12)	31.8(5)
C8	4008(7)	6659(4)	8669.3(13)	38.6(6)
C9	2955(8)	5286(4)	9117.1(14)	44.7(7)
C10	3393(8)	3419(4)	8971.9(14)	43.8(7)
C11	4858(7)	2908(4)	8384.0(14)	39.8(6)
C12	5785(7)	4268(3)	7927.0(13)	33.9(6)
Cl1A	9820(60)	10880(20)	6948(9)	41.1(14)
O1A	2843(13)	7206(6)	4976.3(19)	54.8(10)
C1A	3660(16)	7220(9)	5587(3)	37.5(11)
C2A	6022(14)	8856(11)	5908(3)	34.2(13)
C3A	6890(40)	9040(20)	6571(5)	31(3)
C5A	3120(30)	5854(18)	6682(4)	32.7(18)
C6A	2228(16)	5717(10)	6020(3)	34.1(12)
Cl1B	10030(70)	10840(30)	7044(11)	41.1(14)
O1B	5144(16)	7460(8)	4876(2)	54.8(10)
C1B	5349(19)	7492(11)	5500(3)	37.5(11)
C2B	7479(18)	9065(14)	5901(4)	34.2(13)
C3B	7660(60)	8910(30)	6576(6)	31(3)
C5B	3740(40)	5930(20)	6539(5)	32.7(18)
C6B	3500(20)	5960(13)	5869(4)	34.1(12)

Table 3 Anisotropic Displacement Parameters (Å^2×10^3) for mac180066_fa. The Anisotropic displacement factor exponent takes the form: -$2\pi^2[h^2a^{*2}U_{11}+2hka^*b^*U_{12}+\ldots]$.

Atom	U_{11}	U_{22}	U_{33}	U_{23}	U_{13}	U_{12}

Cl2	93.8(7)	46.4(4)	58.1(5)	14.8(4)	30.1(4)	12.1(4)
N1	31.5(11)	29.9(10)	32.2(11)	-1.0(8)	-2.0(8)	9.2(9)
C4	37.9(13)	29.8(12)	32.1(12)	-1.6(9)	-5.1(10)	11.9(10)
C7	29.6(13)	33.3(12)	32.3(12)	0.2(10)	-2.3(10)	6.0(10)
C8	45.2(15)	33.7(13)	38.2(14)	-2.0(11)	4.6(12)	10.7(11)
C9	55.7(18)	42.0(15)	39.1(15)	1.3(12)	13.0(13)	12.9(13)
C10	52.7(17)	39.6(14)	40.8(15)	7.9(11)	9.3(13)	9.2(12)
C11	46.2(16)	32.3(13)	42.8(15)	1.5(11)	4.5(12)	11.2(12)
C12	35.9(14)	33.5(13)	33.2(13)	-0.3(10)	1.7(10)	9.3(11)
Cl1A	53(2)	29.2(7)	41(4)	-0.5(19)	8(2)	6.6(10)
O1A	89(3)	44.2(16)	27.9(14)	2.6(11)	-7(2)	3(2)
C1A	50(3)	31(2)	30.6(17)	1.0(14)	-1(2)	2(3)
C2A	40(4)	30(2)	33.2(15)	3.9(13)	2(3)	6(3)
C3A	38(7)	26(2)	33.9(13)	-0.9(11)	0(2)	23(4)
C5A	40(4)	30.2(15)	29(3)	-2(2)	-3(3)	11(2)
C6A	41(4)	29(2)	30(2)	1.2(17)	-4(2)	2(2)
Cl1B	53(2)	29.2(7)	41(4)	-0.5(19)	8(2)	6.6(10)
O1B	89(3)	44.2(16)	27.9(14)	2.6(11)	-7(2)	3(2)
C1B	50(3)	31(2)	30.6(17)	1.0(14)	-1(2)	2(3)
C2B	40(4)	30(2)	33.2(15)	3.9(13)	2(3)	6(3)
C3B	38(7)	26(2)	33.9(13)	-0.9(11)	0(2)	23(4)
C5B	40(4)	30.2(15)	29(3)	-2(2)	-3(3)	11(2)
C6B	41(4)	29(2)	30(2)	1.2(17)	-4(2)	2(2)

Table 4 Bond Lengths for mac180066_fa.

Atom	Atom	Length/Å	Atom	Atom	Length/Å
Cl2	C10	1.740(3)	Cl1A	C3A	1.722(9)
N1	C4	1.284(3)	O1A	C1A	1.237(6)
N1	C7	1.411(3)	C1A	C2A	1.474(7)
C4	C3A	1.467(9)	C1A	C6A	1.466(7)
C4	C5A	1.486(8)	C2A	C3A	1.338(9)
C4	C3B	1.496(11)	C5A	C6A	1.338(8)
C4	C5B	1.465(10)	Cl1B	C3B	1.739(11)
C7	C8	1.391(4)	O1B	C1B	1.235(7)
C7	C12	1.399(4)	C1B	C2B	1.469(9)
C8	C9	1.382(4)	C1B	C6B	1.462(8)
C9	C10	1.387(4)	C2B	C3B	1.348(10)
C10	C11	1.382(4)	C5B	C6B	1.330(10)
C11	C12	1.378(4)			

Table 5 Bond Angles for mac180066_fa.

Atom	Atom	Atom	Angle/°	Atom	Atom	Atom	Angle/°
C4	N1	C7	122.1(2)	O1A	C1A	C6A	122.8(5)
N1	C4	C3A	119.0(5)	C6A	C1A	C2A	117.8(5)
N1	C4	C5A	121.0(4)	C3A	C2A	C1A	123.4(7)
N1	C4	C3B	116.1(6)	C4	C3A	Cl1A	117.1(9)
N1	C4	C5B	133.3(5)	C2A	C3A	C4	118.1(9)
C3A	C4	C5A	118.6(6)	C2A	C3A	Cl1A	124.0(9)
C5B	C4	C3B	109.8(7)	C6A	C5A	C4	121.5(7)
C8	C7	N1	117.7(2)	C5A	C6A	C1A	119.8(6)
C8	C7	C12	119.3(2)	O1B	C1B	C2B	121.3(7)
C12	C7	N1	122.8(2)	O1B	C1B	C6B	121.4(6)
C9	C8	C7	120.1(2)	C6B	C1B	C2B	117.3(6)
C8	C9	C10	119.6(3)	C3B	C2B	C1B	116.5(9)
C9	C10	Cl2	119.6(2)	C4	C3B	Cl1B	114.8(12)
C11	C10	Cl2	119.4(2)	C2B	C3B	C4	128.8(11)
C11	C10	C9	121.0(3)	C2B	C3B	Cl1B	115.8(11)
C12	C11	C10	119.2(3)	C6B	C5B	C4	124.4(9)
C11	C12	C7	120.7(2)	C5B	C6B	C1B	122.8(8)
O1A	C1A	C2A	119.3(5)				

Table 6 Hydrogen Atom Coordinates (Å×10^4) and Isotropic Displacement Parameters (Å^2×10^3) for mac180066_fa.

Atom	*x*	*y*	*z*	U(eq)
H8	3835	7924	8776	46
H9	1957	5611	9513	54
H11	5212	1661	8298	48
H12	6726	3929	7526	41
H2A	6960	9809	5636	41
H5A	2101	4933	6958	39
H6A	702	4672	5836	41
H2B	8640	10112	5700	41
H5B	2590	4873	6737	39
H6B	2089	4967	5625	41

Table 7 Atomic Occupancy for mac180066_fa.

Atom	*Occupancy*	Atom	*Occupancy*	Atom	*Occupancy*
Cl1A	0.5481	O1A	0.5481	C1A	0.5481
C2A	0.5481	H2A	0.5481	C3A	0.5481
C5A	0.5481	H5A	0.5481	C6A	0.5481
H6A	0.5481	Cl1B	0.4519	O1B	0.4519
C1B	0.4519	C2B	0.4519	H2B	0.4519
C3B	0.4519	C5B	0.4519	H5B	0.4519

C6B 0.4519	H6B 0.4519

(*E*)-4-(Phenylimino)-3-(*o*-tolylamino)cyclohexa-2,5-dien-1-one, 4.7e

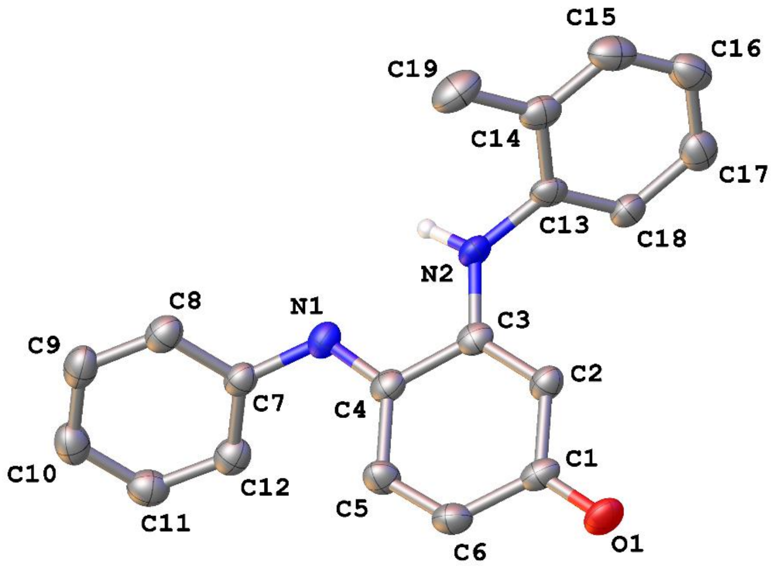

Table 1: Crystal data and structure refinement for mac190041_fa.

Identification code	mac190041_fa
Empirical formula	$C_{19}H_{16}N_2O$
Formula weight	288.34
Temperature/K	150.0(2)
Crystal system	monoclinic
Space group	$P2_1$
a/Å	8.0230(6)
b/Å	7.5722(5)
c/Å	12.4479(11)
α/°	90
β/°	97.540(7)
γ/°	90
Volume/Å^3	749.69(10)
Z	2
ρ_{calc}g/cm^3	1.277
μ/mm^{-1}	0.632
F(000)	304.0
Crystal size/mm^3	0.26 × 0.09 × 0.02
Radiation	CuKα (λ = 1.54184)
2Θ range for data collection/°	7.164 to 133.69
Index ranges	$-9 \le h \le 9$, $-9 \le k \le 8$, $-14 \le l \le 13$

Reflections collected	5768
Independent reflections	2195 [R_{int} = 0.0494, R_{sigma} = 0.0594]
Data/restraints/parameters	2195/1/204
Goodness-of-fit on F^2	1.057
Final R indexes [I>=2σ (I)]	R_1 = 0.0461, wR_2 = 0.0970
Final R indexes [all data]	R_1 = 0.0688, wR_2 = 0.1120
Largest diff. peak/hole / e Å^{-3}	0.27/-0.17
Flack parameter	0.3(5)

Table 2 Fractional Atomic Coordinates (×10^4) and Equivalent Isotropic Displacement Parameters (Å^2×10^3) for mac190041_fa. U_{eq} is defined as 1/3 of of the trace of the orthogonalised U_{IJ} tensor.

Atom	*x*	*y*	*z*	U(eq)
O1	6176(4)	915(4)	3776(3)	39.1(8)
N1	7648(4)	7266(4)	5618(3)	30.0(8)
N2	6300(4)	7181(5)	3561(3)	31.3(8)
C1	6527(5)	2386(6)	4181(3)	30.7(9)
C2	6133(4)	4004(6)	3607(3)	28.9(9)
C3	6543(4)	5602(6)	4071(3)	27.3(9)
C4	7355(5)	5701(5)	5222(3)	28.6(9)
C5	7812(5)	4035(6)	5774(3)	31.5(9)
C6	7433(5)	2490(6)	5290(3)	34.4(10)
C7	8305(4)	7527(6)	6720(3)	28.7(9)
C8	9666(5)	8680(6)	6942(4)	34.7(10)
C9	10316(5)	9049(7)	8002(4)	39.0(10)
C10	9594(5)	8326(6)	8853(4)	38.5(11)
C11	8212(5)	7216(6)	8639(3)	37.6(10)
C12	7570(5)	6808(6)	7576(3)	33.7(10)
C13	5555(5)	7440(5)	2472(3)	29.2(9)
C14	6446(5)	8367(5)	1757(4)	35.0(10)
C15	5643(6)	8696(7)	712(4)	43.9(12)
C16	4033(6)	8113(6)	381(4)	44.4(12)
C17	3171(5)	7179(6)	1074(4)	39.6(11)
C18	3929(5)	6841(5)	2122(3)	32.0(10)
C19	8218(5)	9001(7)	2102(4)	48.3(12)

Table 3 Anisotropic Displacement Parameters (Å^2×10^3) for mac190041_fa. The Anisotropic displacement factor exponent takes the form: -2π^2[h^{2}a*^{2}U$_{11}$+2hka*b*U$_{12}$+…].

Atom	U_{11}	U_{22}	U_{33}	U_{23}	U_{13}	U_{12}
O1	45.4(17)	19.5(17)	51(2)	-1.7(15)	1.2(15)	0.2(13)
N1	27.5(15)	25.9(19)	36.3(19)	-3.8(17)	3.1(14)	-2.4(15)

N2	39.2(18)	18.0(19)	35(2)	-0.1(16)	-1.6(15)	-5.8(15)
C1	27.5(18)	21(2)	45(2)	2(2)	9.8(17)	-0.2(19)
C2	27.3(17)	23(2)	36(2)	-2(2)	3.1(16)	0.0(18)
C3	23.2(18)	25(2)	35(2)	1(2)	8.8(16)	-0.3(18)
C4	24.5(18)	26(2)	36(2)	1(2)	5.7(17)	-2.2(18)
C5	35(2)	26(2)	34(2)	2(2)	2.3(17)	7(2)
C6	38(2)	28(2)	37(2)	7(2)	5.5(19)	1(2)
C7	27.9(18)	23(2)	35(2)	-1(2)	2.6(17)	0.0(18)
C8	31(2)	28(3)	45(3)	-1(2)	4.3(18)	0.0(17)
C9	34(2)	32(2)	48(3)	-6(2)	-5.0(19)	1(2)
C10	41(2)	37(2)	36(3)	-6(2)	-2(2)	5.2(19)
C11	41(2)	34(3)	39(2)	3(2)	8.2(19)	5(2)
C12	31.1(19)	29(2)	41(2)	-2(2)	4.0(18)	2.4(18)
C13	37(2)	16.6(19)	34(2)	2(2)	5.6(18)	3.3(18)
C14	43(2)	22(2)	42(3)	-0.8(19)	12(2)	2.5(19)
C15	62(3)	34(3)	39(3)	5(2)	17(2)	4(2)
C16	60(3)	36(3)	37(3)	4(2)	2(2)	9(2)
C17	45(2)	31(3)	41(2)	-5(2)	0(2)	4(2)
C18	37(2)	22(2)	36(2)	-1.3(19)	3.7(18)	-3.4(17)
C19	46(2)	35(3)	67(3)	-3(3)	21(2)	-8(2)

Table 4 Bond Lengths for mac190041_fa.

Atom	Atom	Length/Å	Atom	Atom	Length/Å
O1	C1	1.240(5)	C7	C12	1.394(6)
N1	C4	1.293(5)	C8	C9	1.382(6)
N1	C7	1.417(5)	C9	C10	1.385(7)
N2	C3	1.356(5)	C10	C11	1.390(7)
N2	C13	1.422(5)	C11	C12	1.391(6)
C1	C2	1.433(6)	C13	C14	1.401(5)
C1	C6	1.475(6)	C13	C18	1.395(5)
C2	C3	1.362(6)	C14	C15	1.397(6)
C3	C4	1.496(6)	C14	C19	1.508(6)
C4	C5	1.460(6)	C15	C16	1.376(7)
C5	C6	1.332(6)	C16	C17	1.371(7)
C7	C8	1.398(6)	C17	C18	1.389(6)

Table 5 Bond Angles for mac190041_fa.

Atom	Atom	Atom	Angle/°	Atom	Atom	Atom	Angle/°
C4	N1	C7	121.5(3)	C12	C7	C8	119.3(4)
C3	N2	C13	125.7(4)	C9	C8	C7	120.2(4)
O1	C1	C2	122.8(4)	C8	C9	C10	120.5(4)

O1	C1	C6	119.1(4)	C9	C10	C11	119.7(4)
C2	C1	C6	118.1(4)	C10	C11	C12	120.2(4)
C3	C2	C1	121.5(4)	C11	C12	C7	120.0(4)
N2	C3	C2	125.0(4)	C14	C13	N2	119.3(3)
N2	C3	C4	114.9(4)	C18	C13	N2	120.8(4)
C2	C3	C4	120.1(4)	C18	C13	C14	119.9(3)
N1	C4	C3	116.5(4)	C13	C14	C19	121.3(4)
N1	C4	C5	126.2(4)	C15	C14	C13	118.0(4)
C5	C4	C3	117.3(4)	C15	C14	C19	120.7(4)
C6	C5	C4	121.2(4)	C16	C15	C14	121.4(5)
C5	C6	C1	121.7(4)	C17	C16	C15	120.6(4)
C8	C7	N1	117.4(4)	C16	C17	C18	119.4(4)
C12	C7	N1	123.0(3)	C17	C18	C13	120.6(4)

Table 6 Hydrogen Atom Coordinates (Å×10^4) and Isotropic Displacement Parameters (Å^2×10^3) for mac190041_fa.

Atom	*x*	*y*	*z*	U(eq)
H2	6560(50)	8150(60)	3930(30)	38
H2A	5573	3962	2886	35
H5	8390	4053	6490	38
H6	7754	1429	5668	41
H8	10145	9213	6364	42
H9	11265	9803	8148	47
H10	10043	8589	9580	46
H11	7703	6734	9222	45
H12	6632	6039	7433	40
H15	6221	9336	218	53
H16	3514	8359	-333	53
H17	2064	6766	840	48
H18	3336	6196	2605	38
H19A	8894	8029	2449	72
H19B	8201	9978	2617	72
H19C	8709	9408	1465	72

(5*E*,5'*E*)-4,4'-Bis(methyl(phenyl)amino)-5,5'-(phenylimino)-[1,1'-bi(cyclohexane)]-3,3',6,6'-tetraene-2,2'-dione, 4.28f

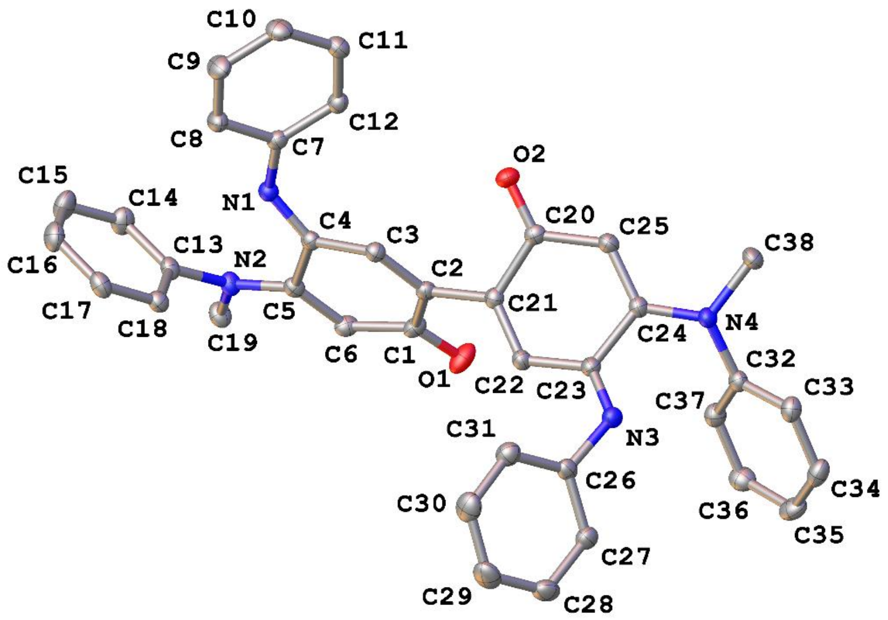

Table 1: Crystal data and structure refinement for mac190044.

Identification code	mac190044
Empirical formula	$C_{38}H_{30}N_4O_2$
Formula weight	574.66
Temperature/K	100.0(2)
Crystal system	monoclinic
Space group	$P2_1/n$
a/Å	16.82010(10)
b/Å	10.48550(10)
c/Å	18.17610(10)
α/°	90
β/°	112.45
γ/°	90
Volume/Å^3	2962.74(4)
Z	4
ρ_{calc}g/cm^3	1.288
μ/mm^{-1}	0.076
F(000)	1208.0
Crystal size/mm^3	0.13 × 0.095 × 0.03
Radiation	Synchrotron (λ = 0.68890)
2Θ range for data collection/°	2.722 to 53.146
Index ranges	$-21 \leq h \leq 21$, $-13 \leq k \leq 13$, $-23 \leq l \leq 23$
Reflections collected	42058
Independent reflections	6790 [R_{int} = 0.0669, R_{sigma} = 0.0403]
Data/restraints/parameters	6790/0/399
Goodness-of-fit on F^2	1.071

Final R indexes [I>=2σ (I)] R_1 = 0.0464, wR_2 = 0.1293
Final R indexes [all data] R_1 = 0.0499, wR_2 = 0.1323
Largest diff. peak/hole / e Å^{-3} 0.43/-0.17

Table 2 Fractional Atomic Coordinates (×10^4) and Equivalent Isotropic Displacement Parameters (Å^2×10^3) for mac190044. U_{eq} is defined as 1/3 of of the trace of the orthogonalised U_{IJ} tensor.

Atom	*x*	*y*	*z*	U(eq)
O1	3902.7(5)	6192.5(9)	6520.5(6)	29.6(2)
O2	2572.5(5)	2503.2(8)	6794.4(5)	21.12(19)
N1	689.5(6)	6050.9(9)	6387.5(6)	17.4(2)
N2	1406.7(6)	8413.6(9)	6416.5(6)	18.8(2)
N3	4139.3(6)	2488.7(9)	4808.7(6)	19.3(2)
N4	4917.2(6)	1003.8(9)	6173.3(6)	19.2(2)
C1	3125.4(7)	6191.0(12)	6379.4(7)	19.2(2)
C2	2614.4(7)	4982.5(11)	6125.5(6)	16.8(2)
C3	1786.3(7)	4970.4(11)	6043.6(6)	16.9(2)
C4	1378.7(7)	6078.7(10)	6242.3(6)	15.7(2)
C5	1825.9(7)	7337.7(11)	6336.0(6)	16.9(2)
C6	2669.8(7)	7333.7(11)	6425.2(7)	19.3(2)
C7	213.3(7)	4947.1(11)	6381.0(6)	17.4(2)
C8	-682.5(7)	5101.3(12)	6048.3(7)	22.4(2)
C9	-1216.6(8)	4106.6(13)	6066.1(8)	27.0(3)
C10	-868.5(8)	2964.0(13)	6439.8(8)	25.3(3)
C11	18.0(8)	2814.8(12)	6785.4(7)	22.4(2)
C12	560.2(7)	3795.1(11)	6750.3(7)	19.0(2)
C13	493.4(7)	8559.0(11)	6025.8(7)	18.5(2)
C14	19.9(8)	9035.4(12)	6446.4(7)	25.4(3)
C15	-867.9(9)	9157.0(14)	6067.0(8)	30.3(3)
C16	-1280.3(8)	8803.7(13)	5275.0(8)	27.6(3)
C17	-803.8(8)	8354.5(11)	4853.8(7)	22.6(2)
C18	85.6(7)	8247.9(11)	5224.4(7)	19.5(2)
C19	1908.8(8)	9570.6(11)	6717.9(7)	22.1(2)
C20	3078.6(7)	2646.8(11)	6460.1(6)	17.1(2)
C21	3068.0(7)	3848.7(11)	6003.0(6)	17.1(2)
C22	3495.0(7)	3865.6(11)	5513.2(7)	18.1(2)
C23	3978.3(7)	2753.4(11)	5425.3(7)	17.4(2)
C24	4256.6(7)	1812.4(11)	6097.9(7)	17.8(2)
C25	3745.1(7)	1720.4(11)	6527.7(7)	19.3(2)
C26	3764.5(7)	3186.7(11)	4093.4(7)	18.8(2)
C27	4300.7(8)	3618.0(12)	3719.3(7)	22.6(2)
C28	3946.7(9)	4230.8(13)	2989.7(8)	27.9(3)
C29	3060.2(9)	4376.7(15)	2615.1(7)	32.7(3)
C30	2525.7(9)	3917.7(15)	2976.4(8)	31.4(3)

C31	2871.7(8)	3326.6(13)	3716.1(7)	24.7(3)
C32	5616.0(7)	1388.9(11)	5961.4(7)	18.9(2)
C33	5965.9(7)	528.9(12)	5584.2(7)	22.3(2)
C34	6609.0(8)	927.7(13)	5335.2(8)	26.7(3)
C35	6909.8(8)	2169.9(14)	5463.0(8)	28.1(3)
C36	6588.3(8)	3007.2(13)	5874.6(8)	26.4(3)
C37	5947.5(8)	2617.6(12)	6127.8(7)	22.0(2)
C38	5028.3(8)	-145.9(12)	6661.8(8)	24.2(3)

Table 3 Anisotropic Displacement Parameters (Å^2×10^3) for mac190044. The Anisotropic displacement factor exponent takes the form: -2π^2[$h^2a^{*2}U_{11}$+2hka*b*U_{12}+…].

Atom	U_{11}	U_{22}	U_{33}	U_{23}	U_{13}	U_{12}
O1	17.7(4)	33.9(5)	39.2(5)	-13.3(4)	13.1(4)	-5.0(4)
O2	20.9(4)	23.9(4)	21.8(4)	0.2(3)	11.7(3)	-1.3(3)
N1	16.9(4)	17.3(5)	17.2(4)	0.8(3)	5.7(3)	0.4(3)
N2	17.9(4)	15.6(5)	19.5(4)	-2.1(4)	3.6(4)	-0.4(4)
N3	20.5(5)	18.8(5)	20.0(5)	1.3(4)	9.2(4)	2.3(4)
N4	19.8(5)	17.0(5)	22.2(5)	4.1(4)	9.6(4)	3.2(4)
C1	17.0(5)	24.1(6)	17.9(5)	-3.4(4)	8.2(4)	-2.5(4)
C2	18.4(5)	18.3(5)	14.4(5)	0.0(4)	6.9(4)	0.4(4)
C3	17.8(5)	16.5(5)	16.2(5)	-0.2(4)	6.4(4)	-0.4(4)
C4	15.0(5)	17.4(5)	13.1(5)	0.7(4)	3.7(4)	0.4(4)
C5	18.8(5)	17.1(5)	13.4(5)	-0.8(4)	4.7(4)	-0.6(4)
C6	20.7(5)	18.1(5)	19.8(5)	-3.7(4)	8.5(4)	-4.8(4)
C7	17.1(5)	19.4(6)	16.9(5)	-0.6(4)	7.7(4)	-0.9(4)
C8	18.3(5)	23.1(6)	25.8(6)	5.6(5)	8.3(4)	2.0(4)
C9	15.6(5)	31.4(7)	31.8(6)	5.5(5)	6.7(5)	-2.0(5)
C10	23.4(6)	24.9(6)	27.6(6)	2.5(5)	9.6(5)	-7.2(5)
C11	25.0(6)	20.0(6)	21.2(5)	3.5(4)	7.9(5)	0.8(4)
C12	16.4(5)	22.4(6)	17.5(5)	0.0(4)	5.7(4)	0.8(4)
C13	18.7(5)	14.1(5)	20.6(5)	0.8(4)	5.0(4)	1.3(4)
C14	26.0(6)	26.4(6)	22.2(6)	-5.2(5)	7.3(5)	2.6(5)
C15	25.9(6)	33.4(7)	33.1(7)	-5.8(5)	12.9(5)	6.6(5)
C16	18.5(6)	27.6(7)	32.1(6)	-0.7(5)	4.6(5)	4.4(5)
C17	23.9(6)	17.8(6)	20.4(5)	1.0(4)	2.2(4)	1.7(4)
C18	21.8(5)	16.5(5)	19.5(5)	1.1(4)	7.1(4)	0.9(4)
C19	23.2(5)	16.2(5)	23.2(5)	-1.6(4)	4.6(4)	-0.8(4)
C20	16.9(5)	19.3(5)	14.6(5)	-1.8(4)	5.4(4)	-1.9(4)
C21	15.3(5)	18.1(5)	16.9(5)	-0.3(4)	5.0(4)	0.5(4)
C22	19.1(5)	17.7(5)	17.6(5)	2.0(4)	7.1(4)	2.7(4)
C23	16.4(5)	18.0(5)	18.7(5)	1.7(4)	7.7(4)	0.6(4)
C24	17.9(5)	16.6(5)	18.1(5)	0.6(4)	6.1(4)	1.2(4)

C25	20.8(5)	19.2(5)	18.1(5)	3.2(4)	7.7(4)	1.5(4)
C26	23.4(5)	17.1(5)	16.9(5)	-0.8(4)	8.6(4)	3.0(4)
C27	23.9(6)	23.4(6)	23.0(6)	-0.9(5)	11.8(5)	2.3(5)
C28	37.0(7)	28.5(7)	23.5(6)	1.8(5)	17.5(5)	1.3(5)
C29	41.5(8)	37.4(8)	16.9(6)	4.8(5)	8.5(5)	8.1(6)
C30	24.5(6)	41.7(8)	21.8(6)	-1.1(5)	2.0(5)	4.8(5)
C31	23.3(6)	28.4(6)	22.9(6)	-1.5(5)	9.2(5)	-0.6(5)
C32	16.3(5)	21.1(6)	17.9(5)	2.3(4)	4.9(4)	2.6(4)
C33	19.0(5)	21.6(6)	24.2(6)	-2.0(5)	5.9(4)	2.2(4)
C34	19.6(5)	35.6(7)	24.8(6)	-4.8(5)	8.2(5)	4.6(5)
C35	18.7(5)	41.4(8)	24.8(6)	0.7(5)	9.1(5)	-4.1(5)
C36	23.7(6)	26.5(6)	26.9(6)	0.5(5)	7.3(5)	-5.3(5)
C37	21.8(6)	21.5(6)	21.8(5)	-0.9(4)	7.5(4)	1.7(4)
C38	25.2(6)	20.6(6)	28.0(6)	8.9(5)	11.6(5)	4.7(5)

Table 4 Bond Lengths for mac190044.

Atom	Atom	Length/Å	Atom	Atom	Length/Å
O1	C1	1.2324(14)	C13	C14	1.3903(16)
O2	C20	1.2295(14)	C13	C18	1.3913(16)
N1	C4	1.2838(14)	C14	C15	1.3911(18)
N1	C7	1.4049(14)	C15	C16	1.3885(19)
N2	C5	1.3675(14)	C16	C17	1.3853(18)
N2	C13	1.4333(14)	C17	C18	1.3909(16)
N2	C19	1.4600(15)	C20	C21	1.5058(16)
N3	C23	1.2799(15)	C20	C25	1.4526(16)
N3	C26	1.4133(15)	C21	C22	1.3406(15)
N4	C24	1.3624(14)	C22	C23	1.4647(15)
N4	C32	1.4278(15)	C23	C24	1.5000(15)
N4	C38	1.4662(15)	C24	C25	1.3686(15)
C1	C2	1.5015(16)	C26	C27	1.3960(16)
C1	C6	1.4418(16)	C26	C31	1.4000(16)
C2	C3	1.3431(15)	C27	C28	1.3867(18)
C2	C21	1.4747(15)	C28	C29	1.391(2)
C3	C4	1.4629(15)	C29	C30	1.386(2)
C4	C5	1.4965(15)	C30	C31	1.3902(18)
C5	C6	1.3658(16)	C32	C33	1.3920(16)
C7	C8	1.4022(15)	C32	C37	1.3905(17)
C7	C12	1.3968(16)	C33	C34	1.3870(17)
C8	C9	1.3851(17)	C34	C35	1.384(2)
C9	C10	1.3914(19)	C35	C36	1.3899(19)
C10	C11	1.3882(17)	C36	C37	1.3854(17)
C11	C12	1.3917(17)			

Table 5 Bond Angles for mac190044.

Atom	Atom	Atom	Angle/°	Atom	Atom	Atom	Angle/°
C4	N1	C7	125.00(10)	C16	C15	C14	120.41(12)
C5	N2	C13	122.25(9)	C17	C16	C15	119.88(11)
C5	N2	C19	118.54(9)	C16	C17	C18	120.13(11)
C13	N2	C19	117.03(9)	C17	C18	C13	119.82(11)
C23	N3	C26	121.60(10)	O2	C20	C21	120.70(10)
C24	N4	C32	121.38(10)	O2	C20	C25	122.27(10)
C24	N4	C38	118.89(9)	C25	C20	C21	116.91(10)
C32	N4	C38	117.91(9)	C2	C21	C20	119.29(9)
O1	C1	C2	120.15(10)	C22	C21	C2	121.93(10)
O1	C1	C6	122.14(11)	C22	C21	C20	118.75(10)
C6	C1	C2	117.68(10)	C21	C22	C23	121.49(10)
C3	C2	C1	119.32(10)	N3	C23	C22	125.45(10)
C3	C2	C21	123.37(10)	N3	C23	C24	117.81(10)
C21	C2	C1	117.28(9)	C22	C23	C24	116.63(9)
C2	C3	C4	121.95(10)	N4	C24	C23	118.69(9)
N1	C4	C3	125.30(10)	N4	C24	C25	124.41(10)
N1	C4	C5	116.79(10)	C25	C24	C23	116.30(10)
C3	C4	C5	117.79(9)	C24	C25	C20	122.52(10)
N2	C5	C4	118.86(10)	C27	C26	N3	118.14(10)
C6	C5	N2	123.00(10)	C27	C26	C31	119.94(11)
C6	C5	C4	117.73(10)	C31	C26	N3	121.54(10)
C5	C6	C1	123.16(10)	C28	C27	C26	119.64(11)
C8	C7	N1	115.08(10)	C27	C28	C29	120.50(12)
C12	C7	N1	125.18(10)	C30	C29	C28	119.85(12)
C12	C7	C8	119.33(10)	C29	C30	C31	120.34(12)
C9	C8	C7	120.19(11)	C30	C31	C26	119.67(12)
C8	C9	C10	120.27(11)	C33	C32	N4	119.74(11)
C11	C10	C9	119.80(11)	C37	C32	N4	120.42(10)
C10	C11	C12	120.36(11)	C37	C32	C33	119.84(11)
C11	C12	C7	120.00(10)	C34	C33	C32	119.64(12)
C14	C13	N2	119.77(10)	C35	C34	C33	120.63(12)
C14	C13	C18	120.20(11)	C34	C35	C36	119.49(12)
C18	C13	N2	120.02(10)	C37	C36	C35	120.30(12)
C13	C14	C15	119.49(12)	C36	C37	C32	119.94(11)

Table 6 Hydrogen Atom Coordinates (Å×10^4) and Isotropic Displacement Parameters (Å^2×10^3) for mac190044.

Atom	*x*	*y*	*z*	U(eq)
H3	1463	4236	5855	20

H6	2965	8105	6520	23
H8	-919	5874	5815	27
H9	-1810	4203	5827	32
H10	-1229	2302	6458	30
H11	251	2056	7042	27
H12	1153	3683	6973	23
H14	295	9271	6977	31
H15	-1187	9477	6346	36
H16	-1875	8868	5028	33
H17	-1079	8124	4322	27
H18	407	7969	4937	23
H19A	2377	9386	7211	33
H19B	1547	10214	6804	33
H19C	2132	9873	6337	33
H22	3484	4600	5223	22
H25	3827	1039	6876	23
H27	4892	3495	3958	27
H28	4305	4547	2749	33
H29	2827	4781	2123	39
H30	1933	4006	2723	38
H31	2512	3025	3959	30
H33	5770	-308	5500	27
H34	6840	355	5080	32
H35	7324	2442	5275	34
H36	6804	3833	5981	32
H37	5739	3177	6409	26
H38A	5469	-672	6606	36
H38B	4497	-612	6489	36
H38C	5191	93	7210	36

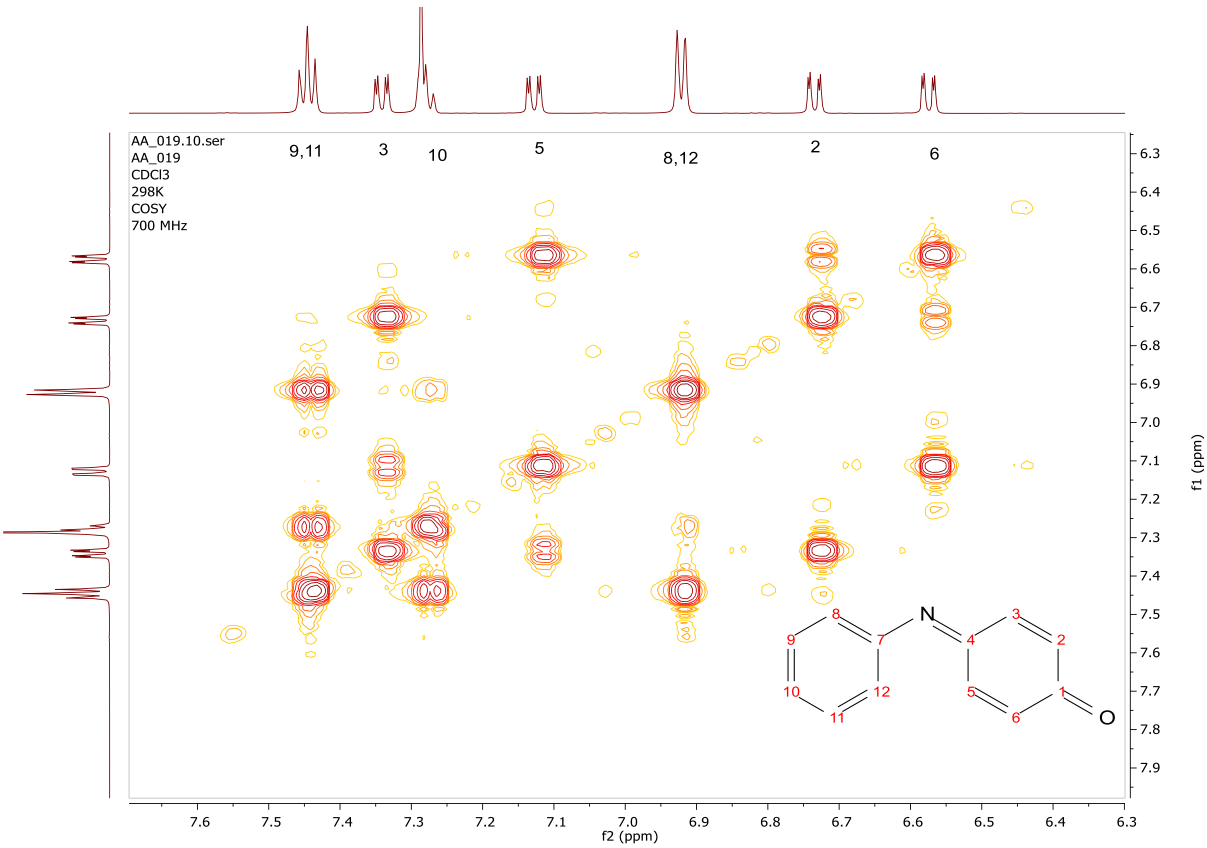

Figure 1: COSY spectrum of **1.24**

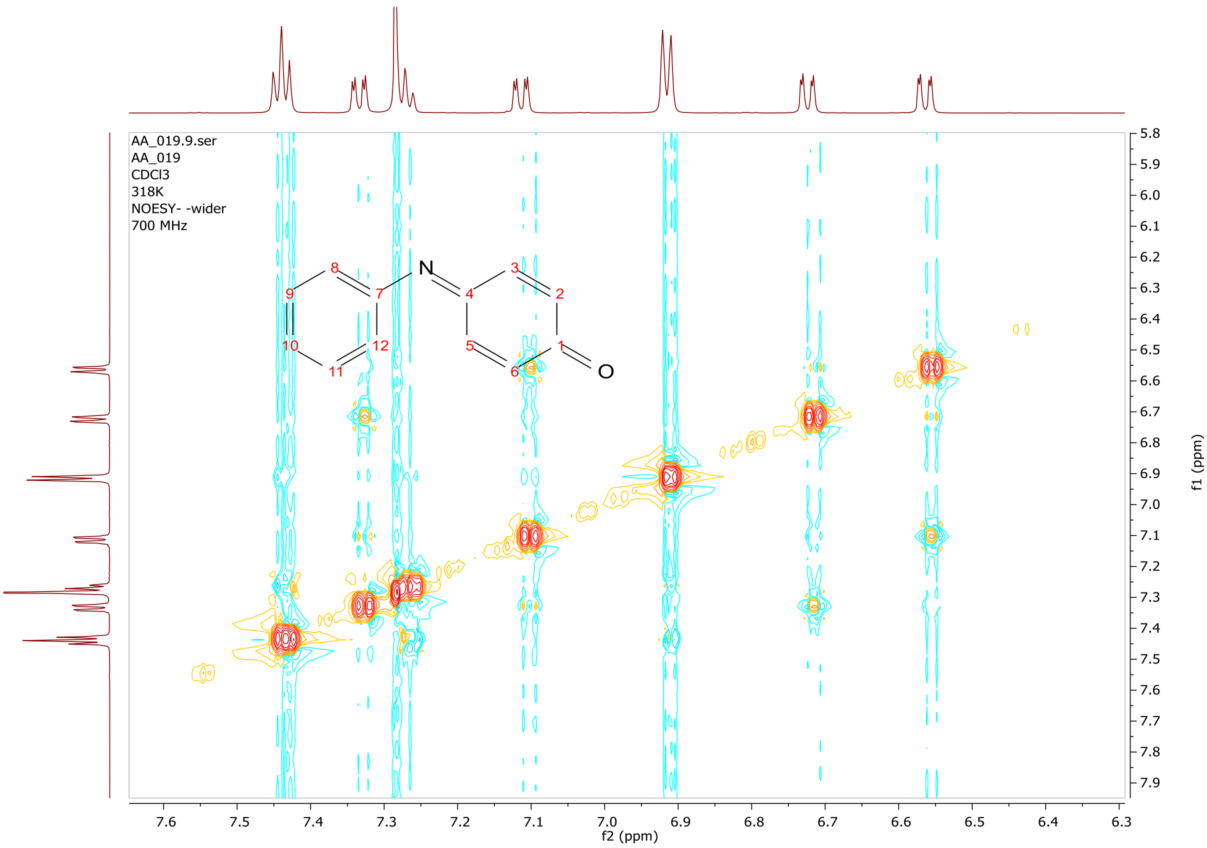

Figure 2: NOESY spectrum of **1.24**

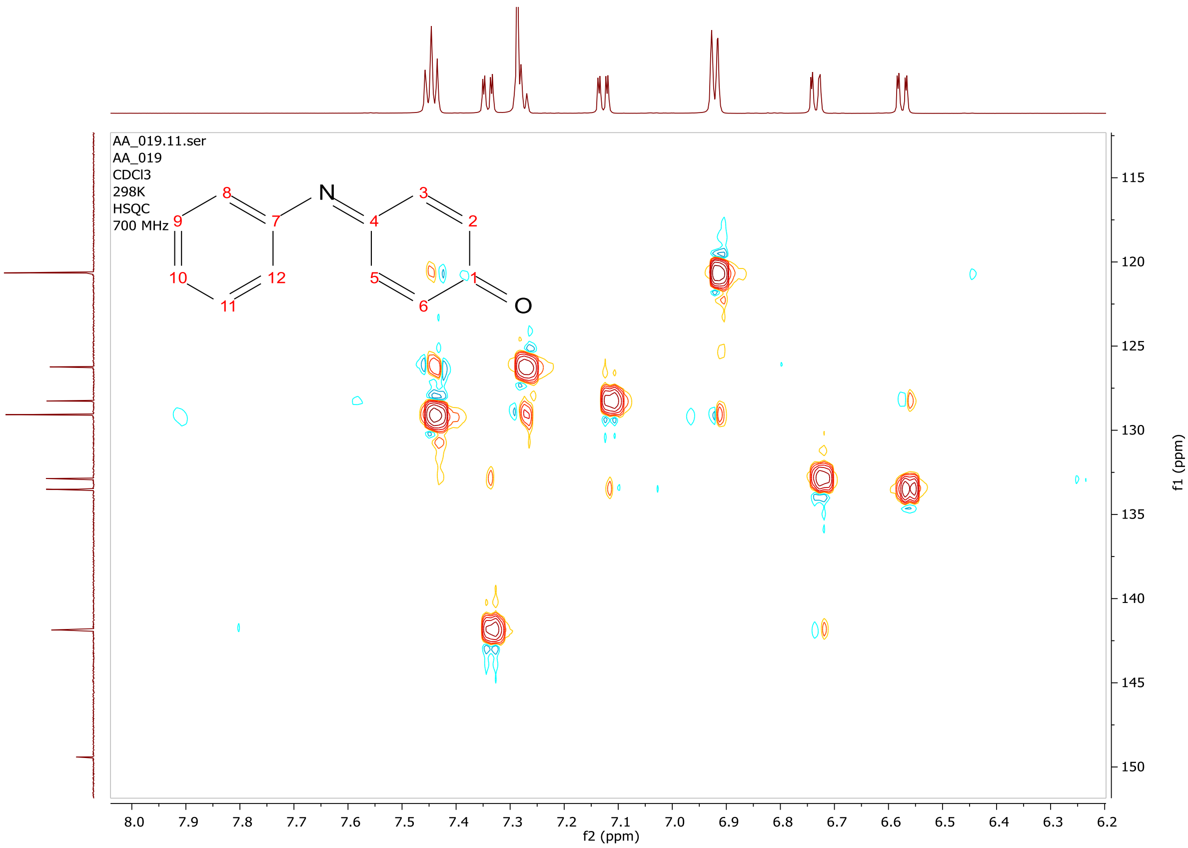

Figure 3: HSQC spectrum of **1.24**

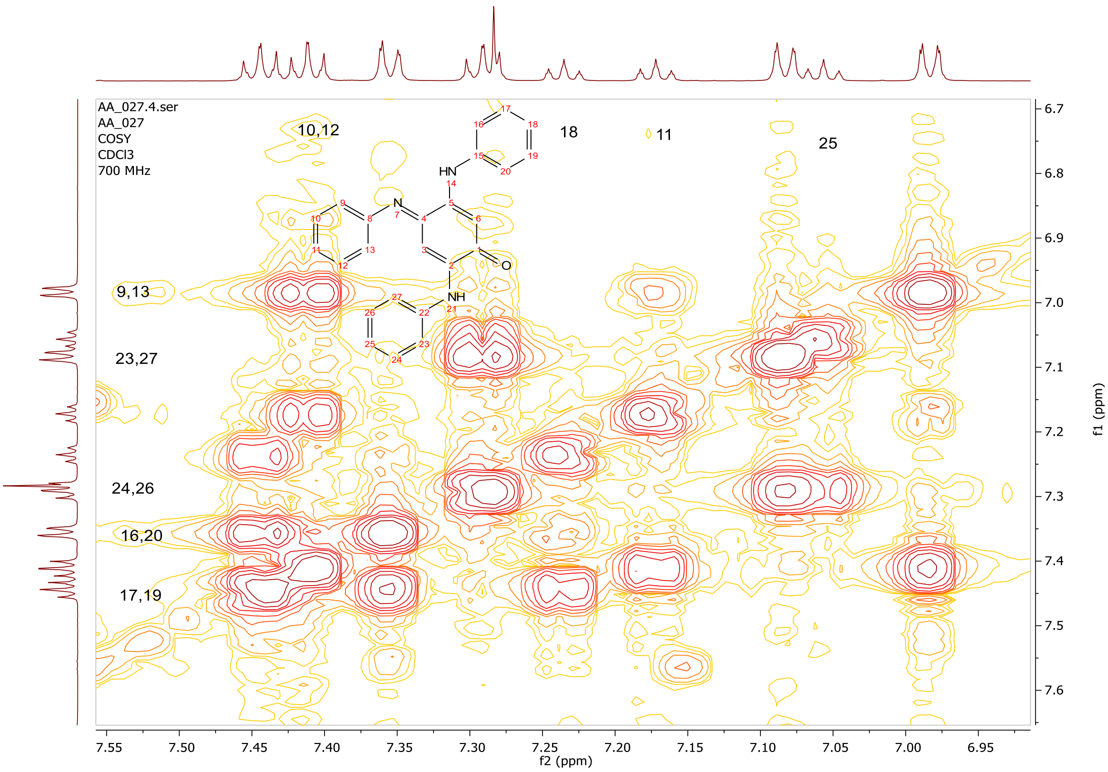

Figure 4: COSY spectrum of **2.9a**

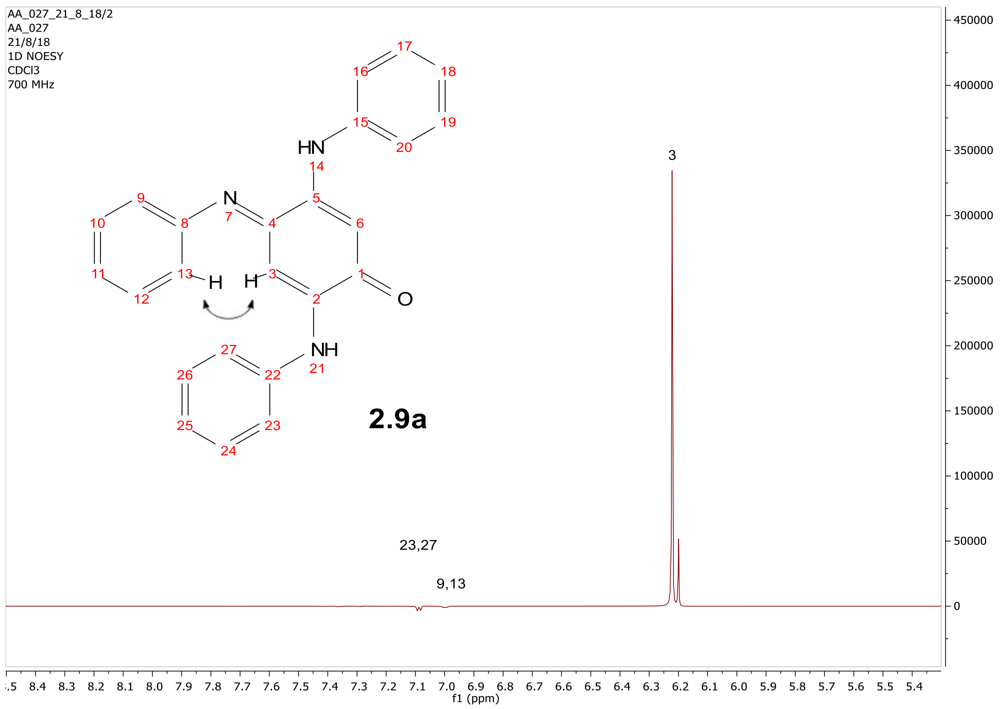

Figure 5: NOESY spectrum of **2.9a**

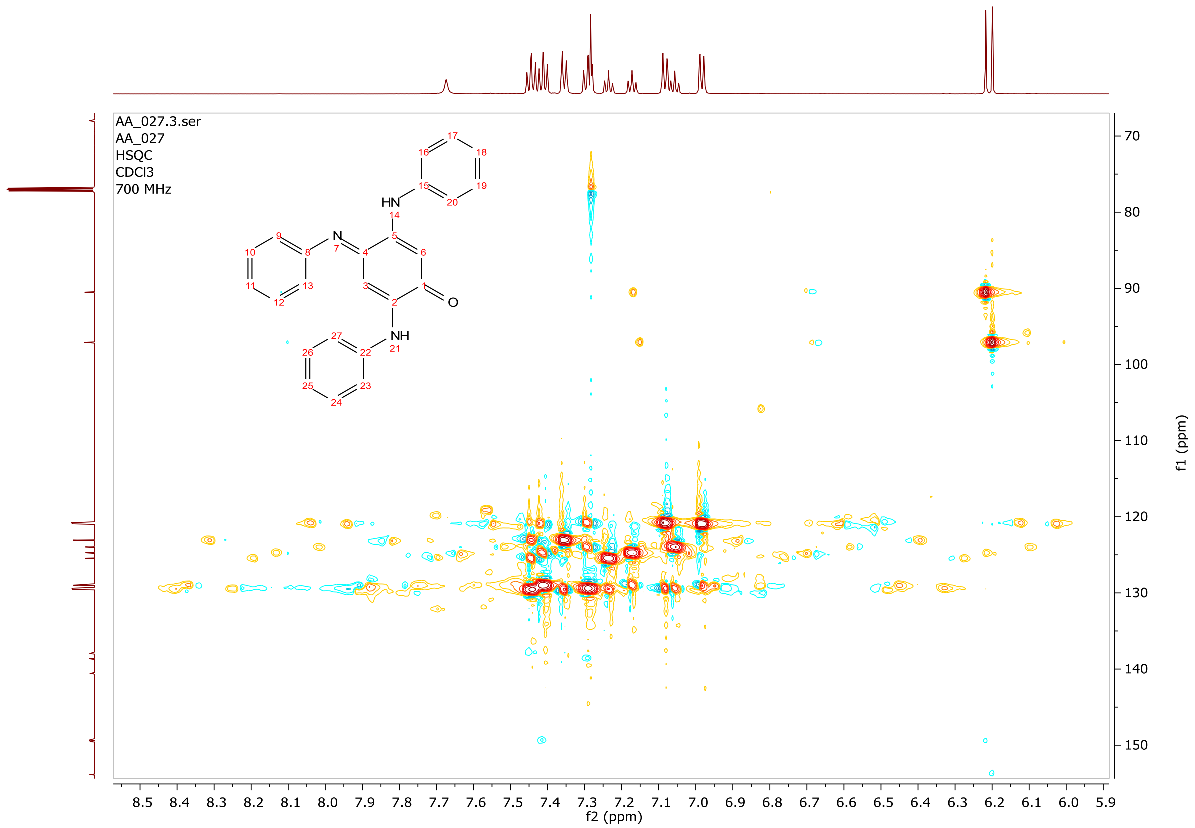

Figure 6: HSQC spectrum of **2.9a**

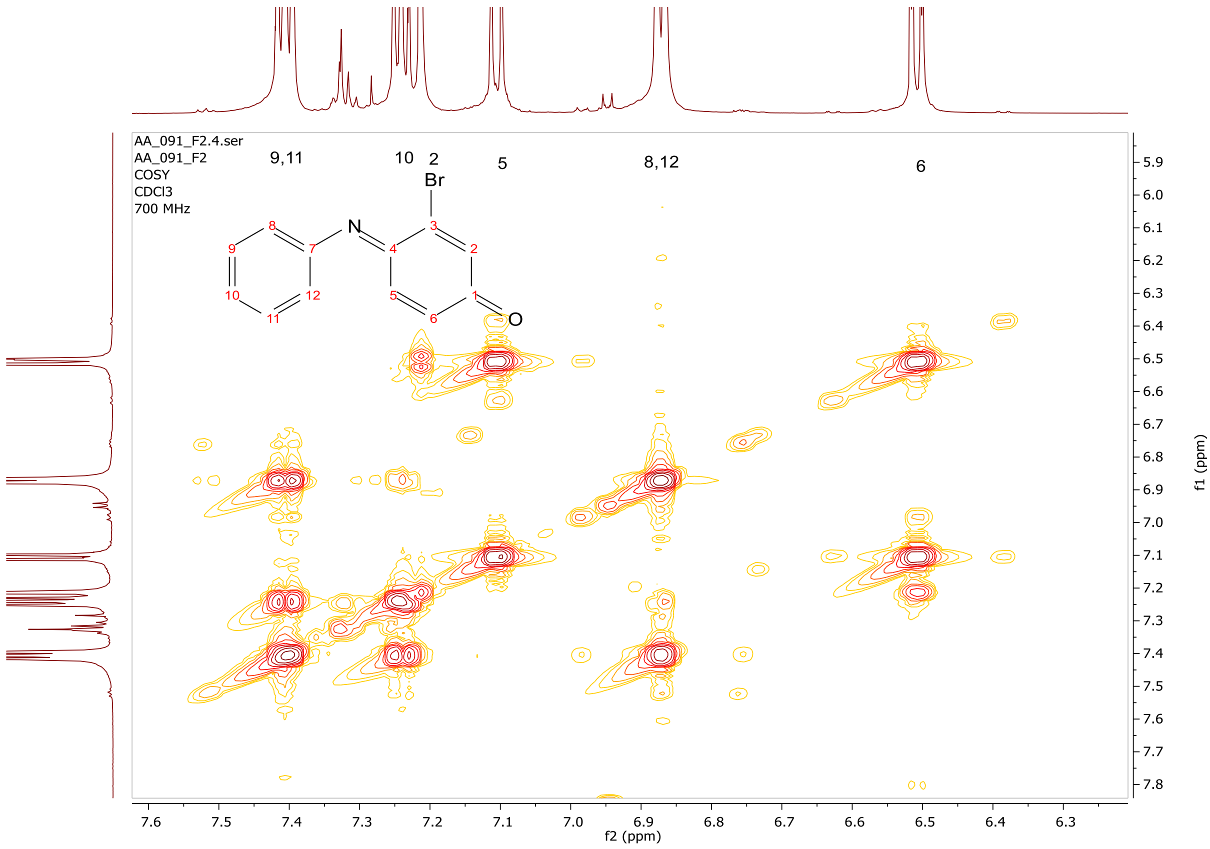

Figure 7: COSY spectrum of **3.2**

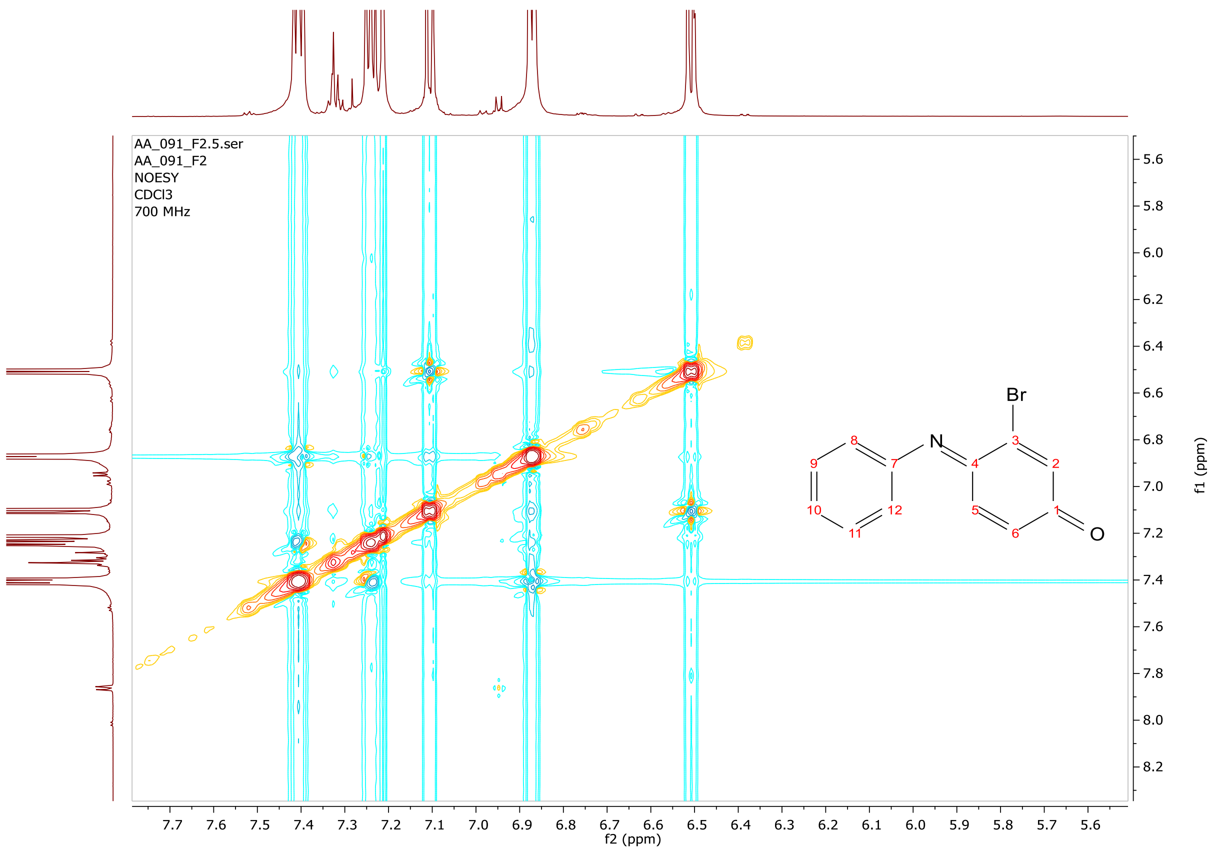

Figure 8: NOESY spectrum of **3.2**

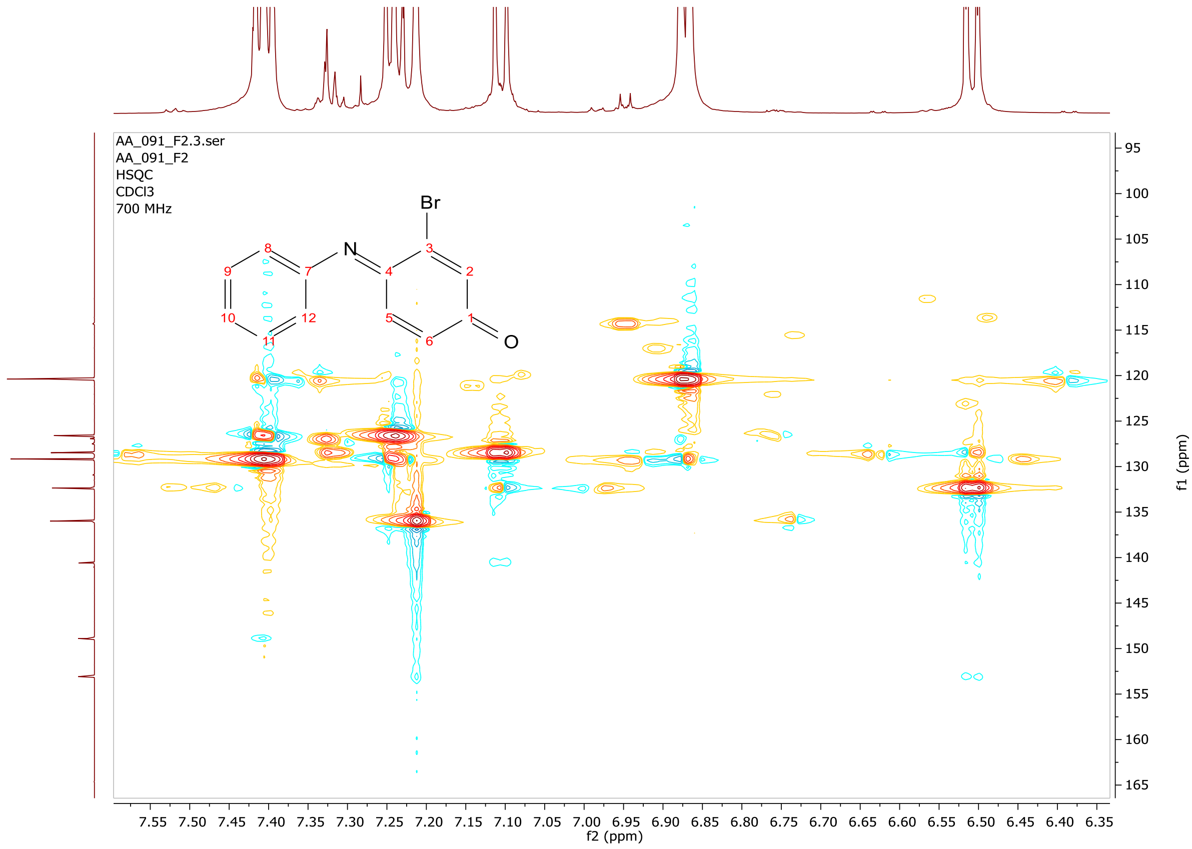

Figure 9: HSQC spectrum of **3.2**

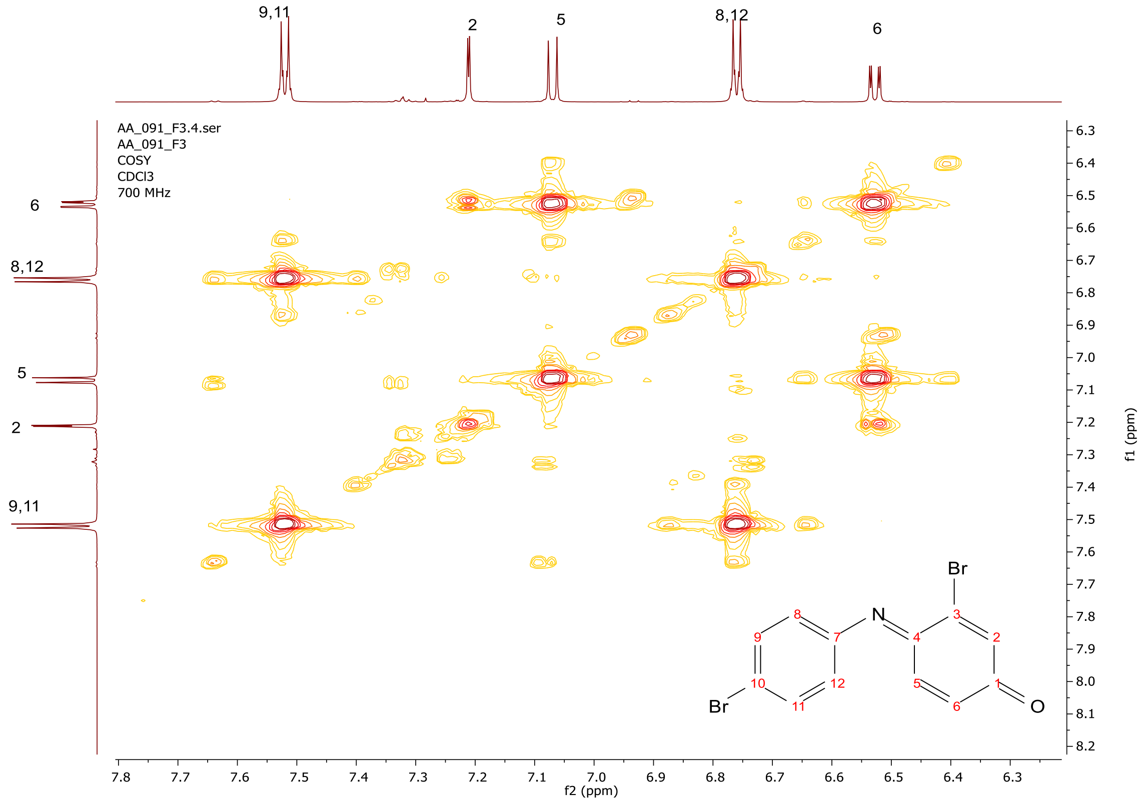

Figure 10: COSY spectrum of **3.30**

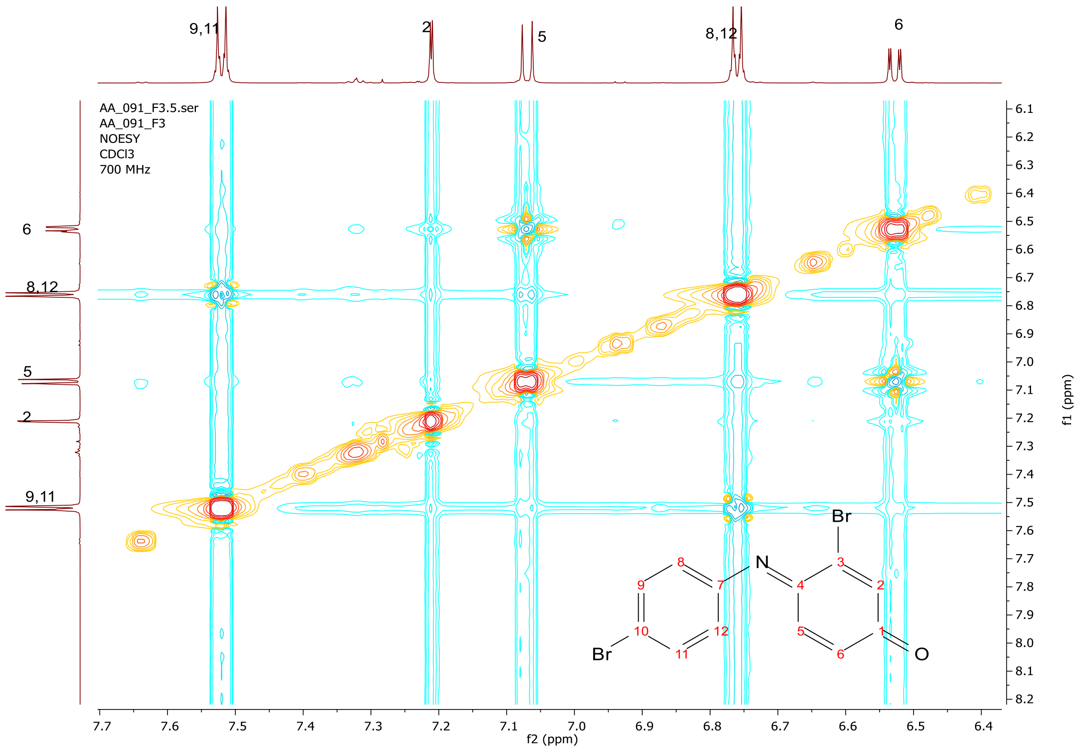

Figure 11: NOESY spectrum of **3.30**

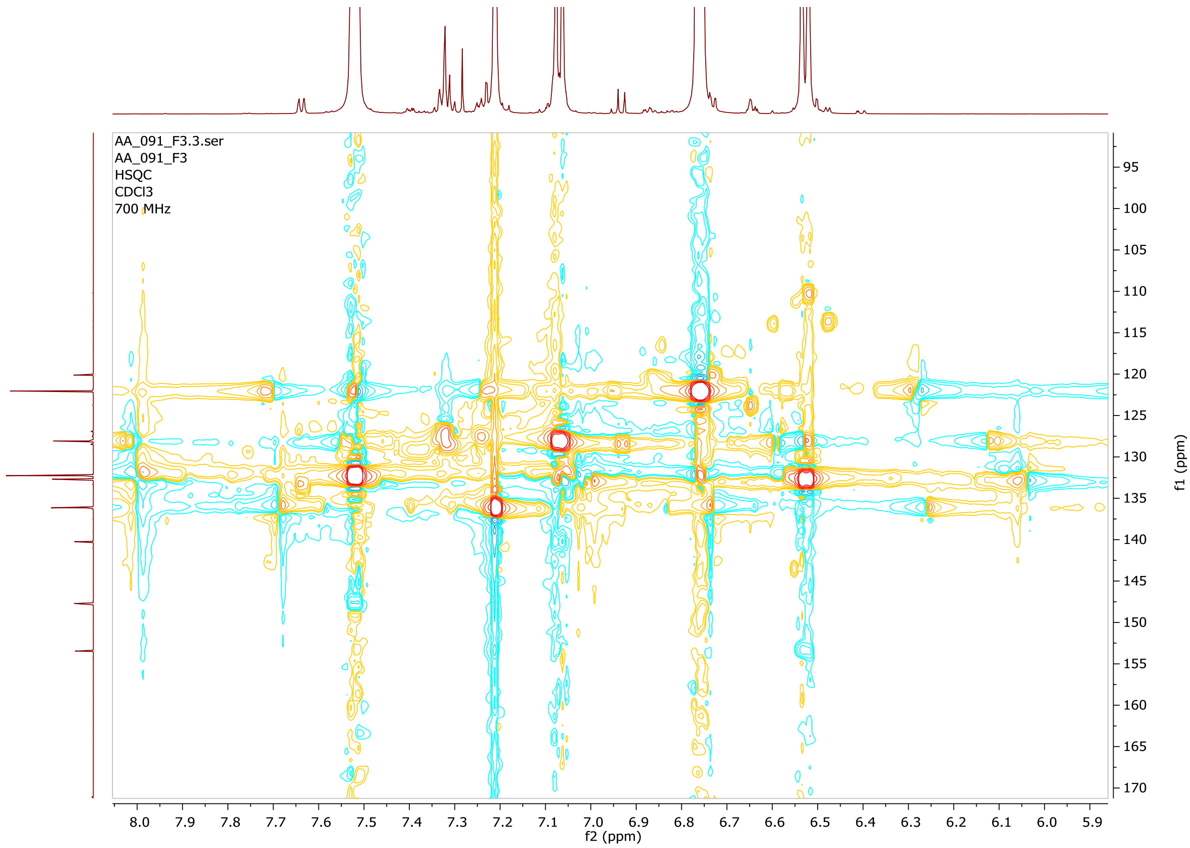

Figure 12: HSQC spectrum of **3.30**